

The significance of sAPP α production to increase cell viability in Alzheimer's disease cell models

Research Masters Thesis

Joshua Bracewell MBiomed Sci (Hons)

Lancaster University

March 2023

I, Joshua Bracewell, confirm that the work presented in this thesis is my own and has not been submitted in substantially the same form for the award of a higher degree elsewhere. Where information has been derived from other sources, I confirm this has been indicated in the thesis.

Signed

Submitted in part fulfilment of the requirements for the degree of Research Masters

Abstract

Alzheimer's disease (AD) is a currently incurable disease. The amyloid hypothesis on causation relates to amyloid precursor protein (APP) which is processed to release soluble APP (α or β) (sAPP) and possibly amyloid β (A β) peptides. The A β can then form amyloid plaques and are neurotoxic in the brain, newly approved antibodies target A β but are not a cure. sAPP α is another possibility predominantly released by ADAM10 processing of APP and has been linked to many neuroprotective/neuroproliferative effects. The objective of this research is to examine the role of APP processing in AD cell models and explore therapies to enhance sAPP α .

Fibrates have previously been used to increase sAPP α release and we tested this in the AD-related cell model Swedish mutant APP₆₉₅ (SweAPP)-SH-SY5Y. However, the fibrates were found to not enhance release of sAPP α via ADAM10 expression. Subsequently, APP processing was examined for Mock-, wild-type APP₆₉₅- (wtAPP-), SweAPP- and BACE1-transfected SH-SY5Y Cells, where BACE1 is responsible for amyloidogenic processing of APP to release sAPP β and A β -peptides.

It was found that the non-amyloidogenic release of sAPP was unaffected by batimastat (ADAM inhibitor) in SH-SY5Y-BACE1 cells, which could be due to the release of sAPP β prime (sAPP β ') by BACE1. By transfecting Mock- and BACE1-SH-SY5Y cells with sAPP α and sAPP β ' constructs, the sAPP α /sAPP β ' axis was shown to rescue the SH-SY5Y-BACE1 cell viability and highlighted the importance of sAPP α release to the cell.

Further work is required to generate a functioning Tet-On system to create an inducible mammalian expression system to selectively overexpress sAPP α .

1. Table of contents

1. Literature review	1
1.1 Introduction.....	2
1.1.1 The pathological hallmarks of Alzheimer's disease	2
1.1.2 Disease causation	4
1.1.3 Amyloid precursor protein (APP).....	9
1.1.4 APP proteolysis	12
1.1.5 sAPP α	17
1.1.6 Existing experimental strategies for the treatment of AD	18
1.1.7 Enhancing sAPP α as a therapeutic strategy	20
1.1.8 Aims of the current project.....	22
2. Materials and Methods	24
2.1 Materials	25
2.2 Methods.....	25
2.2.1 Cell culture.....	25
2.2.2 Freezing and resurrecting cell lines.....	26
2.2.3 Cell treatments	26
2.2.4 A β -peptide quantification.....	27
2.2.5 Cell viability assays	27
2.2.6 Agarose gel electrophoresis	28
2.2.7 DNA fragment gel extraction	28
2.2.8 Polymerase chain reaction (PCR)	28
2.2.9 Restriction digest	32
2.2.10 Ligation.....	32
2.2.11 Bacterial transformation	32
2.2.12 Bacterial cultures.....	33
2.2.13 Plasmid DNA preparation.....	33
2.2.14 Stable and transient transfections of mammalian cells.....	33
2.2.15 Preparation of conditioned medium samples.....	35
2.2.16 Harvesting cells and preparation of cell lysates	35
2.2.17 Bicinchoninic acid (BCA) protein assay	36
2.2.18 Sodium dodecyl sulphate polyacrylamide gel electrophoresis (SDS-PAGE) ...	36
2.2.19 Tris-Tricine gel electrophoresis	38
2.2.20 Immunoblotting.....	39
2.2.21 Amido black staining	41
2.2.22 Statistical analysis.....	41
3. Results; Fibrates do not enhance sAPPα generation in Swedish mutant APP SH-SY5Y cells	42
3.1 Introduction.....	43
3.2 Lack of effect of gemfibrozil on ADAM10 expression and APP processing in Swedish mutant APP SH-SY5Y cells.....	43
3.3 Lack of effect of bezafibrate on ADAM10 expression and APP processing in Swedish mutant APP SH-SY5Y cells.....	47
3.4 Summary	50
4. Results; Beta-prime processing of APP replaces sAPPα generation in BACE1-transfected SH-SY5Y cells	52

4.1	Introduction.....	53
4.2	APP and secretase expression/proteolysis in AD-relevant SH-SY5Y cell lines 53	
4.2.1	APP and secretase expression in AD-relevant SH-SY5Y cell lines.....	54
4.2.2	APP proteolysis in AD-relevant SH-SY5Y cell lines.....	59
4.2.3	Non-amyloidogenically derived soluble APP produced by SH-SY5Y-BACE1 cells results from BACE1 beta-prime activity.....	63
4.3	Viability of AD-relevant SH-SY5Y cell lines	74
4.4	Generation and characterization of sAPP α and sAPP β ' over-expressing Mock- and BACE1-transfected SH-SY5Y cell lines.....	75
4.5	The effect of sAPP α and sAPP β ' over expression on the viability of Mock- and BACE1-transfected SH-SY5Y cells.....	85
4.6	Summary	86
5.	Results; Design of inducible, neuron-specific mammalian expression plasmids	89
5.1	Introduction.....	90
5.2	Design of a dual plasmid doxycycline-inducible neuron-specific expression system.....	90
5.2.1	Dual plasmid system regulator plasmid (pIRES _{hyg} -ESYN-TET3G) design	91
5.2.2	Dual plasmid system response plasmid (pIRES _{zeo} -sAPP α -VPS35) design.....	95
5.3	Design of a single plasmid PiggyBac doxycycline-inducible neuron-specific expression system.....	97
5.4	Summary	101
6.	Results; Stable SH-SY5Y transfectants for the study of protective proteins as potential therapies for AD.....	102
6.1	Introduction.....	103
6.2	Generation of a cytomegalovirus promoter version of the pIRES _{hyg} -ESYN- TET3G regulator plasmid	103
6.3	Transient transfection of pIRES _{hyg} -ESYN-TET3G and pIRES-CMV-TET3G regulator plasmids in SH-SY5Y and HEK cells	106
6.4	Generation of response plasmids for examining the effect of MCS positioning of coding DNA sequences on protein expression	107
6.4.1	pIRES _{zeo} -empty-VPS35.....	108
6.4.2	pIRES _{zeo} -empty-empty	109
6.4.3	pIRES _{zeo} -sAPP α -VPS35.....	110
6.4.4	pIRES _{zeo} -sAPP α -empty	113
6.4.5	pIRES _{zeo} -empty-sAPP α	114
6.4.6	pIRES _{zeo} -VPS35-sAPP α	117
6.4.7	pIRES _{zeo} -VPS35-empty	118
6.5	Removal of the bleomycin coding sequence from pIRES _{zeo} -empty-VPS35 for subsequent PiggyBac plasmid generation	120
6.6	Summary	121
7.	Discussion	123
7.1	Fibrate treatment does not enhance sAPP α release in Swedish mutant APP SH-SY5Y cells.....	124

7.2	Beta-prime processing of APP supersedes sAPP α generation in BACE1-transfected SH-SY5Y cells	126
7.3	The sAPP α /sAPP β ' axis is more important for cell viability than A β -peptide production	129
7.4	Design and generation of a neuroprotective expression system in SH-SY5Y stable transfectants	133
7.5	Future work.....	136
7.6	Conclusions	137
8.	Appendices	138
9.	Bibliography	155

Acknowledgements

I would like to principally thank my supervisor Dr Edward Parkin, his lab and the department for all of their support throughout this project. I would also like to extend this thanks to my family and friends for support during a tumultuous year.

Author's declaration

I Joshua James Bracewell, hereby do swear that this thesis is of my own work and has not been submitted in substantially the same form for the award of a higher degree elsewhere. Elements of this thesis have been published in the paper Owens *et al.*, 2022 and shall be clearly identified. Email permission to reproduce material from Owens *et al.*, 2022 have been attached in Figure S.6.

1. Literature review

1.1 Introduction

Alzheimer's Disease (AD) is an incurable and progressive neurodegenerative disorder and the most common form of dementia, accounting for 50 million cases worldwide, with 10 million new cases each year (World Health Organisation (WHO), 2020). These numbers are perpetuated by an aging population, a major AD risk factor, with the number of people over 65 worldwide predicted to increase from 420 million in 2000 to 1 billion by 2030 (CDC, 2003). The disease begins with minor memory issues and progresses to broad changes in personality, major cognitive difficulties and even hallucinations.

Despite AD being incurable, there are treatments available that marginally slow the rate of cognitive decline including acetylcholinesterase inhibitors such as Donepezil (Shintani and Uchida, 1997), and the glutamate receptor blocker memantine (Kornhuber *et al.*, 1994). However, these treatments only partly mask disease symptoms and do not address the underlying causation. Therefore, with the rising socioeconomic impact of AD in the aging population, there is a pressing need for effective disease treatments.

1.1.1 The pathological hallmarks of Alzheimer's disease

At the macroscopic level, a significant thinning of various cortical regions (including the medial temporal lobe, temporal lobe and superior frontal gyrus) is visible in the AD-afflicted brain (Dickerson *et al.*, 2011). At the microscopic level, AD is characterized neuropathologically by intraneuronal neurofibrillary tangles composed of tau and extracellular neuritic plaques composed of amyloid- β (A β) (Lashley *et al.*, 2018) (Figure 1.1).

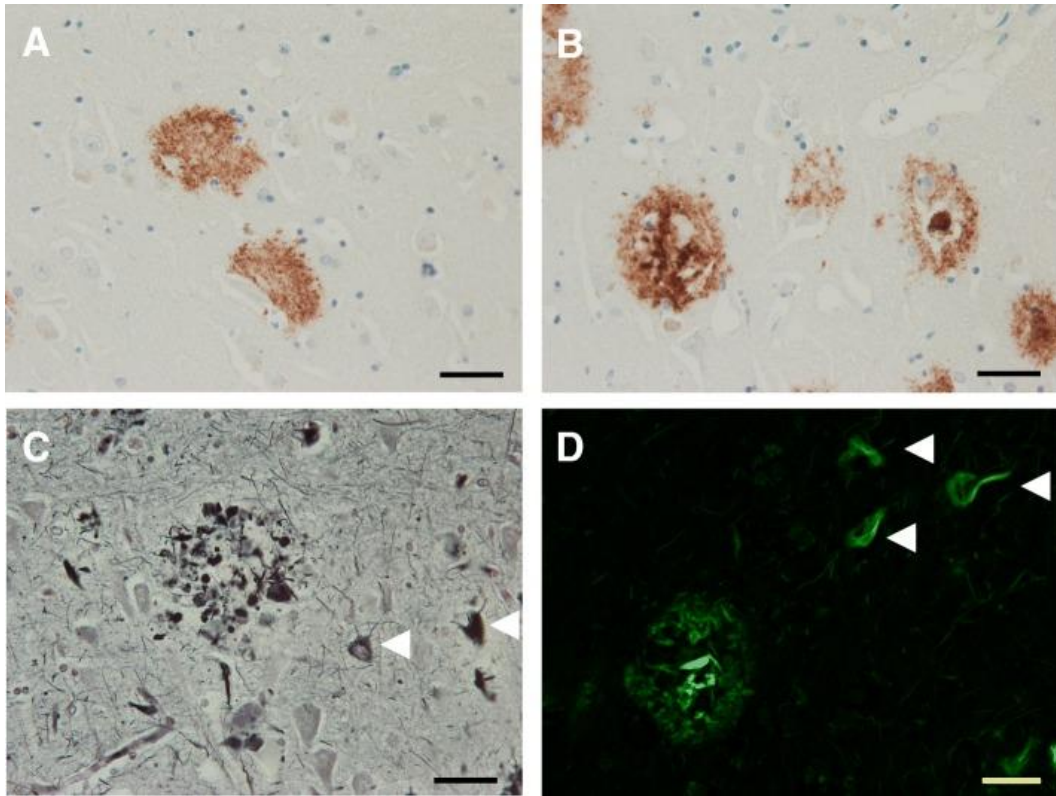


Figure 1.1: Immunohistochemical staining of Alzheimer's disease brain slices. Antibodies raised against amyloid- β ($A\beta$) demonstrate the presence of diffuse (A) and dense core senile plaques (B). Neuritic plaques can be observed with Bielschowsky silver staining (C) and Thioflavin S staining (D). These latter two forms of staining can also highlight neurofibrillary tangles indicated by the arrowheads. Scale bars are 40 μ m. Image taken from (DeTure and Dickson, 2019).

1.1.1.1 Neurofibrillary tangles

Neurofibrillary tangles (NFTs) are composed of paired helical filaments (PHFs) formed from two filaments of the protein Tau (Goedert and Spillantini, 2019). The morphology of NFTs can be categorised into four distinct stages detected using an anti-Tau antibody (Augustinack *et al.*, 2002); stage 0 - diffuse or fine granular staining, stage 1 - some elongated inclusions are evident, stage 2 - characterized by the classic representation of NFTs, stage 3 - extra-neuronal "ghost" NFTs, originating from neuronal death, are detected with no sign of the nucleus or stainable cytoplasm. The topographical spread of NFTs in the brain occurs in six stages (Braak *et al.*, 2006); stage 1 - NFTs appear in the entorhinal cortex proper, stage 2 - NFTs appear in the CA1 region in the hippocampus,

stage 3 - NFTs spread to the subiculum of the hippocampus, stage 4 - NFTs spread across the limbic system (amygdala, thalamus, claustrum), stage 5 – more extensive spread into the associative areas, stage 6 - NFTs appear across the primary sensory, motor and visual areas (isocortex).

1.1.1.2 Amyloid β plaques

Amyloid or ‘senile’ plaques result from the abnormal accumulation and deposition of extracellular A β -peptides and, morphologically, can be divided into diffuse and dense-cored structures (Dickson and Vickers, 2001); the former lack the β -pleated sheet conformation and do not cause neuronal death (Masliah *et al.*, 1990). Dense-cored plaques are associated with neuronal and synaptic loss (D’Andrea and Nagele, 2010). Braak and Braak (1991) proposed a 3-stage model for the spread of plaques within the brain, whereby they originate in the basal portions of the frontal, temporal and occipital lobes then spread to the isocortical association areas followed, finally, by more extensive isocortical deposition and, possibly, deposition in the cerebellum and subcortical nuclei. Notably, A β plaque load does not correlate with the extent of cognitive impairment in AD which, instead, has been arguably attributed to NFTs (Arriagada *et al.*, 1992). The neurotoxic effect of A β more likely originates from early oligomers, whereas the plaques themselves act as non-toxic ‘sinks’ of A β -peptide (Huang and Liu, 2020).

1.1.2 Disease causation

Familial AD (FAD) constitutes 5-10% of cases with the remaining cases consisting of sporadic disease with no known fully penetrative genetic causation. FAD is inherited in an autosomal dominant fashion and is caused by mutations in three genes encoding the amyloid-precursor protein (*APP*), presenilin 1 (*PSEN1*) and presenilin 2 (*PSEN2*) (Cacace, Sleegers and Van Broeckhoven, 2016). To date 358 *PSEN1* and 88 *PSEN2* pathogenic mutations have been identified along with 114 in *APP* (ALZFORUM, 2021). Genome-wide analysis has also identified the ϵ 4 allele of the apolipoprotein E gene (*APOE*) as a major genetic risk factor for late onset disease (Serrano-Pozo, Das and Hyman, 2021).

APOE has been shown to interact with A β in the cerebrospinal fluid (CSF) and the APOE type ϵ 4 (APOE4) allele is significantly associated with this function (Strittmatter *et al.*, 1993). APOE4 can form a complex with A β to promote and stabilise oligomerisation of the peptides, leading to increased risk of late onset AD (Hashimoto *et al.*, 2012). Other alleles such as the triggering receptor expressed on myeloid cells 2 (*TREM2*) gene are also associated with higher risk of developing AD (Jonsson *et al.*, 2013). However, the exact underlying cause of AD has not been fully elucidated, although key theories include the tau and amyloid cascade hypotheses.

1.1.2.1 The tau hypothesis

Tau belongs to the microtubule-associated protein (MAP) family and has a physiological role in the assembly of these structures (Pîrşcoveanu *et al.*, 2017). It is encoded by the *MAPT* gene and exists as six soluble protein isoforms produced by alternate splicing (Park, Ahn and Gallo, 2016). The different isoforms range between 352 and 441 amino acids (

Figure 1.2), and the three/four repeat regions in the C-terminal region are the core component necessary for microtubule stability and assembly (Goedert and Spillantini, 2019), whilst the N-terminal domain is proposed to determine the spacing between microtubules (Chen *et al.*, 1992). Isoform expression in the brain is dependent on developmental stage, the three C-terminal repeat isoform is found in early development and the four C-terminal repeat isoforms are dominant in the adult brain (Takuma, Arawaka and Mori, 2003). There are up to 85 serine, threonine, and tyrosine phosphorylation sites in the tau protein (Noble *et al.*, 2013) and these post translational modification influence the biological functions of the protein (Mietelska-Porowska *et al.*, 2014). Tau phosphorylation is, once again, developmentally regulated, with foetal tau generally more phosphorylated than in the adult developed brain (Kanemaru *et al.*, 1992).

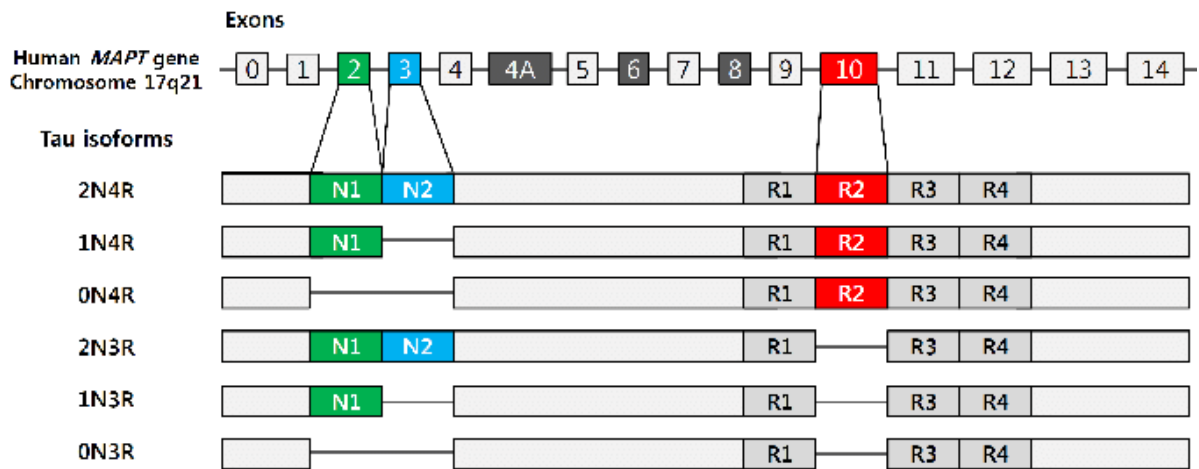


Figure 1.2: Tau protein isoforms in the human brain. Six tau isoforms are produced through alternate splicing of exons 2, 3 and/or 10 from the human *MAPT* gene. The N-terminal projection domains are encoded by exons 2 and 3, which produce N1 and N2, respectively. The C-terminal microtubule-binding domain R2 is encoded by exon 10. Depending on the presence of R2, the tau proteins are either 3R or 4R tau. Taken from (Park, Ahn and Gallo, 2016).

1.1.2.1.1 Tau pathology

Tau is phosphorylated by a number of different kinases and hyperphosphorylation reduces the ability of the microtubule-binding domain to function, disrupting the cytoskeleton of the neuron (Schneider *et al.*, 1999). Hyperphosphorylated tau can also sequester normal tau, further causing disruption (Iqbal, Gong and Liu, 2013). Hyperphosphorylated tau then accumulates in the dendritic spines (Ittner *et al.*, 2010). This disturbs calcium homeostasis and disrupts synaptic function by impairing trafficking and the anchoring of glutamate receptors (Zempel *et al.*, 2010).

Accumulated tau undergoes self-assembly into filaments, modulated by anionic cofactors, such as heparin (Pérez *et al.*, 1996). Phosphorylation of tau by certain kinases such as glycogen synthase kinase-3 (GSK-3) can enhance the formation of oligomers and filaments (Nübling *et al.*, 2012). Two filaments of tau can then match up into PHFs and form NFTs as visualized in AD pathology (Figure 1.1).

There are cellular pathways in place to degrade insoluble proteins such as tau oligomers via the autophagy-lysosomal pathway (or the ubiquitin-proteasome system) (Rubinsztein, 2006). However, these systems are overwhelmed by large tau aggregates (Guo *et al.*, 2016). Insoluble tau is transported for degradation by the endosomal-lysosomal network. This includes the retromer complex, that facilitates the transport of proteins from the endosome to the trans-Golgi network (Seaman *et al.*, 1997). The recognition core of this complex is formed by a vacuolar protein sorting (VPS) trimer of VPS35/VPS26/VPS29. VPS35 is a vital element and appears to be a risk factor for the development of AD (Small *et al.*, 2005). VPS35 haploinsufficiency causes cognitive impairments and synaptic dysfunction, as well as increased A β levels, in AD mouse models (Wen *et al.*, 2011). VPS35 downregulation has also been found in other tauopathies, and VPS35 reduction in a mouse model of tauopathy leads to an accumulation of pathological tau as well as exacerbating motor and learning impairments (Vagnozzi *et al.*, 2019).

1.1.2.2 The amyloid cascade hypothesis

The amyloid cascade hypothesis suggests that A β -peptide deposition is a primary event in the pathogenesis of AD (Hardy and Allsop, 1991). A β -peptides can range from 36-43 amino acids in length, the most common forms found in plaques being A β 40 and A β 42 (Iwatsubo *et al.*, 1994). An increase in A β production marks the trigger for the amyloid cascade, that includes oligomerisation, neuritic injury, NFT formation and neuronal dysfunction, culminating in cell death (Figure 1.3).



Figure 1.3: Amyloid cascade hypothesis flow chart. Image taken from (Haass and Selkoe, 2007).

1.1.2.2.1 Aβ-peptide toxicity

One possible mechanism of Aβ-mediated toxicity might be attributed to the ability of oligomers to form membrane channels leading to massive calcium influx, toxicity to organelles and neuronal death (Arispe, Rojas and Pollard, 1993; Canevari, Abramov and Duchon, 2004). In addition to forming Aβ channels, Aβ-peptides can interact with more than 20 types of cell-surface receptors (Mroczko *et al.*, 2018). One such receptor is the N-methyl-D-aspartate receptor (NMDAR) at the post-synapse (Alberdi *et al.*, 2010). NMDAR binding, in addition to Aβ membrane channels, results in the accumulation of intracellular calcium and mediates Aβ-peptide toxicity by causing mitochondrial dysfunction (Swerdlow,

2018). This dysfunction induces superoxide generation and increased mitochondrial permeability, resulting in neuronal death (Du *et al.*, 2008).

In addition to calcium channels, the peptides can interact with other types of receptor including the p75 neurotrophin receptor (p75NTR) leading to the signalling activation of caspase 8 and 3 and the subsequent generation of reactive oxidative species and, ultimately, cell death (Yaar *et al.*, 1997). The interaction of p75NTR with A β was later shown to induce cyclin-dependent kinase 5 (CDK5) and GSK3 β activity, which phosphorylate tau and induce tau pathology (Shen *et al.*, 2019). A β can similarly induce tau pathology by binding to the α_{2A} adrenergic receptor to activate GSK3 β activity (Zhang *et al.*, 2020).

1.1.3 Amyloid precursor protein (APP)

The *APP* gene is located on chromosome 21 and consists of 18 exons which undergo alternate splicing to form the three major isoforms ubiquitously expressed across the body; APP₇₇₀, APP₇₅₁ and APP₆₉₅ (number denotes amino acid length). APP₇₇₀ and APP₇₅₁ contain a Kunitz-type serine protease inhibitor (KPI) domain and the former also contains an OX-2 domain; both domains are absent in APP₆₉₅ (

Figure 1.4). The expression of the isoforms is tissue-specific and there is a ratio of 1:10:20 of APP 770:751:695 in the cerebral cortex; this balance is disrupted in AD where APP_{751/770} expression increases (Tanaka *et al.*, 1989).

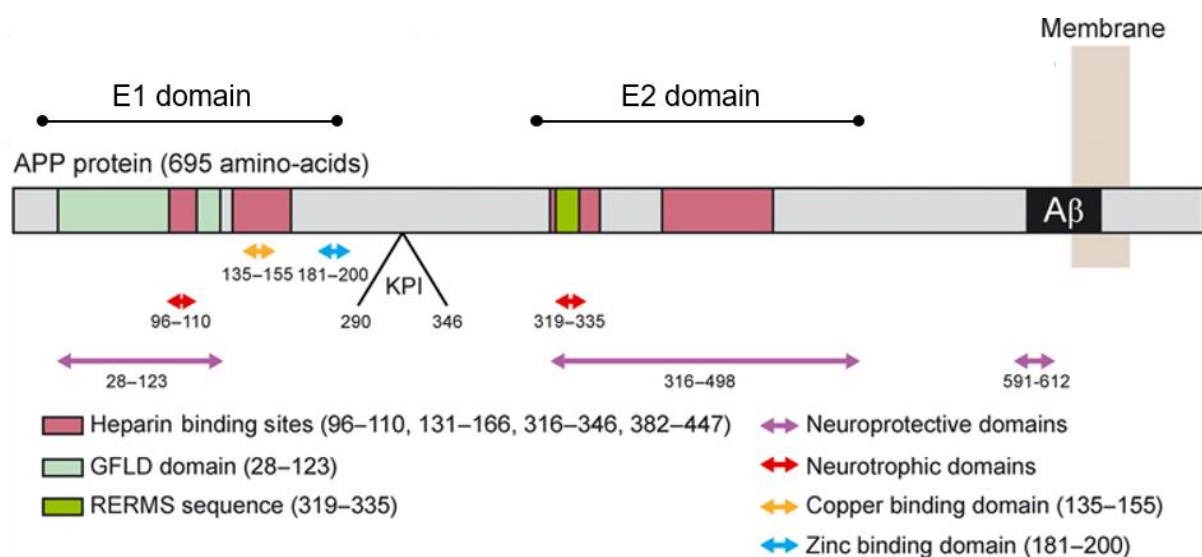


Figure 1.4: Domains and functional subdomains of APP. The heparin binding sites (HBS) are found throughout APP and serve different functions in neuroprotection and neuroproliferation. The C-terminal neuroprotective domain (591-612) is unique to the soluble APP α fragment and not present on soluble APP β . The position of the Kunitz-type serine protease inhibitor (KPI) domain is indicated. Amino-acids are numbered according to the APP₆₉₅ isoform. Adapted from (Chasseigneaux and Allinquant, 2012).

APP is a type I single-pass transmembrane protein consisting of a large extracellular N-terminal region and a shorter cytoplasmic C-terminal region. The extracellular region can be further divided into the E1 and E2 domains (

Figure 1.4). E1 contains a growth factor-like domain and a copper-binding domain (Dahms *et al.*, 2010), whilst E2 contains a high affinity heparin binding site (Wang and Ha, 2004).

Some functionality of APP is dependent on whether the monomeric form of the protein forms *cis* or *trans* dimers. *Cis* homodimers of APP are modulated by E1 or E2 dimerization when bound to heparin (Dahms *et al.*, 2010; Xue, Lee and Ha, 2011). APP can also form *trans* homodimers, which enable them to act as synaptic adhesion molecules at the neuromuscular junction (NMJ) (Wang *et al.*, 2009). The protein is also thought to be involved in several other processes including cortical development, neurite growth and synapse modification (via binding with Fe65), NMJ function, dendritic complexity, spine density and synaptic function (Herms *et al.*, 2004; Sabo *et al.*, 2003; Wang *et al.*, 2005; Tyan *et al.*, 2012; Dawson *et al.*, 1999).

1.1.4 APP proteolysis

APP can be proteolytically cleaved through a range of proteolytic pathways (Andrew *et al.*, 2016). However, the major pathways in neurons are the amyloidogenic and non-amyloidogenic pathways (Figure 1.5).

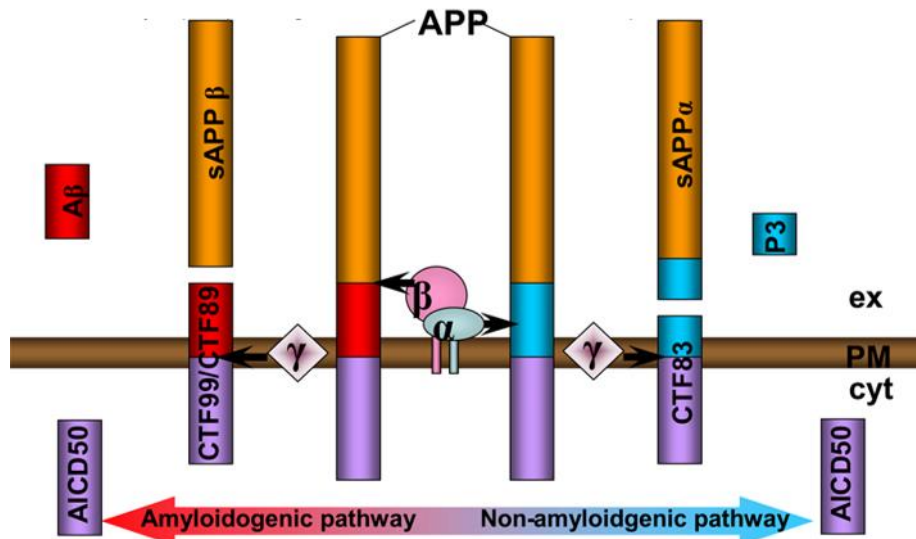


Figure 1.5: Schematic representation of the two possible pathways of amyloid precursor protein (APP) processing and their products. The non-amyloidogenic pathway is represented via the blue pathway (to the right) which involves sequential cleavage by α -secretase to release N-terminal sAPP α and C-terminal fragments 83 (CTF83), the latter is further processed by γ -secretase to yield p3 and AICD50. The amyloidogenic pathway is represented via the red pathway (to the left) and involves sequential cleavage by β -secretase to release N-terminal sAPP β and CTF99 (or CTF89 if the alternate β' site is cleaved). γ -secretase further processes CTF99/89 to produce AICD or A β . ex = extracellular space, PM = plasma membrane, cyt = cell cytosol. Schematic adapted from (Chow *et al.*, 2010).

1.1.4.1 Amyloidogenic proteolysis

Following APP transport to the plasma membrane, a fraction can be reinternalized and processed by the amyloidogenic pathway (Jiang *et al.*, 2014; Hook *et al.*, 2002). In the amyloidogenic pathway APP is sequentially cleaved by a β -secretase identified as BACE1 (beta-site APP cleaving enzyme 1) (Hussain *et al.*, 1999) and the γ -secretase complex (Hitzenberger *et al.*, 2020) (Figure 1.5). Canonical cleavage by BACE1 leads to the generation of the large N-terminal soluble fragment sAPP β and the residual membrane-bound C-terminal fragment 99 (CTF99). γ -secretase further cleaves CTF99 to form A β -peptides and the transcriptionally active APP intracellular domain (AICD). AICD functions by interacting with multiple cofactors and transcription factors (Konietzko, 2012). AICD has been shown to upregulate many different genes, some of which are involved in APP and tau processing including BACE1, neprilysin and GSK3 β (von Rotz *et al.*, 2004; Belyaev *et al.*, 2009; Kim *et al.*, 2003).

1.1.4.1.1 BACE1

BACE1 is a type I transmembrane aspartic protease expressed ubiquitously throughout the body with higher levels of expression in the pancreas and brain (Ehehalt *et al.*, 2002). The transcription of the *BACE1* gene is tightly regulated and is enhanced in response to oxidative stress conditions such as hypoxia and ischemic injury (Guglielmotto *et al.*, 2009). BACE1 is initially synthesized as a zymogen and matures along the trans-Golgi network (Bennett *et al.*, 2000) before being transported to the endosomes where it is most active (Kandalepas *et al.*, 2013).

The enzyme is monomeric and has a catalytic domain ~400 residues long, with two catalytic aspartate residues vital for enzymatic function (Ellis and Shen, 2015). One aspartate residue (Asp228) acts as a base and the other (Asp32) acts as an acid to protonate the substrate, cleaving the proteolytic bond (Toulokhonova *et al.*, 2003). Located above the catalytic site is a β -hairpin loop (also known as the flap) that controls substrate access (Shimizu *et al.*, 2008).

In addition to APP, BACE1 has many other substrates involved in synaptic plasticity and homeostasis including neurexins 1 α and 3 β (involved in synapse assembly and maintenance), neuregulin 1 (NRG1) (which regulates myelination) and amyloid beta precursor like protein 1/2 (APLP1/2) (involved in neurotransmission, synaptic function and plasticity) (Kuhn *et al.*, 2012). Knockout of BACE1 thus causes significant issues, including severe hypo-myelination of peripheral nerves and modest hypo-myelination in the central nervous system (CNS) (Hu *et al.*, 2006). Knockout can also reduce spine density in hippocampal pyramidal neurons and cause alterations to behaviour, cognition and social recognition in mice (Savonenko *et al.*, 2008).

Despite the role of BACE1 in the production of A β , there have been no reported cases of mutations in the *BACE1* coding sequence or single-nucleotide polymorphisms associated with AD (Nicolaou *et al.*, 2001; Zhou *et al.*, 2010). Despite this, BACE1 activity and expression has been shown to increase in the brains of AD patients (Holsinger *et al.*, 2002; Eehalt *et al.*, 2002). Certain mutations within the *APP* gene have been found to increase BACE1-mediated cleavage of the protein. One such mutation is the Swedish double substitution (Lys670/Met671 to Asn670/Leu671) immediately adjacent to the β -secretase cleavage site, which is associated with FAD (Perez, Squazzo and Koo, 1996). The enzymatic efficiency of BACE1 relative to Swedish mutant APP is 100-fold that of the wild-type APP substrate and leads to preferential cleavage by the enzyme rather than α -secretase and an associated increase in A β production (Yang *et al.*, 2004).

In the canonical amyloidogenic pathway, BACE1 cleaves APP between Met671 and Asp672 to release sAPP β and CTF99 (Figure 1.5). Notably, however, the enzyme can also cleave APP in a non-amyloidogenic fashion between Tyr681 and Gln682 at the 'beta prime' site, releasing sAPP β ' and leaving behind a membrane-associated CTF89 (Liu, Doms and Lee, 2002). The latter fragment can then be further processed by γ -secretase to generate A β (11-XX) lacking the first 10 amino acids compared to amyloidogenic processed A β -peptides. In transgenic flies expressing different A β peptides, A β (11-XX) was

shown to exhibit reduced neurotoxicity compared to A β 40/42 (Jonson *et al.*, 2015). The function of sAPP β ' in relation to sAPP α and sAPP β has not been explored.

1.1.4.1.2 γ -secretase

γ -secretase is a multi-subunit protein complex consisting of presenilin 1 or 2 (PS1/PS2), nicastrin (Nct), anterior pharynx-defective 1 (Aph-1) and presenilin enhancer 2 (Pen2) (Gertsik, Chiu and Li, 2014). Presenilin 1/2 contain the catalytic core of the complex and consist of nine transmembrane domains, with the catalytic aspartates located in transmembrane domains six and seven (Sato *et al.*, 2006). Presenilin 2 was identified due to its sequence homology to presenilin 1, with the highest similarity observed in the transmembrane domains (Levy-Lahad *et al.*, 1995; Rogaev *et al.*, 1995). Nct is a type I integral membrane protein with a large, heavily glycosylated ectodomain (Xie *et al.*, 2014) and has a role in substrate selectivity allowing access to the smaller C-terminal fragments generated by substrate ectodomain shedding (e.g. CTF99), but precluding larger substrates from the active site (Bolduc *et al.*, 2016). The seven transmembrane domain protein Aph-1 is involved in the scaffolding of the γ -secretase complex (Gu *et al.*, 2003) initially forming a complex with Nct to which presenilins can bind followed, lastly, by Pen2 to form the active complex (Li, Wolfe and Selkoe, 2009).

The γ -secretase complex is active both at the cell-surface, where it cleaves C83 generated by α -secretase cleavage, and in the endosomes where it tends to cleave C99 generated by prior β -secretase cleavage (Sannerud *et al.*, 2016). In fact, the enzyme complex has more than 90 known substrates including Notch, N-cadherin and E-cadherin (Güner and Lichtenthaler, 2020).

1.1.4.2 Non-amyloidogenic proteolysis

In the non-amyloidogenic pathway cleavage of APP at the cell surface by α -secretase leads to the generation of the large N-terminal soluble fragment sAPP α , as well as C-terminal fragment 83 (CTF83). γ -secretase further cleaves CTF83 into p3 and AICD (Figure 1.5).

The α -secretase-mediated ectodomain shedding of APP can be constitutive or regulated, with the latter stimulated by protein kinases (Lammich *et al.*, 1999). Members of the a disintegrin and metalloproteinase (ADAM) family of zinc metalloproteinases have been implicated in both forms of α -secretase cleavage (Allinson *et al.*, 2003). ADAM17 (TACE; tumour necrosis factor α -converting enzyme) is thought to be the key regulated α -secretase (Buxbaum *et al.*, 1998). In contrast, ADAM10 was originally identified as a constitutive α -secretase when it was shown to enhance sAPP α generation when overexpressed in human embryonic kidney (HEK) cells (Lammich *et al.*, 1999). The authors also demonstrated that a point mutation in the zinc binding site of ADAM10 specifically inhibited APP shedding. The enzyme cleaves between Lys16-Leu17 within the A β region of APP precluding intact A β -peptide production (Lammich *et al.*, 1999) and has been shown to be the key physiological α -secretase (Postina *et al.*, 2004).

ADAM9 was also originally thought to have α -secretase activity but, more recently, it has been shown to exert this role through ADAM10 (Cissé *et al.*, 2005). In fact, the former enzyme, along with ADAM15, have since been shown to shed ADAM10 from the membrane with the resultant ADAM10 CTF being subject to γ -secretase processing and transcriptionally active intracellular domain generation (Parkin and Harris, 2009; Tousseyn *et al.*, 2009).

1.1.4.2.1 ADAM10

ADAM10 is a type I transmembrane endopeptidase that is encoded by the *ADAM10* gene present on chromosome 15 (Yamazaki, Mizui and Tanaka, 1997). As with other members of the ADAM family, the structure of the ADAM10 protein consists of an N-terminal prodomain followed by metalloproteinase, disintegrin, cysteine-rich, epidermal-growth like factor, transmembrane and cytoplasmic tail domains (Seegar and Blacklow, 2019). The enzyme contains a reprotolysin-type active site (HEXGHXXGXXHD) found in the metalloproteinase domain (Cerdà-Costa and Gomis-Rüth, 2014). The three histidine residues co-ordinate a zinc ion, and the glutamate acts as the catalytic residue (Seegar *et al.*, 2017).

ADAM10 is synthesized as an inactive 798 amino acid zymogen which permits cells to spatially and temporally regulate catalytic activity of the enzyme (Anders *et al.*, 2001). During proteolytic maturation the prodomain is cleaved by the membrane-associated endoprotease furin or proprotein convertase (PC) (Moss *et al.*, 2007; Lopez-Perez *et al.*, 2001), in the trans-Golgi network or the plasma membrane.

In addition to APP, ADAM10 can cleave a range of transmembrane proteins including N-cadherin, epidermal growth factor receptor (EGFR) ligands, tumour necrosis factor- α (TNF- α), transforming growth factor- α (TGF- α), notch and ephrin (Kohutek *et al.*, 2009; Le Gall *et al.*, 2009). With so many important substrates, it is perhaps not surprising that total knockout of ADAM10 is embryonically lethal in mice causing major deficits in the development of somites and vasculogenesis (Jorissen *et al.*, 2010).

1.1.5 sAPP α

sAPP α is the main product of ADAM10 cleavage, linked to many functions in neuroprotection and proliferation (Dar and Glazner, 2020). The fragment is nearly identical to sAPP β except that it contains an additional 16 C-terminal amino acids which accounts for the neuroprotective ability unique to sAPP α , whereas sAPP β does not protect neurons against A β -dependent toxicity (Tackenberg and Nitsch, 2019). Another study also showed that the induction of long-term potentiation (LTP) by recombinant sAPP α injection was much more effective than recombinant sAPP β injection in the dentate gyrus of rats (Taylor *et al.*, 2008). In contrast to functionality residing in the C-terminal residues of sAPP, because sAPP α and sAPP β share many common domains, the fragments have similar roles in other events such axonal outgrowth and decreasing cell adhesion (Chasseigneaux *et al.*, 2011).

sAPP α appears to act as a growth factor for cells of epidermal origin and induces proliferation of embryonic and adult neural stem cells (Siemes *et al.*, 2006; Ohsawa *et al.*, 1999). In adult mice, sAPP α induces proliferation of epidermal growth factor (EGF)-responsive neuronal cells in the subventricular

zone (in the lateral ventricle) (Caillé *et al.*, 2004). It was proposed that sAPP α induced proliferation of neuronal cells in association with stimulated extracellular signal-regulated kinase (ERK) signalling and mitogen-activated protein (MAP)-kinase signalling pathways (Demars *et al.*, 2011). Neuroproliferation is facilitated by the heparin binding domain found in APP, that allows it to act as a potential ligand for growth factor receptors (Rossjohn *et al.*, 1999).

In addition to enhancing cell proliferation, sAPP α can also promote neuron survival. The fragment can regulate CDK5 expression and activity (Hartl *et al.*, 2013). CDK5 has a dual neuroprotective function, by suppressing the cell cycle in the nucleus and preventing cell death in the cytoplasm (Zhang and Herrup, 2011).

Early *in vitro* studies demonstrated that sAPP α was able to protect cultured neurons against oxygen-glucose deprivation and excitotoxicity (Mattson *et al.*, 1993; Furukawa *et al.*, 1996) by activating potassium channels to balance calcium influx and protect against glutamate toxicity.

In vivo studies have also reported that sAPP α injections into the CSF enhance learning and memory (Taylor *et al.*, 2008). The authors demonstrated that this was a consequence of increased LTP and enhanced NMDA currents.

1.1.6 Existing experimental strategies for the treatment of AD

Most AD clinical trials so far have attempted to reduce the burden of A β -peptides in the brain (Liu *et al.*, 2019b). Particular attention has been paid to the development of β - and γ -secretase inhibitors (Kumar *et al.*, 2018; Moussa-Pacha *et al.*, 2020). For example, the BACE1 inhibitor, verubecestat (MK-8931) was found to significantly reduce A β levels in the CNS of animal models and AD patients (Kennedy *et al.*, 2016). Unfortunately, the treatment led to unfavourable side effects and did not improve cognitive decline (Egan *et al.*, 2018). Targeting γ -secretase activity has yielded similarly disappointing results; initial trials with semagacestat (LY450139) reduced A β levels but phase 3 trials led to the

worsening of cognitive ability and adverse side effects (Siemers *et al.*, 2005; Doody *et al.*, 2013).

An alternative method of reducing A β -peptide levels is to enhance its clearance from the brain, which has been addressed through the use of anti-amyloid immunotherapy. For example, solanezumab, is able to bind monomeric and soluble A β , to an extent where it can reduce plasma A β levels by 90% yet, when it reached phase III trials, it failed to significantly reverse cognitive decline (Honig *et al.*, 2018). Another promising anti-A β antibody is aducanumab, which showed initial promise in a mouse model of AD (Sevigny *et al.*, 2016). However, during phase III trials Biogen cancelled the trial due to futility. Further analysis concluded that there were benefits in subgroups of patients (Knopman, Jones and Greicius, 2021). Aducanumab has since received first approval for use by the US FDA, despite the benefits being marginal and only appropriate for a minority subgroup of patients (Dhillon, 2021). In addition to aducanumab, there are other anti-amyloid antibodies that have shown success in treating early AD. This includes lecanemab (also funded by Biogen), which was part of a large phase 3 trial conducted in persons with early AD and found significant reductions in amyloid markers and moderately less decline on measures of cognition (van Dyck *et al.*, 2023). Lecanemab has since been approved by the FDA for use in early AD.

Tau has also been targeted in an attempt to develop AD therapeutics. For example, low dose leuco-methylthioninium bis(hydromethanesulphonate) (LMTM), a tau aggregation inhibitor which entered phase 3 trials, may be effective in slowing down brain atrophy in AD patients after 9 months of treatment (Wilcock *et al.*, 2018). Gene therapy to enhance proteins that reduce tau pathology may also be feasible. For example, adeno-associated virus (AAV) vector has been used as a carrier to overexpress VPS35 in a preclinical mouse AD model (Li *et al.*, 2020). The authors demonstrated that enhanced expression of the protein rescued spatial learning and working memory deficits in mice and was also seen to decrease full-length APP along with both A β ₄₀ and sAPP α production in neuroblastoma cells expressing Swedish mutant APP. Similar to aducanumab

and lecanemab, antibodies can also be raised against tau aggregates. This was used to create donanemab, where the TRAILBLAZER-ALZ 2 trial slowed clinical progression of early AD in persons which demonstrated tau pathology (Sims *et al.*, 2023). Donanemab is awaiting FDA consideration as of 2023.

1.1.7 Enhancing sAPP α as a therapeutic strategy

Despite the approval of therapeutics targeting A β -peptides and tau pathologies, their success is restricted to certain sub-populations of AD and none of them are a cure. Therefore, there is still many more avenues of therapy to be approached, in the hopes of finding a more definitive cure to AD. One such approach might come in the form of enhancing the non-amyloidogenic processing of APP thereby potentially precluding A β -peptide production and, at the same time, enhancing the production of beneficial sAPP α (see Section 1.1.5).

1.1.7.1 Enhancing ADAM10

The expression or catalytic activity of ADAM10 can be targeted at several levels (Peron *et al.*, 2018). At the transcriptional level, synthetic analogues of retinoic acid such as Am80 (Tamibarotene) can bind to retinoic acid receptors (RARs) and interact with the ADAM10 promoter to enhance transcription (Kitaoka *et al.*, 2013). The authors demonstrated that the drug increased hippocampal ADAM10 expression in aged mice and improved age-related memory deficits. In a similar vein, acitretin can interact with retinoid acid binding proteins and release RAR/ retinoid X receptor (RXR) signalling to induce ADAM10 transcription (Postina, 2012).

Fibrates have also been used to increase ADAM10 expression. Gemfibrozil, an agonist of peroxisome proliferator-activated receptor α (PPAR α), increased recruitment of co-activators to the *ADAM10* promoter and led to an increase in ADAM10 expression and sAPP α release in mouse hippocampal cells (Corbett, Gonzalez and Pahan, 2015b). PPAR α 's role is not exclusive to

ADAM10, its role in the brain is more systemic and PPAR α is involved with oxidative stress response and lipid metabolism (discussed in Wojtowicz *et al.*, 2020). The benefit of fibrates in combating AD pathology was confirmed in mice with the Swedish and *PSEN1* mutations, whereby gemfibrozil or Wy14643 (another fibrate) treatment decreased A β pathology and reversed memory deficits (Luo *et al.*, 2020). In contrast, there have also been studies showing no effect of fibrates on AD risk (Haag *et al.*, 2009). By activating PPAR α , fibrates can lead to pleiotropic effects that PPAR α is involved with. This has been used to target lipid metabolism and reduce serum low-density lipoprotein cholesterol (LDL-c), triglycerides, apolipoprotein B and increase high-density lipoprotein cholesterol (Singh and Correa, 2023). Possibly due to the systemic effects caused by fibrate treatment, it is also possible to find that fibrates can increase the risk of AD. In one large cohort study, fibrate use significantly increased the risk of decline in visual memory in women and exhibited slightly higher cases of AD (Ancelin *et al.*, 2012). Ancelin *et al.*, 2012 remarks that it was unclear if this was due to treatment resistant LDL-c, or the fibrates themselves play an active role. This association with increased risk of AD was also suggested in another study of lipid-regulating drugs (McGuinness *et al.*, 2021).

At the translational level, ADAM10 is subject to regulation via numerous microRNAs (miRNAs) including miRNA-221, the depletion of which has been shown to increase ADAM10 levels (Manzine *et al.*, 2018). It is also possible to target inhibitory elements within ADAM10 RNA; a screen of methylquinolinium derivatives identified 24 compounds that could bind to the RNA G-quadruplex inhibitory motif within the 5'-untranslated region (Dai *et al.*, 2015). These compounds up-regulated ADAM10 translation and led to significant increases in sAPP α in APP overexpressing human embryonic kidney (HEK) cells.

At the protein level, targeting the ADAM10 prodomain may also be effective. For example, AAV-mediated overexpression of furin (one of the enzymes that cleaves the prodomain) has been shown, in pre-clinical models, to enhance ADAM10 activity (Hwang *et al.*, 2006). A potential issue here is that furin

also cleaves the prodomain from other ADAMs and may, therefore, enhance the shedding of a myriad of ADAM substrates.

1.1.7.2 Gene therapy with sAPP α

One of the key drawbacks of enhancing ADAM10 activity is that the enzyme has a range of other substrates (Saftig and Lichtenthaler, 2015), many of which are involved in adverse events such as cancer invasiveness or tumour cell proliferation (Smith, Tharakan and Martin, 2020). In order to avoid these adverse effects, an alternative strategy might be to circumvent ADAM10 by employing gene therapy to directly overexpress sAPP α , although there are currently very few studies that have examined this approach. AAV has been used to overexpress sAPP α in the brain of an AD model mouse (Fol *et al.*, 2016). The sustained sAPP α overexpression was sufficient to rescue spatial reference memory (assessed via the Morris water maze), in aged AD mice with existing pathology. The authors also showed that the treatment induced recruitment of microglia with ramified morphology in the vicinity of plaques, leading to a significant reduction of soluble A β and plaques. A subsequent study tested the effect of lentivirus-mediated sAPP α overexpression before the onset of plaque pathology (Tan *et al.*, 2018). Here, the authors demonstrated an improved performance in the spatial water maze task and enhanced LTP following sAPP α therapy in AD mouse models.

1.1.8 Aims of the current project

The current project examines the role of soluble APP in Alzheimer's disease and explores experimental therapies based around the enhancement of sAPP α as potential disease therapies. Specifically, the following points will be investigated:

- Fibrate-mediated enhancement of ADAM10 expression
- Characterisation of APP proteolysis in key, AD-relevant, cell lines.

- The design of plasmid systems permitting the neuron-specific inducible co-expression of sAPP α and VPS35.

2. Materials and Methods

2.1 Materials

The generation of the wtAPP₆₉₅ (wtAPP) and BACE1 constructs in the mammalian expression vector pIREShyg (Clontech-Takara Bio Europe, Saint-Germain-en-Laye, France) has been described previously (Parkin *et al.*, 2007). SH-SY5Y human neuroblastoma cells stably expressing Swedish mutant APP₆₉₅ (SweAPP) in pIREShyg were a gift from Prof. Nigel Hooper (University of Manchester, Manchester, UK). pIREShyg-ESYN-TET3G and pRESzeo-EGFP-VPS35 constructs were synthesized by Epoch Life Science (Missouri City, Texas, USA). Mouse monoclonal anti-actin, rabbit polyclonal anti-ADAM10, rabbit polyclonal anti-APP C-terminus (APP-CT), rabbit polyclonal anti-BACE1 and mouse monoclonal anti-APP N-terminus (22C11) antibodies were purchased from Merck Life Science (Gillingham, UK). Mouse monoclonal anti-APP (6E10) and rabbit polyclonal anti-sAPP β antibodies were from Biolegend (San Diego, USA). Mouse monoclonal anti-APP β sw (6A1) antibody was from IBL America (Minneapolis, USA). Mouse monoclonal TetR antibody was from Takara (Saint-Germain-en-Laye, France). All restriction enzymes were from New England Biolabs (Hitchin, UK) unless stated otherwise. All other reagents were from Merck Life Science (Gillingham, UK) unless stated otherwise.

2.2 Methods

2.2.1 Cell culture

All cell culture reagents were purchased from Lonza Ltd. (Basel, Switzerland). SH-SY5Y cells and human embryonic kidney (HEK) 293 cells were cultured in Dulbecco's modified Eagle medium (DMEM) supplemented with 25 mM glucose, 4 mM L-glutamine, 10% (v/v) foetal bovine serum, penicillin (50 U/ml) and streptomycin (50 μ g/ml). All cells were maintained at 37°C and 5% (v/v) CO₂. Cultures were split when the cells reached confluency by removing the growth medium and rinsing cells *in situ* with 1.5 ml trypsin (trypsin EDTA 200 mg/L, 170,000 U trypsin/L), before adding 1.5 ml of fresh trypsin and incubating at 37°C for 5 min (to detach the cells). Once detached, 20 ml of growth medium

was added to neutralise the trypsin and the suspension was centrifuged at 1000 rpm for 5 min in an Allegra X-22R centrifuge (Beckman Coulter, California USA). The cells were then reseeded into new flasks at the required density.

2.2.2 Freezing and resurrecting cell lines

Once a flask reached confluency, the cells were trypsinized as described in the preceding section and the cell pellet was resuspended in 1.5 ml of 10% (v/v) dimethyl sulphoxide (DMSO) in complete growth medium. The suspension was then transferred into a cryovial and frozen at -80°C for 24 hours before transferring into liquid nitrogen. To resurrect cells, the cryovials were thawed at 37°C and the cell suspension immediately transferred into a Falcon tube containing 20 ml pre-warmed growth medium (37°C) before centrifuging at 1000 rpm (Allegra X-22R centrifuge) for 5 min. The supernatant was removed, and the pellet resuspended in 2 ml of growth medium before transferring 1 ml of this to flasks containing 10 ml of complete growth medium.

2.2.3 Cell treatments

Cells were grown to confluence in complete growth medium and then washed with 10 ml UltraMEM™ reduced serum medium before culturing for a further 24 hrs in a fresh 10 ml of the same medium containing the relevant drug treatments. Batimastat (Merck Life Science, Gillingham, UK) and β -secretase inhibitor IV (Tocris Bioscience, Bristol, UK) were prepared as concentrated stocks (10 μ M) in DMSO and added to the UltraMEM™ on cultures to achieve a final concentration of 5 μ M. The fibrates gemfibrozil and bezafibrate (Sigma, Poole, UK) were also prepared as concentrated stocks (1 to 100 μ M) in DMSO and added to UltraMEM™ to create a range of different concentrations (1 μ M, 10 μ M, 25 μ M, 50 μ M and 100 μ M). The relevant volumes of DMSO carrier were incorporated into the medium of control cultures.

2.2.4 A β -peptide quantification

A β -peptides in unconcentrated conditioned medium were quantified using the Mesoscale Discovery (MSD) platform. The MSD platform uses electrochemiluminescent labels conjugated to detection antibodies rather than a standard ELISA, with the addition of electricity this light emission that can be accurately quantified. The A β 40 and A β 42 levels were measured using the V-Plex A β peptide panel (6E10) kit according to the manufacturer's instructions (MSD, Maryland, USA). Within the MSD 96-well plate there are 4 discrete spots in each well, three of the spots are coated with A β 38, A β 40 and A β 42 specific antibodies. When the sample is added each specific A β peptide is captured by its respective antibody and allows for simultaneous detection and quantification.

2.2.5 Cell viability assays

For trypan blue assays, cells were seeded at a density of $2 \times 10^4/\text{cm}^2$. At set time points, the cells were trypsinized (see Section 2.2.1) and resuspended in filter-sterilized phosphate-buffered saline (PBS; 0.15 M NaCl, 20 mM Na₂HPO₄, 2 mM NaH₂PO₄, pH 7.4). Cell resuspensions (20 μ l) were mixed with an equal volume of 0.4% (w/v) trypan blue solution (Merck Life Science, Gillingham, UK) and loaded onto a haemocytometer (Merck Life Science, Gillingham, UK). The average cell count across four quarters of squares (6.25 nL per square) was scaled up to determine the total number of cells in each starting flask.

For the methanethiosulfonate (MTS) viability assay, cells were seeded at a density of $9.38 \times 10^4/\text{cm}^2$ in 96-well plates. At set time points, the cells were incubated with CellTiter 96® Aqueous One Cell Proliferation Assay solution (Promega, Wisconsin, USA) for 35 min at 37°C. The absorbance at 490 nm was measured using a Victor² 1420 multilabel counter microplate reader (Lab Merchant Ltd, London, UK).

2.2.6 Agarose gel electrophoresis

0.7% (w/v) agarose gels were made by adding agarose to tris-acetate-EDTA (TAE) buffer (diluted from a 50 X TAE stock; 242 g Tris, 57.1 ml acetic acid, 100 ml 0.5 M EDTA (pH 8.0), made up to 1 litre with distilled H₂O). Syber safe (1 µl) (Thermo Scientific, Massachusetts, USA) was added and the gel (5 ml) was left to set at room temperature. Samples were prepared by mixing 6 X loading buffer (New England Biolabs, Hitchin, UK) with each sample (1:5 (v/v), loading buffer: sample). Following sample loading, gels were run at 100 V until the dye had reached about halfway down the gel. The finished gels were then visualised on the Chemidoc (BioDoc-IT Transilluminator) or on a blue light box (see Section 2.2.7).

2.2.7 DNA fragment gel extraction

When extracting DNA from gels, bands were visualised and dissected on a blue light box, to protect the DNA from UV damage. The DNA was then purified using the Qiagen gel extraction kit (Hilden, Germany) according to manufacturer's instructions with some adjustments in that the same fragments from multiple agarose gel were purified in the same column to maximise concentration, and, in the final step, 30 µl of filter-sterilized distilled H₂O was added to each column and allowed to stand for 4 min before the final (elution) spin.

2.2.8 Polymerase chain reaction (PCR)

All primers (**Table 2.1**) were reconstituted in filter-sterilized distilled H₂O to a concentration of 100 µM (a 10 X stock relative to the concentration added to PCR reactions). PCR reactions consisted of 12.5 µl Q5 high-fidelity 2 X master mix (New England Biolabs, Hitchin, UK), 1.25 µl each of diluted forward and reverse primer stocks (10 µM), 1 µl of DNA (0.5 ng), made up to 25 µl with nuclease free water. The thermocycler reaction conditions were as follows; heated lid 105°C, preheat lid off, pause off, initial denaturation of 98°C for 30 s, hot start off. After initial denaturation the following conditions were run for 30

cycles: 98°C for 10 s, melting temperature and extension time dependent on primers (**Table 2.1**), and 72°C for 20 s. The final extension was at 72°C for 2 min and samples were then held at 4°C. The PCR reaction was then purified using a Qiagen PCR purification kit (Hilden, Germany) according to the manufacturer's instructions.

Table 2.1: Primer design and usage

Primer Name	Sequence	Fwd/Rev	Use	Melting temperature (°C)	Extension time (seconds)
A	5'-AGCTAGATATCGCCACCATGCTGCCCGGTTTGG -3'	F	Amplification of sAPP α for insertion into pIRESneo	66	20
B	5'-ATAGCGCGGCCGCCTATTTTTGATGATGAACTTCATATCCTGAG-3'	R		65.7	20
C	5'-ACGTAGCGGCCGCTAGTATCCTGAGTCATGTCGGAATTCTG-3'	R	Paired with primer A for amplification of sAPP β ' for insertion into pIRESneo	67	20
D	5'-CGGCACCTTAAGCGTTACATAACTTACGGTAAATGG-3'	F	Amplification of the CMV promoter for insertion into the regulator plasmid pRESHyg-CMV-TET3G	63	15
E	5'-GCCCAGTTAATTAAGAGCTCTGCTTATATAGACCTCC-3'	R		65	15
F	5'-AGCTTTGTTTAAACGCCACCATGCTGCCCGGTTTGG-3'	F	Amplification of sAPP α for insertion into MCS1 of the response plasmid pRESzeo-sAPP α -VPS35	66	30
G	5'-GTCACCGGTCTATTTTTGATGATGAACTTCATATCCTGAG-3'	R		65.7	30
H	5'-TAACTAGTGCCACCATGCTGCCCGGTTTGG-3'	F	Amplification of sAPP α for insertion into MCS2 of the response plasmid pRESzeo-VPS35-sAPP α	66	30

Primer Name	Sequence	Fwd/Rev	Use	Melting temperature (°C)	Extension time (seconds)
I	5'- ATCGTTAGCTACGTACTATTTTTGATGATGAACTTCATATCCTGAG- 3'	R		65.7	30
J	5'-AGCTTTGTTTAAACGCCACCATGCCTACAACAC-3'	F	Amplification of VPS35 for insertion into MCS1 of the response plasmid pIRESzeo-VPS35-sAPP α	64.1	30
K	5'-GTCACCGGTTTAAAGGATGAGACCTTCATAAATTGG-3'	R		64.8	30

2.2.9 Restriction digest

Digests for 1 µg of DNA were set up with 1 µl of restriction enzyme, 5 µl of 10 X digestion buffer (as recommended for the cognate restriction enzyme by New England Biolabs, Hitchin, UK), made up to 50 µl with filter-sterilised distilled H₂O. Digests were incubated at 37°C (unless otherwise recommended) for 1 h (or overnight for PCR fragment digests).

2.2.10 Ligation

Digested plasmids and PCR inserts were visualized on agarose gels and relative concentrations estimated. Reactions consisted of 2 µl of 10 X T4 DNA ligase buffer, 1 µl of T4 ligase (Thermo Scientific, Massachusetts, USA) (diluted 1:5 with nuclease free water to give a final reaction quantity of 1 unit of ligase), plasmid and PCR insert (ratio 1:6 (v/v), plasmid: insert), made up to 20 µl with nuclease free water. The reaction was incubated at 22°C for 10 min before being terminated (and ligase inactivated) by heating at 65°C before bacterial transformation (Section 2.2.11).

2.2.11 Bacterial transformation

For the bulking up of plasmids, β-mercaptoethanol (0.3 µl) was added to 20 µl of XL1-blue competent cells (Agilent, Santa Clara, USA) followed by a 10 min incubation on ice (with gentle swirling every 2 min). Plasmid DNA (0.1 µg) was added to the mixture followed by a further incubation for 15 min on ice. The mixture was heat shocked at 42°C for 45 s, cooled on ice for 2 min, before the entire solution was plated on a pre-warmed LB agar plate.

For transformation of ligation products, XL1-blue supercompetent cells (Agilent, Santa Clara, California, USA) (20 µl) were incubated with 0.34 µl β-mercaptoethanol for 10 min on ice (with gentle swirling every 2 min). Inactivated ligation reaction (3 µl) was then added to the supercompetent cells and they were further incubated on ice for 30 min. The mixture was then heat shocked at 42°C for 45 s, cooled on ice for 2 min, and 0.9 ml of pre-warmed (37°C) LB media was

added. This solution was incubated for 1 h at 37°C with shaking at 250 rpm. After incubation, the cells were pelleted by centrifugation at 2000 rpm in a Spectrafuge 16M, SI50 microfuge for 10 min. The majority of the supernatant (800 µl) was removed and the pellet was resuspended in the remaining 100 µl of liquid before plating on a pre-warmed LB agar plate.

2.2.12 Bacterial cultures

For agar plate culture preparation, 7.5 g of agar was added to 500 ml of liquid broth (LB) (10 g bacto-tryptone, 5 g bacto-yeast extract, 5 g NaCl, made up to 1 litre with distilled H₂O, p H 7.5) and autoclaved. The LB agar was then cooled at 45°C for 1 h before 500 µl of 100 mg/ml filter-sterilized ampicillin was added. The plates were poured by an open flame and allowed to set for 10 min at room temperature before storage at 4°C (whilst inverted).

For mini-suspension cultures, transformant colonies were stabbed and suspended in 3 ml LB containing 3 µl of 100 mg/ml filter-sterilized ampicillin.

To propagate midi-cultures, 500 µl of mini-culture was seeded into 50 ml of LB containing 50 µl of 100 mg/ml filter-sterilized ampicillin. Both types of cultures were grown overnight on an SI-600R orbital incubator at 37°C and 250 rpm.

2.2.13 Plasmid DNA preparation

Plasmid DNA was purified using Qiagen mini- or midi-prep kits (Hilden, Germany) according to the manufacturer's instructions.

2.2.14 Stable and transient transfections of mammalian cells

For stable transfections, 20-30 µg of plasmid was linearized overnight (with AhdI) (see Section 2.2.9). A 1/10 volume of filter-sterilized 3 M sodium acetate (pH 5.2) and 2 volumes of cold absolute ethanol were added to the 50 µl of linearized plasmid. The sample was then centrifuged in a bench top microfuge in a cold room at top speed for 20 min before removing and discarding the

supernatant. Ice cold 80% (v/v) ethanol (300 μ l) was then added to the pellet without resuspending it and the sample was centrifuged at top speed for 5 min as previously described. The supernatant was then removed in a laminar flow hood and the DNA pellet was resuspended in 30 μ l of filter-sterilized distilled H₂O by repeated pipetting.

For stable transfection, cells were grown to 80% confluency, trypsinised and pelleted as previously described (Section 2.2.1). Following resuspension in 0.8 ml of complete growth medium, the cells were transferred into a 2 mm electroporation cuvette, with the DNA, and electroporated using a Biolegend ECM 630 electroporator (square wave, 120V, 25 ms, 2 mm path width). The cells were then transferred from the cuvette into 5 ml of growth medium and resuspended by repeated pipetting before transferring into a fresh 10 ml of complete culture medium in a culture flask. The following morning, the medium was replaced with a fresh 10 ml of the same growth medium. When the cells reached 60% confluence selection with the relevant antibiotic was commenced. For cells transfected with neomycin resistance plasmid a 1 g / 10 ml solution of G418 sulphate (neomycin) in distilled H₂O was prepared and filter-sterilized; 50 μ l of this stock was added to 10 ml of the selection medium. For hygromycin resistance plasmids, 30 μ l of a 50 mg/ml commercial antibiotic stock (Invitrogen, Paisley, UK) was added to 10 ml of selection medium. Selected cells were grown to confluence and passaged for a further time in the presence of antibiotic before freezing or using for experiments.

For the stable transfection of HEK cells, the cells were grown to 60% confluence and linearized DNA (20-30 μ g) was transfected using the Turbofect transient transfection procedure described below. When the cells reached 60% confluence selection was performed as described above.

For transient transfection of both SH-SY5Y and HEK cells, 7.5 μ g of plasmid was used. Cells were grown to 80% confluence before removing and replacing the complete growth medium. The plasmids (7.5 μ g) were diluted in UltraMEM™ (750 μ l including plasmid) and the turbofect reagent (60 μ l) was

added to the plasmid solution and incubated at room temperature for 20 min. The plasmid:turbfect solution was then added dropwise to the cells for transfection. The health of the cells was checked after 24 hrs, then after 48 hrs the cells were harvested for preparation.

2.2.15 Preparation of conditioned medium samples

Following drug treatments or transfections, the conditioned UltraMEM™ medium was centrifuged at 3000 rpm in a Hettich Rotanta 460R centrifuge (Hettich, Tuttlingen, Germany) for 5 min at 4°C to pellet cell debris. The supernatant (8 ml) was concentrated 32-fold to a volume of 250 µl using Amicon Ultra-4 centrifugal filters (10 kDa molecular weight cut off) (Merck Millipore, Darmstadt, Germany).

2.2.16 Harvesting cells and preparation of cell lysates

After the conditioned medium was removed, cells were rinsed *in situ* with 10 ml PBS. The cells were then scraped into a fresh 10 ml of PBS and transferred into a Falcon tube. Residual cells were washed from the culture flask with another 10 ml PBS and added to the existing Falcon tube. Cells were pelleted by centrifugation at 1000 rpm for 10 min at 4°C and the supernatant was discarded. Cell pellets were resuspended in 1.5 ml of lysis buffer (50 mM Tris, 150 mM NaCl, 1% (v/v) IGEPAL, 0.1% (v/v) sodium deoxycholate, 5 mM EDTA, pH 7.4) containing 1% (v/v) protease inhibitor cocktail (Merck Life Science, Gillingham, UK).

Resuspended cells were sonicated at half power for 30 s in a probe sonicator (MSE, Crawley, UK) and the insoluble material was pelleted by centrifugation at 11,600 g for 10 min. The lysate supernatants were then assayed for protein concentration (Section 2.2.17) and samples were equalized in terms of protein content through the addition of lysis buffer before aliquoting and storing at -80°C.

2.2.17 Bicinchoninic acid (BCA) protein assay

Bovine serum albumin (BSA) protein standards of 0, 0.2, 0.4, 0.8 and 1 mg/ml in distilled H₂O were prepared and 10 µl of each standard was placed in duplicate into the wells of a 96 well microtitre plate. Lysate samples (5 µl) were pipetted in duplicate into the same plate and working reagent (200 µl) consisting of a 50:1 (v/v) ratio of BCA protein assay reagent (Pierce, Illinois, USA): 4% (w/v) CuSO₄.5H₂O was added to each well (standards and samples).

The wells were mixed briefly by tapping the plate and the samples were incubated for 30 min at 37°C. Absorbance at 570 nm was then measured using a Victor² 1420 multilabel counter microplate reader (Lab Merchant Ltd, London, UK). The average absorbance reading for each of the standard duplicates was plotted against protein concentration to produce a standard line and associated regression equation from which the protein concentrations of the lysate samples were calculated.

2.2.18 Sodium dodecyl sulphate polyacrylamide gel electrophoresis (SDS-PAGE)

Proteins were resolved on 5-20% or 7-17% gradient gels. Resolving gel solutions were prepared as described in **Table 2.2** and the gels were poured using a gradient mixer. Isopropanol was layered on top of the setting gel to exclude oxygen and facilitate polymerisation and gels were allowed to set for 30 min.

Table 2.2: Resolving gel compositions

Resolving gel concentration				
	20%	17%	7%	5%
Sucrose	0.37 g	0.37 g	N/A	N/A
1M Tris, pH 8.8	N/A	1.39 ml	1.39 ml	1.39 ml
1.5M Tris, pH 8.8	0.93 ml	N/A	N/A	N/A

Resolving gel concentration				
	20%	17%	7%	5%
30% acrylamide, 0.8% Bis	2.5 ml	2.1 ml	0.88 ml	0.63 ml
Distilled H ₂ O	N/A	N/A	1.36 ml	1.64 ml
1.5% (w/v) ammonium persulphate	0.22 ml	0.22 ml	0.1 ml	71 µl
10% (w/v) SDS	37 µl	37 µl	37 µl	37 µl
TEMED (tetramethylethylenediamine)	3 µl	3 µl	3 µl	3 µl

Table 2.3: Stacking gel composition

1M Tris, pH 6.8	1.39 ml
30% acrylamide, 0.8% Bis	0.63 ml
Distilled H ₂ O	1.64 ml
1.5% (w/v) ammonium persulphate	71 µl
10% (w/v) SDS	37 µl
TEMED	3 µl

After setting, the isopropanol was decanted off, a comb was positioned, and the stacking gel (Table 2.3) was layered on top of the resolving gel.

The protein samples for analysis were mixed with dissociation buffer (3.5 ml 1 M Tris/HCl, pH 6.8, 2.5 g SDS, 0.3085 g dithiothreitol (DTT), 5 ml glycerol, made up to 25 ml with d.H₂O, with 0.5 % (w/v) bromophenol blue added dropwise until desired colour) in a ratio of 2:1 (v/v) (sample: buffer) and heated at 90°C for 3 min on a heating block. The molecular weight standards (GE Healthcare, Buckinghamshire, UK) were prepared in the same way.

Samples and standards (30 µl) were loaded onto the gels and proteins resolved at 70 mA (per pair of gels) in Tris/glycine/SDS running buffer (Geneflow Ltd. Bradley, UK) until the dye front reached the base of the gel.

2.2.19 Tris-Tricine gel electrophoresis

For the detection of APP C-terminal fragments, tris-tricine gels were employed. Gels were poured as described in the preceding section but using the resolving and stacking gel compositions described in **Table 2.4** and **Table 2.5**, respectively. After setting and before use, the gels were transferred to a cold room for 1 h at 4°C to equilibrate.

Table 2.4: Tris-tricine resolving gel composition

2.5M Tris-HCl, pH 8.8	12.99 ml
30% acrylamide, 0.8% Bis	15.99 ml
Distilled H ₂ O	402 µl
10% (w/v) ammonium persulphate)	300 µl
10% (w/v) SDS	300 µl
TEMED	18 µl

Table 2.5: Tris-tricine stacking gel composition

2.5M Tris-HCl, pH 8.8	3.04 ml
30% acrylamide, 0.8% Bis	2.64 ml
Distilled H ₂ O	13.52 ml
10% (w/v) ammonium persulphate)	200 µl
10% (w/v) SDS	600 µl
TEMED	20 µl

Protein samples were mixed (2:1, sample: buffer) with dissociation buffer (200 mM Tris-HCl pH 6.8, 2% (w/v) SDS, 40% (v/v) glycerol, 0.193 g DTT, made up to 25 ml with d.H₂O, with 0.4 % (w/v) bromophenol blue added dropwise until desired colour) and heated at 90°C for 3 min on a heating block. The molecular weight standard (Spectra™ Multicolor Low Range Protein Ladder, Thermo Scientific, Massachusetts, USA) was added directly to the loading well. Following

sample loading, gels were run at 200 V in running buffer (250 mM tris, 250 mM tricine and 0.5% (w/v) SDS diluted 1:10 with distilled H₂O) until the dye front reached the base of the gel.

2.2.20 Immunoblotting

For standard SDS-PAGE gels, proteins were transferred from gels to Immobilon P polyvinylidene difluoride (PDVF) membranes (Millipore, Massachusetts, USA). Prior to transfer, the membranes were equilibrated by submerging in methanol for 10 s, distilled H₂O for 2 min and then Towbin transfer buffer (20 mM Tris, 150 mM glycine, 800 ml methanol made up to 4 L with distilled H₂O) for at least 20 min. Gels were also equilibrated for no more than 5 min in Towbin buffer before assembling the transfer sandwiches in a wet blot kit (GE Healthcare, Buckinghamshire, UK) and transferring proteins at 115 V for 1 h. Following transfer, the membranes were rinsed for 5 min in room temperature PBS.

For tris-tricine gels, proteins were transferred to 0.2 µm nitrocellulose membrane (Fisher Scientific, Loughborough, UK). The membranes were equilibrated in modified Towbin transfer buffer (25 mM tris, 192 mM glycine, 800 ml methanol made up to 4 L with distilled H₂O) for at least 20 min prior to transfer. Gels were also equilibrated for no more than 5 min in modified Towbin buffer before assembling transfer sandwiches in a wet blot kit (GE Healthcare, Buckinghamshire, UK) and transferring proteins at 90 V for 1 h. After transfer, membranes were incubated in boiling PBS for 5 min.

For both standard SDS-PAGE and tris-tricine gels, membranes were blocked by incubating them for 1 h at room temperature in 5 % (w/v) marvel in 0.1 % (v/v) Tween-20 (PBS-Tween). After blocking, membranes were rinsed in PBS-tween for 5 min before the addition of the primary antibody (**Table 2.6**) diluted in 2% (w/v) BSA in PBS-tween, followed by overnight incubation at 4°C on a Stuart™ roller mixer (Merck Life Science, Gillingham, UK).

The following morning, membranes were washed in PBS-tween for 1 x 1 min and 2 x 15 min. The secondary antibody (Table 2.6), diluted in 2% (w/v) BSA in PBS-tween (1:4000, antibody: BSA in PBS-tween), was then added and the membranes were incubated for 1 h at room temperature. Membranes were then washed in PBS (1 x 1 min and 2 x 15 min).

For the detection of proteins, membranes were incubated in enhanced chemiluminescence reagent (ECL) (Fisher Scientific, Loughborough, UK) for 2 min with constant shaking. Following sandwiching between sheets of acetate, membranes were exposed to X-ray film (CL-X Posure™ film, Fisher Scientific, Rockford, USA), which was then manually developed.

Table 2.6: Primary and secondary antibody dilutions

Protein	Primary antibody dilution	Secondary antibody (1:4000)
Actin	1:5000	Rabbit anti-mouse
BACE1	1:5000	Goat anti-rabbit
ADAM10	1:1000	Goat anti-rabbit
APP-CTF	1:5000	Goat anti-rabbit
APP (22c11)	1:4000	Rabbit anti-mouse
sAPP α (6e10)	1:5000	Rabbit anti-mouse
sAPP β	1:5000	Goat anti-rabbit
sAPP β sw (6A1)	1:5000	Rabbit anti-mouse
TetR	1:1000	Rabbit anti-mouse

For the quantification of immunoblots, x-ray films were scanned at 600 dpi and saved as pdf files before being converted to tiff and imported into ImageJ for densitometric analysis. For the majority of the bar graphs, the results were normalised to the control and so there was no error bars on the control result. This was to account for the fact that the western blot repetitions were not run on

the same blot at the same time, due to limited space on the gel (and to control external influences).

2.2.21 Amido black staining

PVDF/nitrocellulose immunoblotting membranes were submerged in amido black stain (0.1% (w/v) amido black, 1% (v/v) acetic acid, 40% (v/v) methanol) for 30 s before a brief rinse with tap water to remove excess stain from the membrane. Membranes were then dried on filter paper.

2.2.22 Statistical analysis

Statistical analysis was conducted using analysis of variance (ANOVA) and results are presented as means \pm standard deviation (S.D). All ANOVA analyses were followed by Tukey *post-hoc* analysis. RStudio was used for all statistical analysis.

3. Results; Fibrates do not enhance sAPP α generation in Swedish mutant APP SH-SY5Y cells

3.1 Introduction

Underlying the current thesis is the possibility that enhancing sAPP α may represent a possible therapy for Alzheimer's disease (AD). Fibrates act as an agonist for peroxisome proliferator-activated receptor alpha (PPAR- α) which regulates gene expression and has been implicated in APP metabolism and AD pathology (Wójtowicz *et al.*, 2020). For example, the fibrate GW7647 has previously been shown to reduce sAPP β and A β levels in SweAPP-transfected SH-SY5Y cells but not in their Mock-transfected counterparts (Zhang *et al.*, 2015). Although alternative mechanisms have been postulated Corbett *et al.* (2015) demonstrated that another fibrate, gemfibrozil, stimulated ADAM10 expression thereby enhancing sAPP α release from mouse hippocampal neurons.

In the current study we sought to examine whether gemfibrozil enhanced the non-amyloidogenic pathway in SweAPP-transfected SH-SY5Y cells and, furthermore, we examined the effects of another fibrate, bezafibrate, that hasn't previously been linked to APP metabolism.

3.2 Lack of effect of gemfibrozil on ADAM10 expression and APP processing in Swedish mutant APP SH-SY5Y cells

In order to examine APP expression and proteolysis we grew SH-SY5Y-SweAPP cells to confluence and incubated the cells in reduced serum medium in the absence or presence of increasing concentrations of gemfibrozil (1, 10, 25, 50 or 100 μ M) for 24 h. Cells were then harvested and the lysates and conditioned medium prepared (see Materials and Methods).

Cell lysates were initially immunoblotted with the anti-APP C-terminal (APP-CT) antibody to determine APP holoprotein levels. The results (Figure 3.1A) revealed no significant effect of any gemfibrozil concentration on full-length (FL-APP) expression. Equal protein concentrations were confirmed by immunoblotting with anti-actin antibody (Figure 3.1B). The same cell lysates were also immunoblotted with anti-ADAM10 antibody and the results (Figure 3.1C)

also showed that gemfibrozil had no significant effect on the expression or maturation of the protein.

Next, we examined the effects of gemfibrozil on the secretion of APP proteolytic fragments into the conditioned medium of SweAPP-SH-SY5Y cells. Initially, equal volumes of conditioned medium were immunoblotted with anti-APP 6E10 antibody to examine the non-amyloidogenic shedding of sAPP. The results (Figure 3.2A) showed no significant effect of gemfibrozil on sAPP release. The same conditioned medium samples were then immunoblotted with anti-sAPP β Swe 6A1 antibody as the normal anti-sAPP β antibody would not detect sAPP β generated from Swedish mutant APP holoprotein due to the double substitution mutation immediately N-terminal to the BACE1 cleavage site. The resultant blots (Figure 3.2B) showed no significant effect of gemfibrozil on sAPP β ₆₉₅ release.

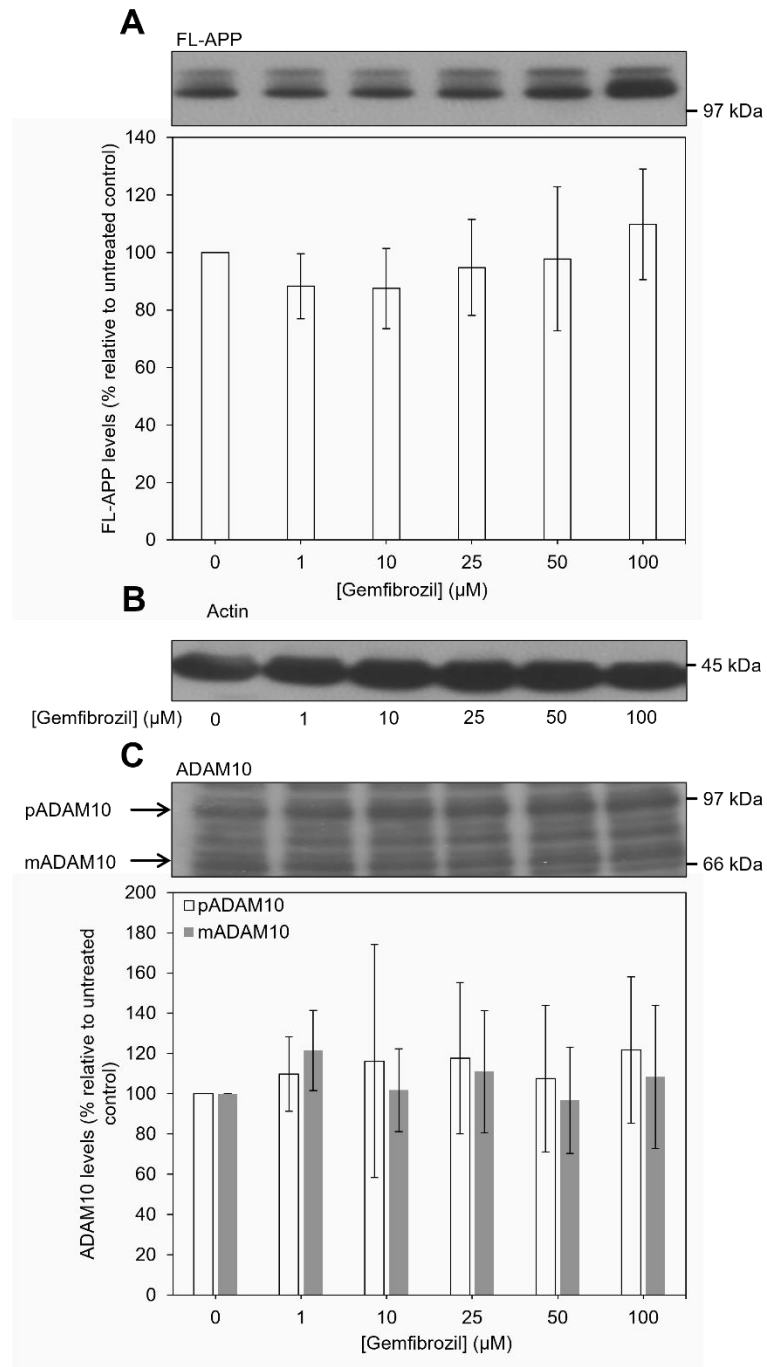


Figure 3.1: Lack of effect of gemfibrozil on APP and ADAM10 expression in SH-SY5Y-SweAPP cells. SweAPP-transfected SH-SY5Y cells were grown to confluence and incubated for 24 h in the absence or presence of increasing concentrations of gemfibrozil (1, 10, 25, 50 and 100 μM). Cells were harvested, lysates prepared and equal amounts of proteins were resolved by SDS-PAGE and immunoblotted (see Materials and Methods). **(A)** Anti-APP (APP-CT) immunoblot. **(B)** Anti-actin immunoblot. **(C)** Anti-ADAM10 immunoblot. Multiple immunoblots were subjected to densitometric quantification and the results expressed relative to the untreated controls; pADAM10, prodomain ADAM10; mADAM10, mature ADAM10. All results are means \pm S.D. (n=3).

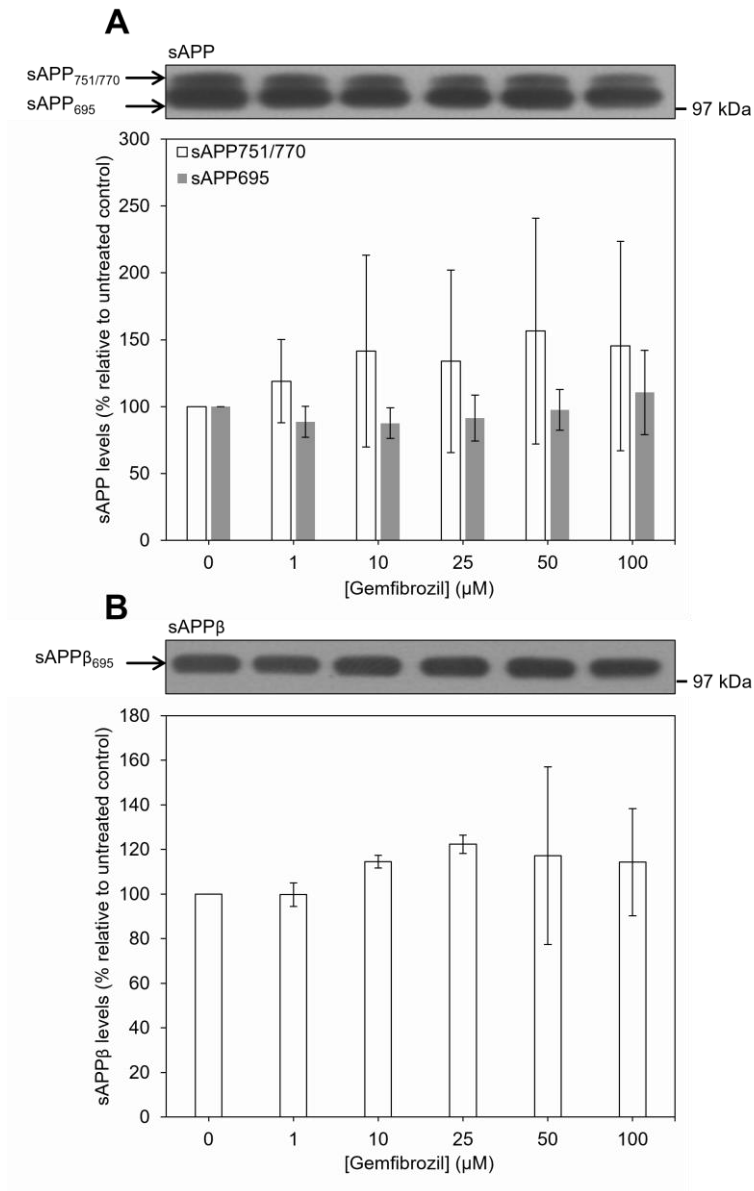


Figure 3.2: Lack of effect of gemfibrozil on soluble APP generation by SH-SY5Y-SweAPP cells. SweAPP-transfected SH-SY5Y cells were grown to confluence and incubated for 24 h in the absence or presence of increasing concentrations of gemfibrozil (1, 10, 25, 50 and 100 μM). Cells were harvested, medium conditioned and equal volumes of samples were resolved by SDS-PAGE and immunoblotted (see Materials and Methods). **(A)** Anti-APP 6E10 immunoblot. **(B)** Anti-sAPPβSwe 6A1 immunoblot. Multiple immunoblots were subjected to densitometric quantification and the results expressed relative to untreated control. All results are means ± S.D. (n=3).

3.3 Lack of effect of bezafibrate on ADAM10 expression and APP processing in Swedish mutant APP SH-SY5Y cells

As gemfibrozil showed no effect on APP expression/proteolysis in SH-SY5Y-SweAPP cells we examined the effects of a second fibrate, bezafibrate, in this respect. As such, we once again grew SH-SY5Y-SweAPP cells to confluence and incubated the cells in reduced serum medium for 24 h in the absence or presence of increasing concentrations of bezafibrate (1, 10, 25, 50 or 100 μ M). The cells were then harvested and the lysates and conditioned medium prepared as described in the Materials and Methods section.

Cell lysates were initially immunoblotted with anti-APP C-terminal (APP-CT) antibody in order to monitor any effects of the fibrate on APP holoprotein levels. The results (Figure 3.3A) demonstrated no effect of bezafibrate on FL-APP levels at any concentration. Equal protein loading was confirmed by immunoblotting with anti-actin antibody (Figure 3.3B). The same cell lysate samples were then also immunoblotted with the anti-ADAM10 antibody and the results (Figure 3.3C) also showed no significant changes in the immature or mature forms of ADAM10 following bezafibrate treatment.

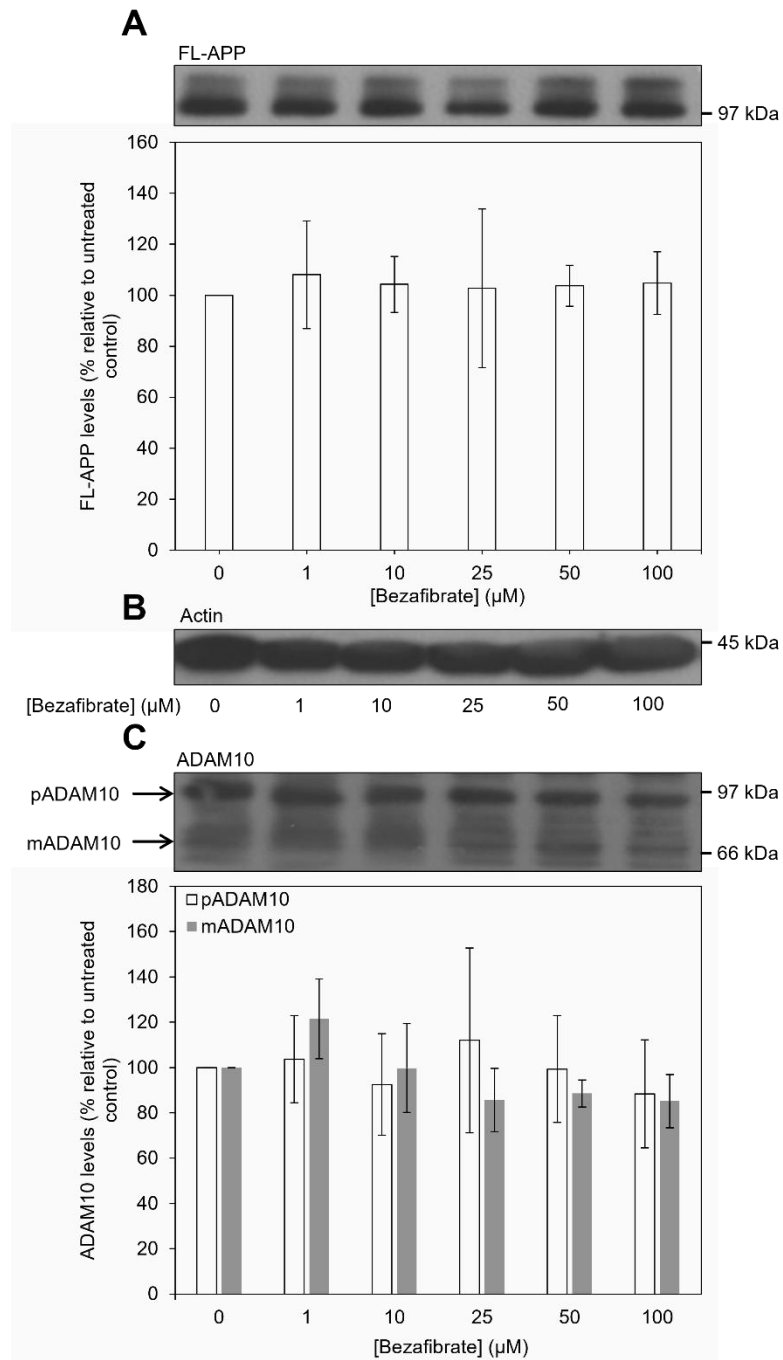


Figure 3.3: Lack of effect of bezafibrate on APP and ADAM10 expression in SH-SY5Y-SweAPP cells. SweAPP-transfected SH-SY5Y cells were grown to confluence and incubated for 24 h in the absence or presence of increasing concentrations of bezafibrate (1, 10, 25, 50 and 100 μM). Cells were harvested, lysates prepared and equal amounts of samples were resolved by SDS-PAGE and immunoblotted (see Materials and Methods). **(A)** Anti-APP (APP-CT) immunoblot. **(B)** Anti-actin immunoblot. **(C)** Anti-ADAM10 immunoblot. Multiple immunoblots were subjected to densitometric quantification and the results expressed relative to the untreated controls; pADAM10, prodomain ADAM10; mADAM10, mature ADAM10. All results are means ± S.D. (n=3).

Next, we examined the effects of bezafibrate on the generation of sAPP proteolytic fragments by SH-SY5Y-SweAPP cells. In order to quantify non-amyloidogenic shedding of sAPP, the conditioned medium from the previous experiments were immunoblotted with anti-APP 6E10 antibody. However, the results (Figure 3.4A) showed no significant changes in the non-amyloidogenic generation of sAPP fragments from any of the APP isoforms. The conditioned medium samples were then immunoblotted with anti-sAPP β Swe (6A1) antibody to determine the effect of bezafibrate on sAPP β release. Once again, however, the fibrate had no significant effects in this respect (Figure 3.4B).

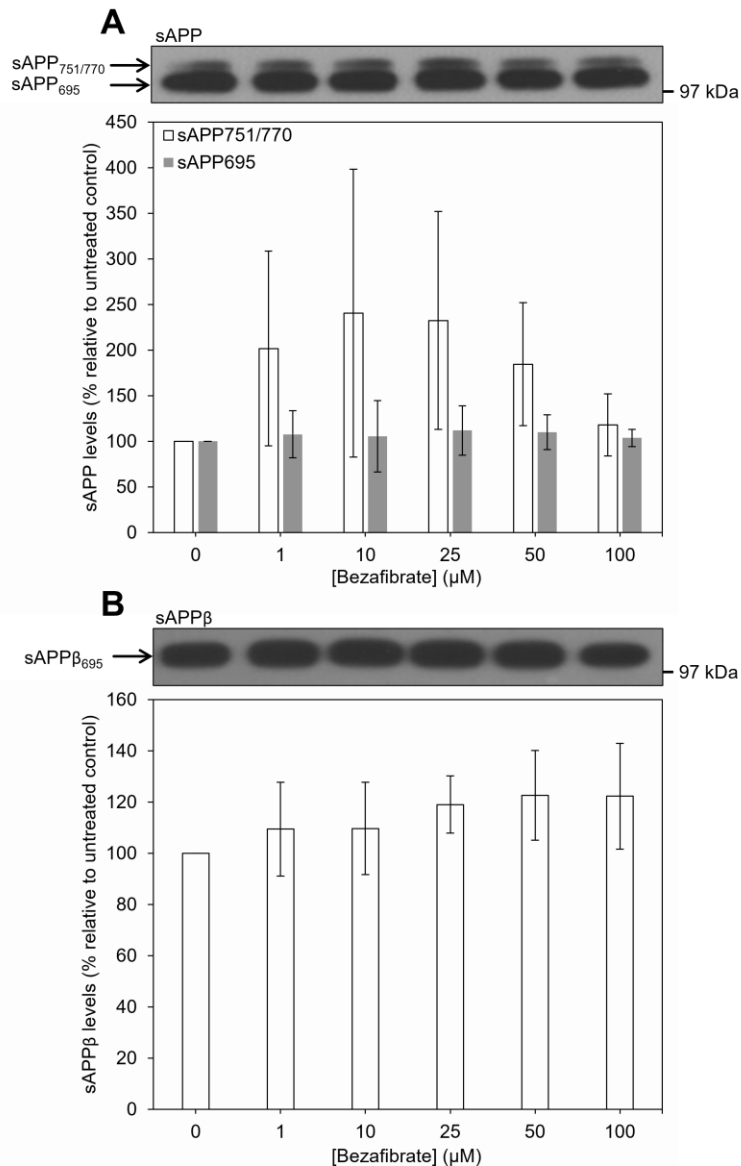


Figure 3.4: Lack of effect of bezafibrate on soluble APP generation by SH-SY5Y-SweAPP cells. SweAPP-transfected SH-SY5Y cells were grown to confluence and incubated for 24 h in the absence or presence of increasing concentrations of bezafibrate (1, 10, 25, 50 and 100 μM). Cells were harvested, medium conditioned and equal volumes of samples were resolved by SDS-PAGE and immunoblotted (see Materials and Methods). **(A)** Anti-APP 6E10 immunoblot. **(B)** Anti-sAPP β Swe 6A1 immunoblot. Multiple immunoblots were subjected to densitometric quantification and the results expressed relative to untreated control. All results are means \pm S.D. (n=3).

3.4 Summary

Despite prior research demonstrating the potential for fibrates to enhance sAPP α production through an increase in ADAM10 expression and maturation

(Zhang *et al.*, 2015; Corbett, Gonzalez and Pahan, 2015a) both gemfibrozil and bezafibrate failed to illicit any effects on either ADAM10 or APP proteolysis in SH-SY5Y-SweAPP cells in the current study. Therefore, we decided to investigate alternative molecular biology-based approaches to enhance sAPP α generation (see Chapters 0 and 6).

4. Results; Beta-prime processing of APP replaces sAPP α generation in BACE1-transfected SH-SY5Y cells

4.1 Introduction

SH-SY5Y neuroblastoma cells are often employed as an *in vitro* model of Alzheimer's disease (de Medeiros *et al.*, 2019) and Parkinson's disease (Xicoy, Wieringa and Martens, 2017). They have several benefits in comparison to primary neuronal cultures including a high rate of proliferation and expression of human neuronal markers not present in primary rodent cells, without the same ethical issues associated with primary human neuronal culture use (Kovalevich and Langford, 2013). Several variants of SH-SY5Y cell lines stably over-expressing BACE1, wild-type APP695 (wtAPP) or Swedish mutant APP695 (SweAPP) have been utilised in AD studies (Parkin *et al.*, 2007; Mattsson *et al.*, 2012; Findlay, Hamilton and Ashford, 2015; Lee *et al.*, 2016; Kong *et al.*, 2020).

During our studies on fibrates as potential enhancers of sAPP α generation we surreptitiously noted that the broad-spectrum ADAM/MMP inhibitor, batismastat, did not inhibit non-amyloidogenic sAPP generation in SH-SY5Y-BACE1 cells. Therefore, in the current chapter, we directly compared APP expression and proteolysis in a range of AD-relevant SH-SY5Y cell lines in an effort to determine the mechanisms underlying this observation.

4.2 APP and secretase expression/proteolysis in AD-relevant SH-SY5Y cell lines

In order to examine APP and secretase expression/proteolysis we grew the three AD-relevant cell lines and Mock-transfected SH-SY5Y cells, to confluence and incubated the cells in reduced serum medium for 24 h in the absence or presence of the broad spectrum MMP/ADAM inhibitor batimastat (5 μ m) (Woods and Padmanabhan, 2013) (see Materials and Methods). The cells were then harvested and the lysates and conditioned medium prepared as described in the Materials and Methods section.

4.2.1 APP and secretase expression in AD-relevant SH-SY5Y cell lines

In order to confirm BACE1 over-expression in the SH-SY5Y-BACE1 cells, equal protein levels from the cell lysates were immunoblotted with anti-BACE1 antibody. The results (Figure 4.1A) showed a strong signal around 70 kDa, corresponding to previously observed banding for BACE1 (Parkin *et al.*, 2007) in SH-SY5Y-BACE1 cells. None of the other cell lines expressed detectable amounts of the enzyme. Equal protein concentrations in samples were then confirmed by immunoblotting with anti-actin antibody (Figure 4.1B).

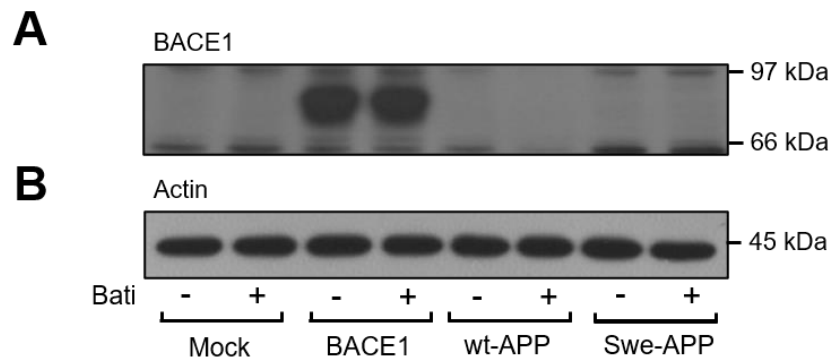


Figure 4.1: BACE1 expression in AD-relevant SH-SY5Y cell lysates. Mock-, BACE1-, wtAPP- and SweAPP-transfected SH-SY5Y cells were grown to confluence and incubated for 24 h in the absence/ presence of batimastat (5 μ M). Cells were harvested, lysates prepared and equal amounts of samples immunoblotted as described in the Materials and Methods section. **(A)** Anti-BACE1 immunoblot. **(B)** Anti-actin immunoblot.

In order to compare the expression and proteolytic maturation of the α -secretase ADAM10 the same lysates were also immunoblotted with anti-ADAM10 antibody. The results (Figure 4.2A) revealed two major bands at 98 and 70 kDa corresponding to published values (Parkin and Harris, 2009) for the proteolytically immature and the mature prodomain-lacking forms of the enzyme, respectively. The absolute levels of either ADAM10 form (in the absence of batimastat treatment) did not differ significantly between any of the cell lines (Figure 4.2A). With the addition of batimastat, the levels of cell-associated mature ADAM10 increased relative to the cognate untreated cell controls by 32.08 ± 10.51 , 54.17 ± 36.71 and 60.87 ± 22.23 %, respectively, in Mock-, BACE1- and SweAPP-transfected cells (Figure 4.2B). Batimastat treatment also caused a significant decrease in prodomain ADAM10 levels in SH-SY5Y-wtAPP cells (38.04 ± 10.94 % relative to the untreated control).

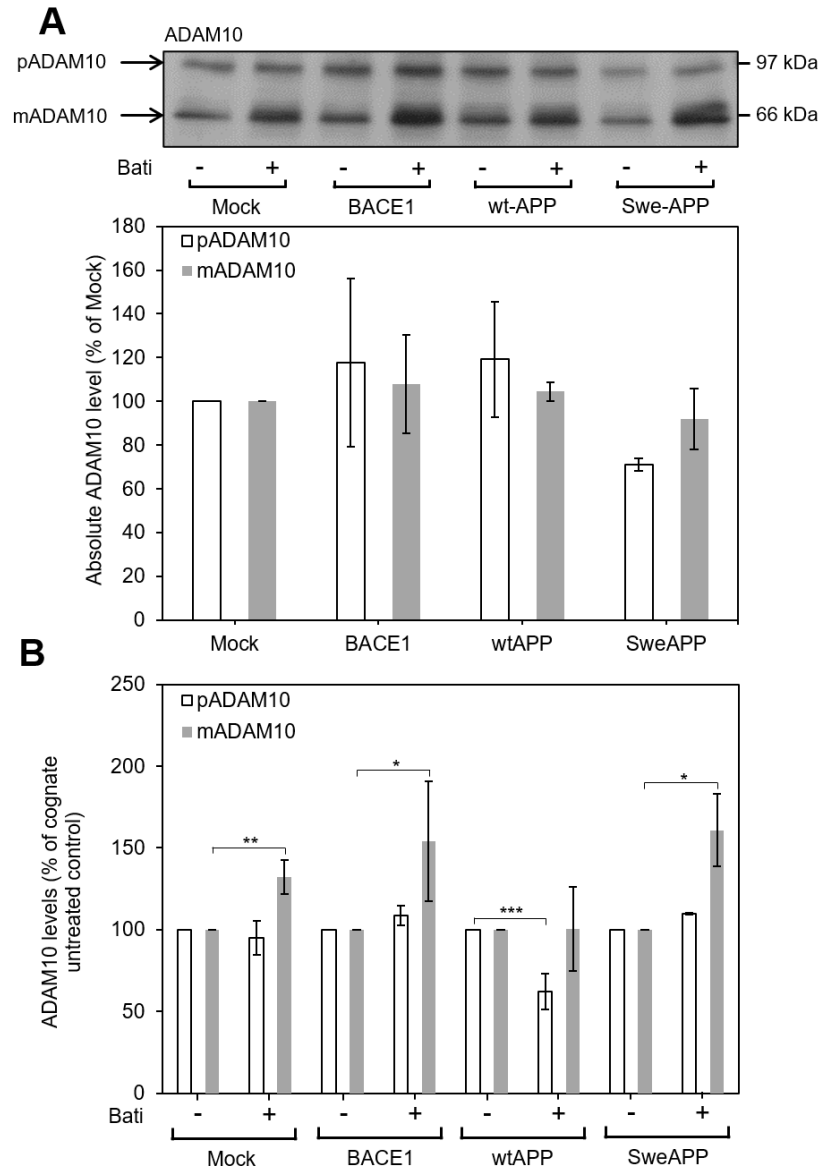


Figure 4.2: ADAM10 expression and proteolytic maturation in AD-relevant SH-SY5Y cell lysates. Mock-, BACE1-, wtAPP- and SweAPP-transfected SH-SY5Y cells were grown to confluence and incubated for 24 h in the absence/presence of batimastat (5 μ M). Cells were harvested, lysates prepared and equal amounts of samples were then resolved by SDS-PAGE and immunoblotted. **(A)** Anti-ADAM10 immunoblot. Multiple immunoblots were subjected to densitometric quantification and the results expressed relative to Mock-transfected controls **(B)** The effect of batimastat on ADAM10 proteolytic maturation. Results are expressed relative to the cognate no batimastat control for each cell line. pADAM10, prodomain ADAM10; mADAM10, mature ADAM10. All results are means \pm S.D. (n=3). Significant results from one-way ANOVA analysis are indicated; * = significant at $p \geq 0.05$; ** = significant at $p \geq 0.01$; *** = significant at $p \geq 0.001$.

Next, we sought to determine APP expression levels and the effect of batimastat on levels of the protein in the four cell lines. As such, the same cell lysates were immunoblotted with anti-APP C-terminus (APP-CT) antibody. The results (Figure 4.3A) revealed several bands on immunoblots just above the 97 kDa marker likely corresponding to a combination of different APP isoforms and glycoforms. As the SH-SY5Y-wtAPP and SH-SY5Y-SweAPP cells both overexpress APP₆₉₅, the 9.09 ± 1.49 - and 10.59 ± 2.60 -fold respective increases in full-length APP (FL-APP) expression (relative to untransfected controls) in these cell lysates were expected (Figure 4.3A). What was not expected was the 2.80 ± 0.53 -fold increase in FL-APP exhibited in the SH-SY5Y-BACE1 cell lysates relative to the Mock-transfected cell lysates.

With the addition of batimastat, there was no significant change in APP expression between the treated cell lines and their cognate untreated controls (Figure 4.3B).

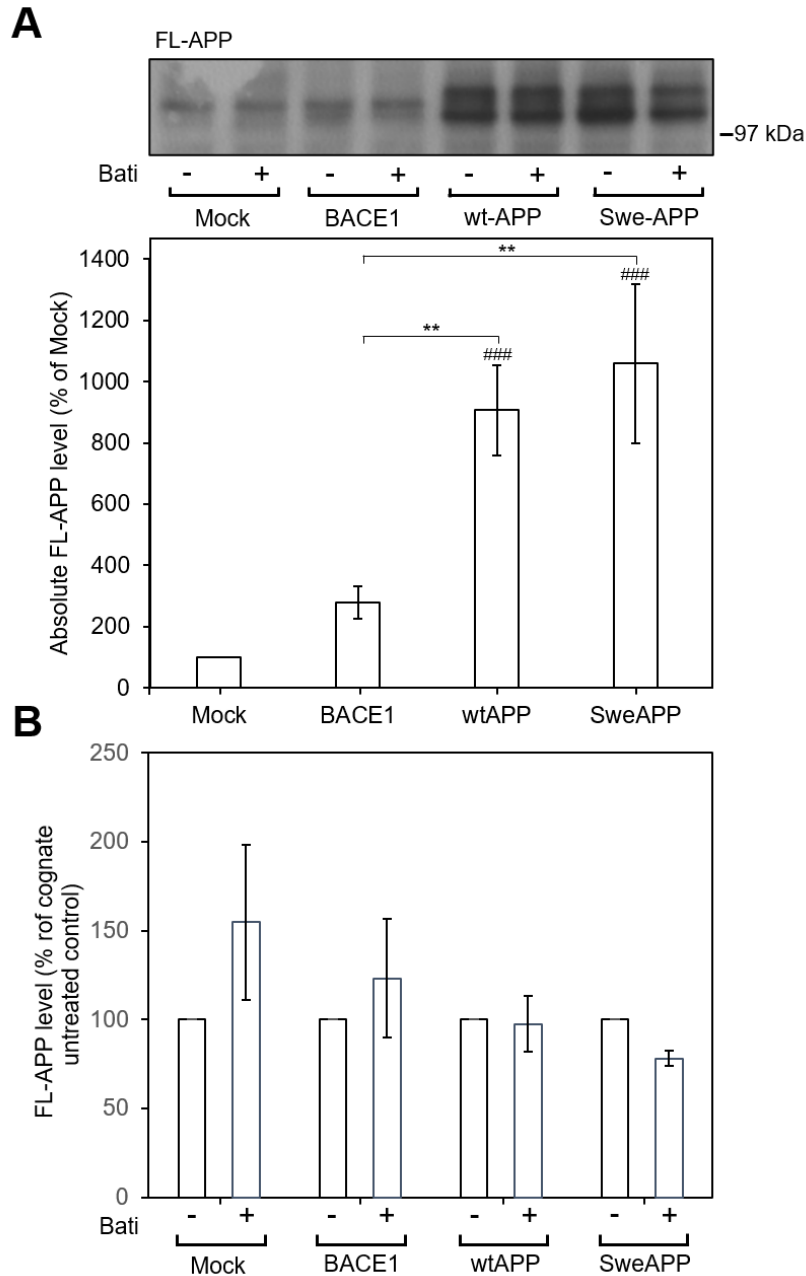


Figure 4.3: Full-length APP expression in AD-relevant SH-SY5Y cell lysates. Mock-, BACE1-, wtAPP- and SweAPP-transfected SH-SY5Y cells were grown to confluence and incubated for 24 h in the absence/presence of batimastat (5 μ M). Cells were harvested, lysates prepared and equal amounts of samples were then resolved by SDS-PAGE and immunoblotted. **(A)** Anti-APP C-terminal (APP-CT) immunoblot. Multiple immunoblots were subjected to densitometric quantification and the results are expressed relative to the Mock-transfected control. **(B)** The effect of batimastat on FL-APP expression. Results are expressed relative to the cognate no batimastat control for each cell line. All results are means \pm S.D. (n=3). Significant results from one-way ANOVA analysis are indicated; ** = significant at $p \geq 0.01$; *** = significant at $p \geq 0.001$. Hash symbols (#) represent the same significance levels relative to the Mock-transfected controls.

4.2.2 APP proteolysis in AD-relevant SH-SY5Y cell lines

In order to compare APP proteolysis and the effect of batimastat on these events between the four different cell lines the conditioned medium from the previously described experiments was collected and processed as described in the Materials and Methods section. Initially, equal volumes of concentrated conditioned medium were immunoblotted with the anti-APP 6E10 antibody to examine non-amyloidogenic shedding of sAPP. The monoclonal 6E10 antibody is raised against residues 1-16 of the amyloid- β region of the APP protein, with the epitope present within amino acids 3-8 of the same region which is present in sAPP α and not in sAPP β (Grant *et al.*, 2019). The results (Figure 4.4A) demonstrated two bands of sAPP with the larger band representing sAPP_{751/770} and the smaller band sAPP₆₉₅ (Belyaev *et al.*, 2010). The latter band was significantly enhanced in medium from both wtAPP- and SweAPP-transfected cells (3.08 ± 0.56 -fold and 2.79 ± 0.06 -fold, respectively, relative to Mock-transfected cells). This result was expected as wtAPP- and SweAPP-transfected cells overexpress the APP₆₉₅ isoform. Also expected, was the reduction in sAPP_{751/770} and sAPP₆₉₅ produced by the SH-SY5Y-BACE1 cells (44.56 ± 13.06 and 46.41 ± 14.74 % reductions, respectively, relative to Mock-transfected cells), which would be expected to favour reciprocal amyloidogenic shedding of APP.

Following batimastat treatment (Figure 4.4B), the non-amyloidogenic shedding of APP_{751/770} from Mock-, wtAPP-, and SweAPP-transfected cells was dramatically reduced by 84.53 ± 3.64 , 44.08 ± 8.23 and 74.30 ± 12.52 %, respectively, compared to cognate untreated cell controls. A similar effect was observed in relation to the non-amyloidogenic shedding of APP₆₉₅ from the same cell lines (reductions of 92.06 ± 7.01 , 14.55 ± 6.90 and 50.21 ± 0.52 %, relative to cognate untreated controls). What was not expected was the lack of a decrease in sAPP shedding in the SH-SY5Y-BACE1 cell line when treated with batimastat.

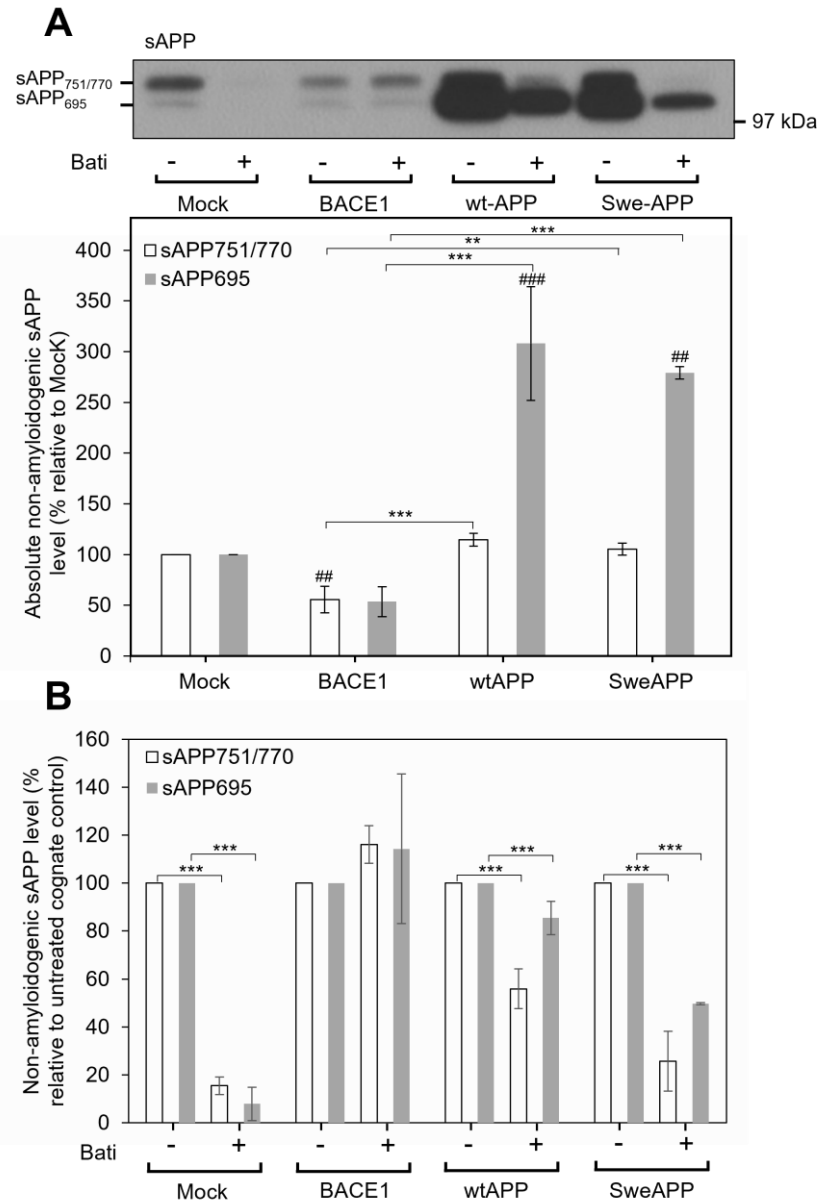


Figure 4.4: Non-amyloidogenic soluble APP in conditioned medium from AD-relevant SH-SY5Y cell lines. Mock-, BACE1-, wtAPP- and SweAPP-transfected SH-SY5Y cells were grown to confluence and incubated for 24 h in the absence/presence of batimastat (5 μ M). Cells were harvested, medium conditioned and equal volumes of medium were then resolved by SDS-PAGE and immunoblotted. **(A)** Anti-APP 6E10 immunoblot. Multiple immunoblots were subjected to densitometric quantification and the results are expressed relative to the Mock-transfected control. **(B)** The effect of batimastat on non-amyloidogenic APP shedding. Results are expressed relative to the cognate no batimastat control for each cell line. All results are means \pm S.D. (n=3). Significant results from one-way ANOVA analysis are indicated; ** = significant at $p \geq 0.01$; *** = significant at $p \geq 0.001$. Hash symbols (#) represent the same significance levels relative to the Mock-transfected controls.

The concentrated conditioned medium samples were also immunoblotted with anti-sAPP β antibody in order to examine canonical β -secretase-mediated shedding of APP by the AD-relevant cell lines. As seen in Figure 4.5A, two bands corresponding to sAPP β were observed with the larger band representing sAPP $\beta_{751/770}$ and the smaller band sAPP β_{695} . Quantification of multiple immunoblots showed that SH-SY5Y-BACE1 cells released significantly higher levels of sAPP $\beta_{751/770}$ and sAPP β_{695} compared to the Mock-transfected cells (5.16 ± 1.86 -fold and 45.15 ± 5.07 -fold increase, respectively). The SH-SY5Y-wtAPP cells also exhibited a significant increase in their sAPP β_{695} release (57.46 ± 23.14 -fold relative Mock-transfected cells) as might be expected for cells over-expressing full-length APP $_{695}$. Notably, using the sAPP β antibody, no changes were observed in the apparent production of these fragments by the SweAPP cells. This was likely due to the nature of the APP Swedish double substitution around the β -secretase-cleavage site (Lys670/Met671 to Asn670/Leu671), such that the anti-sAPP β antibody was unable to detect the sAPP β fragment generated. Therefore, we immunoblotted the same samples with anti-sAPP β Swe 6A1 antibody which detected very intense bands only in medium from the SH-SY5Y-SweAPP cells (Figure 4.5C). Batimastat had no effect on the levels of sAPP β generated by any of the four cell lines (Figure 4.5B).

In order to quantify the A β -peptide levels produced by the different AD-relevant cell lines, unconcentrated medium samples were analysed using the V-Plex A β peptide panel (6E10) kit and quantified using the Mesoscale Discovery (MSD) platform (Materials and Methods). The results (Figure 4.6) revealed that the concentrations of A β 40 increased 3.71 ± 0.55 -, 5.62 ± 0.92 - and 34.36 ± 3.82 -fold relative to Mock cells in BACE1-, wtAPP- and SweAPP-transfected cell medium, respectively. Similar increases were observed in relation to A β 42 whereby concentrations increased 4.03 ± 0.58 -, 5.94 ± 0.47 - and 47.13 ± 2.68 -fold, respectively, in medium from BACE1-, wtAPP- and SweAPP-transfected cells.

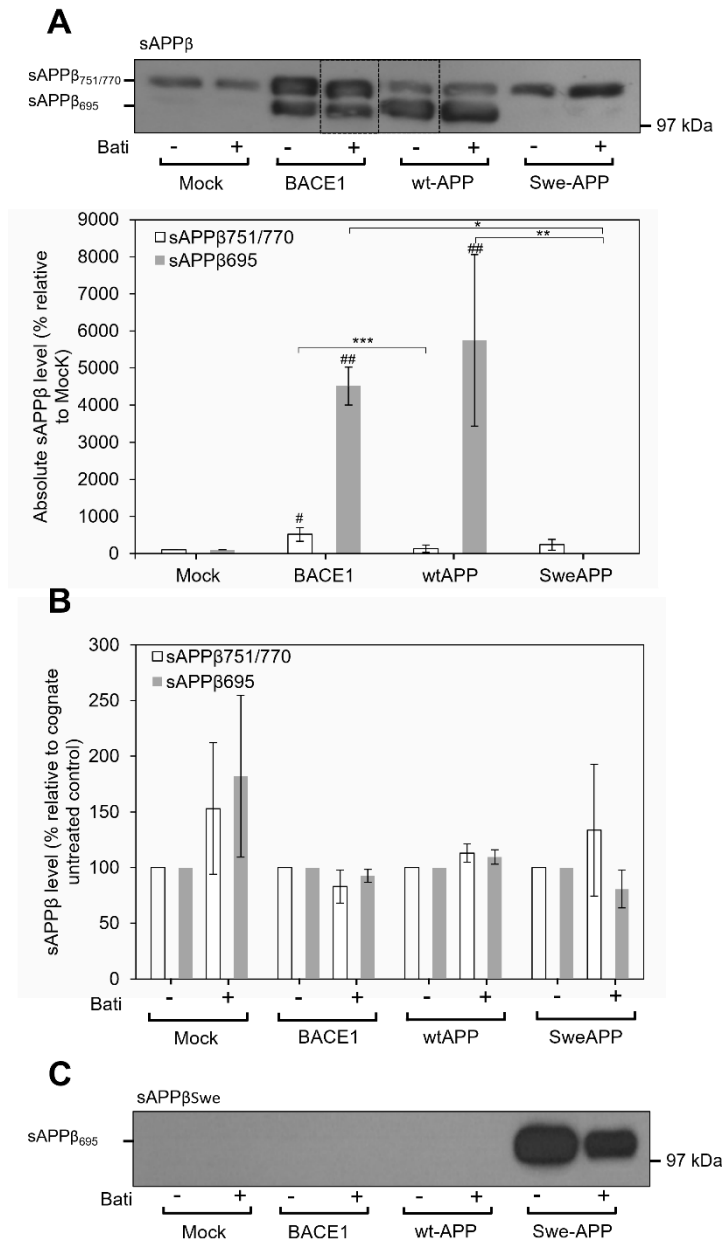


Figure 4.5. sAPPβ in conditioned medium from AD-relevant SH-SY5Y cell cells. Mock-, BACE1-, wtAPP- and SweAPP-transfected SH-SY5Y cells were grown to confluence and incubated for 24 h in the absence/presence of batimastat (5 μM). Cells were harvested, medium conditioned and equal volumes of medium were then resolved by SDS-PAGE and immunoblotted. **(A)** Anti-sAPPβ immunoblot. Multiple immunoblots were subjected to densitometric quantification and the results are expressed relative to the Mock-transfected control. **(B)** The effect of batimastat on amyloidogenic APP shedding. **(C)** Anti-APPβ_{swe} immunoblot. Results are expressed relative to the cognate no batimastat control for each cell line. All results are means ± S.D. (n=3). Significant results from one-way ANOVA analysis are indicated; * = significant at $p \geq 0.05$; ** = significant at $p \geq 0.01$; *** = significant at $p \geq 0.001$. Hash symbols (#) represent the same significance levels relative to the Mock-transfected controls.

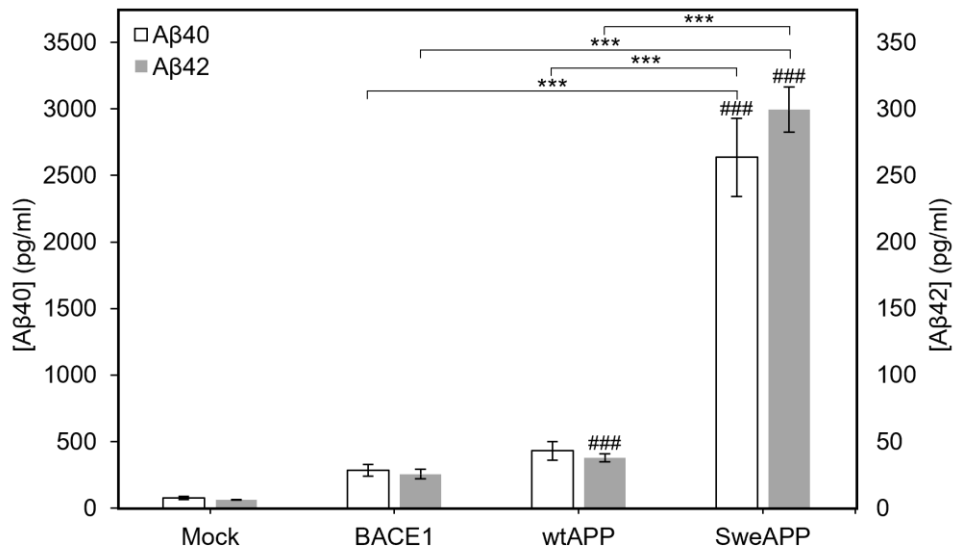


Figure 4.6. Amyloid- β peptide fragments in AD-relevant SH-SY5Y cell medium. A β -peptide levels expressed relative to the Mock-transfected control. Significant results from one-way ANOVA analysis are indicated; *** = significant at $p \geq 0.001$. Hash symbols (#) represent the same significance levels relative to the Mock-transfected controls.

4.2.3 Non-amyloidogenically derived soluble APP produced by SH-SY5Y-BACE1 cells results from BACE1 beta-prime activity

Batimastat treatment did not significantly affect the levels of non-amyloidogenically-derived sAPP produced by BACE1-transfected cells (Figure 4.4B). Therefore, it was hypothesized that the over-expressed BACE1 might be cleaving APP at the 'beta prime' site C-terminal to Tyr10 of the A β region (Liu, Doms and Lee, 2002). The resultant sAPP β' would still contain the minimum 6E10 epitope of amino acids 3-8 of the A β region (Grant *et al.*, 2019) but production of the fragment would not be inhibited by batimastat. As there is no antibody that could specifically detect sAPP β' and not sAPP α in conditioned medium, we examined the reciprocal production of APP C-terminal fragments (CTFs) in cell lysates. As such, the cell lysates from Figure 4.2 were subjected to tris-tricine gel electrophoresis (see Materials and Methods) and immunoblotted with the anti-APP CT antibody. The resultant immunoblot showed three distinct C-terminal fragments of different sizes (Figure 4.7A). The C99 fragment produced via canonical BACE1-mediated processing of APP was significantly increased in lysates from SH-SY5Y-SweAPP cells (15.01 ± 4.58 -fold relative to Mock

transfectants). The fragment was also increased, albeit not significantly in lysates from SH-SY5Y-wtAPP cells (7.64 ± 2.83 -fold relative to Mock transfectants) (Figure 4.7B). Rather surprisingly, C99 levels in BACE1-transfected cells were not significantly enhanced relative to Mock-transfected cells. The α -secretase generated C83 fragment was enhanced in lysates from wtAPP- and SweAPP-transfected cells (3.77 ± 1.10 - and 3.71 ± 1.32 -fold, respectively, relative to Mock transfectants) (Figure 4.7C). Notably, however, there was a complete absence of C83 in SH-SY5Y-BACE1 cell lysates. Instead, a slightly larger fragment, C89, was detected which was likely the result of non-canonical non-amyloidogenic cleavage of APP at the beta prime site by the over-expressed BACE1.

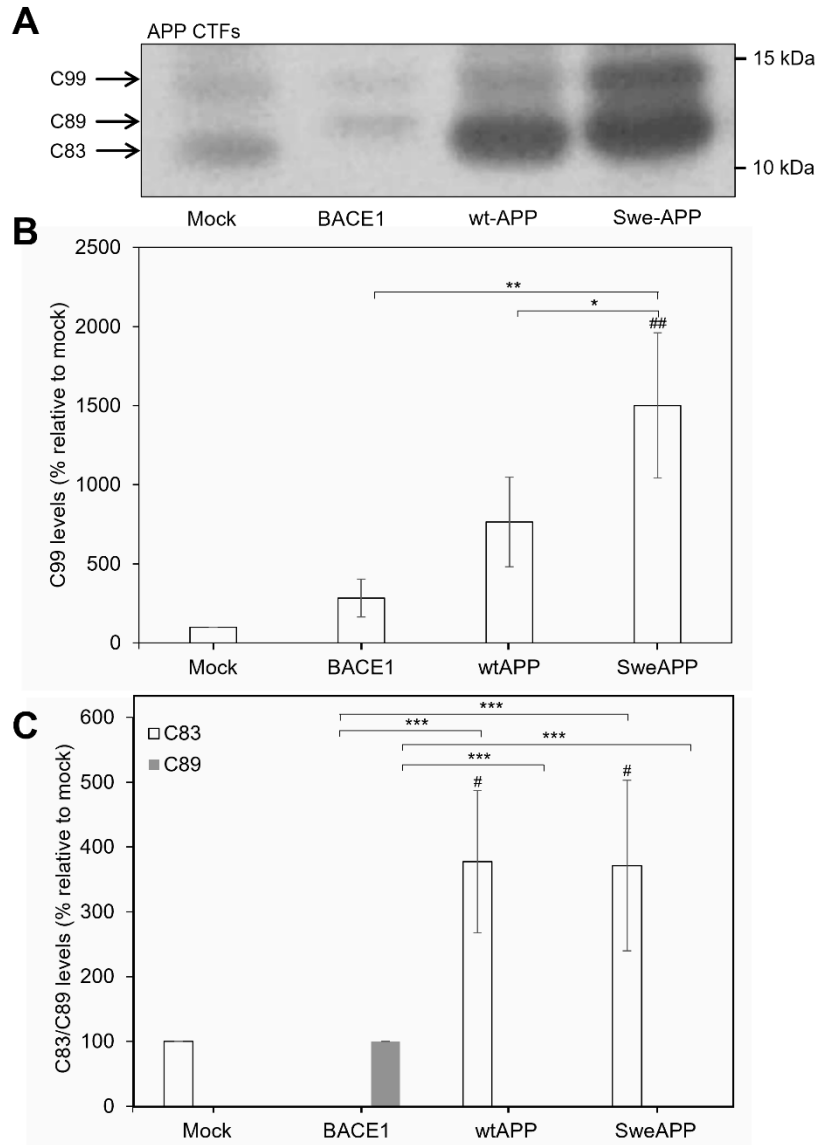


Figure 4.7: APP-CTF quantification in AD-relevant SH-SY5Y cell lysates. Mock-, BACE1-, wtAPP- and SweAPP-transfected SH-SY5Y cells were grown to confluence and incubated for 24 h in the absence/presence of batimastat (5 μ M). Cells were harvested, lysates prepared and immunoblotted as described in the Materials and Methods section. **(A)** Anti-APP C-terminal (CTF) immunoblot. **(B)** Levels of C99, produced by amyloidogenic processing, relative to Mock control. **(C)** Levels of C89 and C83, produced by non-amyloidogenic processing of APP by BACE1 and ADAM10, respectively, are portrayed relative to Mock control C83 levels. Multiple immunoblots were subjected to densitometric quantification and the results are expressed relative to the Mock-transfected control. All results are means \pm S.D. (n=3). Significant results from one-way ANOVA analysis are indicated; * = significant at $p \geq 0.05$; ** = significant at $p \geq 0.01$; *** = significant at $p \geq 0.001$. Hash symbols (#) represent the same significance levels relative to the Mock-transfected controls.

To further confirm that the non-amyloidogenically derived sAPP generated by SH-SY5Y-BACE1 was the consequence of non-canonical BACE1-mediated

processing, we directly compared the effects of batimastat and β -secretase inhibitor IV (Stachel *et al.*, 2004) on APP proteolysis in Mock- and BACE1-transfected SH-SY5Y cells. Initially, Mock-transfected cells were incubated in the absence or presence of either or both inhibitors for 24 hrs in reduced serum medium. Equal amounts of protein from the subsequently prepared cell lysates were then immunoblotted with anti-APP CT antibody (Figure 4.8A). The results showed no changes in full-length APP levels following treatment with any combination of the inhibitors. Equal protein loading was confirmed by immunoblotting for actin (Figure 4.8B).

Equal volumes of conditioned medium from the same experiment were then immunoblotted with anti-APP 6E10 antibody to examine non-amyloidogenic APP processing. The results (Figure 4.8C) demonstrated a near complete inhibition of non-amyloidogenic sAPP_{751/770} and sAPP₆₉₅ release from the Mock-transfected cells following batimastat treatment either alone or in combination with the β -secretase inhibitor. In contrast, β -secretase inhibitor IV alone had no effect.

Immunoblotting the same conditioned medium with anti-sAPP β demonstrated that the addition of β -secretase inhibitor IV, alone or in combination with batimastat, was sufficient to inhibit the release of sAPP β (Figure 4.8D). Treatment with β -secretase inhibitor IV alone reduced sAPP β _{751/770} and sAPP β ₆₉₅ by 95.74 ± 0.49 and 91.42 ± 3.52 %, respectively, relative to untreated controls. In combination with batimastat, β -secretase inhibitor IV reduced sAPP β _{751/770} and sAPP β ₆₉₅ production by 96.15 ± 0.79 % and 91.54 ± 2.51 %, respectively, relative to untreated controls.

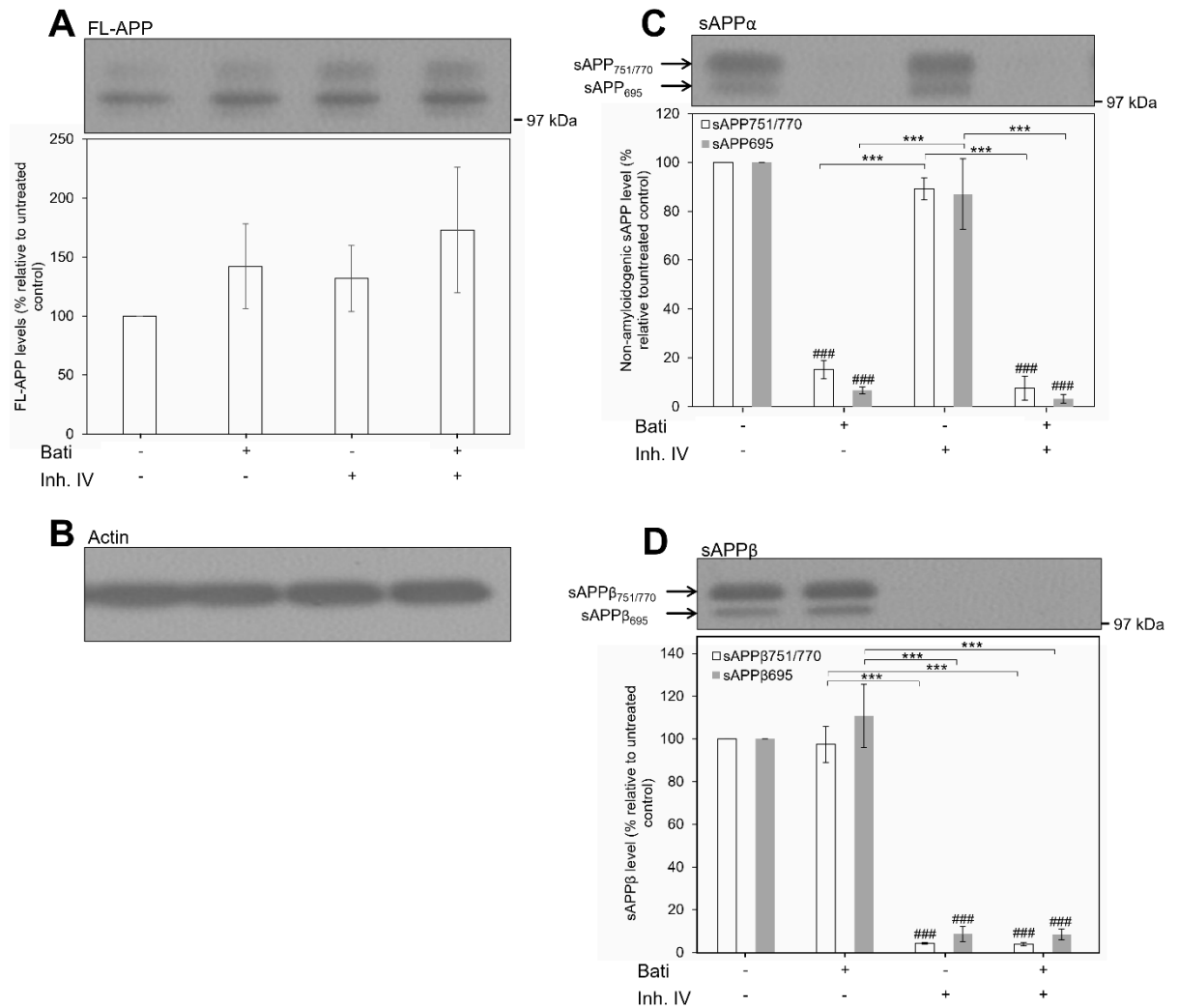


Figure 4.8: The effect of α - and β -secretase inhibitors on APP expression and proteolysis in SH-SY5Y-Mock cells. Mock-transfected SH-SY5Y cells were grown to confluence and incubated for 24 h in the absence/presence of batimastat (5 μ M) and/or β -secretase inhibitor IV (5 μ M). Cells were harvested, lysates prepared and equal amounts of samples were then resolved by SDS-PAGE and immunoblotted (**A and B**). Equal volumes of medium were also resolved by SDS-PAGE and immunoblotted (**C and D**). (**A**) Anti-APP C-terminal (CTF) immunoblot of lysates. (**B**) Anti-actin immunoblot of lysates. (**C**) Anti-APP 6E10 immunoblot of medium. (**D**) Anti-sAPP β immunoblot of medium. Multiple immunoblots were subjected to densitometric quantification and the results are expressed relative to the untreated control. All results are means \pm S.D. (n=3). Significant results from one-way ANOVA analysis are indicated; *** = significant at $p \geq 0.001$. Hash symbols (#) represent the same significance levels relative to the Mock-transfected controls.

The same inhibitor experiments were then repeated using SH-SY5Y-BACE1 cells (Figure 4.9). Immunoblotting of cell lysates using the anti-APP C-terminal antibody showed no significant changes in FL-APP levels following

inhibitor treatment (Figure 4.9A). Equal protein loading was confirmed by anti-actin immunoblotting (Figure 4.9B).

Next, the conditioned medium was immunoblotted with the anti-APP 6E10 antibody. As observed previously (Figure 4.4B) batimastat did not significantly alter the release of non-amyloidogenically-derived sAPP from SH-SY5Y-BACE1 cells (Figure 4.9C). Notably, treatment with β -secretase inhibitor IV alone also did not lead to a reduction in the non-amyloidogenic release of sAPP. Only the combination of both batimastat and β -secretase inhibitor IV resulted in a significant reduction in the release of both sAPP_{751/770} and sAPP₆₉₅ (72.54 ± 24.24 % and 81.26 ± 19.80 % reductions, respectively, relative to untreated controls). Immunoblotting the same conditioned medium with anti-sAPP β antibody confirmed that β -secretase inhibitor IV alone or in combination with batimastat largely inhibited the generation, as would be expected, of sAPP β (65.72 ± 12.56 % and 70.36 ± 12.82 % in relation to sAPP_{751/770} and 90.55 ± 7.07 % and 85.21 ± 9.97 % in relation to sAPP₆₉₅, respectively) (Figure 4.9D).

Collectively, these results suggested the involvement of non-canonical non-amyloidogenic APP cleavage in SH-SY5Y-BACE1 cells. The data also suggest that α -secretase activity can compensate for BACE1 inhibition resulting in their being no reduction in sAPP release from cells when β -secretase inhibitor IV alone was used. The net inference from this is that BACE1 is the key enzyme responsible for non-amyloidogenic APP processing in SH-SY5Y-BACE1 cells.

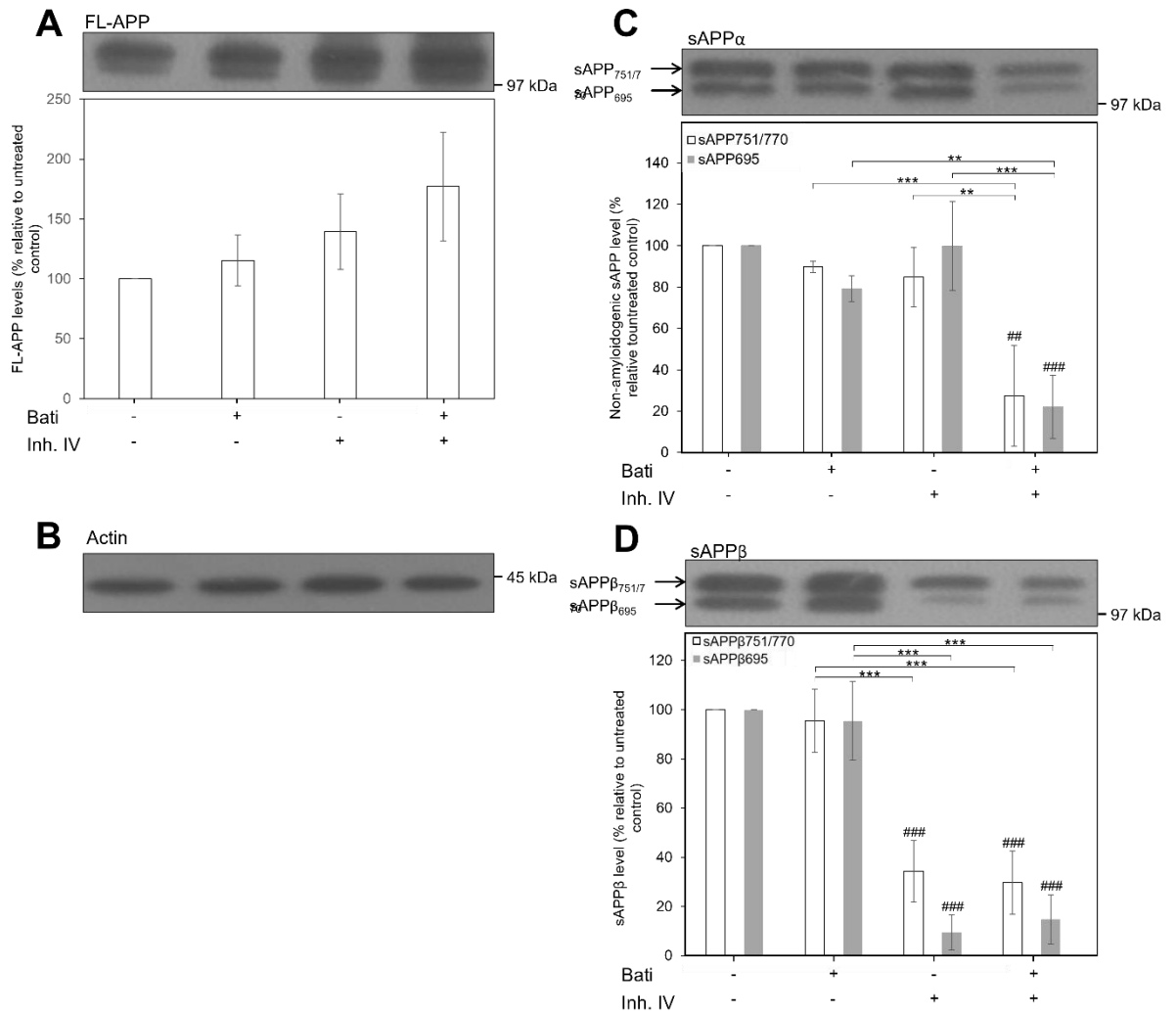


Figure 4.9: The effect of α - and β -secretase inhibitors on APP expression and proteolysis in SH-SY5Y-BACE1 cells. Mock-transfected SH-SY5Y cells were grown to confluence and incubated for 24 h in the absence/presence of batimastat (5 μ M) and/or β -secretase inhibitor IV (5 μ M). Cells were harvested, lysates prepared and equal amounts of samples were then resolved by SDS-PAGE and immunoblotted (**A** and **B**). Equal volumes of medium were also resolved by SDS-PAGE and immunoblotted (**C** and **D**). (**A**) Anti-APP C-terminal (CTF) immunoblot of lysates. (**B**) Anti-actin immunoblot of lysates. (**C**) Anti-APP 6E10 immunoblot of medium. (**D**) Anti-sAPP β immunoblot of medium. Multiple immunoblots were subjected to densitometric quantification and the results are expressed relative to the untreated control. All results are means \pm S.D. (n=3). Significant results from one-way ANOVA analysis are indicated; ** = significant at $p \geq 0.01$, *** = significant at $p \geq 0.001$. Hash symbols (#) represent the same significance levels relative to the Mock-transfected controls.

In an attempt to further investigate the potential role of BACE1 beta prime activity as the key non-amyloidogenic secretase in SH-SY5Y-BACE1 cells we examined the effect of batimastat and β -secretase inhibitor IV on the generation of APP-CTFs in Mock-transfected and SH-SY5Y-BACE1 cells. To this end lysates from inhibitor-treated Mock-transfected cells were initially resolved by tris-tricine electrophoresis and immunoblotted with the anti-APP C-terminal antibody (Materials and Methods). The results (Figure 4.10A) showed that there was no C89 detected in any of the cell lysates with or without inhibitor treatments. C99 levels decreased following β -secretase inhibitor IV treatment alone or in combination with batimastat (by 44.61 ± 6.62 % and 70.47 ± 11.11 %, respectively, relative to untreated controls) (Figure 4.10B). C83 also follow an expected pattern (Figure 4.10C), whereby there was only a reduction in the levels of this fragment when cells were treated with batimastat (a 24.42 ± 6.04 % reduction relative to untreated controls). Notably however, a combination of both treatments did not affect C83 levels.

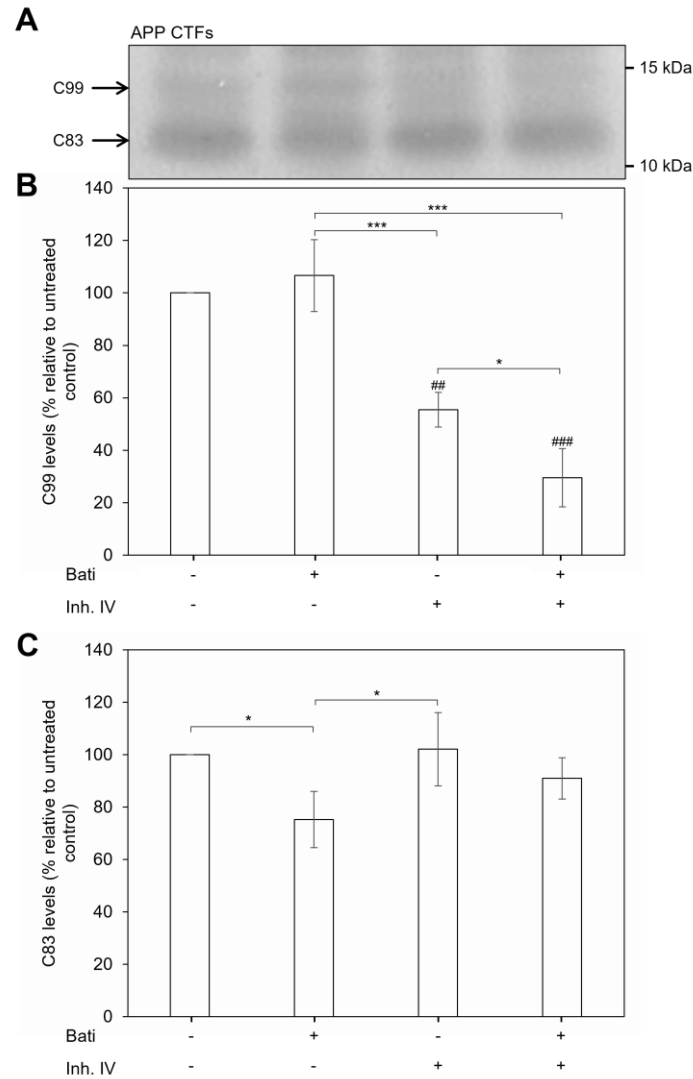


Figure 4.10: The effect of α - and β -secretase inhibitors on APP-CTFs in SH-SY5Y-Mock cell lysates. Mock-transfected SH-SY5Y cells were grown to confluence and incubated for 24 h in the absence/presence of batimastat (5 μ M) and/or β -secretase inhibitor IV (5 μ M). Cells were harvested, lysates prepared and immunoblotted as described in the Materials and Methods section. **(A)** Anti-APP C-terminal (CTF) immunoblot. **(B)** Levels of C99, produced by amyloidogenic processing, relative to Mock control. **(C)** Levels of C83, produced by non-amyloidogenic processing of APP by ADAM10, are portrayed relative to Mock control C83 levels. Multiple immunoblots were subjected to densitometric quantification and the results are expressed relative to the untreated controls. All results are means \pm S.D. (n=3). Significant results from one-way ANOVA analysis are indicated; * = significant at $p \geq 0.05$; ** = significant at $p \geq 0.01$; *** = significant at $p \geq 0.001$. Hash symbols (#) represent the same significance levels relative to the Mock-transfected controls.

Next the CTF analysis was repeated on lysates prepared from inhibitor-treated SH-SY5Y-BACE1 cells. Unlike Figure 4.10, there was no C83 fragment detected in lysates from the untreated control and batimastat-treated cells (Figure 4.11A). Instead, the BACE1 beta prime-generated C89 fragment was clearly visible at a higher molecular weight. The levels of C89 were indistinguishable from the global increase in CTFs that was exhibited following β -secretase inhibitor IV treatment (Figure 4.11B and Figure 4.11C). This is explored further in the Discussion section of the study.

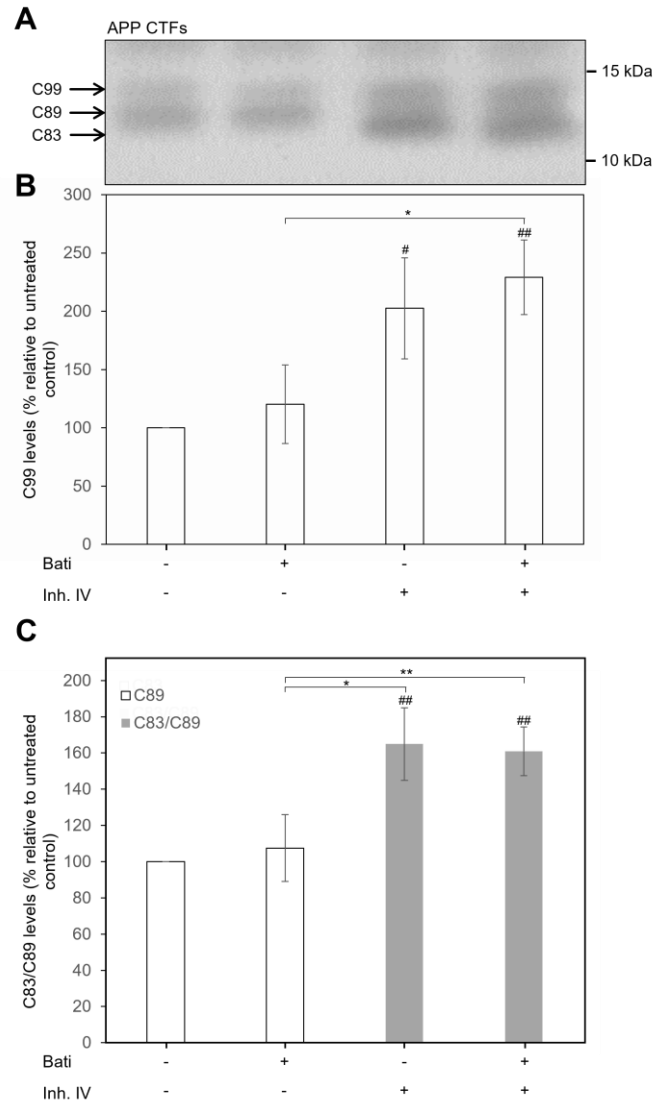


Figure 4.11: The effect of α - and β -secretase inhibitors on levels of APP-CTFs in SH-SY5Y-BACE1 cell lysates. BACE1-transfected SH-SY5Y cells were grown to confluence and incubated for 24 h in the absence/presence of batimastat (5 μ M) and/or β -secretase inhibitor IV (5 μ M). Cells were harvested, lysates prepared and immunoblotted as described in the Materials and Methods section. **(A)** Anti-APP C-terminal (CTF) immunoblot. **(B)** Levels of C99, produced by amyloidogenic processing, relative to BACE1 control. **(C)** Levels of C89 and C83, produced by non-amyloidogenic processing of APP by BACE1 and ADAM10, respectively, are portrayed relative to BACE1 control C89 levels. Multiple immunoblots were subjected to densitometric quantification and the results are expressed relative to the untreated controls. All results are means \pm S.D. (n=3). Significant results from one-way ANOVA analysis are indicated; * = significant at $p \geq 0.05$; ** = significant at $p \geq 0.01$. Hash symbols (#) represent the same significance levels relative to the Mock-transfected controls.

4.3 Viability of AD-relevant SH-SY5Y cell lines

Having previously quantified A β -peptide generation by all four SH-SY5Y cell lines used in the current study (Figure 4.6) we next sought to determine whether levels of the peptides correlated to any degree with cell viability. To this end, the cells were seeded at identical densities and cultured over a 12-day growth period with viability measurements being determined at the stated time points (see Materials and Methods). Initially, the trypan blue assay was employed to monitor viability and the results (Figure 4.12A) demonstrated that wtAPP- and SweAPP-transfected SH-SY5Y cells exhibited slightly higher viability than the Mock-transfected cells. This was possibly due to the increased amounts of non-amyloidogenic sAPP found in the medium of both of these cell lines (Figure 4.4A) and indicates that the effect of enhanced A β -peptide levels (Figure 4.5D) could possibly be countered by the increased sAPP. Notably, SH-SY5Y-BACE1 cells, despite generating less A β than either SH-SY5Y-wtAPP or SH-SY5Y-SweAPP cells, exhibited reduced viability which became increasingly apparent after day 5 (Figure 4.12A). To more effectively demonstrate the differences in cell viability, an area under the curve (AUC) analysis was utilized and the results (Figure 4.12B) demonstrated a highly significant reduction in SH-SY5Y-BACE1 cell viability (11.56 ± 0.47 % relative to Mock transfectants).

Morphologically, the SH-SY5Y-BACE1 cells appeared less healthy than the other cell lines suggesting that the general metabolism of the cells might be impacted more than absolute viable cell numbers. Therefore, we repeated the viability studies using the methanethiosulfonate (MTS) assay (see Materials and Methods). The results (Figure 4.12C-D) more clearly demonstrated a decrease in the viability of SH-SY5Y-BACE1 cells relative to any of the other cell lines employed (a 30.62 ± 4.87 % reduction relative to Mock transfectants), together with an enhanced viability of wtAPP- (28.99 ± 8.55 %) and SweAPP-transfected (21.56 ± 4.54 %) cells relative to Mock transfectants, despite dramatically enhanced A β production by the latter two cell lines.

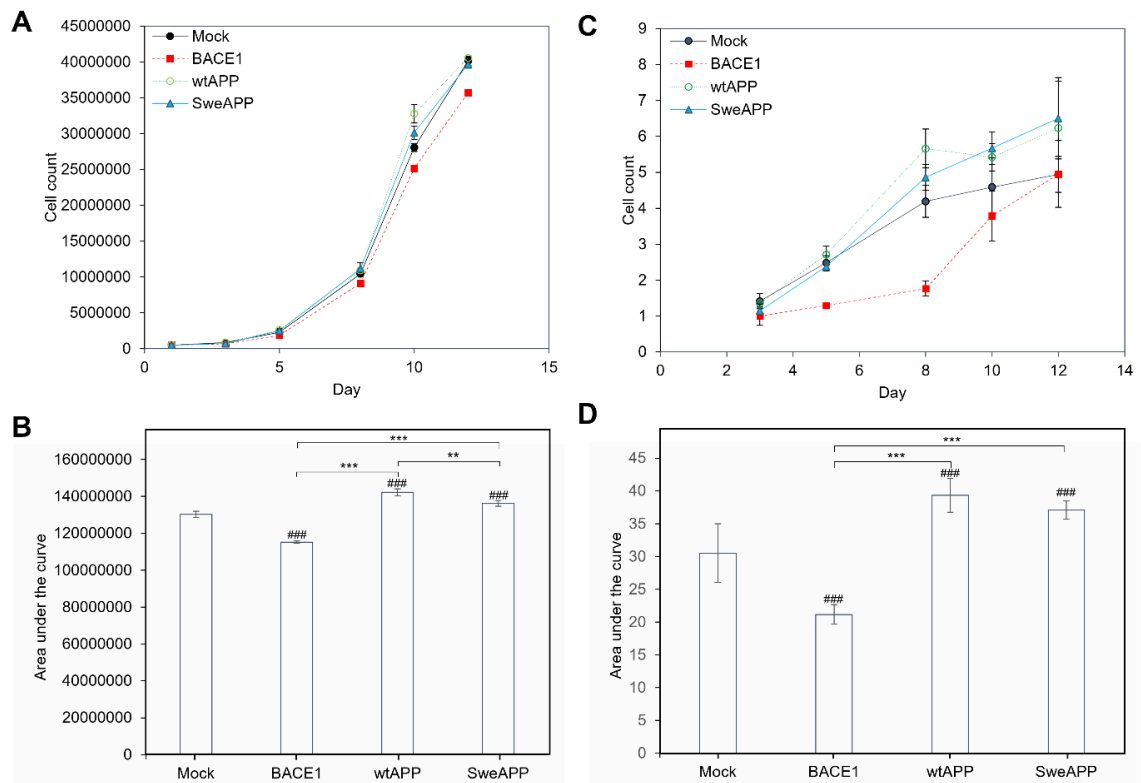


Figure 4.12: Cell viability assays in AD-relevant SH-SY5Y cell models. Mock-, BACE1-, wtAPP- and SweAPP-transfected SH-SY5Y cells were seeded at a density of $2 \times 10^4/\text{cm}^2$ and cultured over a 12-day growth period. At the relevant time points, viability assays were conducted as described in the Materials and Methods. **(A)** Trypan blue cell viability curves. **(B)** Area under the curve analysis (AUC) for Trypan blue cell count. **(C)** Methanethiosulfonate (MTS) assay cell viability curves. **(D)** AUC for MTS assay count. Results for all viability assays are means \pm S.D. ($n=3$ for cell count and $n=6$ for MTS assay). Significant results from one-way ANOVA are indicated; *** = significant at $p \geq 0.001$. Hash symbols (#) represent the same significance relative to the cognate experiment controls.

4.4 Generation and characterization of sAPP α and sAPP β' over-expressing Mock- and BACE1-transfected SH-SY5Y cell lines

The results in the preceding section suggested that the decreased viability of SH-SY5Y-BACE1 cells might have been more to do with depleted sAPP α and/or enhanced sAPP β' prime levels than enhanced A β production. Therefore, we endeavored to over-express sAPP α and sAPP β' in SH-SY5Y-BACE1 and Mock-transfected SH-SY5Y cells in order to examine the effects of these fragments on cell viability.

The pIRES_{hyg}-wtAPP₆₉₅ plasmid (Parkin *et al.*, 2007) containing the coding DNA for full-length APP₆₉₅ was used as a template for the generation of an sAPP α PCR fragment. Forward Primer A (Table 2.1, Materials and Methods) containing a 5' EcoRV restriction site and Kozak sequence and reverse Primer B (Table 2.1, Materials and Methods) (with a 3' NotI restriction site) possessing a stop codon after the codon encoding Lys16 of the A β region of APP were employed. Initially, the PCR efficiency was tested at 64, 65, 66 and 67°C annealing temperatures (based around the 65.7-66°C melting temperature of the reverse and forward primers) in order to optimise product generation. Resolving reaction products on agarose gels (Materials and Methods) demonstrated that 64°C was the optimum annealing temperature for the reaction (Figure 4.13A).

Multiple PCR reactions were then performed at 64°C and the PCR product was isolated and ligated into the mammalian expression vector pIRESneo. Following bacterial transformation and overnight culture growth, colonies were stabbed into mini-cultures and plasmid DNA subsequently isolated from each culture. PCR was then performed using the same primers in order to make a provisional determination of which preparations contained the desired sAPP α plasmid. The results (Figure 4.13B) demonstrated that 6 of the 7 colonies tested contained the sAPP α coding sequence and repeat 3 was selected for midi-culture growth.

Restriction digests were then performed to test for the presence of the sAPP α PCR fragment in the plasmid isolated from the midiprep. The results (Figure 4.13C) showed that EcoRV linearized the empty pIRESneo control vector to give an expected band size of 5.3 kb. Digests of the midiprep plasmid were successfully linearized by EcoRV or NotI to produce a band size of 7.1 kb; 1.8 kb higher than the empty pIRESneo (the difference equivalent to the sAPP α coding sequence). Furthermore, a double digest resulted in two bands; one at 5.3 kb corresponding to empty pIRESneo and the other at 1.8 kb corresponding to the sAPP α coding DNA insert.

In order to confirm the correct sequence of the sAPP α coding region the plasmid was sequenced by the MRC DNA Sequencing Service (University of Dundee, Dundee, UK). Although the completed construct was sequenced, in particular, the results showed the correct insertion of the TAG stop codon downstream of the codon encoding Lys16 of the APP A β region (Figure 4.13D).

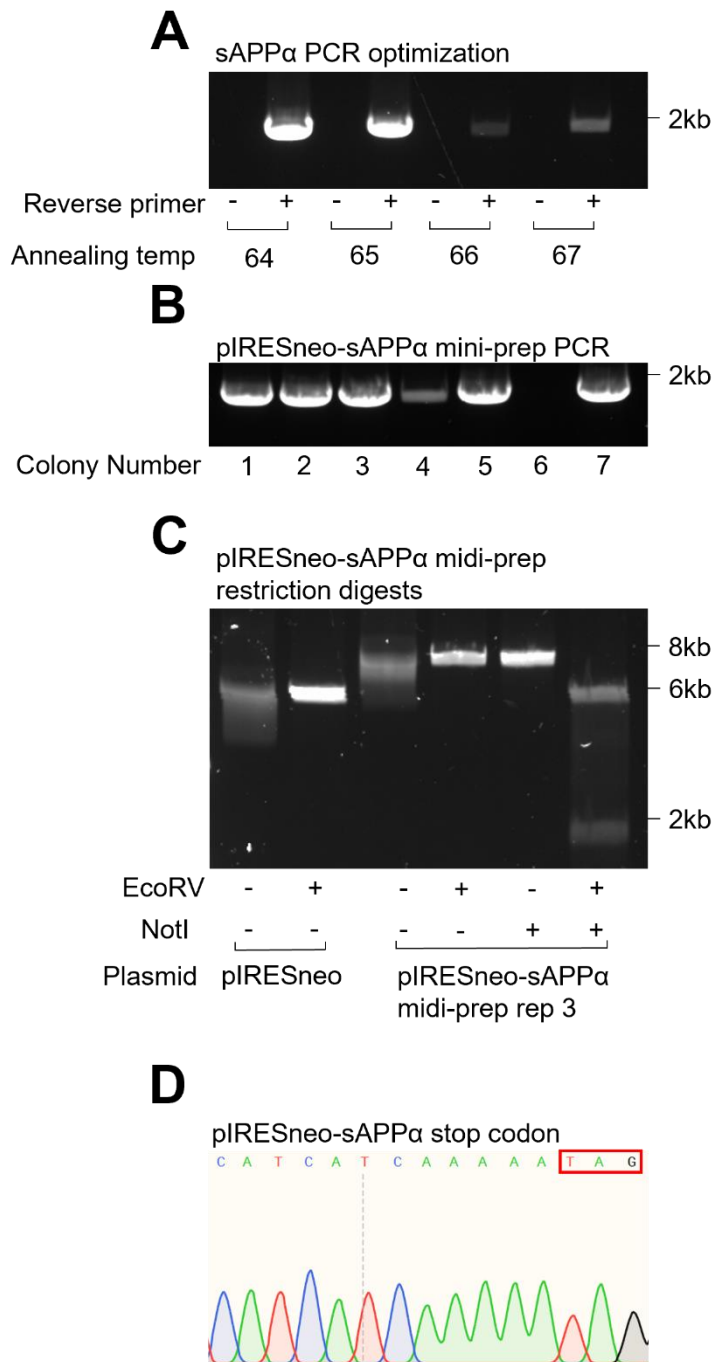


Figure 4.13: Generation of the pIRESneo-sAPP α construct. pIRESHyg-wtAPP₆₉₅ was used as a template for the amplification of sAPP α for insertion into the pIRESneo vector. **(A)** PCR

optimization to amplify sAPP α at different annealing temperatures. **(B)** PCR to confirm presence of sAPP α in different pIRESneo-sAPP α mini-preps. **(C)** Restriction digests to confirm presence of sAPP α in pIRESneo-sAPP α midi-prep colony number 3. **(D)** The 3' coding region of pIRESneo-sAPP α with the stop codon highlighted.

pIRESHyg-wtAPP₆₉₅ was also used as a PCR template for the generation of an sAPP β ' construct. PCR optimizations were performed as described in the Materials and Methods section using Forward Primer A (Table 2.1, Materials and Methods) containing a 5' EcoRV restriction site and Kozak sequence. Reverse Primer C (Table 2.1, Materials and Methods) (with a 3' NotI restriction site) was designed to introduce a stop codon after the codon encoding Tyr10 of the A β region of APP generating a sequence analogous to sAPP β '. Note that the TAT codon encoding tyrosine was altered to TAC (a non-coding change) in the primer to facilitate a suitable primer melting temperature. The PCR efficiency was again tested at 64, 65, 66 and 67°C annealing temperatures to optimize product generation (based around the 66-67°C melting temperature of the primers as found in Table 2.1). Resolving the reaction products on agarose gels (Materials and Methods) demonstrated the optimum annealing temperature was again 64°C (Figure 4.14A).

Multiple PCR reactions were then performed at 64°C and the PCR product was isolated and ligated into pIRESneo. Following bacterial transformation and overnight culture growth, colonies were stabbed into mini-cultures and plasmid DNA subsequently isolated from each culture. PCR was then performed using the same primers in order to make a provisional determination of which preparations contained the desired sAPP β ' insert. The results (Figure 4.14B) demonstrated that 5 of the 7 colonies tested contained the sAPP β ' coding sequence and colony 4 was selected for midi-culture growth.

Restriction digests were then performed to test for the presence of sAPP β ' in the plasmid isolated from the midiprep. The results (Figure 4.14C) show that EcoRV again linearized pIRESneo to produce a fragment size of 5.3 kb. The putative sAPP β ' midiprep plasmid was successfully linearized by EcoRV or NotI

to give a band size of 7.1 kb; 1.8 kb higher than the empty pIRESneo (the difference equivalent to the sAPP β ' coding sequence). Furthermore, a double digest with both enzymes resulted in two bands; one at 5.3 kb corresponding to empty pIRESneo and the other at 1.8 kb corresponding to the sAPP β ' coding DNA insert.

In order to confirm the correct sequence of the sAPP β ' coding region the plasmid was sequenced as described previously and the results, in particular, demonstrated the correct insertion of the TAG stop codon downstream of the codon encoding Tyr10 of the APP A β region (Figure 4.14D).

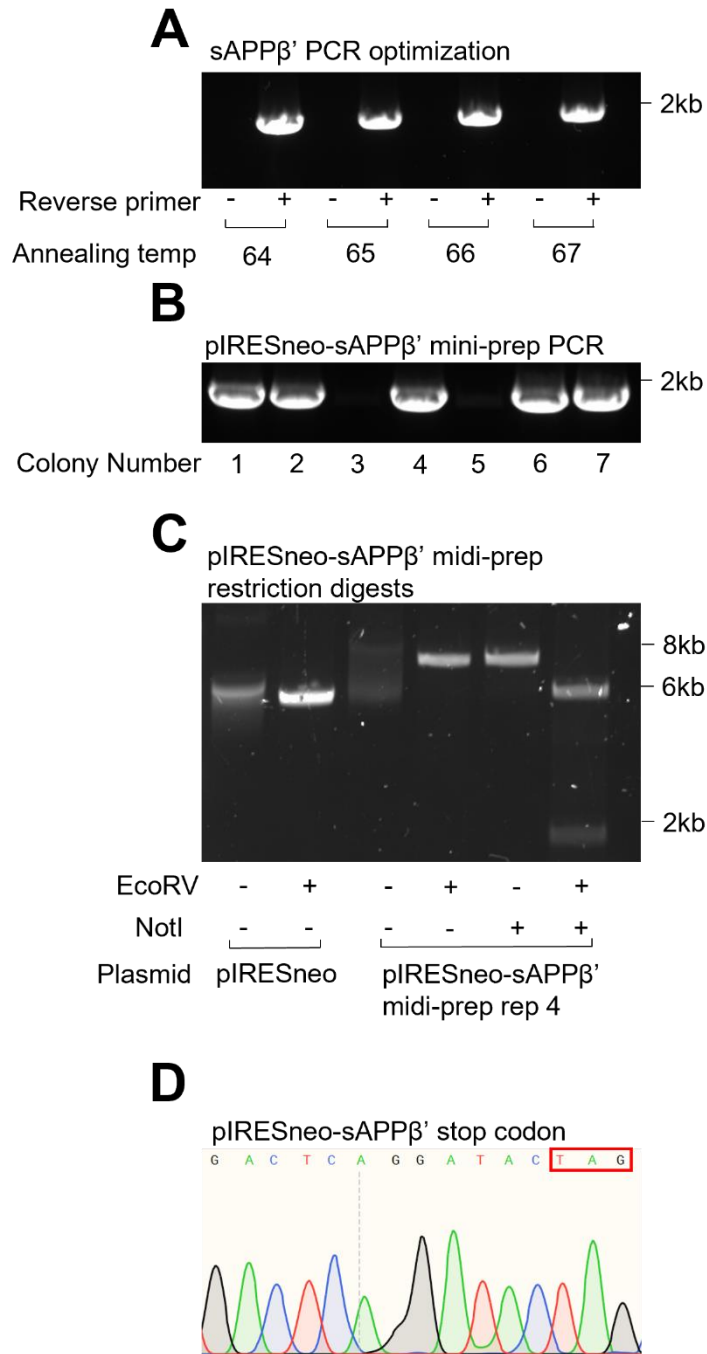


Figure 4.14: Generation of the pIRESneo-sAPP β ' construct. pIRESHyg-wtAPP₆₉₅ was used as a template for the amplification of sAPP β ' for insertion into the pIRESneo vector. **(A)** PCR optimization to amplify sAPP β ' at different annealing temperatures. **(B)** PCR to confirm presence of sAPP β ' in different pIRESneo-sAPP β ' mini-preps. **(C)** Restriction digests to confirm presence of sAPP β ' in pIRESneo-sAPP β ' midi-prep colony number 3. **(D)** The 3' coding region of pIRESneo-sAPP β ' with the stop codon highlighted.

The pIRESneo-sAPP α and pIRESneo-sAPP β' constructs or the empty pIRESneo vector were then stably transfected into Mock (pIRESHyg)- and BACE1-transfected SH-SY5Y cells as described in the Materials and Methods section. The cells were then grown to confluence and medium conditioned. In order to determine whether sAPP α or sAPP β' over-expression had any effect on endogenous full-length APP expression, equal amounts of protein from the resultant lysates were resolved and immunoblotted with anti-APP C-terminal antibody. The results (Figure 4.15A and C) showed little change in full-length APP expression in the Mock- and BACE1-transfected cells following sAPP α or sAPP β' over expression. The exception was a slight reduction in full-length APP expression in SH-SY5Y-BACE1 cells transfected with sAPP α (a 17.36 ± 10.78 % reduction relative to the pIRESneo-transfected controls) (Figure 4.15C). Equal protein loading was confirmed by immunoblotting for actin (Figure 4.15B and D).

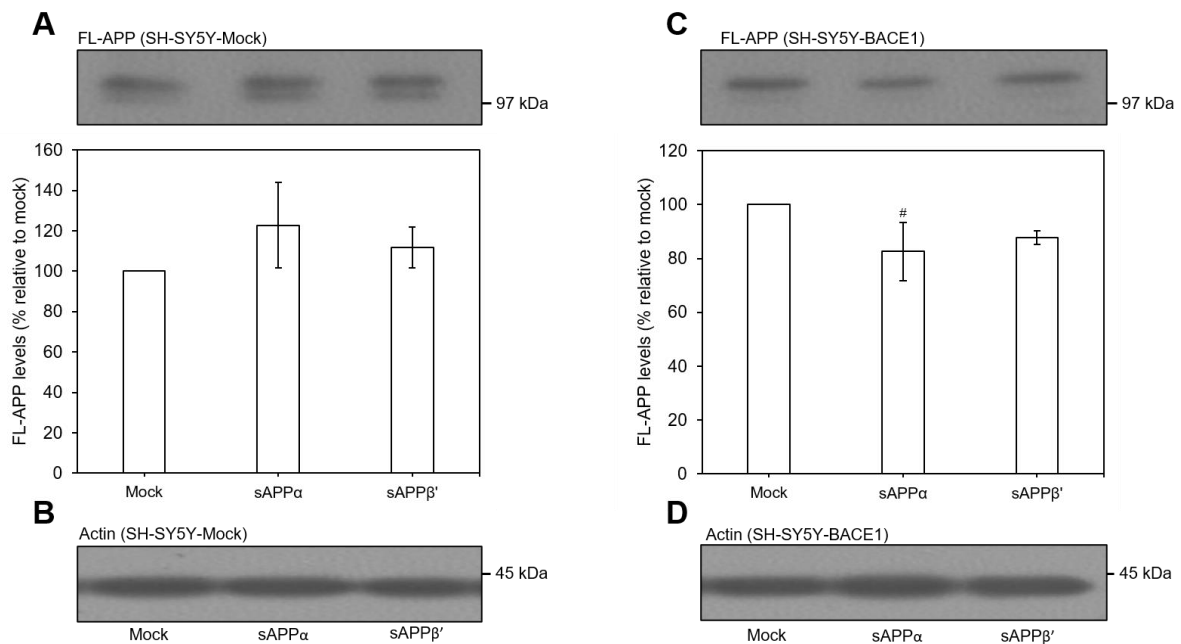


Figure 4.15: Endogenous APP expression in sAPP α - and sAPP β' -transfected stable cell lines. Mock- (**A and B**) and BACE1-transfected (**C and D**) SH-SY5Y cell lines were double transfected with pIRESneo-sAPP α or -sAPP β' constructs. (**A and C**) Anti-APP immunoblots. Multiple immunoblots were subjected to densitometric quantification and the results are expressed relative to the Mock-transfected control. (**B and D**) Anti-actin immunoblots. All results are means \pm S.D. (n=3). Significant results from one-way ANOVA analysis are indicated; * = significant at $p \geq 0.05$. Hash symbols (#) represent the same significance levels relative to the Mock-transfected controls.

In order to confirm the correct over-expression of the soluble APP constructs, equal volumes of concentrated conditioned medium from the pIREShyg Mock-transfected SH-SY5Y cells double transfected with the sAPP constructs or empty pIRESneo were initially immunoblotted with anti-APP 6E10 antibody. The results (Figure 4.16A) revealed increases in the sAPP₆₉₅ band in SH-SY5Y-Mock cells double transfected with sAPP α and sAPP β' constructs (3.16 ± 0.53 -fold and 2.59 ± 0.59 -fold, respectively, relative to the double Mock-transfected control). This confirmed that the 6E10 antibody was cross-reacting with both sAPP α and sAPP β' . There was also a significant decrease in the endogenous sAPP_{751/770} band when cells were transfected with the sAPP α construct (37.90 ± 18.18 % relative to the double Mock-transfected control).

The same conditioned medium samples were also immunoblotted with the anti-sAPP β antibody (Figure 4.16B). Quantification of the resultant immunoblots revealed significant decreases in the sAPP β _{751/770} band following transfection of SH-SY5Y pIREShyg-Mock cells with the sAPP α and sAPP β' constructs (57.01 ± 22.49 and 50.55 ± 2.09 %, respectively, relative to controls).

Finally, to confirm that sAPP α and sAPP β' were the dominant soluble APP fragments produced in their cognate transfectants, the conditioned medium was immunoblotted with anti-APP N-terminal (22C11) antibody (Figure 4.16C). pIRESneo-sAPP α and pIRESneo-sAPP β' transfection increased sAPP₆₉₅ levels by 4.18 ± 0.50 -fold and 3.89 ± 0.37 -fold, respectively, relative to the double Mock-transfected controls. This was coupled with significant reductions in the intensities of the sAPP_{751/770} bands (by 65.34 ± 14.23 and 64.18 ± 15.56 %, respectively in the case of sAPP α and sAPP β' transfectants).

The same experiments were then repeated in the SH-SY5Y-BACE1 cells. Immunoblotting of conditioned medium using anti-APP 6E10, again, revealed the expected increases in sAPP released from the sAPP α - and sAPP β' -transfected cells (3.27 ± 0.92 - and 3.33 ± 0.28 -fold, respectively, compared to pIRESneo transfected SH-SY5Y-BACE1 controls) (Figure 4.16D). Concomitant reductions in sAPP_{751/770} production were also observed (by 44.82 ± 2.16 and 11.33 ± 4.19

%, respectively, in sAPP α - and sAPP β '-transfected cells relative to pIRESneo transfected SH-SY5Y-BACE1 controls).

When the medium from the SH-SY5Y-BACE1 cell double transfectants was immunoblotted using the anti-sAPP β antibody the results (Figure 4.16E) showed a slight increase in the amounts of sAPP β ₆₉₅ produced following transfection with sAPP α and sAPP β ' (41.12 \pm 14.65 % and 58.77 \pm 8.28 % relative to the pIRESneo-transfected SH-SY5Y-BACE1 control cells).

Finally, immunoblotting the conditioned medium samples using the anti-APP N-terminal (22C11) antibody confirmed that the stably transfected sAPP α and sAPP β ' were the major soluble APP fragments generated by their cognate transfectants (Figure 4.16F).

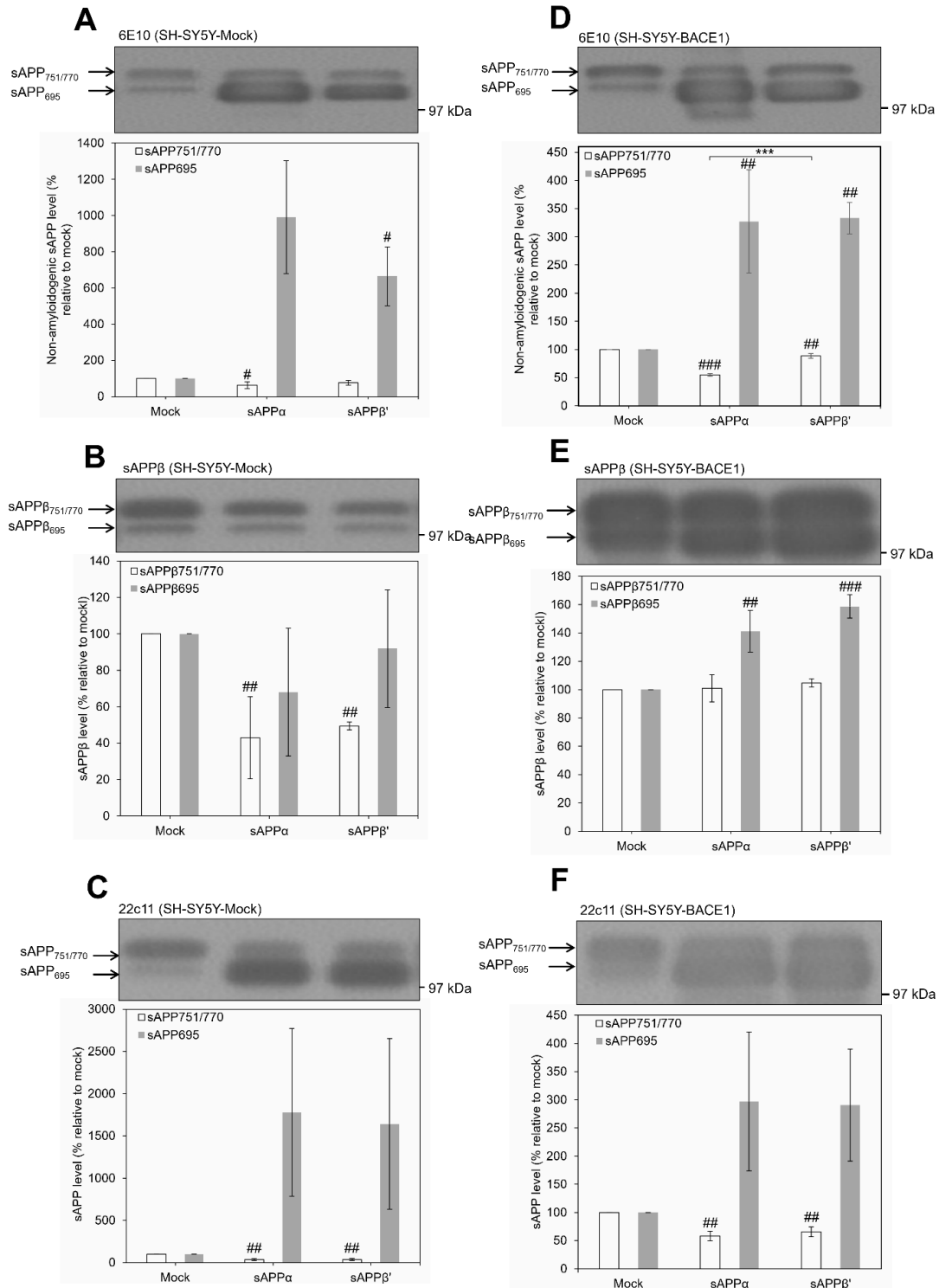


Figure 4.16: Soluble APP production by sAPP α and sAPP β' stable cell lines. Mock- (A,B,C) and BACE1-transfected (D,E,F) SH-SY5Y cells double transfected with sAPP α and sAPP β' were grown to confluence and incubated in reduced serum medium for 24 hours. Cells were harvested, medium conditioned and equal volumes of proteins were then resolved by SDS-PAGE. (A and B) Anti-APP 6E10 immunoblots. (B and E) Anti-sAPP β immunoblots. (C and F) Anti-APP NT 22C11 immunoblots. Multiple immunoblots were subjected to densitometric quantification and the results are expressed relative to the Mock-transfected control. All results are means \pm S.D. (n=3). Significant results from one-way ANOVA analysis are indicated; * = significant at $p \geq 0.05$; ** =

significant at $p \geq 0.01$; *** = significant at $p \geq 0.001$. Hash symbols (#) represent the same significance levels relative to the Mock-transfected controls.

4.5 The effect of sAPP α and sAPP β' over expression on the viability of Mock- and BACE1-transfected SH-SY5Y cells

Having verified the overexpression of sAPP α and sAPP β' in the various SH-SY5Y transfectants, we next sought to determine the effects of these fragments on cell viability. To achieve this the Mock- and BACE1-double transfected SH-SY5Y cells were seeded at identical densities and cultured over a 12-day growth period with viability measured at stated time points (see Materials and Methods). Initial trypan blue assays demonstrated that the sAPP α constructs in Mock- and BACE1-transfected SH-SY5Y cells significantly increased their cell viability relative to their respective Mock-transfected controls (Figure 4.17A and B). In contrast, the sAPP β' construct caused a significant reduction in viability by 9.39 ± 0.47 and 26.99 ± 1.36 %, respectively, in Mock- and BACE1-transfected cells, relative to the double Mock-transfected controls (Figure 4.17B).

The viability experiment was then repeated using the MTS assay (see Materials and Methods). The results (Figure 4.17C-D) more clearly demonstrate the negative effect of sAPP β' overexpression in SH-SY5Y-BACE1 cells, leading to a 40.89 ± 5.24 % reduction in viability compared to the pIRESneo-transfected SH-SY5Y-BACE1 cells. The MTS assay also recapitulated the beneficial effect of sAPP α overexpression on cell viability in both Mock- and BACE1-transfected cells (19.67 ± 2.37 and 24.95 ± 5.83 % increases in viability, respectively, relative to cognate pIRESneo-transfected controls).

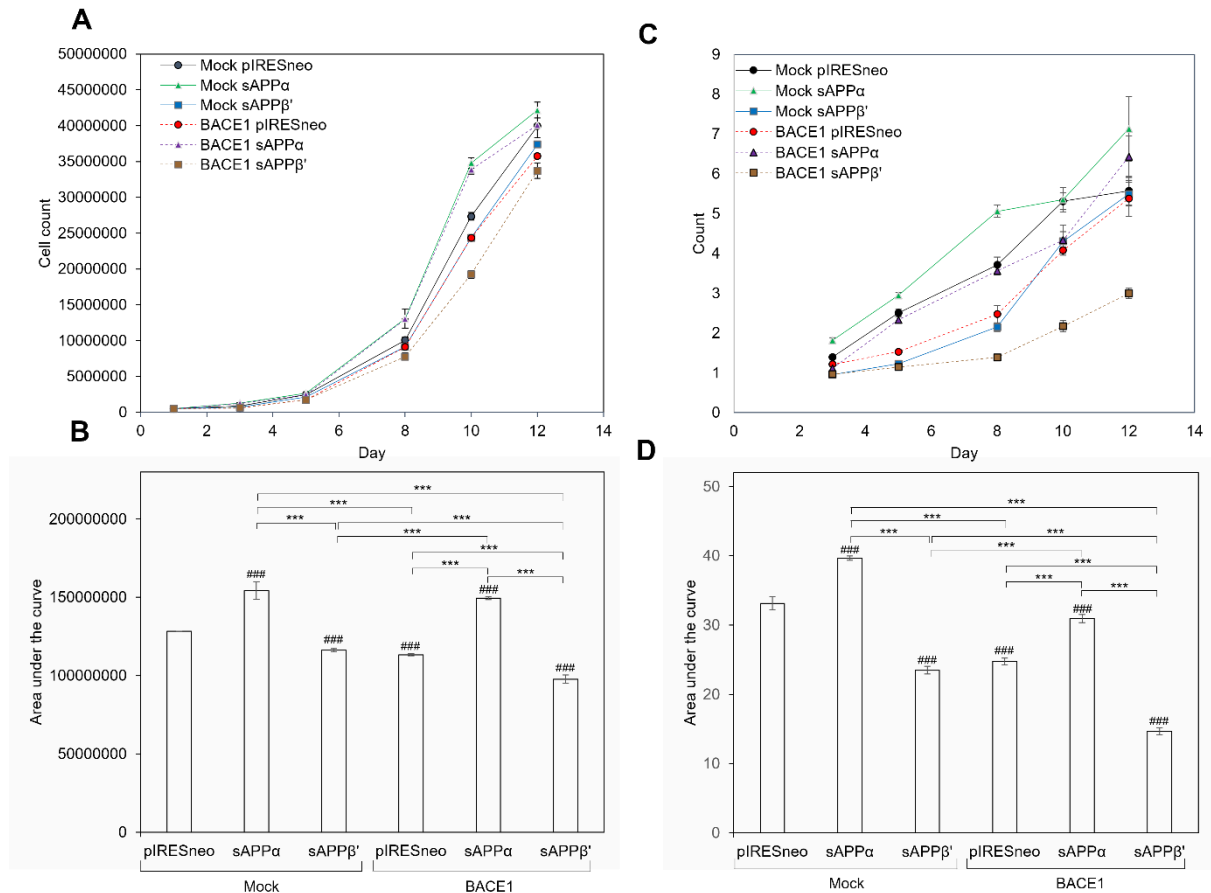


Figure 4.17: Cell viability assays in Mock- and BACE1-transfected SH-SY5Y cells. Mock- and BACE1-transfected SH-SY5Y cells double transfected with sAPP α and sAPP β' were seeded at a density of $2 \times 10^4/\text{cm}^2$ and cultured over a 12 day growth period. At the relevant time points, the viability assays were employed as described in the Materials and Methods. **(A)** Trypan blue cell viability curve. **(B)** Area under the curve analysis (AUC) for Trypan blue cell count. **(C)** Methanethiosulfonate (MTS) assay cell viability curve. **(D)** AUC for MTS assay count. Results for all viability assays are means \pm S.D. ($n=3$ for cell count and $n=6$ for MTS assay). Significant results from one-way ANOVA are indicated; *** = significant at $p \geq 0.001$. Hash symbols (#) represent the same significance relative to the cognate experiment controls.

4.6 Summary

Examining the non-amyloidogenic release of soluble APP from SH-SY5Y-BACE1 cells revealed a surprising effect in that batimastat did not inhibit the production of these fragments. Reciprocal analysis of C-terminal fragments demonstrated that, in the SH-SY5Y-BACE1 cells, C83 was completely absent in lieu of C89; a BACE1 beta prime generated fragment (represented in Figure

4.18). The ability of β -secretase inhibitor IV, in combination with batimastat, to completely impair sAPP generation by the cells further indicated the involvement of non-canonical BACE1 cleavage of APP.

Despite wtAPP- and Swe-APP-transfected cells generating far more A β -peptides than Mock or BACE1-transfected cells, neither of the former cell lines exhibited corresponding decreases in viability. However, SH-SY5Y-BACE1 cells, despite exhibiting much more moderate increases in A β -peptide production, did exhibit reduced viability relative to Mock transfectant controls. This suggested that it was the lack of sAPP α and/or alternate production of sAPP β ' that caused decreased SH-SY5Y-BACE1 cell viability rather than elevated A β -peptide levels.

When sAPP α and sAPP β ' constructs were overexpressed in Mock- and BACE1-transfected SH-SY5Y cells it was confirmed that the anti-APP 6E10 antibody cross-reacted with both of these soluble fragments. Furthermore, the overexpression of sAPP α was able to restore the viability of BACE1-transfected cells back up to control cell levels. In contrast, sAPP β ' overexpression reduced cell viability in both Mock- and BACE1-transfected cells.

Collectively these data imply that the loss of sAPP α perhaps as much as enhanced A β levels might be neurotoxic in Alzheimer's disease. Furthermore, previous studies employing antibody 6E10 to determine the suitability of changes in sAPP α levels as a biomarker for AD need to be reassessed in light of the cross-reactivity of the antibody with sAPP β '.

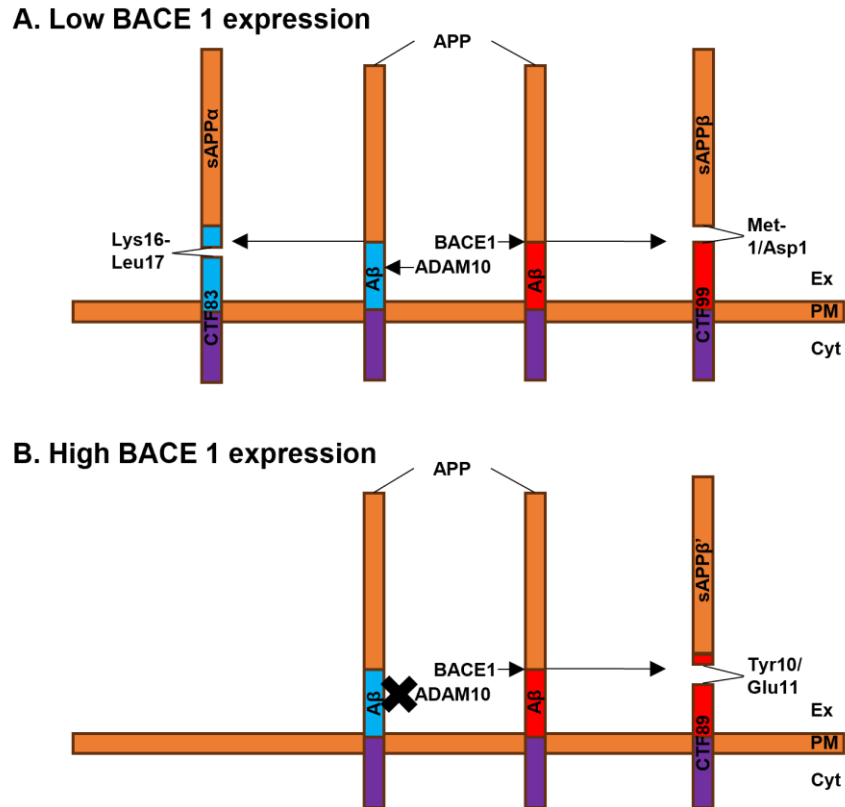


Figure 4.18: Schematic representation of APP metabolism in SH-SY5Y-mock and SH-SY5Y-BACE1 cells. **A.** In SH-SY5Y-mock cells BACE1 expression is low and full-length APP is cleaved predominantly by ADAM10 (α -secretase) between lysine 16 and leucine 17 of the A β region to generate the beneficial sAPP α fragment and the C-terminal fragment CTF83, thus precluding functional A β peptide release. To a lesser extent, APP is cleaved by BACE1 (β -secretase) between methionine 1 and aspartic acid 1, to generate sAPP β and CTF99. CTF99 will go on to release functional A β peptides which are neurotoxic. **B.** In SH-SY5Y-BACE1 cells, BACE1 expression is high and this competes with ADAM10 activity. The result of this is BACE1 cleaving APP at an alternate site between tyrosine 10 and glutamic acid 11, to generate sAPP β' and CTF89. This cleavage once again precludes function A β peptide formation. Ex = extracellular space, PM = plasma membrane, Cyt = cell cytosol. Schematic adapted from Chow et al., 2010 and Owens *et al.*, 2022.

5. Results; Design of inducible, neuron-specific mammalian expression plasmids

5.1 Introduction

In our hands, the two fibrates gemfibrozil and bezafibrate failed to elicit an increase in ADAM10-mediated processing of APP (see Chapter 3). However, we subsequently demonstrated that, at least in SH-SY5Y-BACE1 cells, a decrease in sAPP α production may well have been, at least in part, responsible for the decreased viability of these cells (see Chapter 4). Therefore, we sought to develop an alternative approach to enhancing cellular generation of sAPP α through the design of inducible, neuron-specific mammalian expression plasmids encoding this non-amyloidogenically-derived fragment. Furthermore, as AD is a multi-causational disease, we aimed to create expression systems that could selectively overexpress both sAPP α and a protein that might simultaneously target tau pathology; vacuolar protein sorting-associated protein 35 (VPS35) (Fol *et al.*, 2016; Vagnozzi *et al.*, 2019).

5.2 Design of a dual plasmid doxycycline-inducible neuron-specific expression system

Constitutively over-expressing proteins in a manner that is not cell or tissue specific might well have undesirable consequences/side effects. For example, (Hinderer *et al.*, 2018) reported that the adeno-associated virus-mediated over-expression of survival of motor neuron (SMN) protein in non-human primates resulted in, *inter alia*, ataxia, impaired ambulation, proprioceptive deficits and damaged dorsal root ganglia. Therefore, in the current study, we initially sought to generate a dual plasmid neuron-specific inducible co-expression system for sAPP α and VPS35 based on the commonly used Tet-On plasmid system (Das, Tenenbaum and Berkhout, 2016). This system consists of a **regulator** plasmid encoding a suitable transactivator protein which binds tetracycline/doxycycline and is then able to interact with the promoter on a second, **response**, plasmid controlling expression of downstream genes of interest (Figure 5.1).

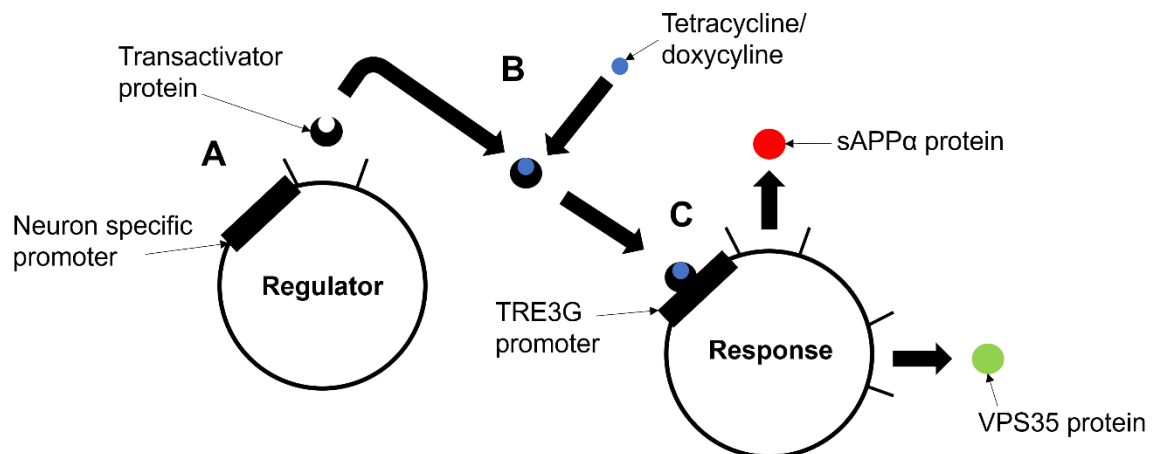


Figure 5.1: Schematic of a neuron-specific Tet-On plasmid system. **A.** A neuron specific promoter controls the expression of a transactivator protein (Tet-On3G) on the regulator plasmid. **B.** The transactivator protein is not functional without the introduction of tetracycline/doxycycline into the system. **C.** The induced transactivator can bind to the TRE3G promoter of the response plasmid which includes the expression of the downstream sAPP α and VPS35 coding sequences.

5.2.1 Dual plasmid system regulator plasmid (pIRESHyg-ESYN-TET3G) design

Initially, we designed a regulator plasmid incorporating the coding DNA for the Tet-On3G transactivator protein under the control of a neuron-specific hybrid promoter consisting of the human cytomegalovirus (CMV) enhancer fused to the human synapsin 1 promoter, which has previously been shown to yield high levels of neuron-specific expression (Hioki *et al.*, 2007). The resultant plasmid, pIRESHyg-ESYN-TET3G, was then synthesized by Epoch Life Science (Missouri City, Texas, USA).

The synthesis of pIRESHyg-ESYN-TET3G, utilized a backbone from the commercial mammalian stable expression vector, pIRESHyg (Clontech-Takara Bio Europe, Saint-Germain-en-Laye, France) (Figure 5.2A). This vector (see Appendix Figure S.1 for full sequence) contains several elements permitting the high-level expression of proteins in mammalian cell cultures. The transcription of downstream coding DNA is under the regulation of the human CMV promoter between nucleotides 232 and 820 (Figure 5.2A) which enables high constitutive protein expression regardless of mammalian cell-type (Yu *et al.*, 2017). This is

followed by a limited multiple cloning site (MCS) between nucleotides 911-971 and an intervening sequence (IVS) between nucleotides 938-1233. The IVS increases the efficiency of RNA processing and accumulation of cytoplasmic RNA (Huang and Gorman, 1990). Of particular importance in this vector is the internal ribosome entry site sequence (IRES) of the encephalomyocarditis virus (ECMV) between nucleotides 1270 and 1856, which permits translation of the resultant mRNA at the ribosome both from this element and the upstream promoter (Jang *et al.*, 1988). Downstream of the IRES is the coding DNA sequence (CDS) for hygromycin phosphotransferase (nucleotides 1869 to 2903), permitting the hygromycin B selection of cells co-expressing any protein encoded within the MCS along with the antibiotic resistance protein (thereby alleviating the requirement for colony selection; (Gurtu, Yan and Zhang, 1996). Following the hygromycin phosphotransferase CDS is a polyA translation termination sequence (nucleotides 3192-3468). Finally, the vector also contains an ampicillin resistance sequence (nucleotides 5548-4727), permitting the selection of effectively transformed bacteria.

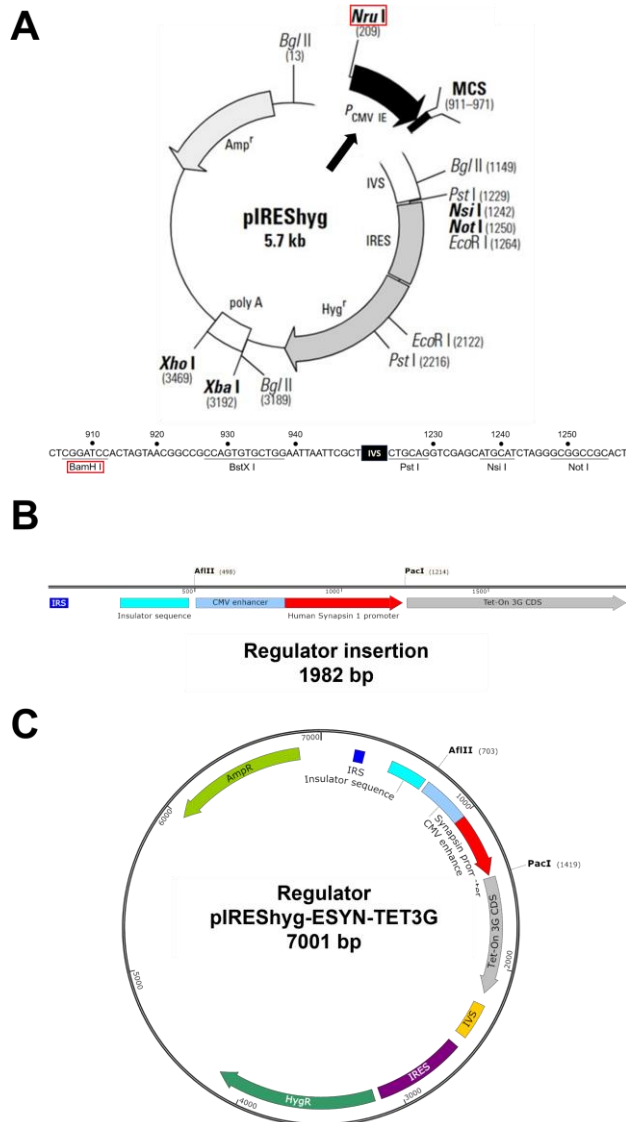


Figure 5.2: Generation of pIRESHyg-ESYN-TET3G from pIRESHyg. **A.** pIRESHyg schematic with NruI and BamH1 restriction sites highlighted. **B.** A new DNA fragment containing, *inter alia*, the neuron-specific hybrid promoter and Tet-On 3G CDS was synthesized *de novo* and ligated into the NruI and BamH1 sites in the larger of the two fragments generated in panel A. **C.** Schematic of the final pIRESHyg-ESYN-TET3G regulator plasmid.

In order to generate pIRESHyg-ESYN-TET3G, the pIRESHyg parent vector was cleaved with NruI and BamH1 which cleave in unique sites, respectively, upstream of the CMV promoter and within the MCS (Figure 5.2A). The smaller cleaved fragment (consisting essentially of the CMV promoter and the first part of the MCS) was removed and the BamH1 overhang of the remaining pIRESHyg backbone was filled in to generate a blunt end (NruI cleaves to give a

blunt end anyway). A newly synthesized sequence consisting, *inter alia*, of the new neuron-specific hybrid promoter and CDS for the Tet-On3G transactivator protein (Figure 5.2B), was then blunt-end ligated into the vector to generate the final pIREShyg-ESYN-TET3G plasmid (Figure 5.2C; full sequence shown in Appendix Figure S.2).

The new promoter (Figure 5.3) was designed to provide neuron-specific expression of the downstream transactivator protein and consisted of the enhancer region of the CMV promoter fused to the promoter region of human synapsin 1. This type of 'hybrid' promoter has previously been shown to provide for an effective balance of neuronal specificity, whilst maintaining suitable high levels of protein expression (Hioki *et al.*, 2007). Note that AflIII and PacI restriction sites were incorporated, respectively, at the 5' and 3' ends of the promoter sequence in order to permit the subsequent excision and replacement of this element with an alternative pan cell-type promoter sequence (Figure 5.2B).

```
CTTAAGCGTTACATAACTTACGGTAAATGGCCCGCCTGGCTGACCGCCCAACGAC
CCCCGCCCATTTGACGTCAATAATGACGTATGTTCCCATAGTAACGCCAATAGGGACTTTCC
ATTGACGTCAATGGGTGGAGTATTTACGGTAAACTGCCCACTTGGCAGTACATCAAGTGTA
TCATATGCCAAGTACGCCCCCTATTGACGTCAATGACGGTAAATGGCCCGCCTGGCATTAT
GCCCAGTACATGACCTTATGGGACTTTCTACTTGGCAGTACATCTACGTATTAGTCATCG
CTATTACCATGGCTGCAGAGGGGCCCTGCGTATGAGTGCAAGTGGGTTTTAGGACCAGGAT
GAGGCGGGGTGGGGGTGCCTACCTGACGACCCGACCCGACCCACTGGACAAGCACCCAA
CCCCATTCCCAAATTGCGCATCCCCTATCAGAGAGGGGGGAGGGGAAACAGGATGCGG
CGAGGCGCGTGCGCACTGCCAGCTTCAGCACCGCGGACAGTGCCTTCGCCCCCGCCTGG
CGGCGCGCGCCACCGCCGCCTCAGCACTGAAGGCGCGCTGACGTCACTCGCCGGTCCC
CCGCAAACCTCCCTTCCCGGCCACCTTGGTCGCGTCCGCGCCGCGCCGCGCCAGCCGG
ACCGCACACGCGAGGCGCGAGATAGGGGGGCACGGGCGCGACCATCTGCGCTGCGGC
GTTAATTAA
```

Figure 5.3: Nucleotide sequence of the hybrid promoter region incorporated into pIREShyg-ESYN-TET3G. The CMV promoter enhancer region (cyan) is fused directly to the human synapsin 1 promoter region (red). The entire sequence is then flanked with AflIII and PacI (5' and 3', respectively) restriction sites (green) in order to permit subsequent excision and replacement of the hybrid promoter sequence.

5.2.2 Dual plasmid system response plasmid (pIRESzeo-sAPP α -VPS35) design

In order to generate the response plasmid (pIRESzeo-sAPP α -VPS35), pIRESHyg was digested with NruI and XhoI which cleave upstream of the CMV promoter and directly downstream of the polyA termination sequence, respectively (Figure 5.4A). Following removal of the larger fragment (consisting of all the elements from the CMV promoter through to and including the polyA tail), the XhoI sticky end of the smaller fragment was filled in to give a blunt end (NruI cleaves in a blunt fashion).

A newly synthesized insert (Figure 5.4B) was then blunt-end ligated in such that the original NruI and XhoI sites were retained. The key elements of the new insert consisted of a TRE3G promoter (between nucleotides 218 and 596 of the complete response plasmid sequence) gleaned from the sequence of the commercial vector pTRE3G-mCherry (Clontech, Paisley, UK). This was followed by a first MCS flanking the human sAPP α CDS (between nucleotides 622 and 2460), an IVS (nucleotides 2523-2752), the first of two IRES sequences (nucleotides 2810-3383), a second MCS this time flanking the CDS of human VPS35 (nucleotides 3506-5896), the second of two IRES sequences (nucleotides 5938-6511), the CDS for *sh ble* encoding zeocin resistance (nucleotides 6559-6933) and, finally, a polyA tail (nucleotides 7225 and 7501).

The resultant pIRESzeo-sAPP α -VPS35 response plasmid is shown in Fig. 5.4C and the full sequence is detailed in Appendix Figure S.3.

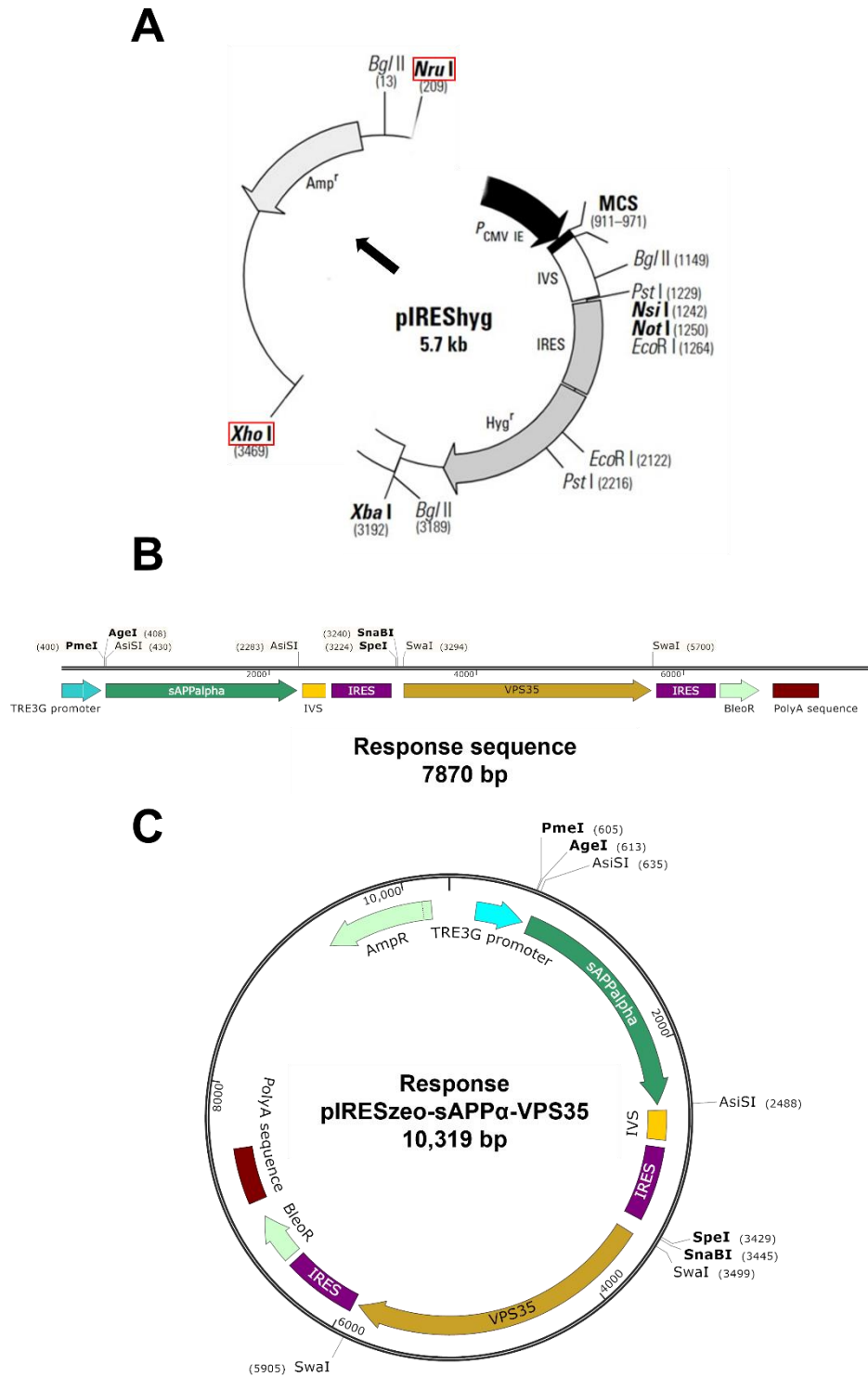


Figure 5.4: Generation of pIRESzeo-sAPP α -VPS35 from pIREShyg. **A.** pIREShyg schematic with NruI and XhoI restriction sites highlighted. **B.** A new DNA fragment containing, *inter alia*, the TRE3G promoter, IRES sequence, sAPP α and VPS35 CDS was synthesized *de novo* and ligated into the NruI and BamH1 sites in the larger of the two fragments generated in panel A. **C.** Schematic of the final pIRESzeo-sAPP α -VPS35 response plasmid.

5.3 Design of a single plasmid PiggyBac doxycycline-inducible neuron-specific expression system

In the dual plasmid expression system described above, all three coding DNA sequences, including that of hygromycin phosphotransferase, were separated by IRES elements and under the transcriptional control of the same TRE3G promoter. This design dictates that the expression of the genes of interest (in this case sAPP α and VPS35) would have to be induced in order to simultaneously induce hygromycin phosphotransferase expression and impart antibiotic resistance to cells for the purpose of selection. This design would become problematic should the genes of interest being expressed be toxic to cells; in this case it would be impossible to select successfully transfected cells.

In order to circumvent this issue, both the regulator and response plasmids of the dual plasmid system were future-proofed to incorporate core insulator (CI) and inverted terminal repeat (ITR) sequences that would permit their molecular combination to generate a single PiggyBac plasmid expression system. This process is discussed below.

Beginning with the original response plasmid, pIRESzeo-sAPP α -VPS35, the zeocin resistance CDS (sh ble), which would be redundant in the final PiggyBac plasmid, was removed by cleaving it out using the flanking BsiWI restriction sites (Figure 5.5A). Additionally, as the sAPP α CDS contained a XhoI site that would subsequently interfere with PiggyBac plasmid generation, this too was removed from pIRESzeo-sAPP α -VPS35 by PmeI/AgeI restriction digest (Figure 5.5A). The resultant response plasmid (Fig. 5.5B) was then digested with XhoI and the larger fragment shown in Fig. 5.5B was isolated.

The pIREShyg-ESYN-TET3G regulator plasmid (Figure 5.5C) was then also digested with XhoI and the fragment shown in Figure 5.5D was isolated. The two fragments shown in Figure 5.5B and Figure 5.5D were then ligated to produce the pre-PiggyBac plasmid shown in Figure 5.5E and the final PiggyBac plasmid shown in Figure 5.6F (full sequence provided in Appendix Figure S.5) can be

completed with the sAPP α CDS cloned back into MCS1 as desired. The schematic of the full PiggyBac plasmid can be seen in Figure 5.6.

The original regulator and response plasmids possess ITR and CI elements essential for PiggyBac formation. The ITRs enable self-complementary base pairing as featured in transposable agents whilst the insulators protect the PiggyBac transposon from coming under the influence of other coding regions in the eukaryotic cell and can increase the likelihood of stable cell transfections (Mossine *et al.*, 2013).

These elements (the sequences for which were taken from the commercial pB513B-1 vector System Biosciences, Mountain View, USA) are positioned preceding the promoter in the regulator plasmid and after the final polyA tail of the response plasmid. Following combination of the two plasmids as described above, these elements flank the entire transposon sequence in the resultant PiggyBac plasmid (Figure 5.6).

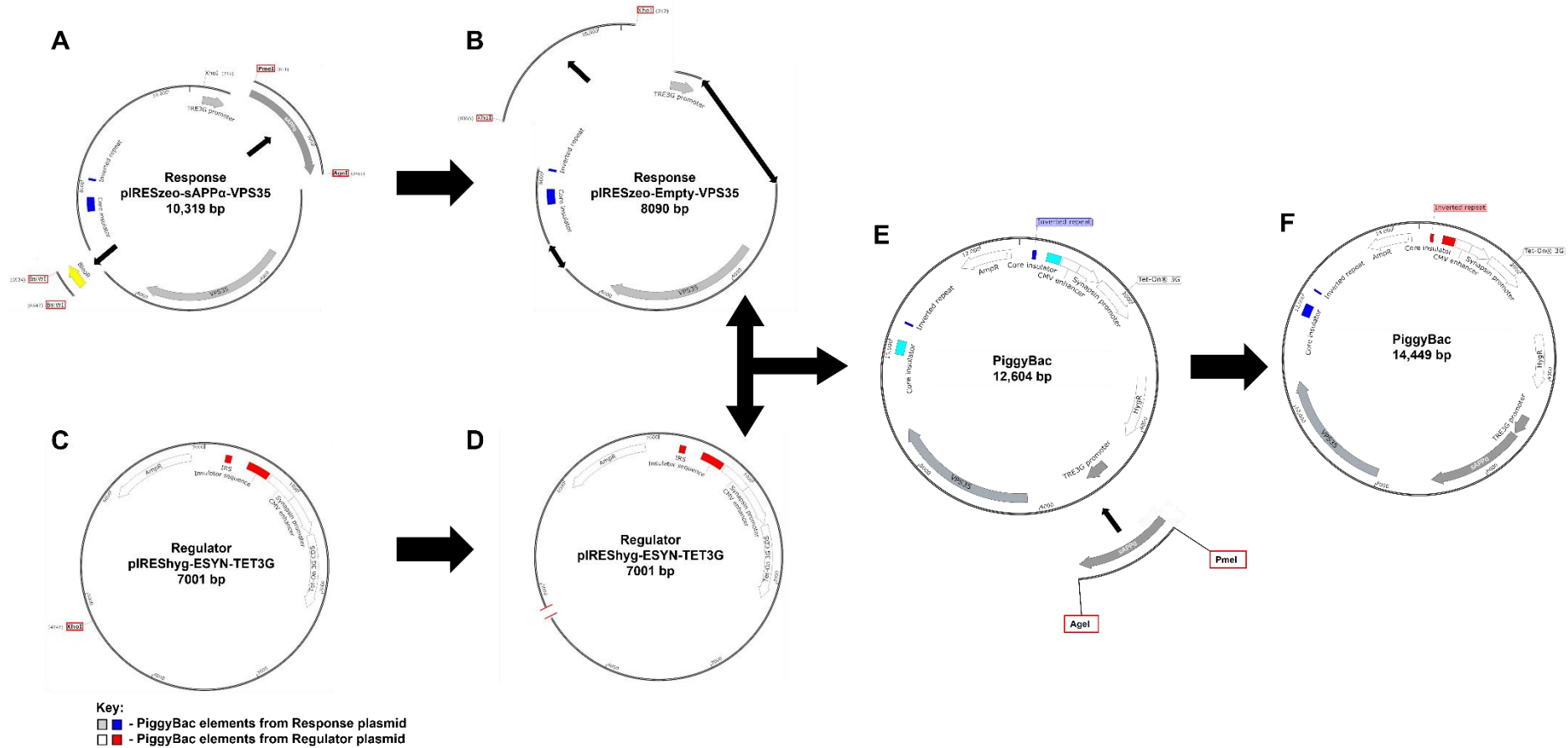


Figure 5.5: Generation of the PiggyBac plasmid. **A.** pIRESzeo-sAPP α -VPS35 was sequentially digested with BsiWI restriction sites to excise the *sh ble* coding sequence (zeocin resistance) and PmeI/Agel to remove sAPP α . **B.** The resultant response plasmid is then cleaved with XhoI (both sites highlighted in red) and the large fragment is isolated. **C.** pIREShyg-ESYN-TET3G with a single XhoI restriction site for response insertion. **D.** The resultant regulator large fragment generated from XhoI cleavage, ready for PiggyBac generation. **E.** A combination of the XhoI digested regulator and response plasmids (B and D), to

generate a single PiggyBac plasmid. sAPP α is PCR amplified and inserted into the PiggyBac utilising PmeI and AgeI restriction sites. **F.** The final PiggyBac plasmid.

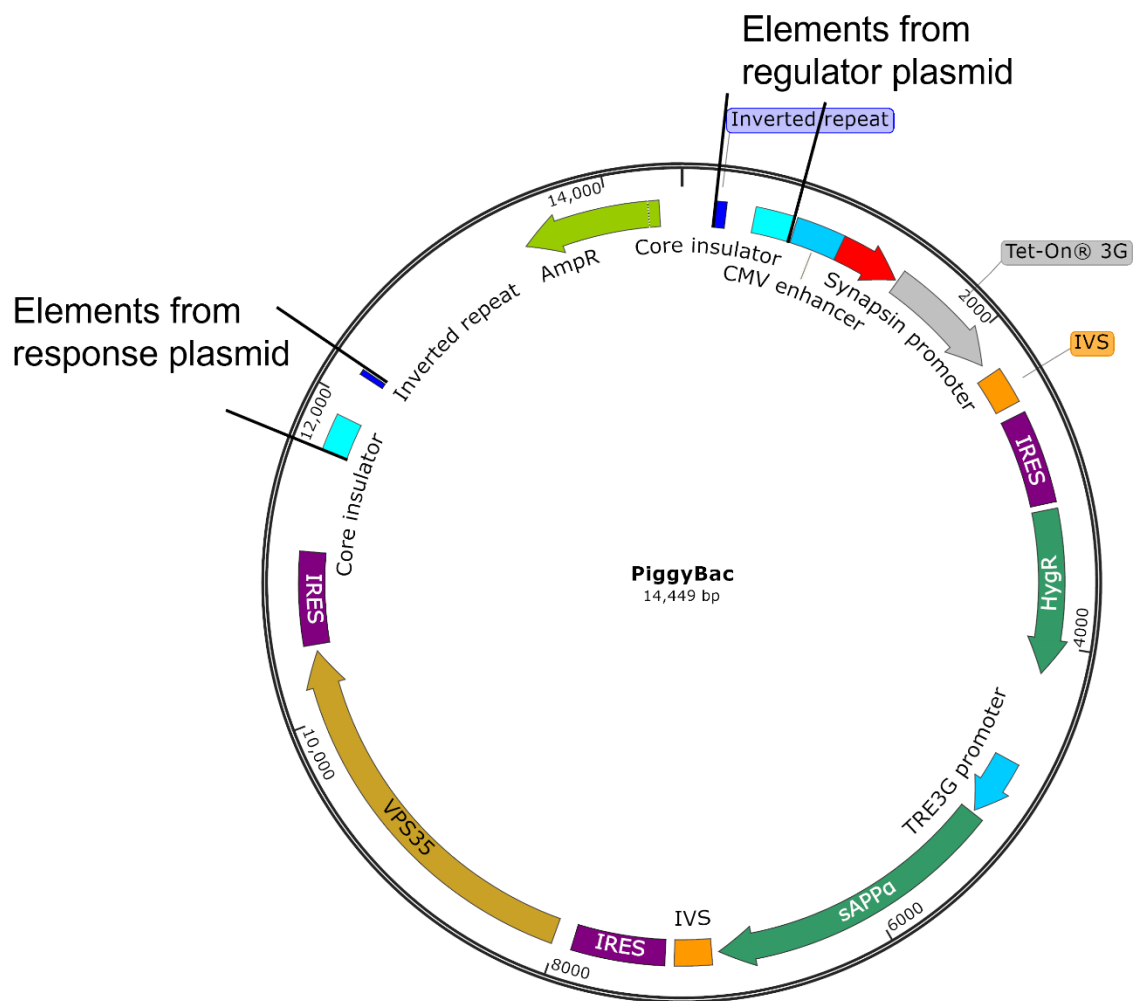


Figure 5.6: Schematic of the transposon region and PiggyBac plasmid. A. Schematic of the transposon region highlighting which elements are from the original dual plasmid system response and regulator plasmids. **B.** A full schematic of the PiggyBac plasmid. The key elements discussed in the main text are: the inverted repeat sequences (nucleotides 212-274 and 12161-12194) and the core insulator sequence from the pB513B-1 vector (nucleotides 451-685 and 11652-11885).

5.4 Summary

The plasmid designs detailed in the current chapter describe, first, a dual plasmid system for the neuron-specific inducible expression of sAPP α and VPS35 and, second, the combination of this first system to generate a PiggyBac transposon plasmid. The latter system should circumvent the selection issues inherent in the design of the two-plasmid system (in the event that the genes of interest are cytotoxic). The experimental generation of some of the plasmids and their derivatives are detailed in the following chapter.

6. Results; Stable SH-SY5Y transfectants for the study of protective proteins as potential therapies for AD

6.1 Introduction

Initially the synthesis of the regulator (pIRES_{hyg}-ESYN-TET3G) and response (pIRES_{zeo}-sAPP α -VPS35) plasmids designed in the previous chapter was outsourced to Epoch Life Science (Missouri City, Texas, USA). The current chapter describes the downstream characterisation of these plasmids and the generation of next generation versions required for the neuron-specific inducible expression of sAPP α and VPS35.

6.2 Generation of a cytomegalovirus promoter version of the pIRES_{hyg}-ESYN-TET3G regulator plasmid

As described in the previous chapter, pIRES_{hyg}-ESYN-TET3G was originally synthesized by Epoch Life Science to contain a neuron specific promoter flanked by AflII and PacI restriction sites to enable the facile replacement of the promoter with a pan cell-type relevant promoter i.e. the cytomegalovirus (CMV) promoter (Wilkinson and Akrigg, 1992).

The original empty pIRES_{hyg} vector (Clontech-Takara Bio Europe, Saint-Germain-en-Laye, France) was used as a template for the PCR of the CMV promoter. The PCR was performed as described in the Materials and Methods section using forward Primer D (Table 2.1, Materials and Methods) containing a 5' Afl II restriction site and reverse Primer E (Table 2.1, Materials and Methods) containing a 3' PacI restriction site. Initially, the PCR efficiency was tested at 61, 63 and 65°C annealing temperatures (based upon the 63 and 65°C melting temperatures of the primers) to optimize product generation. The resultant reactions were run on agarose gels (Materials and Methods) and the results (Figure 6.1A) showed that 61°C was the optimum annealing temperature resulting in the formation of the highest quantity of a 500 bp fragment as expected for amplification of the CMV promoter from pIRES_{hyg}.

Multiple PCR reactions were then performed using an annealing temperature of 61°C and, once isolated, the PCR product and original pIRES_{hyg}-ESYN-TET3G regulator plasmid were both restriction digested with PacI and

AfIII. Following gel resolution of the regulator plasmid (now lacking the ESYN promoter) and the digested PCR-generated CMV promoter fragment, the two were ligated to generate the CMV regulator plasmid (pIREShyg-CMV-TET3G). Following bacterial transformation of the ligation reaction and overnight culture growth, colonies were stabbed into mini-cultures (see Materials and Methods). PCR using the afore mentioned primers was then performed on the DNA isolated from these mini-cultures in order to determine which contained the desired plasmid. Resolution of these reactions on an agarose gel (Figure 6.1B) revealed that each of the colonies contained the CMV coding sequence and colony 1 was selected for midi-culture growth. The plasmid isolated from this midi-culture along with the original pIREShyg-ESYN-TET3G regulator plasmid were then subjected to restriction digests in order to confirm the presence of the CMV promoter in the former plasmid (Figure 6.1C). Both AfIII and PacI, individually, linearized pIREShyg-ESYN-TET3G to generate a fragment of 7.0 kb. Double digest of the same plasmid with the two enzymes, in addition to a band at about 6.8 kb, yielded a fragment at about 0.7 kb consistent with the 706 bp size of the excised ESYN promoter. Whilst double digest of the putative pIREShyg-CMV-TET3G plasmid also generated a 6.8 kb band, the band corresponding to the excised CMV promoter ran slightly smaller (0.5 kb) than the excised ESYN promoter consistent with the expected 508 bp size of the former promoter.

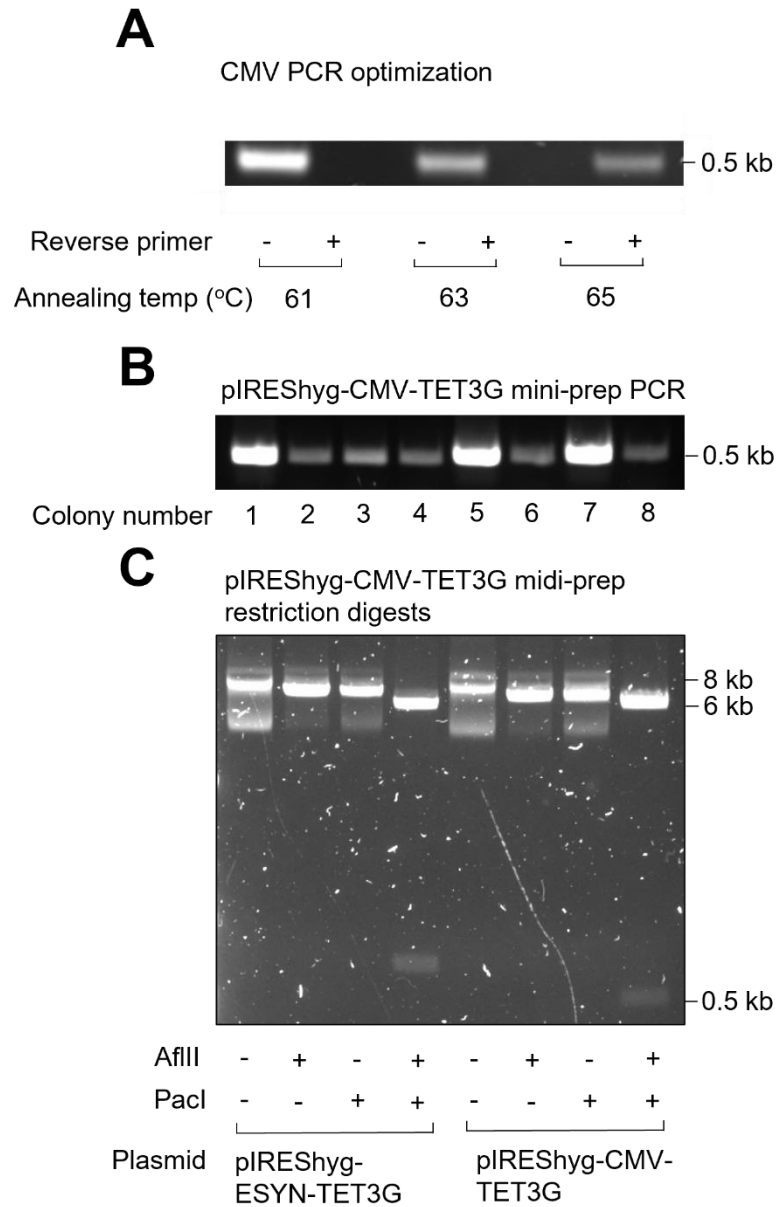


Figure 6.1: Generation of the pIRESHyg-CMV-TET3G construct. pIRESHyg was used as a template for the amplification of the CMV promoter for insertion into the restriction digested pIRESHyg-ESYN-TET3G plasmid. **(A)** PCR optimization of CMV promoter PCR product generation at different annealing temperatures. **(B)** PCR to confirm the presence of CMV promoter in different pIRESHyg-CMV-TET3G mini-preps. **(C)** Restriction digests to confirm the presence of CMV promoter in pIRESHyg-CMV-TET3G midi-prep cultured from colony number 1.

6.3 Transient transfection of pIREShyg-ESYN-TET3G and pIRES-CMV-TET3G regulator plasmids in SH-SY5Y and HEK cells

Having now obtained regulator plasmids containing both neuron-specific (ESYN) and non-cell type-specific (CMV) promoters, both of these constructs were transiently transfected into SH-SY5Y and HEK cells as described in the Materials and Methods section. Cell lysates were subsequently prepared and equal protein concentrations immunoblotted with anti-TetR antibody (Takara, Saint-Germain-en-Laye, France) in order to monitor cell-type specific expression of the transactivator protein. The results (Figure 6.2A) revealed the expression of a strong band at around 20.1 kDa in HEK cells transfected with pIREShyg-CMV-TET3G but not with the neuron-specific ESYN promoter. In SH-SY5Y cells, neither configuration of the regulator plasmid resulted in definitive TET3G expression (Figure 6.2C). There is a possibility of some TET3G expression in the pIREShyg-CMV-TET3G lane but this is not in the same order of magnitude as in HEK cells. Equal protein loading from both cell lines was confirmed by reprobing blots with the anti-actin antibody (Figure 6.2B and D). Notably, we also attempted stable transfection of the plasmids into SH-SY5Y and HEK cells using electroporation (Materials and Methods) but, despite apparent positive antibiotic colony selection, the resultant transfectants did not express detectable levels of transactivator protein from either plasmid (data not shown).

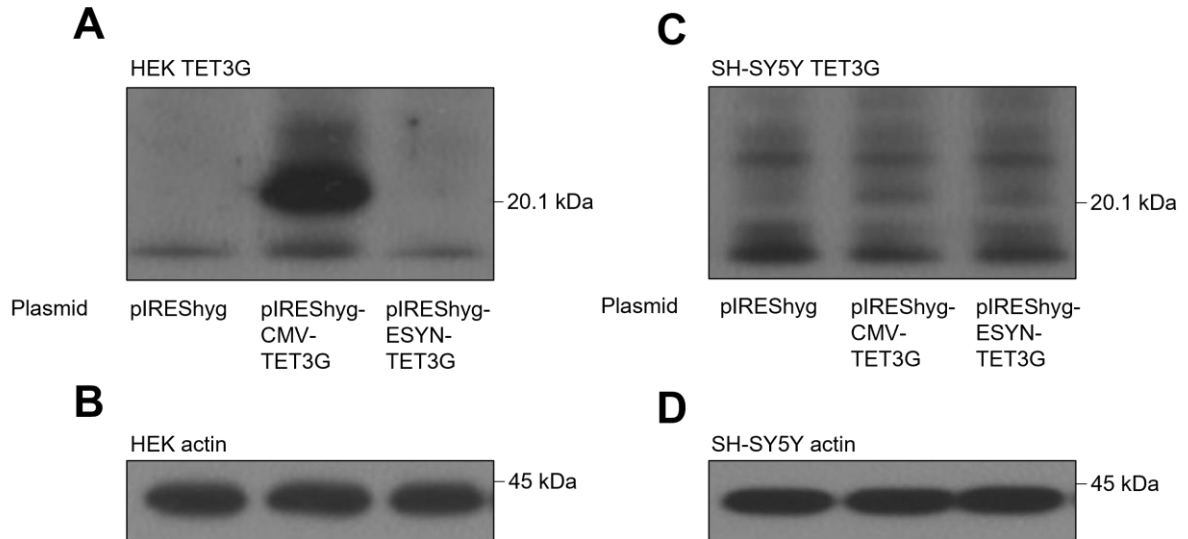


Figure 6.2: TET3G transactivator protein transient transfections in HEK and SH-SY5Y cells. HEK and SH-SY5Y cells were grown to 80% confluence and transiently transfected with pIREShyg-CMV-TET3G or pIREShyg-ESYN-TET3G as described in the Materials and Methods section. Cells were then harvested, lysates prepared and equal amounts of protein immunoblotted. **(A and C)** Anti-TetR immunoblot. **(B and D)** Anti-actin immunoblot.

6.4 Generation of response plasmids for examining the effect of MCS positioning of coding DNA sequences on protein expression

The response plasmid of our initial dual plasmid system itself contained two different multiple cloning sites in theory permitting the expression of two different genes of interest (in addition to hygromycin phosphotransferase for selection purposes). These MCS are separated by internal ribosome entry sites (IRES) and it has been demonstrated that genes of interest downstream of IRES sites can have reduced expression relative to those immediately after the initial plasmid promoter (Mizuguchi *et al.*, 2000). As such, in the current study, it was important to test how the positioning of sAPP α and VPS35 coding DNA sequences in MCS1 versus MCS2 impacted on protein expression. This section details the generation of the response plasmids necessary for this purpose.

6.4.1 pIRESzeo-empty-VPS35

The response plasmid originally synthesized by Epoch Life Science (Missouri City, Texas, USA) actually contained the coding DNA for Enhanced Green Fluorescent Protein (EGFP) within MCS1; it was originally hoped that this might provide an easy visual readout of successful protein induction. In order to generate a version of the plasmid containing just VPS35 in MCS2 (pIRESzeo-empty-VPS35) the EGFP CDS was removed using ASi S1 restriction digest (these sites had been incorporated into the response plasmid for future proofing at the point of synthesis). Agarose gel resolution of the digests (Figure 6.3A) demonstrated the main plasmid fragment at ~10 kb and the excised EGFP coding sequence at ~0.7 kb. The larger fragment was then gel extracted, re-ligated and transformed into bacteria. Several colonies were stabbed into mini-cultures and the plasmid DNA isolated from each culture subjected to NsiI linearization before resolving on an agarose gel. The results (Figure 6.3B) showed that each of the minipreps contained plasmid 720 bp smaller than the original response plasmid; colony 1 was subsequently selected for midi-culture growth and bulk plasmid purification.

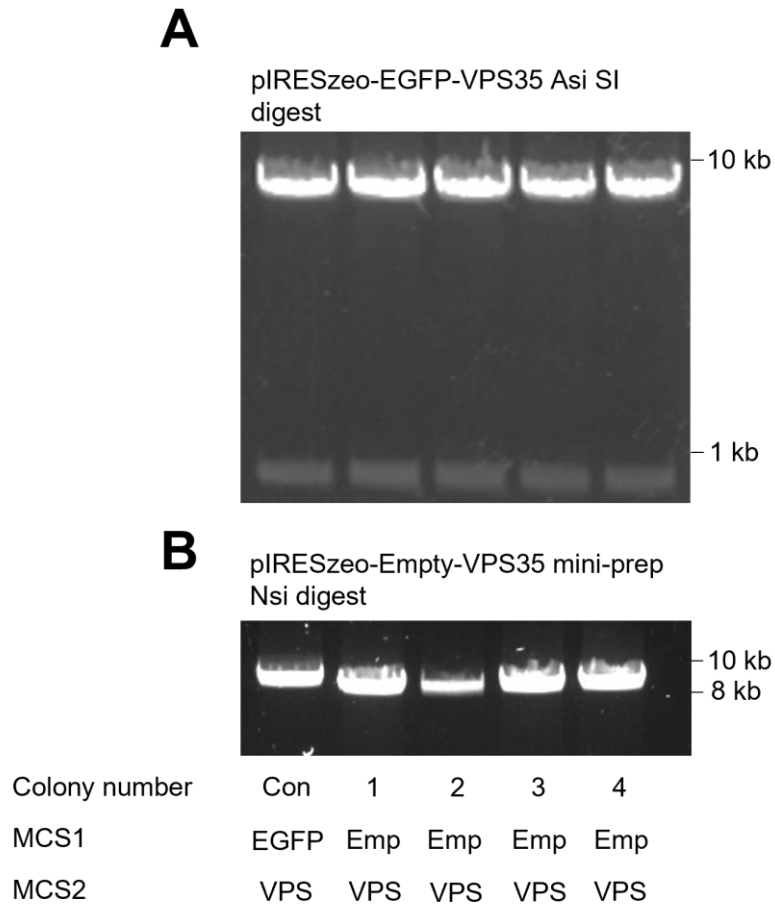


Figure 6.3: Generation of pIRESzeo-empty-VPS35. (A) Asi SI restriction digest of the original pIRESzeo-EGFP-VPS35 plasmid to excise the EGFP coding DNA sequence. (B) NsiI restriction digest of putative pIRESzeo-empty-VPS35 colony plasmid isolates to confirm removal of EGFP coding sequence. EGFP = Enhanced Green Fluorescent Protein, Emp = Empty, VPS = VPS35.

6.4.2 pIRESzeo-empty-empty

The pIRESzeo-empty-VPS35 plasmid generated in the previous section was then used to produce a response plasmid lacking coding DNA sequences in both MCS1 and MCS2 (pIRESzeo-empty-empty). The VPS35 coding DNA was excised from the former plasmid using Swal (Swal restriction sites had been incorporated on either side of the CDS at the point of synthesis). Agarose gel resolution of the digests (Figure 6.4A) exhibited the main plasmid fragment below 8 kb and the excised VPS35 coding sequence above 2 kb. The larger fragment was then gel extracted, re-ligated and transformed into bacteria. Several colonies were stabbed into mini-cultures and the plasmid DNA isolated from each culture,

to be subjected to Nsi linearization and resolution on an agarose gel. The gel (Figure 6.4B) showed that each of the minipreps contained plasmid 3.1 kb smaller than the original plasmid and 2.4 kb smaller than the pIRESzeo-empty-VPS35 plasmid. Colony 1 was, therefore, selected for midi-culture growth and bulk plasmid purification.

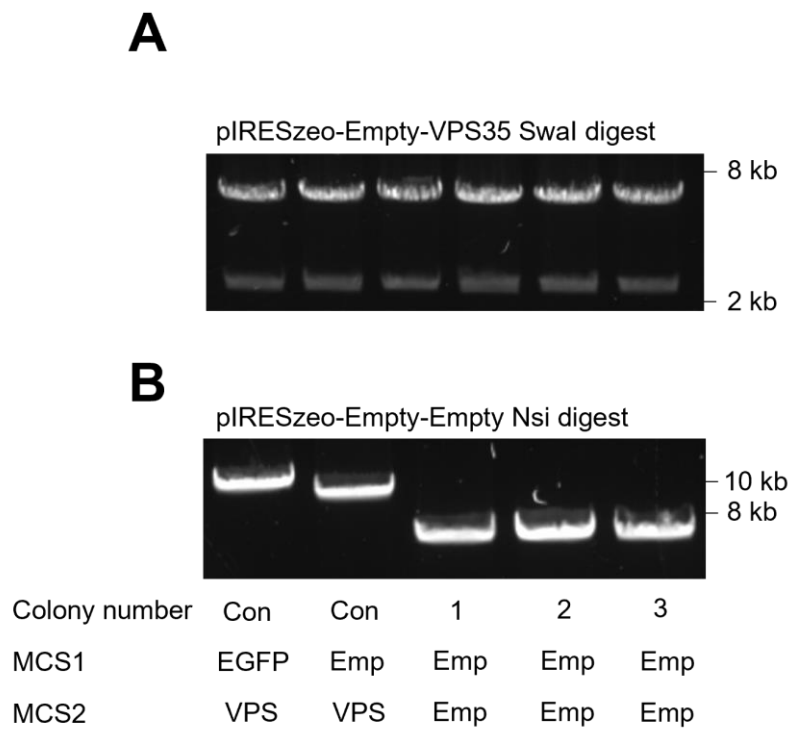


Figure 6.4: Removal of the VPS35 coding sequence from pIRESzeo-Empty-VPS35. Swal restriction enzyme was used to excise the VPS35 coding sequence from the pIRESzeo-Empty-VPS35 plasmid. **(A)** Resultant gel after Swal digest. **(B)** Restriction digest to confirm removal of VPS35 coding sequence. EGFP = Enhanced green-fluorescent-protein, Emp = Empty, VPS = VPS35.

6.4.3 pIRESzeo-sAPP α -VPS35

In order to generate the response plasmid designed in Figure 5.4C, pIRESzeo-empty-VPS35 was used as the foundation. The pRESHyg APP₆₉₅

plasmid (Parkin *et al.*, 2007) containing the coding DNA sequence for full-length APP₆₉₅ was once again used as a template for the generation of an sAPP α PCR fragment (as seen in Section 4.4). Forward Primer F (Table 2.1, Materials and Methods) containing a 5' PmeI restriction site and Kozak sequence and reverse Primer G (Table 2.1, Materials and Methods) (with a 3' AgeI restriction site) possessing a stop codon after the codon encoding Lys16 of the A β region of APP were used. Initially, the PCR efficiency was tested at 63, 64 and 65°C annealing temperatures (based below and around the 66 and 65.7°C melting temperatures of the primers) to optimise product generation. The resultant gel (Figure 6.5A) demonstrated that 63°C was the optimal annealing temperature, resulting in the formation of the highest quantity of an 1845 bp fragment as expected for amplification of the sAPP α CDS from pIRES_{hyg} APP₆₉₅.

Multiple PCR reactions were then carried out at 63°C and the PCR product was isolated, restriction digested using PmeI and AgeI and ligated into the equivalent sites in pIRES_{zeo}-empty-VPS35. Following bacterial transformation, colonies were stabbed into mini-cultures and the plasmid DNA isolated from each culture. The plasmid DNA was then subjected to Nsi linearization to make a provisional determination of which preparation contained the sAPP α CDS. The results of this (Figure 6.5B) demonstrated that 4 of the 5 colonies could possibly contain the sAPP α CDS and colony 3 was selected for midi-culture growth.

A series of restriction digests were then set-up to test for the presence of the sAPP α CDS in the plasmid isolated from the midiprep. The results (Figure 6.5C) show that PmeI linearized the pIRES_{zeo}-empty-VPS35 control vector to an expected size of 8.5 kb. Linearization of the midiprep plasmid with PmeI then produced a band size of 10.3 kb; 1.8 kb higher than pIRES_{zeo}-empty-VPS35 (the difference equivalent to the sAPP α CDS). In addition to this, a double digest with PmeI and AgeI resulted in two bands; one at 8.5 kb corresponding to pIRES_{zeo}-empty-VPS35 and the other at 1.8 kb corresponding to the sAPP α CDS.

To confirm that the correct sequence of sAPP α coding region had been inserted into the plasmid, sequencing was undertaken by MRC DNA Sequencing

Service (University of Dundee, Dundee, UK). In particular, the sequencing demonstrated the correct incorporation of the TAG stop codon downstream of the Lys16 codon of the APP A β region (**Figure 6.5D**).

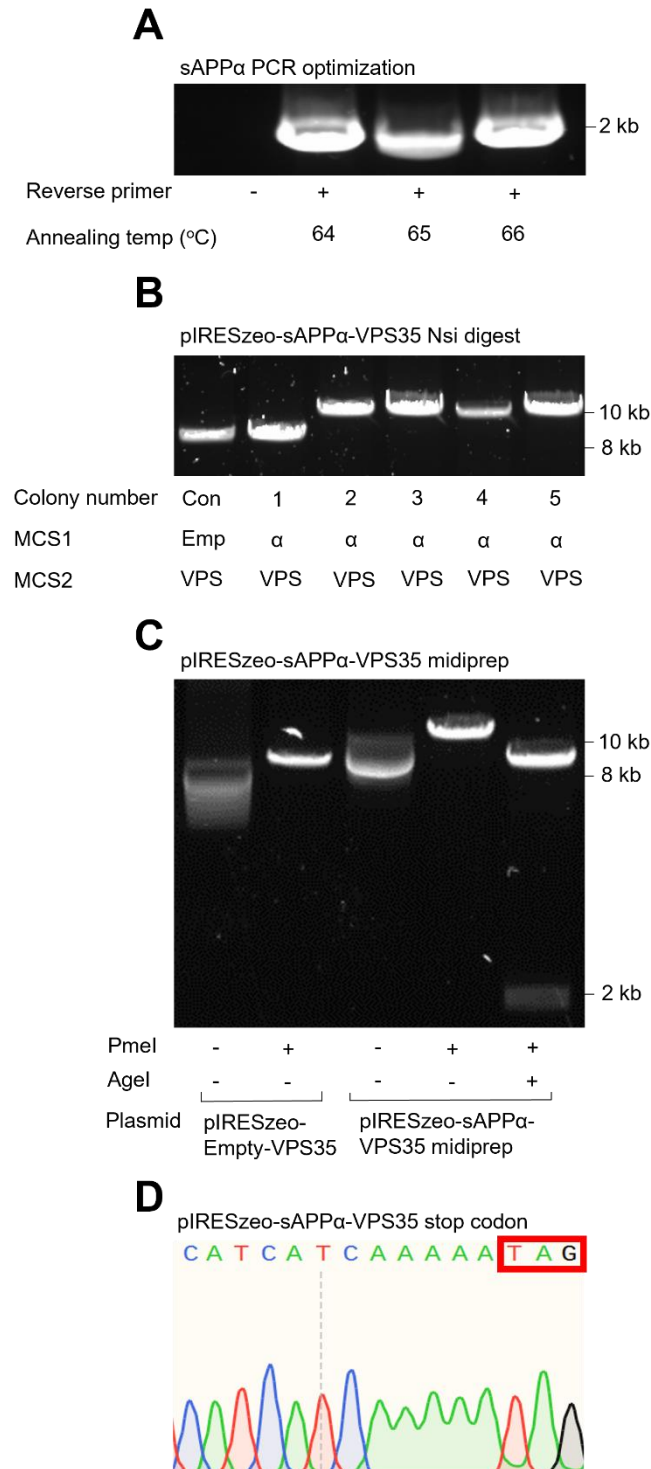


Figure 6.5: Generation of the pIRESzeo-sAPP α -VPS35 construct. pIRESHyg-wtAPP₆₉₅ was used as a template for the amplification of sAPP α for insertion into the pIRESzeo-Empty-VPS35

vector. **(A)** PCR optimization to amplify sAPP α at different annealing temperatures. **(B)** Restriction digest to confirm presence of sAPP α in different pIRESzeo-sAPP α -VPS35 mini-preps. **(C)** Restriction digests to confirm presence of sAPP α in pIRESzeo-sAPP α -VPS35 midi-prep colony number 3. **(D)** The 3' coding region of sAPP α in pIRESzeo-sAPP α -VPS35 with the TAG stop codon highlighted. α = sAPP α , Emp = Empty, VPS = VPS35.

6.4.4 pIRESzeo-sAPP α -empty

The pIRESzeo-empty-empty plasmid generated in Section 6.4.2 was used to produce a response plasmid with the sAPP α CDS inserted into MCS1. Similar to the plasmid generation in Section 6.4.3 (to create pIRESzeo-sAPP α -VPS35), pIRESHyg APP₆₉₅ plasmid (Parkin *et al.*, 2007) was used to amplify a sAPP α PCR fragment using forward Primer F and reverse Primer G (Table 2.1, Materials and Methods). Multiple reactions were performed at the 63°C optimum and the PCR product was isolated and ligated into pIRESzeo-empty-empty using the PmeI and AgeI restriction enzymes. After bacterial transformation, colonies were stabbed into mini-cultures and the plasmid DNA isolated. The plasmid DNA was then subjected to Nsi linearization to determine which of the preparations contained the sAPP α CDS. The resultant digest (Figure 6.6A) showed that only colony 1 was the correct size to contain the sAPP α insert and so this colony was subsequently taken forward for midi-culture growth.

A series of restriction digests were set up to confirm the presence of the sAPP α CDS in the plasmid isolated from the midiprep (Figure 6.6B). Incubation with PmeI linearized the plasmid midiprep to produce a band size of 7.9 kb; 1.8 kb higher than pIRESzeo-empty-empty (equivalent to the size of the sAPP α CDS). Further to this, double digest with both PmeI and AgeI created two bands; one at 6.1 kb corresponding to the pIRESzeo-empty-empty and a smaller band at 1.8 kb corresponding to the sAPP α CDS. Final confirmation of the sAPP α insertion was performed by sequencing via the MRC DNA Sequencing Service (University of Dundee, Dundee, UK). This confirmed the complete construct sequence, and once again showed the correct incorporation of the TAG stop codon downstream of the Lys16 codon of the APP A β region (Figure 6.6C).

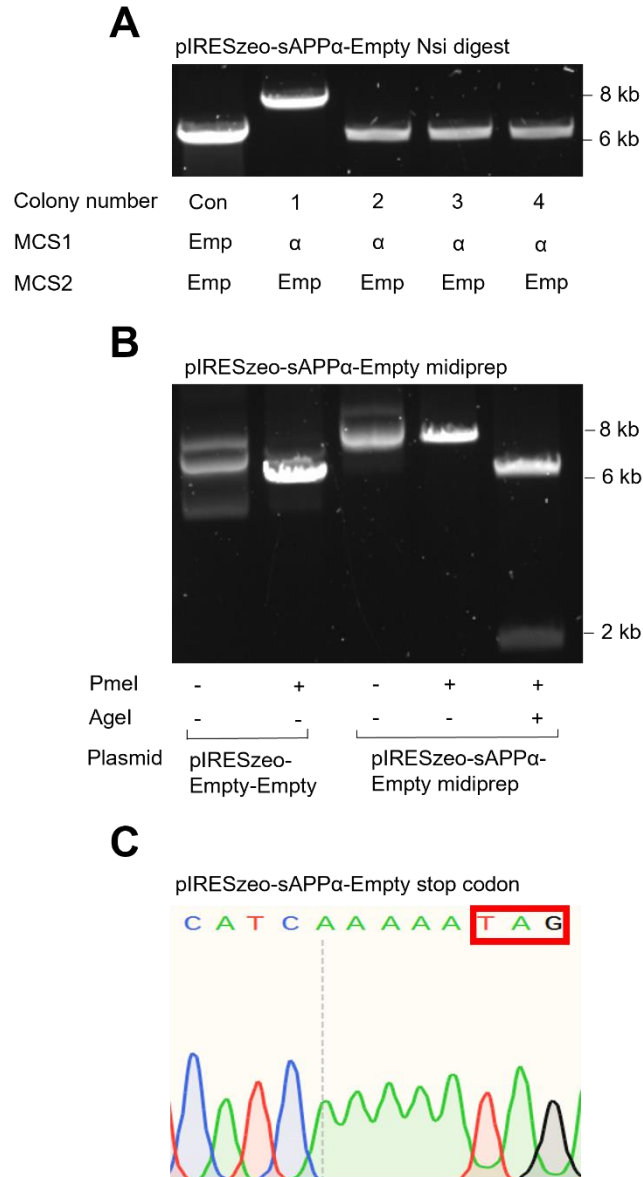


Figure 6.6: Generation of the pIRESzeo-sAPP α -Empty construct. pIREShyg-wtAPP₆₉₅ was used as a template for the amplification of sAPP α for insertion into the pIRESzeo-Empty-Empty vector. **(A)** Restriction digest to confirm presence of sAPP α in different pIRESzeo-sAPP α -Empty mini-preps. **(B)** Restriction digests to confirm presence of sAPP α in pIRESzeo-sAPP α -Empty midi-prep colony number 3. **(C)** The 3' coding region of sAPP α in pIRESzeo-sAPP α -Empty with the TAG stop codon highlighted. α = sAPP α , Emp = Empty, VPS = VPS35.

6.4.5 pIRESzeo-empty-sAPP α

In addition to generating pIRESzeo-sAPP α -empty, pIRESzeo-empty-empty was also used as a basis to generate pIRESzeo-empty-sAPP α . This again utilized the pIREShyg APP₆₉₅ plasmid (Parkin *et al.*, 2007) to amplify the sAPP α

CDS. Forward Primer H (Table 2.1, Materials and Methods) containing a 5' *SpeI* restriction site and Kozak sequence and reverse Primer I (Table 2.1, Materials and Methods) (with a 3' *SnaB1* restriction site) possessing a stop codon after the codon encoding Lys16 of the A β region of APP were used. The PCR efficiency was tested at 64, 65 and 66°C annealing temperatures (based on 66 and 65.7°C primer melting temperatures) to optimise sAPP α amplification. The results (Figure 6.7A) showed that 64°C was the annealing temperature that resulted in the highest formation of a 1845 bp fragment as expected for amplification of the sAPP α CDS.

Multiple PCR reactions were then performed at 64°C and the amplified sAPP α fragment was isolated and ligated into pIRESzeo-empty-empty with the use of *SpeI* and *SnaB1* restriction sites. After bacterial transformation, colonies were stabbed into mini-cultures and the plasmid DNA was isolated from each culture. *Nsi* linearization was employed for the plasmid DNA to predict which preparation contained sAPP α . Of the 5 colonies tested (Figure 6.7B), only colony 5 was the correct size to contain sAPP α (7.9 kb) and was selected for midi-culture growth.

The midi-prep was then subjected to a series of restriction digests to determine the presence of the sAPP α insert in the midiprep plasmid. *SpeI* successfully linearized the midiprep to produce a band size of 7.9 kb (Figure 6.7C). This was 1.8 kb higher than the linearized pIRESzeo-empty-empty control vector. A double digest with *SpeI* and *SnaB1* resulted in two bands; the larger of the two corresponding to pIRESzeo-empty-empty at 6.1 kb and the smaller, at 1.8 kb, corresponding to the size of the sAPP α CDS. The insert was then sequenced and confirmed by the MRC DNA Sequencing Service (University of Dundee, Dundee, UK) demonstrating the correct incorporation of the TAG stop codon downstream of the Lys16 codon (Figure 6.7D).

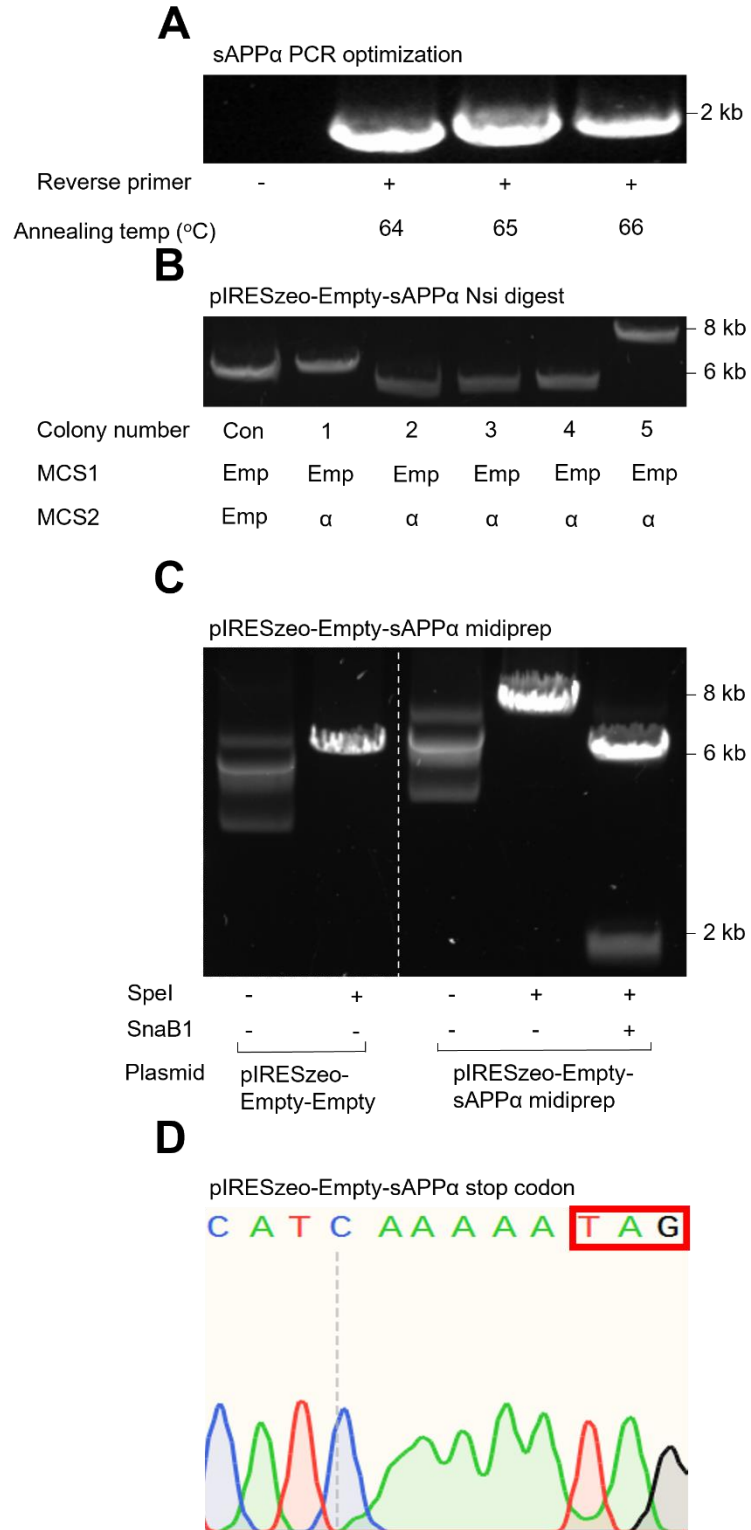


Figure 6.7: Generation of the pIRESzeo-Empty-sAPP α construct. pIRESHyg-wtAPP₆₉₅ was used as a template for the amplification of sAPP α for insertion into the pIRESzeo-Empty-Empty vector. **(A)** PCR optimization to amplify sAPP α at different annealing temperatures. **(B)** Restriction digest to confirm presence of sAPP α in different pIRESzeo-Empty-sAPP α mini-preps. **(C)** Restriction digests to confirm presence of sAPP α in pIRESzeo-Empty-sAPP α midi-prep colony

number 5. **(D)** The 3' coding region of sAPP α in pIRESzeo-Empty-sAPP α with the TAG stop codon highlighted. α = sAPP α , Emp = Empty, VPS = VPS35.

6.4.6 pIRESzeo-VPS35-sAPP α

To generate pIRESzeo-VPS35-sAPP α , pIRESzeo-empty-sAPP α was used as the starting point. The original response plasmid pIRESzeo-EGFP-VPS35 supplied by Epoch Life Science (Missouri City, Texas, USA) was used as a template for the generation of a VPS35 PCR fragment. Forward Primer J containing a 5' PmeI restriction site and reverse Primer K (Table 2.1, Materials and Methods) (with a 3' AgeI restriction site) were used. PCR efficiency was tested at 63, 64 and 65°C annealing temperatures (based on the 64.1 and 64.8°C melting temperatures of the primers, respectively) to optimise VPS35 product generation. The resultant gel (Figure 6.8A) showed that 63°C was the optimum.

Multiple PCR reactions at 63°C were then performed and the VPS35 PCR product was isolated and ligated into pIRESzeo-empty-sAPP α via PmeI and AgeI digested restriction sites. Following bacterial transformation, colonies were stabbed into mini-cultures and the plasmid DNA isolated. Each plasmid DNA preparation was subjected to Nsi linearization to determine which minipreps contained the VPS35 CDS. All five colonies tested demonstrated that they could contain VPS35 and colony 2 was selected for midi-culture (Figure 6.8B).

A series of restriction digests were then employed to test for the presence of VPS35 CDS in the plasmid isolated from the midiprep. The results (Figure 6.8C) show that PmeI linearized pIRESzeo-empty-sAPP α control vector ran at an expected size of 7.9 kb, whereas linearized pIRESzeo-VPS35-sAPP α produced a band size of 10.3 kb; the difference in the two corresponding to the size of the VPS35 insert. The double digest with PmeI and AgeI showed the VPS35 band at 2.4 kb and pIRESzeo-empty-sAPP α vector at 7.9 kb.

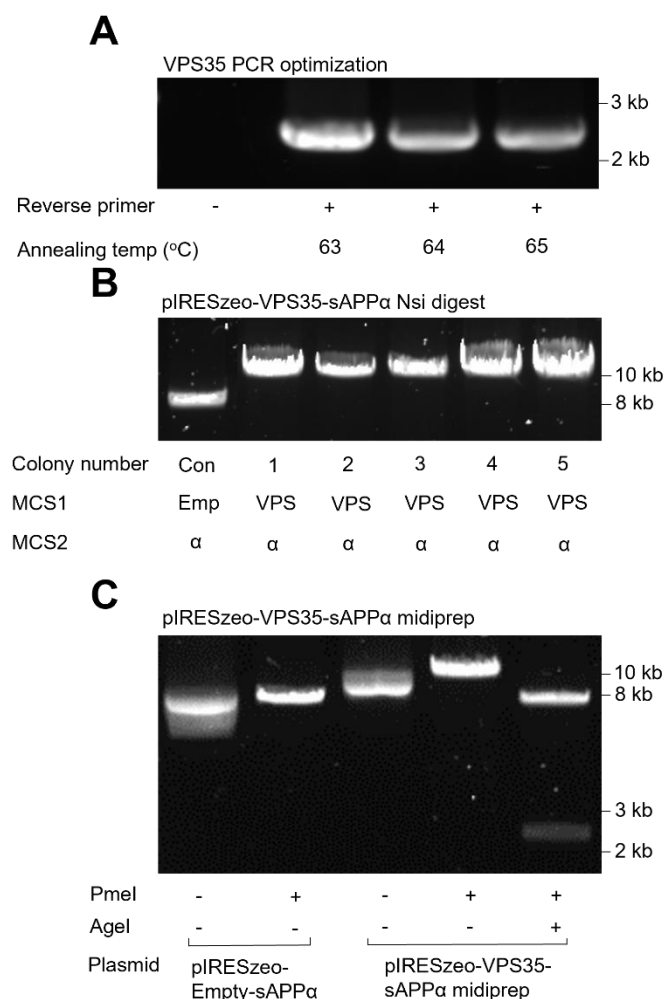


Figure 6.8: Generation of the pIRESzeo-VPS35-sAPP α construct. pIRESHyg-EGFP-VPS35 was used as a template for the amplification of VPS35 for insertion into the pIRESzeo-Empty-sAPP α vector. **(A)** PCR optimization to amplify VPS35 at different annealing temperatures. **(B)** Restriction digest to confirm presence of VPS35 in different pIRESzeo-VPS35-sAPP α mini-preps. **(C)** Restriction digests to confirm presence of VPS35 in pIRESzeo-VPS35-sAPP α midi-prep colony number 5. α = sAPP α , Emp = Empty, VPS = VPS35.

6.4.7 pIRESzeo-VPS35-empty

The pIRESzeo-empty-empty plasmid generated in Section 6.4.2 was used to produce a response plasmid with VPS35 inserted into MCS1 (pIRESzeo-VPS35-empty). pIRESzeo-EGFP-VPS35 supplied by Epoch Life Science (Missouri City, Texas, USA) was used as a template for the amplification of the

VPS35 PCR fragment with Primers J and K (Table 2.1, Materials and Methods). Multiple PCR reactions were set up at 63°C and the amplified VPS35 product was isolated and ligated into pIRESzeo-empty-empty using digested PmeI and AgeI restriction sites. After bacterial transformation and colony selection for mini-culture growth, the plasmid DNA was isolated. One of the five colonies appeared to contain the VPS35 insert following Nsi linearization and this was subsequently taken forward for midi-culture inoculation (Figure 6.9A).

To test for the presence of VPS35 CDS in the midiprep, a series of restriction digests were performed. The results (Figure 6.9B) show that PmeI linearization of pIRESzeo-empty-empty control vector produced a band 2.4 kb lower than linearized pIRESzeo-VPS35-empty (at 8.4 kb). Double digest with both PmeI and AgeI resulted in two bands; one at 6.1 kb corresponding to pIRESzeo-empty-empty and the other at 2.4 kb corresponding to the VPS35 CDS.

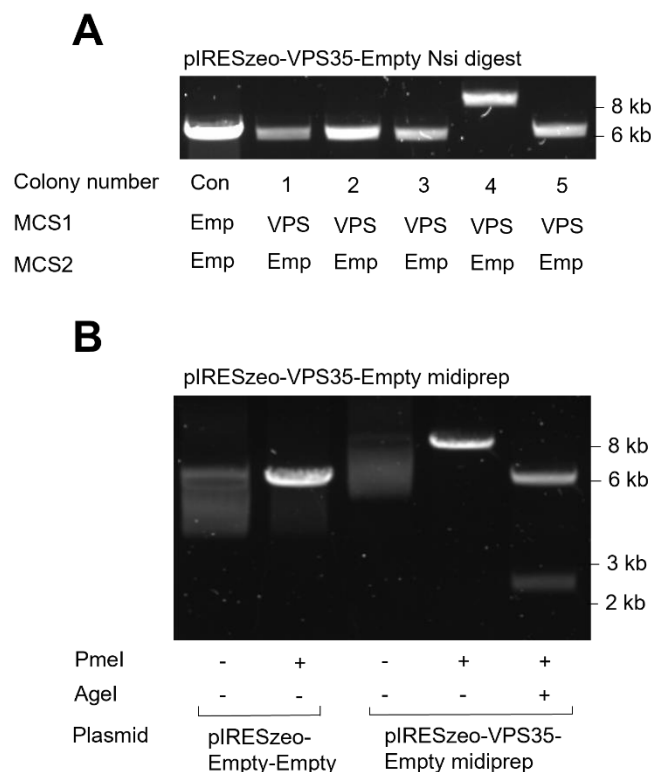


Figure 6.9: Generation of the pIRESzeo-VPS35-Empty construct. pIRESzeo-EGFP-VPS35 was used as a template for the amplification of VPS35 for insertion into the pIRESzeo-Empty-Empty vector. **(A)** Restriction digest to confirm presence of VPS35 in different pIRESzeo-VPS35-Empty mini-preps. **(B)** Restriction digests to confirm presence of VPS35 in pIRESzeo-VPS35-Empty midiprep colony number 3.

6.5 Removal of the bleomycin coding sequence from pIRESzeo-empty-VPS35 for subsequent PiggyBac plasmid generation

In the PiggyBac plasmid design detailed in the preceding chapter (Figure 5.6B), the bleomycin coding DNA sequence would be redundant and its removal would, therefore, reduce overall plasmid size and potentially improve transfection efficiency. The combination of the original regulator and response plasmids to generate the PiggyBac plasmid involved XhoI digestion of both of the former plasmids. However, the sAPP α CDS contains a XhoI restriction site and, as such, this sequence would need to be absent from the response plasmid during PiggyBac plasmid preparation (and then subsequently PCR generated and ligated back into the latter plasmid). Therefore, the response plasmid containing only VPS35 in MCS2 (pIRESzeo-empty-VPS35) was used as the source plasmid from which to remove the bleomycin CDS.

In order to remove the bleomycin resistance CDS, the BsiWI restriction sites flanking this sequence were used. Resolution of the digests (Figure 6.10A) demonstrated the main plasmid fragment at 8.1 kb and the excised bleomycin CDS at 0.4 kb. The larger fragment was then gel extracted, re-ligated and transformed into competent bacteria. Colonies were stabbed into mini-cultures and the plasmid DNA isolated from each culture was subjected to NsiI linearization. The results (Figure 6.10B) showed that each of the minipreps contained a plasmid 345 bp smaller than pIRESzeo-empty-VPS35 that contained the bleomycin resistance CDS. Miniprep 3 was then selected for midculture growth and bulk plasmid purification.

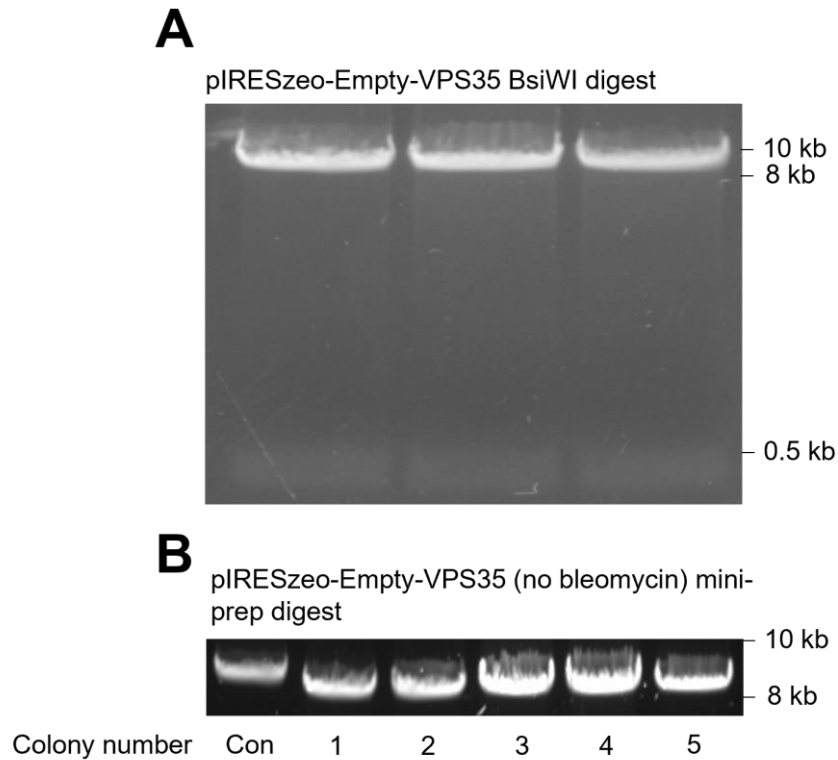


Figure 6.10: Removal of the bleomycin resistance coding DNA sequence from pIRESzeo-Empty-VPS35. (A) BsiWI restriction enzyme was used to excise the bleomycin resistance coding DNA sequence from the pIRESzeo-Empty-VPS35 plasmid. **(B)** BsiWI restriction digest to confirm removal of the bleomycin coding DNA sequence. VPS = VPS35.

6.6 Summary

In the current chapter, versions of the original regulator plasmid containing the ESYN neuron-specific promoter or the CMV promoter were obtained. However, only the CMV promoter version (pIRESHyg-CMV-TET3G) was successfully expressed and only using transient methodology and only in HEK cells. Neither version of the regulator plasmid produced detectable levels of transactivator protein in SH-SY5Y cells following either transient or stable transfection.

Multiple configurations of the response plasmid (pIRESHyg-empty-VPS35, pIRESzeo-empty-empty, pIRESzeo-sAPP α -VPS35, pIRESzeo-sAPP α -empty, pIRESzeo-empty-sAPP α , pIRESzeo-VPS35-sAPP α and pIRESzeo-VPS35-

empty) were generated which would enable future studies to investigate the effect of MCS positioning on the expression efficiency of sAPP α and VPS35.

Finally, the bleomycin resistance CDS was removed from the pIRESzeo-empty-VPS35 regulator plasmid as a precursor to the future combining of regulator and response plasmids in order to generate a PiggyBac transposon plasmid.

The future applications of these plasmids are discussed further in the Discussion section of the current work.

7. Discussion

7.1 Fibrate treatment does not enhance sAPP α release in Swedish mutant APP SH-SY5Y cells

In the current study we sought to enhance the release of sAPP α in SH-SY5Ys that stably over-expressed Swedish mutant APP₆₉₅ (SweAPP). This was attempted using two different fibrates (gemfibrozil and bezafibrate) that had been previously shown to stimulate ADAM10 expression and enhance sAPP α release (Corbett, Gonzalez and Pahan, 2015a). Neither of the fibrates yielded a beneficial effect in SweAPP cells.

Fibrates act as an agonist to peroxisome proliferator-activated receptor alpha (PPAR- α) which is implicated in APP metabolism and AD pathology (Wójtowicz *et al.*, 2020). Specifically, the fibrate gemfibrozil has been demonstrated to stimulate ADAM10 expression and enhance sAPP α release (Corbett, Gonzalez and Pahan, 2015b). This effect was demonstrated in hippocampal neurons dissected from mouse embryos rather than an immortalized cell line such as SH-SY5Y. To more closely replicate the hippocampal cells the SH-SY5Y in the current study could be differentiated to more closely represent neuronal cells (Shipley, Mangold and Szpara, 2016). Another issue with Corbett *et al.*, 2015 is the use of the anti-APP 6E10 antibody to detect the sAPP α fragment. As discovered later in the current study the 6E10 antibody cross-reacts with different sAPP fragments and so the validity of any results from this antibody would have to be repeated. Corbett *et al.*, 2015 also examined the reciprocal CTF α release in cell lysates which was shown to significantly increase with the addition of gemfibrozil. This current study could repeat the experiment with gemfibrozil and examine CTF α release to see if correlates to results in Corbett *et al.*, 2015, which could overcome the issues with using the 6E10 antibody.

Another study demonstrated that gemfibrozil reduced extracellular A β levels in U251 glioma cell cultures (Tang *et al.*, 2021). A future experiment could test the effect of gemfibrozil on A β release in SH-SY5Y-Swe-APP cells, to determine whether the inability of gemfibrozil to influence amyloidogenic

processing would then lead to an inability to influence A β release. Or the results could suggest that gemfibrozil regulates A β release independently of amyloidogenic processing. Important to note, both Corbett *et al.*, 2015 and Tang *et al.*, 2021 utilised models that are not as closely related to AD-pathology than our SH-SY5Y models of AD, which could in part explain why we were not able to recreate their results.

We also demonstrated that a second fibrate, bezafibrate, did not influence ADAM10 or APP processing in SH-SY5Y-SweAPP cells. Bezafibrate, in theory, should function in a similar manner to gemfibrozil as it interacts with PPAR- α (Kamata *et al.*, 2020). However, whereas there have been no studies into the effect of this fibrate on APP metabolism, it has been linked to tauopathy and can provide neuroprotection in sporadic AD models of rats (Lin *et al.*, 2022). The authors noted that there was only a small amount of A β detectable in the brains of the rats and so amyloid metabolism could not be investigated.

The results of this current study have contrasted the other studies discussed and have failed to highlight any beneficial effect of fibrate treatment on yielding increase sAPP α release. Repeat experiments in other AD-related cell (used in Corbett *et al.*, 2015, Tang *et al.*, 2021 and then Lin *et al.*, 2022) would be required to determine whether our results are an anomaly, or fibrates can have an impact previously reported. It is also possible that in the current setup using SH-SY5Y-SweAPP cells, the fibrates are not interacting with PPAR- α and therefore will have no influence on APP metabolism through PPAR- α -influenced gene expression. Therefore, during the repeat experiments it would be important to demonstrate that gemfibrozil and bezafibrate are in fact interacting with PPAR- α (and determine drug-target binding affinity), before looking at the downstream effects.

7.2 Beta-prime processing of APP supersedes sAPP α generation in BACE1-transfected SH-SY5Y cells

During the fibrinate experiments discussed in the preceding section, we noted that the broad-spectrum ADAM/MMP inhibitor, batimastat, did not inhibit non-amyloidogenic sAPP generation in SH-SY5Y cells that overexpressed BACE1, responsible for release of amyloidogenic sAPP. In an attempt to elucidate this phenomenon we directly compared APP expression and proteolysis in three different AD-related cell lines of SH-SY5Y that stably overexpressed BACE1, wild-type APP₆₉₅ (wtAPP) or Swedish mutant APP₆₉₅.

When each of the AD-related cell lines were treated with batimastat (Figure 4.4), non-amyloidogenic sAPP release in SH-SY5Y-BACE1 cells was not affected by batimastat. The treatment caused significant decreases of non-amyloidogenic sAPP₆₉₅ and sAPP_{751/770}, but following BACE1 over-expression there was no significant difference. As BACE1 is responsible for the generation of amyloidogenic sAPP β , and not sAPP α , this effect was not expected. This has not been observed in previous studies and batimastat has been shown to have no effect on BACE1 gene expression (this paper did not look at the efficiency of BACE1 processing however) (Liu *et al.*, 2019a). Conversely batimastat has no significant effect on amyloidogenic sAPP β in any of the cell lines (Figure 4.5). We hypothesised in this current study that over-expressed BACE1 could be cleaving APP at the 'beta prime' site C-terminal to Tyr10 of the A β region (Liu, Doms and Lee, 2002). The result of this would be a sAPP β ' fragment that still contains the minimum epitope of amino acids 3-8 of the A β region which would be detected by anti-APP 6E10 antibody (Grant *et al.*, 2019). This would mean that when batimastat is applied to SH-SY5Y-BACE1 as in Figure 4.4, we are detecting sAPP β ' by anti-APP 6E10 antibody rather than non-amyloidogenic sAPP (illustrated in Figure 7.1).



Figure 7.1: β' site cleavage overlap with anti-APP 6E10 antibody epitope. The β' cleavage site is labelled by the orange rectangle and the 6E10 epitope (EFRHDS) lies within the red rectangle. β- and α-site shown for reference.

As there was no antibody available that could specifically detect sAPPβ' versus sAPPα, we employed tris-tricine based gel electrophoresis to look at the reciprocal production of APP C-terminal fragments (CTFs) in the cell lysates. The resultant immunoblot yielded 3 distinct CTF fragments (Figure 4.7A). The C99 fragment produced by canonical BACE1 processing of APP was significantly increased in SH-SY5Y-SweAPP cells, coinciding with the high levels of sAPPβ₆₉₅ detected by the anti-APPβ_{sw} immunoblot (Figure 4.5C). Despite enhanced BACE1 activity due to its over-expression, SH-SY5Y-BACE1 cells did not produce significantly higher levels of C99 than Mock-transfected cells (albeit the levels were slightly higher). C99 levels would be expected to follow results found by (Zhang *et al.*, 2012), where an increase in BACE1 protein level caused significant C99 increase compared to WT. Zhang *et al.*, 2012 did, however, increase BACE1 levels achieved through UCHL1 gene disruption which may not be as high as in the current study whereby the enzyme was simply over-expressed. Further experiments could test the role of BACE1, with a WT control, overexpressed-BACE1 similar to this current study, UCHL1 gene disruption and genetic knockdown of BACE1. The levels of BACE1 in each cell line could be compared and the resultant effects on APP processing (and C99 release).

Conventional non-amyloidogenic processing of APP results in the C83 fragment detected in SH-SY5Y-wtAPP and -SweAPP cells (Figure 4.7A). This fragment was, notably, not present in BACE1-transfected cell lysates in the current study; whereas the slightly larger C89 fragment was detected as a result of non-canonical non-amyloidogenic cleavage of APP at the beta prime site by the over-expressed BACE1 (Figure 4.7A and C). This effect has been observed previously following the overexpression of BACE1 in the H4 human cell line

(Repetto *et al.*, 2004). The H4 cell line is of epithelial origin from a subject with neuroglioma, therefore it is used for neuroscience research. The study demonstrated that H4 BACE1 cell lysates exhibited a higher amount of C89 coupled with reduced C83. Repetto *et al.*, 2004 did not find a reduction in C83 as prominent as the current study, but their results do follow a similar effect. Greater effects similar to the current were observed by (Deng *et al.*, 2013), where BACE1 and APP₆₉₅ were double transfected into HEK293 cells. In western blots of the BACE1/APP₆₉₅ transfected cells, (Deng *et al.*, 2013) demonstrated that C89 and C99 were the major products of APP processing, and a lack of C83. Overall the literature supports the switch from C83 fragments to C89 fragments when BACE1 is overexpressed, regardless of the different cell models.

We then conducted subsequent experiments to confirm that non-amyloidogenically derived sAPP generated by SH-SY5Y BACE1 was the consequence of non-canonical BACE1-mediated processing. It required a combination of both batimastat and β -secretase inhibitor IV to inhibit non-amyloidogenic sAPP (Figure 4.9C). This suggests a reciprocal relationship between amyloidogenic and non-amyloidogenic APP proteolysis such that, when BACE1 was inhibited, α -secretase could take over. Such a relationship has been observed previously by Sun *et al.*, 2018 where significantly more sAPP α was released when P15 cells were treated with 5 μ M β -secretase inhibitor IV. The effect was then not significant in P5 cells. P15 and P5 cells are senescent human blood-brain barrier endothelial cells that would be expected to react in similar manner. Sun *et al.*, 2018 also noted utilising β -secretase inhibitor IV and a α -secretase inhibitor (Ang II) did not affect sAPP α production, due to decreased expression of APP. This was however in senescent cells and not dividing cells used in the current experiment. In the current study, converse production of C89 in the cell lysates of SH-SY5Y-BACE1 cells was also explored. This led to mixed results, where the C83 fragment via α -secretase production was missing with control or batimastat treatment alone (Figure 4.11A and C), but a combination of both batimastat and β -secretase inhibitor IV lead to significantly increased levels of C99, the product of BACE1 processing. This could be possible due to the

interaction of BACE1 with γ -secretase, where disrupting this process could lead to an accumulation of CTFs unprocessed by γ -secretase (Cui *et al.*, 2015).

The combination of these results demonstrate that BACE1 is the key enzyme for non-amyloidogenic APP processing specifically in SH-SY5Y-BACE1 cells. It remains to be investigated whether the effect of BACE1 is significant with more physiological levels of BACE1, and whether *in vivo* models of AD also follow the effects of BACE1 overexpression.

7.3 The sAPP α /sAPP β ' axis is more important for cell viability than A β -peptide production

After determining that sAPP β ' is the predominant fragment released in BACE1-overexpressing cells, we wanted to ascertain how this would affect amyloid- β (A β) peptide production and cell viability.

Initial screens for A β -peptide levels produced by each of the AD-relevant cells lines demonstrated high A β 40 increases relative to Mock cells in all the cell lines (Figure 4.6), with similar increases in A β 42 compared to Mock. The greatest increase occurred in Swe-APP transfected cells; the Swedish mutation has long been shown to increase A β levels which coincides with our results (Haas *et al.*, 1995). In SH-SY5Y-wtAPP cells, APP₆₉₅ is overexpressed so it is expected that all products of APP processing will be high, coupled with the preferential amyloidogenic cleavage demonstrated by Haas *et al.*, 1995. For BACE1 overexpressing cells, an increased activity in BACE1 has also been shown to increase A β levels (Haass *et al.*, 1995). In addition, it has been suggested that A β 42 forms a positive feedback loop through the JNK pathway to further promote BACE1 transcription (Guglielmotto *et al.*, 2011). Both of these points would suggest we should see high A β -peptide levels in SH-SY5Y-BACE1 similar to wtAPP and SweAPP in Figure 4.6. However, SH-SY5Y-BACE1 cells are limited by the full-length APP available (significantly lower than wtAPP- and SweAPP-transfected cells in Figure 4.3A) and it is possible that due to the extreme increase of A β levels exhibited by SH-SY5Y-SweAPP the statistical significance of the

BACE1 over-expression is masked. Repeats of the experiment with just WT and SH-SY5Y-SweAPP cells would allow for a Student's t test to be carried out to determine the significant difference between the two means.

With these results and paradigm that A β -peptide accumulation is harmful to the viability of the cell, we then sought to determine whether the high A β -peptide correlated to any degree of reduced cell viability. Despite high levels of A β (Figure 4.6), the wtAPP-transfected SH-SY5Y cells demonstrated significantly higher growth than all other cell models. In addition to this, with extremely high levels of both A β isoforms, the SH-SY5Y-SweAPP cells were significantly more viable than Mock-transfected cells. Such growth assays *in vitro* in SH-SY5Y cell models have not been performed before. However, *in vivo* studies in transgenic mice have shown that SweAPP overexpressed cells did not have a significant effect on pyramidal cells (Simon *et al.*, 2009). Whereas wtAPP overexpression caused neurodegeneration and a significant reduction in the number of CA1 neurons over time (Kreis *et al.*, 2021; Simon *et al.*, 2009).

Neither study was able to determine a specific cause for the neurodegeneration but suggested that it is linked to GABAergic receptors. This effect was demonstrated when a presynaptic GABA_BR antagonist was able to rescue the CA1 neurodegeneration (Kreis *et al.*, 2021). A similar paper found that overexpressing wtAPP caused higher levels of A β , yet determined that reducing A β levels did not affect the number of neurons and that the wtAPP itself was more likely inhibiting adult neurogenesis (Pan *et al.*, 2016). Combining the results of these studies, it could be suggested that the negative effect of wtAPP/SweAPP overexpression is dependent on the interaction of neurons via synapses which is not present in this current monoculture of undifferentiated SH-SY5Y cells. In addition, as the growth of cells were irrespective of A β -levels, the abundance of sAPP α and its growth factor abilities could have led to the significant increases in cell viability. To try to replicate the results from the literature, the SH-SY5Y cells could be differentiated into neuronal cultures following a similar procedure as found here (Shipley, Mangold and Szpara, 2016), with the formation of synapses

that could be driven to express GABAergic/glutamate receptors, the growth assays could be repeated.

Examining the health of the cells under the microscope, SH-SY5Y-BACE1 appeared the least viable under the microscope, with the fewest clusters of cells. In terms of the cell viability assays, BACE1 overexpression was significantly less viable for both the cell count and methanethiosulfonate (MTS) assay compared to all other cell lines (Figure 4.12B and D). Previous literature has shown that BACE1 knock-in can significantly alter the mouse brain metabolome and lead to upregulated A β production (Pan and Green, 2019). If the viability of the cell lines is dependent on sAPP α as hypothesized for wtAPP- and SweAPP-SH-SY5Y cells, then SH-SY5Y-BACE1 viability could be explained by the significant decrease of non-amyloidogenic sAPP from Fig. 4.4A, coupled with the lack of the converse C83 release (and lack of sAPP α) as a result of APP processing (Figure 4.7A). Instead, there is a dominance of sAPP β and sAPP β' which do not convey the neuroproliferative effects of sAPP α .

To confirm the results from the cell viability assay, we next sought to generate and characterize Mock- and BACE1-SH-SY5Y cell lines that overexpress sAPP α and sAPP β' (Figure 4.14 and Figure 4.15). Confirmation that the 4 constructs were successful in releasing non-amyloidogenic sAPP came in Figure 4.16A and D, where the constructs released significantly higher non-amyloidogenic sAPP in SH-SY5Y-Mock and -BACE1 cells. Important to note was that the increase in sAPP₆₉₅ was not significantly different between sAPP α and sAPP β' constructs for either Mock- or BACE1-transfected cells. This confirmed that the anti-APP 6E10 antibody was cross-reacting between sAPP α and sAPP β' and explained how SH-SY5Y-BACE1 resisted the effects of batimastat in Figure 4.4B. This undermines much previous literature that has used 6E10 to detect sAPP α exclusively and makes the use of it invalid as a biomarker for AD (Kim *et al.*, 2019; Grant *et al.*, 2019; Schupf *et al.*, 2008). Therefore, a second antibody, anti-APP 22C11 that binds to the N-terminus was used to confirm that sAPP α and sAPP β' were the dominant soluble fragments in their cognate transfectants.

As hypothesized, when sAPP α is overexpressed in BACE1-transfected cells, it caused the cell count and MTS viability to be rescued and then significantly increased the viability of pIRESneo Mock-transfected cells (Figure 4.17B and D). As previously discussed, the proliferative effects of sAPP α have been demonstrated before (Demars *et al.*, 2011), but has not been shown to do so in direct comparison with sAPP β' . The opposite effect of sAPP α was then present when sAPP β' was overexpressed, where the overexpression significantly reduced cell viability compared to pIRESneo-Mock and even compared to pIRESneo-BACE1 Mock transfected. There are unfortunately no studies into the function of sAPP β' and sAPP β' has only been implicated in BACE1-overexpression as a therapeutic target as it leads to the production of non-amyloidogenic A β , which also demonstrates that switching BACE1 cleavage to the β' site is not toxic to the cell itself (Volloch and Rits-Volloch, 2022). However, the research presented here demonstrates that overproduction of sAPP β' is at the deficit of the beneficial effect of sAPP α release and causes a reduction in cell viability.

Each of the cell lines used in this study were SH-SY5Y based and have been used in previous literature (Parkin *et al.*, 2007; Mattsson *et al.*, 2012; Findlay, Hamilton and Ashford, 2015; Lee *et al.*, 2016; Kong *et al.*, 2020). However, none of these studies discuss the use of SH-SY5Y as a model. The undifferentiated cells are non-polarized, rapidly proliferate and do not express mature neuronal markers. This makes undifferentiated SH-SY5Y cells easier to culture, manipulate and economically viable to use. Proteomics of SH-SY5Y cells show that undifferentiated cells express proteins involved in cell proliferation, whereas differentiation cells express proteins related to neuronal development (Murillo *et al.*, 2017). As mentioned in the Introduction (1.1.2.2.1), A β -mediated toxicity could be dependent on the complex neuronal system which would be only present in differentiated neurons, where functional synapses appear. This provides a significant disadvantage to the current model used and could in part explain the lack of A β -toxicity found in Figure 4.12. Differentiation of SH-SY5Y cells also gives rise to KEGG enriched pathways specifically related to AD and

suggests its use a model for AD (Murillo *et al.*, 2017). Looking more specifically at APP expression, when SH-SY5Y cells are differentiated by retinoic acid and stimulated with brain-derived neurotrophic factor, the APP changes localisation from the Golgi apparatus and vesicles to the mitochondria (Riegerova *et al.*, 2021). This is coupled with a reduction of full-length APP in the cell. Therefore, despite the advantages provided by differentiating the SH-SY5Y cells to a more neuronal-like state, the results of the sAPP α /sAPP β ' axis could have entirely been missed in differentiated cells. With lower APP, the balance of ADAM10 and BACE1 activity could change when there is limited APP available.

7.4 Design and generation of a neuroprotective expression system in SH-SY5Y stable transfectants

To circumnavigate the enhancement of ADAM10 via treatment (by fibrates) we utilised gene therapy to directly overexpress sAPP α in the AD cell models. This involved the designing of a Tet-on system employing a neuron-specific hybrid promoter consisting of the human cytomegalovirus (CMV) enhancer fused to the human synapsin 1 promoter, that has been shown to yield high levels of neuron-specific expression (Hioki *et al.*, 2007). In this system sAPP α and VPS35 coding DNA sequences could be stably expressed on a response plasmid and regulated by the introduction of tetracycline to the regulator plasmid. These two plasmids could then be incorporated into a second generation PiggyBac (Ding *et al.*, 2005) single plasmid expression system.

However, due to issues stably transfecting the regulator plasmid into SH-SY5Y cells and time limitations it was not possible to go further than the generation of multiple regulator and response plasmid variants ready for transfection. The regulator and response plasmids were designed to be able to selectively overexpress sAPP α and potentially another protein to simultaneously target tau pathology (VPS35). This involved the use of a commonly used Tet-On plasmid system (Das, Tenenbaum and Berkhout, 2016), which consisted of a regulator plasmid encoding a transactivator protein (TET3G) that can be activated when bound to tetracycline/doxycycline and then able to interact with

the response plasmid promoter; which would control sAPP α and VPS35 expression. The Tet-On system has previously been employed in other AD research, including the Tet-On A β -GFP SH-SY5Y model to test compound VB-037 and herbal formula B401 inhibition of A β aggregation (Chiu *et al.*, 2019; Hsu *et al.*, 2016). The end goal was to combine this system to create a PiggyBac plasmid that could act more similar to other gene therapies. Such gene therapy-based approaches have been employed to successfully treat neurodegenerative diseases such as neuroblastoma (Pesonen *et al.*, 2010), and spinal muscular atrophy where onasemnogene abeparvovec overexpresses the SMN1 gene (Mercuri *et al.*, 2021). There are currently no successful gene therapies focused on AD that have been approved for use and options are only in pre-clinical stages.

The first aim of the plasmid design was to generate a cytomegalovirus (CMV) promoter version of the pIREShyg-ESYN-TET3G regulator plasmid (Figure 6.1). The resultant pIREShyg-CMV-TET3G and pIREShyg-ESYN-TET3G regulator plasmids were then transiently transfected into HEK-293 and SH-SY5Y cells as described in Materials and Methods. The result of this was expression of TET3G from the pIREShyg-CMV-TET3G in HEK cells, and possibly some minor expression from SH-SY5Y cells. The CMV version of the regulator plasmid was to act as a control if the ESYN promoter would not be activated due to the specific nature of the ligand required, which would only arise if the SH-SY5Y cells were fully differentiated to neurons. It was not expected however, that the CMV version was less functional in SH-SY5Y cells, whereas it functioned in HEK cells. The advantage of HEK-293 cells is that they have high transfection efficiency, and high division rate, which has caused HEK cells to be the choice for recombinant protein expression (Baldi *et al.*, 2007). However, they derive from human embryonic kidney cells and were not expected to produce neuron specific factors to induce the ESYN promoter found in pIREShyg-ESYN-TET3G (Hioki *et al.*, 2007). Therefore, SH-SY5Y cells were selected as they derive from neuroblastoma cells. Important to note, undifferentiated SH-SY5Y cells rapidly proliferate but do not express markers of mature neurons including growth-associated protein (GAP-43), neuronal nuclei (NeuN), synaptic vesicle protein II

(SV2), neuron specific enolase (NSE), microtubule associated protein (MAP) and the relevant synaptophysin (SYN) (Gimenez-Cassina, Lim and Diaz-Nido, 2006; Pahlman *et al.*, 1984; Xie, Hu and Li, 2010; Cheung *et al.*, 2009). However, neither regulator plasmid yielded any TET3G production in the SH-SY5Y cells and this could be due to a number of different reasons. As the transient transfection worked in HEK cells it can be assumed that the DNA was of good quality and the 80% confluence of adherent cells (as specified in Turbofect manual) was sufficient for successful transfection, in addition the SH-SY5Y cells did not exhibit signs of cellular toxicity after the check at 24 hrs or 48 hrs. In a comparison with other cells lines using TurboFect, SH-SY5Y demonstrated 27% transfection efficiency, lower than the 47.1% in primary rabbit articular chondrocytes and 37.2% in EMT6 cells (Wu *et al.*, 2017). It is possible to use different reagents to successfully transiently transfect SH-SY5Y cells such as FuGene HD which could prove to be optimal for SH-SY5Y cells (Skommer and Brittain, 2012).

Concurrently alongside the work on the regulator plasmid, we generated multiple versions of the response plasmid. The purpose of the multiple versions of the regulator plasmid was due to the reduced expression that can occur downstream of the IRES sites (Mizuguchi *et al.*, 2000) ranging from 6.4-100% downstream of the first IRES sequence and 0.1-0.8% downstream of the second IRES sequence. The IRES sequence permits the translation of multiple mRNA sequences and allowed for both the sAPP α and VPS35 CDS to be included onto the plasmid. IRES sequences have also been used in other areas of AD research such as the delivery of a modified antibody to combat A β progression (Elmer *et al.*, 2019). The response plasmid was also prepared for the generation of the PiggyBac plasmid by removing the bleomycin coding sequence in the pIRESzeo-Empty-VPS35 variant. Unfortunately, due to time constraints for this project the PiggyBac plasmid could not be generated and tested. This was coupled with issues with transient transfection previously discussed, and failure in attempts of stable transfection via electroporation or a modified Turbofect method. The SH-SY5Y cells would remain viable after transfection but unfortunately there would

be no evidence of TET3G expression; without the regulator stably transfected there was no logic to then double transfect any version of the response plasmid.

7.5 Future work

With refinements and optimization to the methodology for transfection the regulator plasmid could first be stably transfected into SH-SY5Y cells (with CMV and ESYN-promoter versions) and tested for TET3G expression as attempted in Figure 6.2C. Subsequent multiplication of these cells would then be double-transfected with each version of the generated response plasmid (Figure 6.3 to Figure 6.10). Utilizing Tet system approved FBS (Takara, Saint-Germain-en-Laye, France) and the induction of the system with doxycycline, antibodies to select for sAPP α (6E10 or 22c11) and VPS35 (with anti-VPS35 (Abcam, Cambridge, Massachusetts, USA) used in (Niu *et al.*, 2021)) could then test which configuration of the response system yields the highest production of either protein. In conducting the western blots to test for sAPP α and VPS35, it would be prudent to run multiple controls on the same blot so that error bars could be generated unlike the current study. This could then remove any potential bias from normalizing the data to the control. This could be then taken forward by repeating cell viability assays to show that sAPP α overexpression is still beneficial as found in (Figure 4.17) and that VPS35 is not harmful to cell viability. The induction of the ESYN promoter protein would be further enhanced by differentiating the SH-SY5Y down the neuronal cell line (Shipley, Mangold and Szpara, 2016), at the cost of rapid proliferation. It would be then possible to repeat this process in the AD-relevant cell models used in this paper (SH-SY5Y-BACE1, -wtAPP and -SweAPP) that have higher levels of A β . There are also a host of tau-pathology models of AD that could be assessed, including Tau-40 and Tau-46 isoforms modelled in HEK and SH-SY5Y cells, respectively (Bandyopadhyay *et al.*, 2007; Nonaka *et al.*, 2010). The culmination of this work would to be to combine the regulator plasmid with the response plasmid prepared in Figure 6.10 to generate the singular PiggyBac plasmid in preparation for insertion into a viral vector, for instance a similar viral vector was used to then infect an *in vivo* model of AD such as Tg2576 mice (Hsiao *et al.*, 1996). Further tests would need to be

carried out to determine whether the employment of the PiggyBac plasmid was therapeutic in either *in vitro* and *in vivo* models.

7.6 Conclusions

To conclude, in the current study we have demonstrated the sAPP α -sAPP β ' axis generated by BACE1 overexpression. It remains to be seen if this effect is found more widely in more complex models of AD. The effect of the sAPP α -sAPP β ' axis were found to be more influential on cell viability than A β -peptide levels, where sAPP α is vital for health growth of AD-related cell lines. This highlighted the importance of stimulating sAPP α release which was not found with gemfibrozil or bezafibrate treatment in our hands. Going forward, the development of the Tet-On mammalian expression system to selectively overexpress sAPP α in neurons (and subsequent PiggyBac generation) could prove to be therapeutic in combating AD.

8. Appendices

GACGGATCGGGAGATCTCCCGATCCCCTATGGTCGACTCTCAGTACAATCTGCTCTGATG
CCGCATAGTTAAGCCAGTATCTGCTCCCTGCTTGTGTGTTGGAGGTCGCTGAGTAGTGCG
CGAGCAAATTTAAGCTACAACAAGGCAAGGCTTGACCGACAATTGCATGAAGAATCTGCT
TAGGGTTAGGCGTTTTGCGCTGCTTCGCGATGTACGGGCCAGATATACGC**GTTGACATTG**
ATTATTGACTAGTTAATAAGTAATCAATTACGGGGTCATTAGTTCATAGCCCATATATGGA
GTTCCGCGTTACATAACTTACGGTAAATGGCCCGCTGGCTGACCGCCCAACGACCCCGC
CCCATTGACGTCAATAATGACGTATGTTCCCATAGTAACGCCAATAGGGACTTTCCATTGA
CGTCAATGGGTGGACTATTTACGGTAAACTGCCCACTTGGCAGTACATCAAGTGTATCATA
TGCCAAGTACGCCCCCTATTGACGTCAATGACGGTAAATGGCCCGCTGGCATTATGCC
AGTACATGACCTTATGGGACTTTCTACTTGGCAGTACATCTACGTATTAGTCATCGCTATT
ACCATGGTGATGCGGTTTTGGCAGTACATCAATGGGCGTGGATAGCGGTTTGACTCACGG
GGATTTCCAAGTCTCCACCCATTGACGTCAATGGGAGTTTGTGGCACCAAAATCAAC
GGGACTTTCCAAAATGTCGTAACAACCTCCGCCATTGACGCAAATGGGCGGTAGGCGTG
TACGGTGGGAGGTCTATATAAGCAGAGCTCTCTGGCTAACTAGAGAACCCACTGCTTACTG
GCTTATCGAAATTAATACGACTCACTATAGGGAGACCCAAGCTTGGTACCGAGCTCGGATC
CACTAGTAACGGCCGCCAGTGTGCTGGAATTAATTGCTGTCTGCGAGGGCCAGCTGTTG****
GGTGAGTACTCCCTCTCAAAGCGGGCATGACTTCTGCGCTAAGATTGTCAGTTTCCAAA
AACGAGGAGGATTTGATATTCACCTGGCCCGCGGTGATGCCTTTGAGGGTGGCCGCGTCC
ATCTGGTCAGAAAAGACAATCTTTTTGTTGTCAAGCTTGAGGTGTGGCAGGCTTGAGATCT
GGCCATACACTTGAGTGACAATGACATCCACTTTGCCTTTCTCTCCACAGGTGTCCACTCC
CAGGTCCAACTGCAGTGC**ATCGAGCATGCATCTAGGGCGGCCGCACTAGAGGA**ATTGC****
CCCCTCTCCCTCCCCCCCCCTAACGTTACTGGCCGAAGCCGCTTGAATAAGGCCGGTG
TGTGTTTGTCTATATGTGATTTTCCACCATATTGCCGTCTTTGGCAATGTGAGGGCCCGGA
AACCTGGCCCTGTCTTCTTGACGAGCATTCTAGGGGTCTTCCCCTCTCGCCAAAGGAAT
GCAAGGTCTGTTGAATGTCGTGAAGGAAGCAGTTCCTCTGGAAGCTTCTGAAGACAAACA
ACGCTGTAGCGACCCCTTTCAGGCAGCGGAACCCCCACCTGGCGACAGGTGCCTCTG
CGGCCAAAAGCCACGTGTATAAGATACACCTGCAAAGGCCGACACAACCCAGTGCCACGT
TGTGAGTTGGATAGTTGTGGAAGAGTCAAATGGCTCTCCTCAAGCGTAGTCAACAAGGG
GCTGAAGGATGCCCAGAAGGTACCCATTGTATGGGAATCTGATCTGGGGCCTCGGTGCA
CATGCTTTACATGTGTTTAGTCGAGGTTAAAAAGCTCTAGGCCCCCGAACCCAGGGGAC
GTGGTTTTCTTTGAAAACACGATGATAAGCTTGCCACAACCCCGTACCAAAGATGGATA
GATCCGAAAGCCTGAACTCACCGCAGCTCTGTGCGAGAAGTTTCTGATCGAAAAGTTCCG
ACAGCGTCTCCGACCTGATGCAGCTCTCGGAGGGCGAAGAATCTCGTGCTTTAGCTTCCG
ATGTAGGAGGGCGTGATATGTCCTGCGGGTAAATAGCTGCGCCGATGGTTTCTACAAG
ATCGTTATGTTTATCGGCACCTTTGCATCGGCCGCTCCCGATTCCCGAAGTGCTTGACAT
TGGGAATTCAGCGAGAGCCTGACCTATTGCATCTCCCGCCGTGCACAGGGTGTACGTT
GCAAGACCTGCCTGAAACCGAACTGCCCGCTGTTCTGCAGCCGGTCGCGGAGGCCATGG
ATGCGATCGCTGCGGCCGATCTTAGCCAGACGAGCGGGTTCGGCCATTTCGACCGCAA
GGAATCGGTCAATACACTACATGGCGTGATTTCATATGCGCGATTGCTGATCCCATGTGT
ATCACTGGCAAACCTGTGATGGACGACACCGTCAAGTGCCTCCGTCGCGCAGGCTCTCGATG
AGCTGATGCTTTGGGCCGAGGACTGCCCCGAAGTCCGGCACCTCGTGCACGCGGATTTCC
GGCTCCAACAATGTCCTGACGGACAATGGCCGCATAACAGCGGTCAATTGACTGGAGCGAG
GCGATGTTCCGGGATTCCCAATACGAGGTGCGCAACATCTTCTTCTGGAGGCCGTGGTTG
GCTTGTATGGAGCAGCAGACGCGCTACTTCGAGCGGAGGCATCCGGAGCTTGCAGGATC
GCCGCGGCTCCGGGCGTATATGCTCCGCATTGGTCTTGACCAACTCTATCAGAGCTTGGT
TGACGGCAATTTTCGATGATGCAGCTTGGGCGCAGGGTCGATGCGACGCAATCGTCCGATC
CGGAGCCGGGACTGTGCGGGCGTACACAAATCGCCCGCAGAAGCGCGGCCGTCTGGACC
GATGGCTGTGTAGAAGTACTCGCCGATAGTGGAACCGACGCCCCAGCACTCGTCCGAG
GGCAAAGGAATAGAGTAGATGCCGACCGAACAAGAGCTGATTTTCGAGAACGCCTCAGCCA
GCAACTCGCGCGAGCCTAGCAAGGCAAATGCGAGAGAACGGCCTTACGCTTGGTGGCAC
AGTTCTCGTCCACAGTTCGCTAAGCTCGCTCGGCTGGGTGCGGGGAGGGCCGGTGCAG
TGATTCAGGCCCTTCTGGATTGTGTTGGTCCCCAGGGCACGATTGTCATGCCACGCACT
CGGGTGTCTGACTGATCCCGCAGATTGGAGATCGCCGCCCGTGCCTGCCGATTGGGTG
CAGATCTAGAGCTCGCTGATCAGCCTCGACTGTGCCTCTAGTTGCCAGCCATCTGTTGTTT
GCCCTCCCCCGTGCCTTCTTGACCCTGGAAGGTGCCACTCCCACTGTCCTTTCTAATA
AAATGAGGAAATTGCATCGCATTGTCTGAGTAGGTGTCATTCTATTCTGGGGGTGGGGTG
GGGCAGGACAGCAAGGGGGAGGATTGGGAAGACAATAGCAGGCATGCTGGGGATGCGG

TGGGCTCTATGGCTTCTGAGGCGGAAAGAACCAGCTGGGGCTCGAGTGCATTCTAGTTGT
 GGTGGTCCAACTCATCAATGTATCTTATCATGTCTGTATACCGTTCGACCTCTAGCTAGAG
 CTTGGCGTAATCATGGTCATAGCTGTTTCTGTGTGAAATTGTTATCCGCTCACAATTCCAC
 ACAACATACGAGCCGGAAGCATAAAGTGTAAGCCTGGGGTGCCTAATGAGTGAGCTAAC
 TCACATTAATTGCGTTGCGCTCACTGCCCGCTTCCAGTCGGGAAACCTGTCGTGCCAGCT
 GCATTAATGAATCGGCCAACGCGCGGGGAGAGGCGGTTTGCCTATTGGGCGCTCTTCCG
 CTTCTCGCTCACTGACTCGCTGCGCTCGGTCTCGGCTGCGGCGAGCGGTATCAGCTC
 ACTCAAAGGCGGTAATACGGTTATCCACAGAATCAGGGGATAACGCAGGAAAGAACATGT
 GAGCAAAGGCCAGCAAAGGCCAGGAACCGTAAAAAGGCCGCGTTGCTGGCGTTTTTCC
 ATAGGCTCCGCCCCCTGACGAGCATCACAAAAATCGACGCTCAAGTCAGAGGTGGCGAA
 ACCCGACAGGACTATAAAGATACCAGGCGTTTTCCCCCTGGAAGCTCCCTCGTGCGCTCTC
 CTGTTCCGACCTGCCGCTTACCGGATACCTGTCCGCTTCTCCCTTCGGGAAGCGTGG
 CGCTTCTCAATGCTCAGCTGTAGGTATCTCAGTTCCGCTGTAGGTCGTTCCGCTCCAAGCT
 GGGCTGTGTGCACGAACCCCCGTTACGCCGACCGCTGCGCCTTATCCGGTAACTATCG
 TCTTGAGTCCAACCCGGTAAGACACGACTTATCGCCACTGGCAGCAGCCACTGGTAACAG
 GATTAGCAGAGCGAGGTATGTAGGCGGTGCTACAGAGTTCTTGAAGTGGTGGCCTAACTA
 CGGCTACACTAGAAGGACAGTATTTGGTATCTGCGCTCTGCTGAAGCCAGTTACCTTCGGA
 AAAAGAGTTGGTAGCTCTTGATCCGGCAAACAAACCACCGCTGGTAGCGGTGGTTTTTTTG
 TTTGCAAGCAGCAGATTACGCGCAGAAAAAAGGATCTCAAGAAGATCCTTTGATCTTTTCT
 ACGGGGTCTGACGCTCAGTGGAACGAAACTCACGTTAAGGGATTTTGGTCATGAGATTAT
 CAAAAAGGATCTTCACCTAGATCCTTTTAAATTAATAAATGAAGTTTTAAATCAATCTAAAGTA
 TATATGAGTAAACTTGGTCTGACAGT**TACCAATGCTTAATCAGTGAGGCACCTATCTCAGC**
GATCTGTCTATTTTCGTTCCATCCATAGTTGCCTGACTCCCCGTCGTGTAGATAACTACGATAC
GGGAGGGCTTACCATCTGGCCCCAGTGCTGCAATGATACCGCGAGACCCACGCTCACCG
GCTCCAGATTTATCAGCAATAAACCAGCCAGCCGGAAGGGCCGAGCGCAGAAGTGGTCCCT
GCAACTTTATCCGCCTCCATCCAGTCTATTAATTGTTGCCGGGAAGCTAGAGTAAGTAGTT
CGCCAGTTAATAGTTTTCGCAACGTTGTTGCCATTGCTACAGGCATCGTGGTGTACCGCTC
GTGTTTTGGTATGGCTTCATTACGCTCCGGTTCCCAACGATCAAGGCGAGTTACATGATCC
CCCATGTTGTGCAAAAAAGCGGTTAGCTCCTTCGGTCTCCGATCGTTGTGAGAAGTAAGT
TGGCCGCAAGTGTATCACTCATGGTTATGGCAGCACTGCATAATTCTCTTACTGTGATGCC
ATCCGTAAGATGCTTTTCTGTGACTGGTGAGTACTCAACCAAGTCATTCTGAGAATAGTGTA
TGCGGCGACCGAGTTGCTCTTGCCCCGGCGTCAATACGGGATAATACCGCGCCACATAGCA
GAACTTTAAAAGTGCTCATCATTGGAAAACGTTCTTCGGGGCGAAAACCTCTCAAGGATCTT
ACCGCTGTTGAGATCCAGTTTCGATGTAACCCACTCGTGCACCCAACTGATCTTCAGCATCT
TTTACTTTTACCAGCGTTTTCTGGGTGAGCAAAAAACAGGAAGGCAAAATGCCGCAAAAAAGG
GAATAAGGGCGACACGGAAATGTTGAATACTCATACTCTTCTTTTCAATATTATTGAAGC
ATTTATCAGGGTTATTGTCTCATGAGCGGATACATATTTGAATGTATTTAGAAAAATAAACAA
ATAGGGGTTCCGCGCACATTTCCCCGAAAAGTGCCACCTGACGTC

Figure S.1: Total nucleotide sequence for the pRESHyg vector. Important elements discussed in the text are indicated by the colour scheme: Human CMV promoter (cyan) (nucleotides 232-820), synthetic intron (IVS) known to enhance mRNA stability (orange) (nucleotides 938-1233), internal ribosome entry site (IRES) (purple) (nucleotides 1270-1856), hygromycin B phosphotransferase (Hyg^r) coding DNA sequence (nucleotides 1869-2903), polyA termination sequence (nucleotides 3192-3468) (red) and beta-lactamase ampicillin resistance (olive) (nucleotides 5584-4727).

GACGGATCGGGAGATCTCCCGATCCCCTATGGTCGACTCTCAGTACAATCTGCTCTGATG
CCGCATAGTTAAGCCAGTATCTGCTCCCTGCTTGTGTGTTGGAGGTCGCTGAGTAGTGCG
CGAGCAAATTTAAGCTACAACAAGGCAAGGCTTGACCGACAATTGCATGAAGAATCTGCT
TAGGGTTAGGCGTTTTGCGCTGCTTCGCGACCCCTAGAAAGATAATCATATTGTGACGTACG
TTAAAGATAATCATGCGTAAAATTGACGCATGTGTTTTATCGGTCTGTATATCGAGGTTTATT
TATTAATTTGAATAGATATTAAGTTTTATTATATTTACACTTACATACTAATAATAAATTCACA
AACAAATTTATTTATGTTTATTTATTTATTAATAAAAAACAAAACTCAAAATTTCTTCTATAAAG
TAACAAAATTTTATGAGGGACAGCCCCCCCCAAAGCCCCCAGGGATGTAATTACGTCCC
TCCCCCGCTAGGGGGCAGCAGCGAGCCGCCCGGGGCTCCGCTCCGGTCCGGCGCTCCC
CCCGCATCCCCGAGCCGGCAGCGTGCGGGGACAGCCCGGGCAGGGGAAGGTGGCAGC
GGATCGCTTTCTCTGAACGTTCTCGCTGCTCTTTGAGCCTGCAGACACCTGGGGGAT
ACGGGGAAAAGGCCTCCAAGGCCTACTAGTCTTAAGCGTTACATAACTTACGGTAAATGGC
CCGCCTGGCCCAACGACGCCCCGCTTACGCTCAATAATGACGTATGTTCCC
ATAGTAACGCCAATAGGGACTTTCCATTGACGTCAATGGGTGGAGTATTTACGGTAAACTG
CCCATTGGCAGTACATCAAGTGTATCATATGCCAAGTACGCCCCCTATTGACGTCAATGA
CGGTAATGGCCCGCCTGGCATTATGCCAGTACATGACCTTATGGGACTTTCTACTTGG
CAGTACATCTACGTATTAGTCATCGCTATTACCATGGCTGCAGAGGGCCCTGCGTATGAGT
GCAAGTGGGTTTTAGGACCAGGATGAGGCGGGGTGGGGTGCCTACCTGACGACCGACC
CCGACCCACTGGACAAGCACCCAACCCCATTCCCCAAATTGCGCATCCCCTATCAGAGA
GGGGGAGGGGAAACAGGATGCGGCGAGGCGCGTGCCTGCGCACTGCCAGCTTCAGCACCGG
GACAGTGCCTTCGCCCCCGCTGGCGGCGCGGCCACCGCCGCTCAGCACTGAAGGC
GCGCTGACGTCACTCGCCGCTCCCCCGCAAACCTCCCCTTCCCGCCACCTTGGTGCCT
CCGCGCCGCGCCGCGCCAGCCGGACCGCACCGAGGCGCGAGATAGGGGGGCA
CGGGCGCGACCATCTGCGCTGCGGCGTTAATTAAGCCACCATGTCTAGACTGGACAAGAG
CAAAGTCATAAACTCTGCTCTGGAATTACTCAATGGAGTCGGTATCGAAGGCCTGACGACA
AGGAAACTCGCTCAAAAGCTGGGAGTTGAGCAGCCTACCCTGTACTGGCACGTGAAGAAC
AAGCGGGCCCTGCTCGATGCCCTGCCAATCGAGATGCTGGACAGGCATCATACCCACTCC
TGCCCCCTGGAAGGCGAGTCATGGCAAGACTTTCTGCGGAACAACGCCAAGTCATACCGC
TGTGCTCTCCTCTCACATCGCGACGGGGCTAAAGTGCATCTCGGCACCCGCCAACAGAG
AAACAGTACGAAACCCTGGAAAATCAGCTCGCGTTCCTGTGTCAGCAAGGCTTCTCCCTG
GAGAACGCACTGTACGCTCTGTCCGCGTGGGCCACTTTACACTGGGCTGCGTATTGGAG
GAACAGGAGCATCAAGTAGCAAAAAGAGGAAAGAGAGACACCTACCACCGATTCTATGCCC
CCACTTCTGAAACAAGCAATTGAGCTGTTGACCGGCGAGGGAGCCGAACCTGCCTTCCTT
TTCGGCCTGGAACATAATCATATGTGGCCTGGAGAAACAGCTAAAGTGCGAAAGCGCGGG
CCGACCGAGCCCTTGACGATTTTGACTTAGACATGCTCCAGCCGATGCCCTTGACGAC
TTTGACCTTGATATGCTGCTGCTGACGCTCTTGACGATTTTGACCTTGACATGCTCCCCG
GGTAA GATATCGGATCCACTAGTAACGGCCG **CCAGTGTGCTGG** AATTAATTCGCTGTCTGC
GAGGGCCAGCTGTTGGG **GTGAGTACTCCCTCTCAAAGCGGGCATGACTTCTGCGCTAAG**
ATTGTCAGTTTCAAACAGAGGAGATTTGATATTCACCTGGCCCGCGGTGATGCCTTTG
AGGGTGGCCGCGTCCATCTGGTCAGAAAAGACAATCTTTTTGTTGTCAAGCTTGAGGTGTG
GCAGGCTTGAGATCTGGCCATACTTGAGTGACAATGACATCCACTTTGCCTTTCTCTCC
ACAGGTGTCCACTCCAGGTCCAACCTGCAGGTGCATCGAGCATGCATCTAGGGCGGCCG
CACTAGAGGAATTCGCCCTCTCCCTCCCCCCCCCTAACGTTACTGGCCGAAGCCGCTT
GGAATAAGGCCGGTGTGTGTTGTCTATATGTGATTTTCCACCATATTGCCGTCTTTGGCA
ATGTGAGGGCCCGGAAACCTGGCCCTGTCTTCTTGACGAGCATTCTAGGGGTCTTTCCC
CTCTCGCAAAGGAATGCAAGGTCTGTTGAATGTCGTGAAGGAAGCAGTTCTCTGGAAG
CTTCTTGAAGACAAACAACGTCTGTAGCGACCTTTGCAGGCAGCGGAACCCCCCACCTG
GCGACAGGTGCCTCTGCGGCCAAAAGCCACGTGTATAAGATACACCTGCAAAGGCGGCAC
AACCCAGTGCCACGTTGTGAGTTGGATAGTTGTGAAAGAGTCAAATGGCTCTCCTCAAG
CGTAGTCAACAAGGGGCTGAAGGATGCCAGAAGGTACCCATTGTATGGGAATCTGATC
TGGGGCCTCGGTGCACATGCTTTACATGTGTTTAGTCGAGGTTAAAAAGCTCTAGGCCCC
CCGAACCACGGGGACGTGGTTTTCTTTGAAAAACACGATGATAAGCTTGCCACAACCCC
GTACCAAAGATGGATAGATCCGGAAGCCTGAACTCACCGCAGCTCTGTGAGAAAGTTT
CTGATCGAAAAGTTGACAGCGTCTCCGACCTGATGCAGCTCTCGGAGGGCGAAGAATCT
CGTGCTTTGACGTTTCGATGTAGGAGGGCGTGGATATGTCCTGCGGGTAAATAGCTGCGCC
GATGGTTTCTACAAAGATCGTTATGTTTATCGGCACCTTTCATCGGCCGCGCTCCCGATT
CGGAAGTGCTTGACATTGGGGAATTCAGCGAGAGCCTGACCTATTGCATCTCCCGCCGTG

CACAGGGTGTACGTTGCAAGACCTGCCTGAAACCGAACTGCCCGCTGTTCTGCAGCCGG
TCGCGGAGGCCATGGATGCGATCGCTGCGGCCGATCTTAGCCAGACGAGCGGGTTCCGGC
CCATTCGGACCGCAAGGAATCGGTCAATACACTACATGGCGTGATTCATATGCGCCGATTG
CTGATCCCCATGTGTATCACTGGCAAACCTGTGATGGACGACACCGTCAGTGCGTCCGTCG
CGCAGGGCTCTCGATGAGCTGATGCTTTGGGCCGAGGACTGCCCCGAAGTCCGGCACCTC
GTGCACGCGGATTTCCGGCTCCAACAATGTCTGACGGACAATGGCCGCATAACAGCGGTC
ATTGACTGGAGCGAGGCGATGTTCCGGGATTCCCAATACGAGGTCGCCAACATCTTCTTC
TGGAGGCCGTGGTTGGCTTGTATGGAGCAGCAGACGCGCTACTTCGAGCGGAGGCATCC
GGAGCTTGCAGGATCGCCGCGGCTCCGGGCGTATATGCTCCGCATTGGTCTTGACCAACT
CTATCAGAGCTTGGTTGACGGCAATTCGATGATGCAGCTTGGGCGCAGGGTCGATGCGA
CGCAATCGTCCGATCCGGAGCCGGGACTGTCGGGCGTACACAATCGCCCGCAGAAAGCG
CGGCCGTCTGGACCGATGGCTGTGTAGAAGTACTCGCCGATAGTGAAACCGACGCCCC
AGCACTCGTCCGAGGGCAAAGGAATAGAGTAGATGCCGACCGAACAAGAGCTGATTTGCA
GAACGCCTCAGCCAGCAACTCGCGCGAGCCTAGCAAGGCAAATGCGAGAGAACGGCCTT
ACGCTTGGTGGCACAGTTCTCGTCCACAGTTCGCTAAGCTCGCTCGGCTGGGTCCGGGA
GGGCCGGTCCGAGTGATTCAGGCCCTTCTGGATTGTGTTGGTCCCCAGGGCACGATTGTC
ATGCCACGCACTCGGGTGTACTGACTGATCCCGCAGATTGGAGATCGCCGCCCGTGCCT
GCCGATTGGGTGCAGATCTAGAGCTCGCTGATCAGCCTCGACTGTGCCTCTAGTTGCCAG
CCATCTGTTGTTTGGCCCTCCCCCGTGCCTTCTTGACCCTGGAAGGTGCCACTCCCACT
GTCCTTCTCTAATAAAATGAGGAAATTGCATCGCATTGTCTGAGTAGGTGTCATTCTATTCT
GGGGGGTGGGGTGGGGCAGGACAGCAAGGGGGAGGATTGGGAAGACAATAGCAGGCAT
GCTGGGGATGCGGTGGGCTCTATGGCTTCTGAGGCGGAAAGAACCAGCTGGGGCTCGAG
TGCATTCTAGTTGTGGTTTGTCCAAACTCATCAATGTATCTTATCATGTCTGTATACCGTCC
ACCTCTAGCTAGAGCTTGGCGTAATCATGGTCATAGCTGTTTCCTGTGTGAAATTGTTATCC
GCTCACAATTCCACACAACATACGAGCCGGAAGCATAAAGTGTAAGCCTGGGGTGCCTA
ATGAGTGAGCTAACTCACATTAATTGCGTTGCGCTCACTGCCCGCTTTCAGTCCGGGAAAC
CTGTGCTGCCAGCTGCATTAATGAATCGGCCAACGCGCGGGGAGAGGGGTTTGCCTATT
GGGCGCTCTTCCGCTTCTCGCTCACTGACTCGCTGCGCTCGGTGCTTCGGCTGCGGCG
AGCGGTATCAGCTCACTCAAAGGCGGTAATACGGTTATCCACAGAATCAGGGGATAACGC
AGGAAAGAACATGTGAGCAAAAGGCCAGCAAAAGGCCAGGAACCGTAAAAAGGCCGCGTT
GCTGGCGTTTTTCCATAGGCTCCGCCCCCTGACGAGCATCACAATAATCGACGCTCAAG
TCAGAGGTGGCGAAACCCGACAGGACTATAAAGATACCAGGCGTTTCCCCCTGGAAGCTC
CCTCGTGCCTCTCCTGTTCCGACCCTGCCGCTTACCGGATACCTGTCCGCTTTCTCCCT
TCGGGAAGCGTGGCGCTTCTCAATGCTCACGCTGATAGGTATCTCAGTTCGGGTGATGCT
GTTGCTCCAAGCTGGGCTGTGTGCACGAACCCCGTTACGCCGACCGCTGCGCCTTA
TCCGTAACATATCGTCTTGAGTCCAACCCGTAAGACACGACTTATCGCCACTGGCAGCA
GCCACTGGTAACAGGATTAGCAGAGCGAGGTATGTAGGCGGTGCTACAGAGTTCTTGAAG
TGGTGGCCTAACTACGGCTACACTAGAAGGACAGTATTTGGTATCTGCGCTCTGCTGAAGC
CAGTTACCTTCGGAAAAAGAGTTGGTAGCTCTTGATCCGGCAAACAACCACCGCTGGTAG
CGGTGGTTTTTTTTGTTTGAAGCAGCAGATTACGCGCAGAAAAAAGGATCTCAAGAAGAT
CCTTTGATCTTTTCTACGGGGTCTGACGCTCAGTGGAAACGAAAACCTCACGTTAAGGGATTT
TGGTCATGAGATTATCAAAAAGGATCTTACCTAGATCCTTTTAAATTAATAAAGTTTAA
AATCAATCTAAAGTATATATGAGTAACTTGGTCTGACAGTTACCAATGCTTAATCAGTGAG
GCACCTATCTCAGCGATCTGTCTATTTTCGTTCCATCAGTTGCCTGACTCCCCGTCGTGT
AGATAACTACGATACGGGAGGGCTTACCATCTGGCCCCAGTGCTGCAATGATACCGCGAG
ACCCACGCTCACCGGCTCCAGATTTATCAGCAATAAACCAGCCAGCCGGAAGGGCCGAGC
GCAGAAGTGGTCTGCAACTTTATCCGCCTCCATCCAGTCTATTAATTGTTGCCGGGAAGC
TAGAGTAAGTAGTTCGCCAGTTAATAGTTTGCGCAACGTTGTTGCCATTGCTACAGGCATC
GTGGTGTACGCTCGTCTGTTTGGTATGGCTTCAATCAGCTCCGGTTCCTAACGATCAAGG
CGAGTTACATGATCCCCATGTTGTGCAAAAAAGCGGTTAGCTCCTTCGGTCTCCGATCG
TTGTCAGAAGTAAGTTGGCCGCAAGTGTATCACTCATGGTTATGGCAGCACTGCATAATTC
TCTTACTGTATGCCATCCGTAAGATGCTTTTCTGTGACTGGTGGTACTCAACCAAGTCAT
TCTGAGAATAGTGTATGCGGCGACCGAGTTGCTCTTGCCCGGCGTCAATACGGGATAATA
CCGCGCCACATAGCAGAACTTTAAAAGTGCTCATCATTGGAAAACGTTCTTCCGGGGCGAAA
ACTCTCAAGGATCTTACCGCTGTTGAGATCCAGTTTCGATGTAACCCACTCGTGCACCCAAC
TGATCTTCAGCATCTTTTACTTTTACCAGCGTTTCTGGGTGAGCAAAAACAGGAAGGCAAA
ATGCCGCAAAAAAGGGAATAAGGGCGACACGGAAATGTTGAATACTCATACTTCTCTTTT

TCAATATTATTGAAGCATTATCAGGGTTATTGTCTCATGAGCGGATACATATTTGAATGTAT
TTAGAAAAATAAACAAATAGGGGTTCCGCGCACATTTCCCCGAAAAGTGCCACCTGACGTC

Figure S.2: Final nucleotide sequence of pIRES_{hyg}-ESYN-TET3G. Each element discussed in the text is indicated by a different colour scheme: enhancer region of the human CMV promoter (**cyan**) (nucleotides 709-1013), human synapsin 1 promoter region (**red**) (nucleotides 1014-1414), TET-On3G CDS (**grey**) (nucleotides 1429-2175), BstXI restriction site (**black text, yellow highlight**) (nucleotide 2202-2213), synthetic intron (IVS) (**orange**) (nucleotides 2249-2478), internal ribosome entry site (IRES) (**purple**) (nucleotides 2549-3122), hygromycin phosphotransferase CDS (**green**) (nucleotides 3162-4181), poly A termination sequence (**dark red**) (nucleotides 4311-4746) and the XhoI restriction site (**green text, yellow highlight**) (nucleotide 4747-4752).

GACGGATCGGGAGATCTCCCGATCCCCTATGGTCGACTCTCAGTACAATCTGCTCTGATG
CCGCATAGTTAAGCCAGTATCTGCTCCCTGCTTGTGTGTTGGAGGTCGCTGAGTAGTGCG
CGAGCAAATTTAAGCTACAACAAGGCAAGGCTTGACCGACAATTGCATGAAGAATCTGCT
TAGGGTTAGGCGTTTTGCGCTGCTTCGGCACTCGAGGAGTTTACTCCCTATCAGTGATAGA
GAACGTATGAAGAGTTTACTCCCTATCAGTGATAGAGAACGTATGCAGACTTTACTCCCTAT
CAGTGATAGAGAACGTATAAGGAGTTTACTCCCTATCAGTGATAGAGAACGTATGACCACT
TTACTCCCTATCAGTGATAGAGAACGTATCTACAGTTTACTCCCTATCAGTGATAGAGAACG
TATATCCAGTTTACTCCCTATCAGTGATAGAGAACGTATAAGCTTTAGGCGTGTACGGTGG
GCGCCTATAAAAGCAGAGCTCGTTTAGTGAACCGTCAGATCGCCTGGAGCAATTCACAA
CACTTTTGTCTTATACCAACTTTCCGTACCACTTCTACCCTCGTAAAATAATTAATTTGTTT
AAACGCCACCATGCTGCCCGGTTTGGCACTGCTCCTGCTGGCCGCTGGACGGCTCGGG
CTCTGGAGGTACCCACTGATGTAATGCTGCGCTGCTGGCTGAACCCAGATTGCCATGT
TCTGTGGCAGACTGAACATGCACATGAATGTCCAGAATGGGAAGTGGATTAGATCAGTATC
AGGGACCAAACCTGCATTGATACCAAGGAAGGCATCCTGCAGTATTGCCAAGAAGTCTAC
CCTGAACTGCAGATACCAATGTGGTAGAAGCCAACCAACCAGTGACCATCCAGAACTGG
TGCAAGCGGGGCCGCAAGCAGTGCAAGACCCATCCCCACTTTGTGATTCCCTACCGCTGC
TTAGTTGGTGAGTTTGTAAAGTATGCCCCTTCTCGTTCCTGACAAGTGCAAATTTACACCA
GGAGAGGATGGATGTTTGCGAAACTCATCTTCACTGGCACACCCGTCGCCAAAGAGACATG
CAGTGAGAAGAGTACCAACTTGCATGACTACGGCATGTTGCTGCCCTGCCGAATTGACAA
GTTCCGAGGGGTAGAGTTTGTGTTGCCACTGGCTGAAGAAAGTGACAATGTGGATTC
TGCTGATGCGGAGGAGGATGACTCGGATGTCTGGTGGGGCGGAGCAGACACAGACTATG
CAGATGGGAGTGAAGACAAAGTAGTAGAAGTAGCAGAGGAGGAAGAAGTGGCTGAGGTG
GAAGAAGAAGAAGCCGATGATGACGAGGACGATGAGGATGGTATGAGGTAGAGGAAGA
GGCTGAGGAACCCTACGAAGAAGCCACAGAGAGAACCACCAGCATTGCCACCACCACCAC
CACCACCACAGAGTCTGTGGAAGAGGTGGTTTCGAGTTCCTACAACAGCAGCCAGTACCCC
TGATGCCGTTGACAAGTATCTCGAGACACCTGGGGATGAGAATGAACATGCCCATTTCCAG
AAAGCCAAAGAGAGGCTTGAGGCCAAGCACCGAGAGAGAATGTCCAGGTCATGAGAGAA
TGGGAAGAGGCAGAACGTCAAGCAAAGAAGTGCCTAAAGCTGATAAGAAGGCAGTTATC
CAGCATTTCAGGAGAAAGTGAATCTTTGGAACAGGAAGCAGCCAACGAGAGACAGCAG
CTGGTGGAGACACACATGGCCAGAGTGAAGCCATGCTCAATGACCGCCGCCGCTGGC
CCTGGAGAACTACATCACCGCTCTGCAGGCTGTTCTCCTCGGCCTCGTCACGTGTTCAAT
ATGCTAAAGAAGTATGTCCGCGCAGAACAGAAGGACAGACAGCACACCCTAAAGCATTTC
GAGCATGTGCGCATGGTGGATCCCAAGAAAGCCGCTCAGATCCGGTCCCAGGTTATGACA
CACCTCCGTGTGATTTATGAGCGCATGAATCAGTCTCTCCTGCTCTACAACAGTGCCTT
CAGTGGCCGAGGAGATTGAGGATGAAGTTGATGAGCTGCTTCAGAAAGGCAAAAATTT
CAGATGAGCTCTTGCCAAACATGATTAGTGAACCAAGGATCAGTTACGGAACGATGCTCT
CATGCCATCTTTGACCGAAACGAAAACCACCGTGGAGCTCCTTCCCCTGAATGGAGAGTT
CAGCCTGGACGATCTCCAGCCGTGGCATTCTTTTGGGGCTGACTCTGTGCCAGCCAACAC
AGAAAACGAAGTTGAGCCTGTTGATGCCCGCCCTGCTGCCGACCGAGGACTGACCACTCG
ACCAGGTTCTGGGTTGACAAATATCAAGACGGAGGAGATCTCTGAAGTGAAGATGGATGC
AGAATTCGACATGACTCAGGATATGAAGTTCATCATCAAAAATAGACCGGTAAAGGCGCGC
CAAGCGATCGCGAATTAATTCGCTGTCTGCGAGGGCCGGCTGTTGGGGTGAGTACTCCCT
CTCAAAAGCGGGCATGACTTCTGCGCTAAGATTGTCAGTTTCCAAAACGAGGAGGATTTG
ATATTCACCTGGCCCGCGGTGATGCCTTTGAGGGTGGCCGCGTCCATCTGGTCAGAAAAG
ACAATCTTTTTGTTGTCAAGCTTGAGGTGTGGCAGGCTTGAGATCTGGCCATACACTTGAG
TGACAATGACATCCACTTTGCCTTTCTCTCCACAGGTGTCCACTCCCAGGTCCAACCTGCAG
GTCGATCGAGCCATCTAGGGCGGCCAATTCGCCCTCTCCCTCCCCCCCCCTAACGTTA
CTGGCCGAAGCCGCTTGGAATAAGGCCGGTGTGTGTTTGTCTATATGTGATTTCCACCAT
ATTGCCGTCTTTTGGCAATGTGAGGGCCCGGAAACCTGGCCCTGTCTTTGACGAGCATT
CCTAGGGGTCTTTCCCTCTCGCCAAAGGAATGAAGGTCTGTTGAATGTGCTGAAGGAA
GCAGTTCCTCTGGAAGCTTCTTGAAGACAAACAACGTCTGTAGCGACCCTTTGCAGGCAG
CGGAACCCCCACCTGGCGACAGGTGCCTCTGCGGCCAAAAGCCACGTGTATAAGATACA
CCTGCAAAGGCGGCACAACCCCAAGTGCACGTTGTGAGTTGGATAGTTGTGGAAAGAGTC
AAATGGCTCTCCTCAAGCGTAGTCAACAAGGGGCTGAAGGATGCCCAGAAGGTACCCCAT
TGTATGGGAATCTGATCTGGGGCCTCGGTGCACATGCTTTACATGTGTTTAGTCGAGGTTA
AAAAGCTCTAGGCCCCCCGAACCACGGGACGTGGTTTTTCTTTGAAAACACGATGATA
AGCTTGCCACAACCATCGAGCACATCTAGGGCGGCCAATTCACTAGTGCCTCATCTACGTA

GCCTGGGCCTTGAGACCTTTGTCCTTGGGCCTACGCGTTTGGGCCTATTTAAATTGCCAC
CATGCCTACAACACAGCAGTCCCCTCAGGATGAGCAGGAAAAGCTCTTGGATGAAGCCAT
ACAGGCTGTGAAGGTCCAGTCATTCCAAATGAAGAGATGCCTGGACAAAAACAAGCTTATG
GATGCTCTAAAACATGCTTCTAATATGCTTGGTGAACCTCCGGACTTCTATGTTATCACCAA
GAGTTACTATGAACTTTATATGGCCATTTCTGATGAACTGCACTACTTGGAGGTCTACCTGA
CAGATGAGTTTGCTAAAGGAAGGAAAGTGGCAGATCTCTACGAACTTGTACAGTATGCTGG
AAACATTATCCCAAGGCTTTACCTTTTGATCACAGTTGGAGTTGTATATGTCAAGTCATTT
CTCAGTCCAGGAAGGATATTTTAAAAGATTTGGTAGAAATGTGCCGTGGTGTGCAACATCC
CTTGAGGGGTCTGTTTCTCGAAATTACCTTCTTCAAGTGTACCAGAAATATCTTACCTGATG
AAGGAGAGCCAACAGATGAAGAAACAACCTGGTGACATCAGTATTCCATGGATTTTGTACT
GCTCAACTTTGCAGAAATGAACAAGCTCTGGGTGCGAATGCAGCATCAGGGACATAGCCG
AGATAGAGAAAAAGAGAAGAGAAAGACAAGAAGTGAAGATTTAGTGGGAACAATTTG
GTGCGCCTCAGTCAGTTGGAAGGTGTAATGTGGAACGTTACAACAGATTTTGTACTG
GCATATTGGAGCAAGTTGTAACTGTAGGGATGCTTTGGCTCAAGAATATCTCATGGAGTG
TATTATTCAGTTTTCCCTGATGAATTTACCTCCAGACTTTGAATCCTTTTCTTCGGGCCT
GTGCTGAGTTACACCAGAATGTAAATGTGAAGAACATAATCATTGCTTTAATTGATAGATTA
GCTTTATTTGCTCACCGTGAAGATGGACCTGGAATCCCAGCGGATATTAACTTTTTGATAT
ATTTTCACAGCAGGTGGCTACAGTGATACAGTCTAGACAAGACATGCCCTCAGAGGATGTT
GTATCTTTACAAGTCTCTCTGATTAATCTTGCCATGAAATGTTACCCTGATCGTGTGGACTA
TGTTGATAAAGTTCTAGAAACAACAGTGGAGATTTCAATAAGCTCAACCTTGAACATATTG
CTACCAGTAGTGACGTTTCAAAGGAACTCACAGACTTTTAAAATACCAGTTGACACTTAC
AACAATATTTAACAGTCTTGAATTTAAACATTTTCAACCCACTCTTTGAGTACTTTGACTAC
GAGTCCAGAAAGAGCATGAGTTGTTATGTGCTTAGTAATGTTCTGGATTATAACACAGAAAT
TGTCTCTCAAGACCAGGTGGATTCCATAATGAATTTGGTATCCACGTTGATTCAAGATCAGC
CAGATCAACCTGTAGAAGACCCTGATCCAGAAGATTTTGGCTGATGAGCAGAGCCTTGTGG
GCCGCTTCATTCATCTGCTGCGCTCTGAGGACCCTGACCAGCAGTACTTGATTTTGAACAC
AGCACGAAAACATTTTGGAGCTGGTGGAAATCAGCGGATTCGCTTCACTGCCACCTTTG
GTATTTGCAGCTTACCAGCTGGCTTTTCGATATAAAGAGAATTCTAAAGTGGATGACAAATG
GGAAAAGAAATGCCAGAAGATTTTTTCATTTGCCACCAGACTATCAGTGCCTTGATCAAAAG
CAGAGCTGGCAGAATTGCCCTTAAGACTTTTTCTTCAAGGAGCACTAGCTGCTGGGGAAAT
TGGTTTTGAAAATCATGAGACAGTCGCATATGAATTCATGTCCCAGGCATTTTCTGTATG
AAGATGAAATCAGCGATTCCAAGCACAGCTAGCTGCCATCACCTTGATCATTGGCACTTT
TGAAAGGATGAAGTGCCTCAGTGAAGAGAATCACGAACCTCTGAGGACTCAGTGTGCCCTT
GCTCATCCAACTTCTAAAGAAACCTGATCAGGGCCGAGCTGTGAGCACCTGTGCACAT
CTCTTCTGGTCTGGCAGAAACACGGACAAAAAATGGGGAGGAGCTTACAGGAGGCAAGAG
GGTAATGGAGTGCCTAAAAAAGCTCTAAAAATAGCAAATCAGTGCATGGACCCCTCTCTA
CAAGTGCAGCTTTTTATAGAAATTCTGAACAGATATATCTATTTTTATGAAAAGGAAAATGAT
GCGGTAACAATTCAGTTTTAAACCAGCTTATCCAAAAGATTTCGAGAAGACCTCCCGAATC
TTGAATCCAGTGAAGAAACAGAGCAGATTAACAAACATTTTCATAACACACTGGAGCATTTG
CGCTTGCGGCGGGAATCACCGAATCCGAGGGGCCAATTTATGAAGGTCTCATCCTTTAA
ATTTAAATATGATATCGAGCCATCTAGGGCGGCCAATTCGCCCTCTCCCTCCCCCCCC
CTAACGTTACTGGCCGAAGCCGCTTGAATAAGGCCGGTGTGTGTTTGTCTATATGTGATT
TTCCACCATATTGCCGTCTTTTGGCAATGTGAGGGCCCGAAACCTGGCCCTGTCTTCTTG
ACGAGCATTCTAGGGGTCTTTCCCCTCTCGCCAAAGGAATGCAAGGTCTGTTGAATGTGC
TGAAGGAAGCAGTTCCTCTGGAAGCTTCTTGAAGACAAACAACGTCTGTAGCGACCCTTG
CAGGCAGCGGAACCCCCACCTGGCGACAGGTGCCTCTGCGGCCAAAAGCCACGTGTAT
AAGATACACCTGCAAAGGCGGCACAACCCAGTGCCACGTTGTGAGTTGGATAGTTGTGG
AAAGAGTCAAATGGCTCTCCTCAAGCGTAGTCAACAAGGGGCTGAAGGATGCCCAGAAGG
TACCCATTGTATGGGAATCTGATCTGGGGCCTCGGTGCACATGCTTTACATGTGTTTAGT
CGAGGTTAAAAAAGCTCTAGGCCCCCGAACCCACGGGGACGTGGTTTTCTTTGAAAAC
ACGATGATAAGCTTGGCACAACCCCGGATAATTCCTGCAGCCAACTGACG GCCACCATG
GCCAAGTTGACCAGTGCCGTTCCGGTGCTCACCGCGCGGACGTCGCCGGAGCGGTCTGA
GTTCTGGACCGACCGGCTCGGGTTCTCCCGGGACTTCGTGGAGGACGACTTCGCCGGTG
TGGTCCGGGACGACGTGACCCTGTTTATCAGCGCGGTCCAGGACCAGGTGGTGC CGGAC
AACACCCTGGCCTGGGTGTGGGTGCGCGGCCTGGACGAGCTGTACGCCGAGTGGTCCGA
GGTCGTGTCCACGAACCTCCGGGACGCCTCCGGGCCGCCATGACCGAGATCGGCCGAGC
AGCCGTGGGGGCGGGAGTTCCGCCCTGCGCGACCCGGCCGCAACTGCGTGCACCTTCGT

GGCCGAGGAGCAGGACTGACGTACGAGTAGATGCCGACCGAACAAAGAGCTGATTTTCGAG
AACGCCTCAGCCAGCAACTCGCGGAGCCTAGCAAGGCAAATGCGAGAGAACGGCCTTA
CGCTTGGTGGCACAGTTCTCGTCCACAGTTCGCTAAGCTCGCTCGGCTGGGTTCGCGGA
GGGCCGGTTCGAGTGATTCAGGCCCTTCTGGATTGTGTTGGTCCCCAGGGCACGATTGTC
ATGCCACGCACTCGGGTGATCTGACTGATCCCGCAGATTGGAGATCGCCGCCCGTGCCT
GCCGATTGGGTGCAGATCTAGAGCTCGCTGATCAGCCTCGACTGTGCCTCTAGTTGCCAG
CCATCTGTTGTTTGGCCCTCCCCCGTGCCTTCCTTGACCCTGGAAGGTGCCACTCCCACT
GTCCTTTCCTAATAAAATGAGGAAATTGCATCGCATTGTCTGAGTAGGTGTCATTCTATTCT
GGGGGGTGGGGTGGGGCAGGACAGCAAGGGGGAGGATTGGGAAGACAATAGCAGGCAT
GCTGGGGATGCGGTGGGCTCTATGGCTTCTGAGGCGGAAAGAACCAGCTGGGTAGGGC
CCATTGGTATGGCTTTTTCCCGTATCCCCCAGGTGTCTGCAGGCTCAAAGAGCAGCGA
GAAGCCTCAGAGGAAAGCGATCCCGTGCCACCTTCCCCGTGCCGGGCTGCCCGCA
CGCTGCCGGCTCGGGGATGCGGGGAGCGCCGACCCGAGCGGAGCCCGGGCCCGGGC
TCGCTGCTGCCCCCTAGCGGGGAGGGACGTAATTACATCCCTGGGGGCTTTGGGGGG
GGCTGTCCCTGATATCTATAACAAGAAAATATATATAATAAGTTATCACGTAAGTAGAAC
ATGAAATAACAATATAATTATCGTATGAGTTAAATCTTAAAAGTCACGTAAGATAATCATG
CGTCATTTTACTCACGCGGTGCTTATAGTTCAAATCAGTGACACTTACCGCATTGACAA
GCACGCCTCACGGGAGCTCCAAGCGGCGACTGAGATGTCCTAAATGCACAGCGACGGAT
TCGCGCTATTTAGAAAGAGAGCAATATTTCAAGAATGCATGCGTCAATTTTACGCAGACT
ATCTTTCTAGGGCTCGAGTGCATTCTAGTTGTGTTTGTCCAACTCATCAATGTATCTTAT
CATGTCTGTATACCGTGCACCTCTAGCTAGAGCTTGGCGTAATCATGGTCATAGCTGTTTC
CTGTGTGAAATTGTTATCCGCTCACAATCCACACAACATACGAGCCGGAAGCATAAAGTG
TAAAGCCTGGGGTGCCTAATGAGTGAGCTAACTCACATTAATTGCGTTGCGCTCACTGCC
GCTTTCCAGTCGGGAAACCTGTCGTGCCAGCTGCATTAATGAATCGGCCAACGCGCGGGG
AGAGGCGGTTTGCCTATTGGGCGCTTCCGCTTCCCTCGCTCACTGACTCGCTGCGCTCG
GTCTCGGCTGCGGCGAGCGGTATCAGCTCACTCAAAGGCGGTAATACGGTTATCCACA
GAATCAGGGGATAACGCAGGAAAGAACATGTGAGCAAAAAGGCCAGCAAAAAGGCCAGGAA
CCGTA AAAAGGCCGCGTGGCTGGCGTTTTCCATAGGCTCCGCCCCCTGACGAGCATCA
CAAAAATCGACGCTCAAGTCAGAGGTGGCGAAACCCGACAGGACTATAAAGATACCAGGC
GTTTCCCCCTGGAAGCTCCCTCGTGCCTCTCCTGTTCCGACCCTGCCGCTTACCGGATA
CCTGTCCGCTTTCTCCCTTCGGGAAGCGTGGCGCTTTCTCAATGCTCACGCTGTAGGTAT
CTCAGTTCGGTGTAGGTGCTTCCGCTCCAAGCTGGGCTGTGTGCACGAACCCCCGTTAG
CCCGACCCTGCGCCTTATCCGGTAACATCGTCTTGAGTCCAACCCGGTAAGACACGAC
TTATCCGACTGGCAGCAGCCACTGGTAACAGGATTAGCAGAGCGAGGTATGTAGGGGT
GCTACAGAGTCTTGAAGTGGTGGCCTAACTACGCTACACTAGAAGGACAGTATTTGGTA
TCTGCGCTCTGCTGAAGCCAGTTACCTTCGGA AAAAGAGTTGGTAGCTCTTGATCCGGCAA
ACAAACCACCGCTGGTAGCGGTGGTTTTTTTTGTTTGAAGCAGCAGATTACGCGCAGAAAA
AAAGGATCTCAAGAAGATCCTTTGATCTTTTTCTACGGGGTCTGACGCTCAGTGGAACGAAA
ACTCACGTTAAGGGATTTTGGTTCATGAGATTATCAAAAAGGATCTTACCTAGATCCTTTTA
AATTA AAAATGAAGTTTTAAATCAATCTAAAGTATATAGTAAACTTGGTCTGACAGTTAC
CAATGCTTAATCAGTGAGGCACCTATCTCAGCGATCTGTCTATTTTCGTTTACCCATAGTTGC
CTGACTCCCCGTCGTGTAGATAACTACGATACGGGAGGGCTTACCATCTGGCCCCAGTGC
TGCAATGATACCGCGAGACCCACGCTCACCGGCTCCAGATTTATCAGCAATAAACCAGCC
AGCCGGAAGGGCCGAGCGCAGAAGTGGTCTGCAACTTTATCCGCCTCCATCCAGTCTAT
TAATTGTTGCCGGGAAGCTAGAGTAAGTAGTTCGCCAGTTAATAGTTTTCGCAACGTTGTT
GCCATTGCTACAGGCATCGTGGTGTACGCTCGTCTGTTTGGTATGGCTTCATTGAGCTCCG
GTTCCCAACGATCAAGGCGAGTTACATGATCCCCATGTTGTGCAAAAAGCGGTTAGCTC
CTTCGGTCTCCGATCGTTGTCAGAAGTAAGTTGGCCGAGTGTATCACTCATGGTTATG
GCAGCACTGCATAATTCTTACTGTCATGCCATCCGTAAGATGCTTTTTCTGTGACTGGTGA
GTA CTCAACCAAGTCATTCTGAGAATAGTGTATGCGGCGACCGAGTTGCTCTTGGCCGGC
GTCAATACGGGATAATACCGCGCCACATAGCAGAACTTTAAAAGTGCTCATCATTGAAAA
CGTTCTTCGGGGCGAAA ACTCTCAAGGATCTTACCGCTGTTGAGATCCAGTTTCGATGTAAC
CCACTCGTGCACCCAACTGATCTTCAGCATCTTTTACTTTTACCAGCGTTTCTGGGTGAGC
AAAAACAGGAAGGCAAAAATGCCGCAAAAAGGGGAATAAGGGCGACACGGAAATGTTGAAT
ACTCATACTCTTCTTTTTCAATATTATTGAAGCATTTATCAGGGTTATTGTCTCATGAGCGG
ATACATATTTGAATGTATTTAGAAAAATAAACAAATAGGGGTTCCGCGCACATTTCCCCGAA
AAGTGCCACCTGACGTC

Figure S.3: Final nucleotide sequence of pIRESzeo-sAPP α -VPS35. Each important element discussed in the text is indicated by a different colour scheme: XhoI restriction sites (black text, yellow highlight) (nucleotides 212-217 & 8484), TRE3G promoter (blue) (nucleotides 218-596), the first MCS including Pac I, PmeI, AgeI, AscI and Asi SI (black text, green highlight) (nucleotides 597-615 and 2461-2486), human sAPP α coding sequence (green) (nucleotides 622-2460), synthetic intron (IVS) (orange) (nucleotides 2523-2752), the 1st internal ribosome entry site (IRES) (purple) (nucleotides 2810-3383), the second MCS including Spe I, SnaBI, PshAI, MluI and Swa I (black text, green highlight) (nucleotides 3424-3498 and 5897-5913), human VPS35 coding sequence (gold) (nucleotides 3506-5869), the 2nd IRES (purple) (nucleotides 5938-6511), BsiWI restriction sites (black text, blue highlight) (nucleotides 6547-6552 and 6934-6939), *sh ble* coding sequence (zeocin resistance) (dark blue) (nucleotides 6559-6933) and the poly A termination sequence (red) (nucleotides 7225-7501).

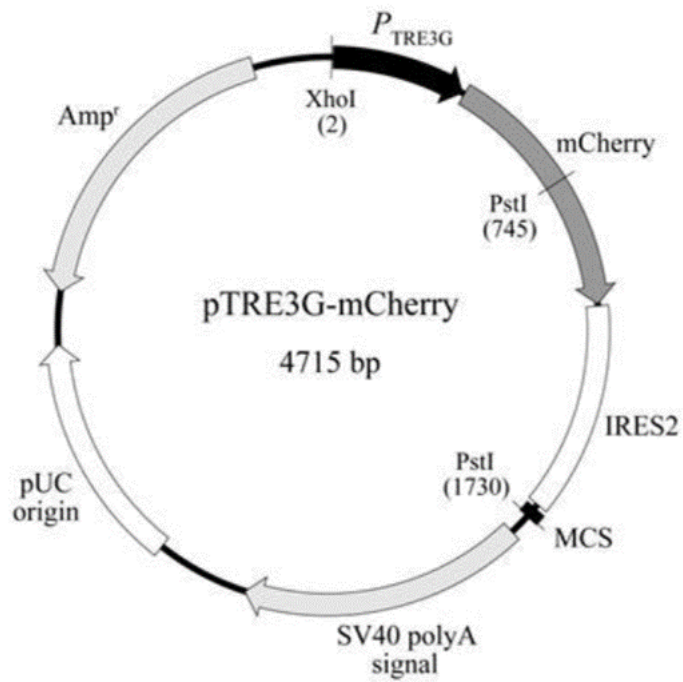


Figure S.4: Schematic of the commercial pTRE3G-mCherry vector. Restriction sites XhoI (nucleotide 2) and Pac I (nucleotide 383), were excised to remove the TET-On3G sensitive promoter fragment (P_{TRE3G}) for incorporation into the response plasmid.

CACAGGGTGTACGTTGCAAGACCTGCCTGAAACCGAACTGCCCGCTGTTCTGCAGCCGG
TCGCGGAGGCCATGGATGCGATCGCTGCGGCCGATCTTAGCCAGACGAGCGGGTTCCGGC
CCATTCGGACCGCAAGGAATCGGTCAATACACTACATGGCGTGATTTTCATATGCGCCGATTG
CTGATCCCCATGTGTATCACTGGCAAACCTGTGATGGACGACACCGTCAGTGCGTCCGTCCG
CGCAGGCTCTCGATGAGCTGATGCTTTGGGCCGAGGACTGCCCCGAAGTCCGGCACCTC
GTGCACGCGGATTTCCGGCTCCAACAATGTCTTGACGGACAATGGCCGCATAACAGCGGTC
ATTGACTGGAGCGAGGCGATGTTCCGGGATTCCCAATACGAGGTCGCCAACATCTTCTTC
TGGAGGCCGTGGTTGGCTTGTATGGAGCAGCAGACGCGCTACTTCGAGCGGAGGCATCC
GGAGCTTGACAGGATCGCCGCGGCTCCGGGCGTATATGCTCCGCATTGGTCTTGACCAACT
CTATCAGAGCTTGTTGACGGCAATTCGATGATGCAGCTTGGGCGCAGGGTCGATGCGA
CGCAATCGTCCGATCCGGAGCCGGGACTGTCCGGCGTACACAATCGCCCGCAGAAAGCG
CGCCCGTCTGGACCGATGGCTGTGTAGAAGTACTCGCCGATAGTGGAAACCGACGCCCC
AGCACTCGTCCGAGGGCAAAGGAATAGAGTAGATGCCGACCGAACAAGAGCTGATTTGCA
GAACGCCTCAGCCAGCAACTCGCGCGAGCCTAGCAAGGCAAATGCGAGAGAACGGCCTT
ACGCTTGGTGGCACAGTTCTCGTCCACAGTTCGCTAAGCTCGCTCGGCTGGGTCCGGGA
GGGCCGGTCCGAGTGATTCAGGCCCTTCTGGATTGTGTTGGTCCCCAGGGCACGATTGTC
ATGCCACGCACTCGGGTGTCTGACTGATCCCGCAGATTGGAGATCGCCGCCCGTGCCT
GCCGATTGGGTGCAGATCTAGAGCTCGCTGATCAGCCTCGACTGTGCCTCTAGTTGCCAG
CCATCTGTTGTTGCCCCCTCCCCCGTGCCTTCTTGACCCTGGAAGGTGCCACTCCCACT
GTCCTTTCCTAATAAAATGAGGAAATTGCATCGCATTGTCTGAGTAGGTGTCATTCTATTCT
GGGGGGTGGGGTGGGGCAGGACAGCAAGGGGGAGGATTGGGAAGACAATAGCAGGCAT
GCTGGGGATGCGGTGGGCTCTATGGCTTCTGAGGCGGAAAGAACCAGCTGGGGCTCGAG
TTTACTCCCTATCAGTGATAGAGAACGTATGAAGAGTTTACTCCCTATCAGTGATAGAGAAC
GTATGCAGACTTTACTCCCTATCAGTGATAGAGAACGTATAAGGAGTTTACTCCCTATCAGT
GATAGAGAACGTATGACCAGTTTACTCCCTATCAGTGATAGAGAACGTATCTACAGTTTACT
CCCTATCAGTGATAGAGAACGTATATCCAGTTTACTCCCTATCAGTGATAGAGAACGTATAA
GCTTTAGGCGTGTACGGTGGGCGCCTATAAAAGCAGAGCTCGTTTAGTGAACCGTCAGAT
CGCCTGGAGCAATTCACAACACTTTTGTCTTATACCAACTTTCCGTACCCTTCTACCCCT
CGTAAAATAATTAATTTGTTAAACGCCACCATGCTGCCCGGTTTGGCACTGCTCCTGCTG
GCCGCCTGGACGGCTCGGGCGCTGGAGGTACCCACTGATGGTAATGCTGGCCTGCTGGC
TGAACCCAGATTGCCATGTTCTGTGGCAGACTGAACATGCACATGAATGTCCAGAATGGG
AAGTGGGATTCAGATCCATCAGGGACCAAAACCTGCATTGATACCAAGGAAGGCATCCTG
CAGTATTGCCAAGAAGTCTACCCTGAACTGCAGATCACCAATGTGGTAGAAGCCAACCAAC
CAGTGACCATCCAGAAGTGGTGAAGCGGGCGCAAGCAGTGAAGCAACCCATCCCCAC
TTTGTGATTCCCTACCCTGCTTAGTTGGTGAGTTTGTAAAGTATGATGCCCTTCTCGTTCCCTGA
CAAGTGCAAATTTACACCAGGAGAGGATGGATGTTTGCGAAACTCATCTTCACTGGCAC
ACCGTCGCCAAAGAGACATGCAGTGAGAAGAGTACCAACTTGCATGACTACGGCATGTTG
CTGCCCTGCGGAATTGACAAGTCCGAGGGGTAGAGTTTGTGTGTTGCCACTGGCTGAA
GAAAGTGACAATGTGGATTCTGCTGATGCGGAGGAGGATGACTCGGATGTCTGGTGGGGC
GGAGCAGACACAGACTATGCAGATGGGAGTGAAGACAAAGTAGTAGAAGTAGCAGAGGAG
GAAGAAGTGGCTGAGGTGGAAGAAGAAGAAGCCGATGATGACGAGGACGATGAGGATGG
TGATGAGGTAGAGGAAGAGGCTGAGGAACCCTACGAAGAAGCCACAGAGAGAACCACCA
GCATTGCCACCACCACCACCACCACAGAGTCTGTGGAAGAGGTGGTTTCGAGTTCTTA
CAACAGCAGCCAGTACCCTGATGCCGTTGACAAGTATCTCGAGACACCTGGGGATGAGA
ATGAACATGCCATTTCCAGAAAGCCAAAGAGAGGCTTGAGGCCAAGCACCGAGAGAGAA
TGTCCCAGGTGATGAGAGAATGGGAAGAGGCAGAACGTCAAGCAAAGAAGTTCCTAAAG
CTGATAAGAAGGCAGTTATCCAGCATTTCAGGAGAAAGTGAATCTTTGGAACAGGAAGC
AGCCAACGAGAGACAGCAGCTGGTGGAGACACACATGGCCAGAGTGGAAAGCCATGCTCA
ATGACCGCCGCCCGCTGGCCCTGGAGAACTACATCACCGCTCTGCAGGCTGTTCTCCTC
GGCCTCGTCACGTGTTCAATATGCTAAAGAAGTATGTCCGCGCAGAACAGAAGGACAGAC
AGCACACCCTAAAGCATTTCGAGCATGTGCGCATGGTGGATCCCAAGAAAGCCGCTCAGA
TCCGGTCCCAGGTTATGACACACCTCCGTGTGATTTATGAGCGCATGAATCAGTCTCTCTC
CCTGCTCTACAACGTGCCTGCAGTGGCCGAGGAGATTCAGGATGAAGTTGATGAGCTGCT
TCAGAAAGAGCAAACTATTGAGATGACGCTTGGCCAACATGATTAGTGAACCAAGGATC
AGTTACGGAAACGATGCTCTCATGCCATCTTTGACCGAAACGAAAACCCAGTGGAGCTCC
TTCCCGTGAATGGAGAGTTCAGCCTGGACGATCTCCAGCCGTGGCATTCTTTGGGGCTG
ACTCTGTGCCAGCCAACACAGAAAACGAAGTTGAGCCTGTTGATGCCCGCCCTGCTGCCG

ACCGAGGACTGACCACTCGACCAGGTTCTGGGTTGACAAATATCAAGACGGAGGAGATCT
CTGAAGTGAAGATGGATGCAGAATTCGACATGACTCAGGATATGAAGTTCATCATCAAAA
ATAGACCGGTAAAGGCGCGCCAAGCGATCGCGAATTAATTCGCTGTCTGCGAGGGCCGCGC
TGTTGGGGTGAGTACTCCCTCTCAAAGCGGGCATGACTTCTGCGCTAAGATTGTCAGTTT
CCAAAAACGAGGAGGATTTGATATTCACCTGGCCCGCGGTGATGCCTTTGAGGGTGGCCG
CGTCCATCTGGTCAGAAAAGACAATCTTTTTGTTGTCAAGCTTGAGGTGTGGCAGGCTTGA
GATCTGGCCATACACTTGAGTGACAATGACATCCACTTTGCCTTTCTCTCCACAGGTGTCC
ACTCCAGGTCCAACCTGCAGGTGCATCGAGCCATCTAGGGCGGCCAATTCGCCCTCTCC
CTCCCCCCCCCTAACGTTACTGGCCGAAGCCGCTTGAATAAGGCCGGTGTGTGTTTGT
CTATATGTGATTTCCACCATATTGCCGTCTTTTGGCAATGTGAGGGCCCGGAAACCTGGC
CCTGTCTTCTTGACGAGCATTCTAGGGGTCTTTCCCTCTCGCCAAAGGAATGCAAGGTG
TGTGAATGTGTGAAGGAAGCAGTTCCTCTGGAAGCTTCTTGAAGACAAACAACGTCTG
AGCCACCTTTGCAGGCAGGCAACCCCACTGGCGACAGGTGCCCTCTGCGGCCAAA
AGCCACGTGTATAAGATACACCTGCAAAGCGGCACAACCCCAAGTGCCACGTTGTGAGTT
GGATAGTTGTGAAAGAGTCAAATGGCTCTCCTCAAGCGTAGTCAACAAGGGGCTGAAGG
ATGCCAGAAGGTACCCATTGTATGGGAATCTGATCTGGGGCCTCGGTGCACATGCTTT
ACATGTGTTTAGTCGAGGTAAAAAAGCTCTAGGCCCCCGAACCACGGGGACGTGTTTT
TCCTTTGAAAAACACGATGATAAGCTTGCCACAACCATCGAGCACATCTAGGGCGGCCAAT
TCACTAGTGCGTCATCTACGTAGCCTTGGGCCTTGAGACCTTTGTCCTTGGGCCTACGCGT
TTGGGCCTATTTAAATGGCCACCATGCCTACAACACAGCAGTCCCCTCAGGATGAGCAGGA
AAAGCTCTTGGATGAAGCCATACAGGCTGTGAAGGTCCAGTCATTCCAAATGAAGAGATGC
CTGGACAAAAACAAGCTTATGGATGCTCTAAAACATGCTTCTAATATGCTTGGTGAACCTCCG
GACTTCTATGTTATCACCAAAGAGTTACTATGAACTTTATATGGCCATTTCTGATGAACTGC
ACTACTTGGAGGTCTACCTGACAGATGAGTTTGCTAAAGGAAGGAAAGTGGCAGATCTCTA
CGAACTTGTACAGTATGCTGGAAACATTATCCCAAGGCTTTACCTTTTGATCACAGTTGGAG
TTGTATATGTCAAGTCATTTCCCTCAGTCCAGGAAGGATATTTTGAAGATTGGTAGAAATG
TGCCGTGGTGTGCAACATCCCTTGAGGGGTCTGTTTCTTCGAAATTACCTTCTCAGTGTA
CCAGAAATATCTTACCTGATGAAGGAGAGCCAACAGATGAAGAAACAACCTGGTGACATCAG
TGATTCCATGGATTTTGTACTGCTCAACTTTGCAGAAATGAACAAGCTCTGGGTGCGAATG
CAGCATCAGGGACATAGCCGAGATAGAGAAAAAGAGAACGAGAAAGACAAGAAGTGAAG
ATTTTAGTGGGAACAAATTTGGTGCGCCTCAGTCAGTTGGAAGGTGTAATGTGGAACGTT
ACAAACAGATTGTTTTGACTGGCATATTGGAGCAAGTTGTAAACTGTAGGGATGCTTTGGC
TCAAGAATATCTCATGGAGTGTATTATTCAGTTTTCCCTGATGAATTTACCTCCAGACTT
TGAATCCTTTTCTCGGGCCTGTGCTGAGTTACACCAGAATGTAATGTGAAGAACATAATC
ATTGCTTTAATTGATAGATTAGCTTTATTTGCTCACCGTGAAGATGGACCTGGAATCCCAAG
GGATATTAACCTTTTTGATATATTTTACAGCAGGTGGCTACAGTGATACAGTCTAGACAAG
ACATGCCTTCAGAGGATGTTGTATCTTTACAAGTCTCTCTGATTAATCTTGCCATGAAATGT
TACCCTGATCGTGTGGACTATGTTGATAAAGTTCTAGAAACAACAGTGGAGATATTCAATAA
GCTCAACCTTGAACATATTGCTACCAGTAGTGCAGTTTTCAAAGGAACTCACCAGACTTTTGA
AAATACCAGTTGACACTTACAACAATATTTAACAGTCTTGAATTTAAACATTTTACCCAC
TCTTTGAGTACTTTGACTACGAGTCCAGAAAGAGCATGAGTTGTTATGTGCTTAGTAATGTT
CTGGATTATAACACAGAAATTGTCTCTCAAGACCAGGTGGATTCCATAATGAATTTGGTATC
CACGTTGATTCAAGATCAGCCAGATCAACCTGTAGAAGACCCTGATCCAGAAGATTTTGTCT
GATGAGCAGAGCCTTGTGGGCCGCTTCATTCATCTGCTGCGCTCTGAGGACCCTGACCAG
CAGTACTTGATTTTGAACACAGCACGAAAACATTTTGGAGCTGGTGGAAATCAGCGGATTC
GCTTCACACTGCCACCTTTGGTATTTGCAGCTTACCAGCTGGCTTTTTCGATATAAAGAGAAT
TCTAAAGTGGATGACAAATGGGAAAAGAAATGCCAGAAGATTTTTTCAATTTGCCACCAGA
CTATCAGTGCTTTGATCAAAGCAGAGCTGGCAGAATTGCCCTTAAGACTTTTTCTTCAAGGA
GCACTAGCTGCTGGGGAAATTGGTTTTGAAAATCATGAGACAGTCGCATATGAATTCATGT
CCCAGGCATTTTCTCTGTATGAAGATGAAATCAGCGATTCCAAAGCACAGCTAGCTGCCAT
CACCTTGATCATTGGCACTTTTGAAGGATGAAGTGCTTCAGTGAAGAGAATCACGAACCT
CTGAGGACTCAGTGTGCCCTTGTGCATCCAACTTCTAAAGAACTGATCAGGGCCGA
GCTGTGAGCACCTGTGCACATCTTCTGGTCTGGCAGAAACACGGACAAAAATGGGGAG
GAGCTTCACGGAGGCAAGAGGGTAATGGAGTGCCTAAAAAAGCTCTAAAAATAGCAAATC
AGTGCATGGACCCCTCTCTACAAGTGCAGCTTTTTATAGAAATTCTGAACAGATATATCTAT
TTTTATGAAAAGGAAAATGATGCGGTAACAATTCAGGTTTTAAACCAGCTTATCCAAAAGAT
TCGAGAAGACCTCCCGAATCTTGAATCCAGTGAAGAAACAGAGCAGATTAACAAACATTTT

CATAACACACTGGAGCATTGCGCTTGCGGCGGGAATCACCAGAATCCGAGGGGCCAATT
TATGAAGGTCTCATCCTTTAAATTAAATATTGATATCAGGCCATCTAGGGCGGCCAATTCC
CCCCTCTCCCTCCCCCCCCCTAACGTTACTGGCCGAAGCCGCTTGAATAAGGCCGGTG
TGTGTTTGTCTATATGTGATTTCCACCATATTGCCGTCTTTGGCAATGTGAGGGCCCGGA
AACCTGGCCCTGTCTTCTTGACGAGCATTCTAGGGGTCTTTCCCCTCTCGCCAAAGGAAT
GCAAGGTCTGTTGAATGTCGTGAAGGAAGCAGTTCCTCTGGAAGCTTCTTGAAGACAAACA
ACGTCTGTAGCGACCCCTTTCAGGGCAGCGGAACCCCCACCTGGCGACAGGTGCCTCTG
CGGCCAAAAGCCACGTGTATAAGATACACCTGCAAAGGCGGCACAACCCAGTGCCACGT
TGTGAGTTGGATAGTTGTGGAAGAGTCAAATGGCTCTCCTCAAGCGTAGTCAACAAGGG
GCTGAAGGATGCCAGAAGGTACCCATTGTATGGGAATCTGATCTGGGGCCTCGGTGCA
CATGCTTTACATGTGTTTAGTCGAGGTTAAAAAAGCTTAGGCCCCCCGAACCACGGGGAC
GTGGTTTTCTTTGAAAAACAGATGATAAGCTTGCCACAACCCCGGATAATTCCTGCAG
CCAACGCTACGAGTAGATGCCGACCGAACAAAGAGCTGATTTTCGAGAACGCCCTCAGCCAGCA
ACTCGCGAGCCCTAGCAAGGCAAATGCGAGAGAACGGCCTTACGCTTGGTGCCACAGTT
CTCGTCCACAGTTCGCTAAGCTCGCTCGGCTGGGTGCGGGAGGGCCGGTGCAGTGAT
TCAGGCCCTTCTGGATTGTGTTGGTCCCAGGGCAGGATTGTCATGCCACGCACTCGGG
TGATCTGACTGATCCCGCAGATTGGAGATCGCCGCCCGTGCCTGCCGATTGGGTGCAGAT
CTAGAGCTCGCTGATCAGCCTCGACTGTGCCTCTAGTTGCCAGCCATCTGTTGTTTGGCCC
TCCCCCGTGCCTTCTTGACCCTGGAAGGTGCCACTCCCCTGCTCTTCTAATAAAATG
AGGAAATTGCATCGCATTGTCTGAGTAGGTGCTATTCTATTCTGGGGGGTGGGGTGGGGC
AGGACAGCAAGGGGGAGGATTGGGAAGACAATAGCAGGCATGCTGGGGATGCGGTGGG
CTCTATGGCTTCTGAGGCGGAAAGAACCAGCTGGGTAGGGCCATTGGTATGGCTTTTT
CCCCGTATCCCCCAGGTGTCTGCAGGCTCAAAGAGCAGCGAGAAGCGTTCAGAGGAAA
GCGATCCCGTGCCACCTTCCCCGTGCCGGGCTGTCCCCGCACGCTGCCGGCTCGGGGA
TGCGGGGGGAGCGCCGACCGGAGCGGAGCCCGGGCGGCTCGCTGCTGCCCCCTAG
CGGGGGAGGGACGTAATTACATCCCTGGGGGCTTTGGGGGGGGGCTGTCCCTGATATCT
ATAACAAGAAAATATATATAATAAGTTATCACGTAAGTAGAACATGAAATAACAATATAAT
TATCGTATGAGTTAAATCTTAAAAGTCACGTAAGATAATCATGCGTCATTTTGACTCACG
CGGTGCTTATAGTTCAAATCAGTGACACTTACCGCATTGACAAGCACGCCTCACGGGAGC
TCCAAGCGGCGACTGAGATGTCCTAAATGCACAGCGACGGATTGCGGCTATTTAGAAAAGA
GAGAGCAATATTTCAAGAATGCATGCGTCAATTTTACGCAGACTATCTTTCTAGGGCTCGA
GTGCATTCTAGTTGTGGTTTGTCCAACTCATCAATGTATCTTATCATGTCTGTATAACCGTC
GACCTCTAGCTAGAGCTTGGCGTAATCATGGTCATAGCTGTTTCTGTGTGAAATTGTTATC
CGTCAACAATCCACACAACATACGAGCCGGAAGCATAAAGTGTAAAGCCTGGGGTGCCT
AATGAGTGAGCTAACATTAATTGCGTTGCGCTCACTGCCCGCTTTCAGTCCGGGAAA
CCTGCTGCCAGCTGATTAATGAATCGGCCAACGCGCGGGGAGAGGCGGTTTGCAT
TGGGCGCTCTTCCGCTTCTCGCTCACTGACTCGCTGCGCTCGGTGCTTCCGGTGCAGC
GAGCGGTATCAGCTCACTCAAAGGCGGTAATACGGTTATCCACAGAATCAGGGGATAACG
CAGGAAAGAACATGTGAGCAAAAGGCCAGCAAAAGGCCAGGAACCGTAAAAAGGCCGCG
TTGCTGGCGTTTTTCCATAGGCTCCGCCCCCTGACGAGCATCACAAAATCGACGCTCAA
GTCAGAGGTGGCGAAACCCGACAGGACTATAAAGATACCAGGCGTTTTCCCCTGGAAGCT
CCCTCGTGCCTCTCCTGTTCCGACCCTGCCGCTTACCGGATACCTGTCCGCCTTTCTCC
CTTCGGGAAGCGTGGCGCTTTCTCAATGCTCACGCTGTAGGTATCTCAGTTCGGTGTAGG
TCGTTGCTCCAAGCTGGGCTGTGTGCACGAACCCCGTTTCAGCCCGACCGCTGCGCC
TTATCCGGTAACATCGTCTTGAGTCCAACCCGGTAAGACACGACTTATCGCCACTGGCAG
CAGCCACTGGTAACAGGATTAGCAGAGCGAGGTATGTAGGCGGTGCTACAGAGTTCTTGA
AGTGGTGGCCTAACTACGGCTACACTAGAAGGACAGTATTTGGTATCTGCGCTCTGCTGAA
GCCAGTTACCTTCGGAAAAGAGTTGGTAGCTCTTGATCCGGCAAACAACACCGCTGG
TAGCGGTGGTTTTTTTTGTTTGAAGCAGCAGATTACGCGCAGAAAAAAGGATCTCAAGAA
GATCCTTTGATCTTTTCTACGGGGTCTGACGCTCAGTGGAACGAAAACCTCACGTTAAGGGA
TTTTGGTCATGAGATTATCAAAAAGGATCTTACCTAGATCCTTTTAAATTAATAAATGAAGTT
TAAATCAATCTAAAGTATATAGATAAAGTGGTCTGACAGTTACCAATGCTTAATCAGTG
AGGCACCTATCTCAGCGATCTGTCTATTTGTTTCCATAGTTGCCTGACTCCCCGTCGT
GTAGATAACTACGATACGGGAGGGCTTACCATCTGGCCCCAGTGCTGCAATGATACCGCG
AGACCCACGCTCACCGGCTCCAGATTTATCAGCAATAAACCAGCCAGCCGGAAGGGCCGA
GCGCAGAAGTGGTCTGCAACTTTATCCGCTCCATCCAGTCTATTAATTGTTGCCGGGAA
GCTAGAGTAAGTAGTTCCGAGTAAATAGTTTGCACAACGTTGTTGCCATTGCTACAGGCA

TCGTGGTGTCACGCTCGTCGTTTGGTATGGCTTCATTCAGCTCCGGTTCCTCAACGATCAAG
GCGAGTTACATGATCCCCATGTTGTGCAAAAAAGCGGTTAGCTCCTTCGGTCCTCCGATC
GTTGTCAGAAGTAAGTTGGCCGCAGTGTTATCACTCATGGTTATGGCAGCACTGCATAATT
CTCTTACTGTCATGCCATCCGTAAGATGCTTTTTCTGTGACTGGTGAGTACTCAACCAAGTCA
TTCTGAGAATAGTGTATGCGGCGACCGAGTTGCTCTTGCCCGGCGTCAATACGGGATAAT
ACCGCGCCACATAGCAGAACTTTAAAAGTGCTCATCATTGGAAAACGTTCTTCGGGGCGAA
AACTCTCAAGGATCTTACCGCTGTTGAGATCCAGTTCGATGTAACCCACTCGTGCACCCAA
CTGATCTTCAGCATCTTTTACTTTACCCAGCGTTTCTGGGTGAGCAAAAACAGGAAGGCAA
AATGCCGCAAAAAAGGGAATAAGGGCGACACGGAAATGTTGAATACTCATACTCTTCCTTT
TTCAATATTATTGAAGCATTATCAGGGTTATTGTCTCATGAGCGGATACATATTTGAATGTA
TTAGAAAAATAAACAAATAGGGGTTCCGCGCACATTTCCCCGAAAAGTGCCACCTGACGT
C

Figure S.5: Final nucleotide sequence of PiggyBac plasmid. Each element discussed in the text is indicated by a different colour scheme: enhancer region of the human CMV promoter (cyan) (nucleotides 709-1013), human synapsin 1 promoter region (red) (nucleotides 1014-1414), TET-On3G CDS (grey) (nucleotides 1429-2175), synthetic intron (IVS) (orange) (nucleotides 2249-2478), internal ribosome entry site (IRES) (purple) (nucleotides 2549-3122), hygromycin phosphotransferase CDS (green) (nucleotides 3162-4181), poly A termination sequence (dark red) (nucleotides 4311-4746) and the XhoI restriction site (green text, yellow highlight) (nucleotide 4747-4752), TRE3G promoter (blue) (nucleotides 4753-5131), human sAPP α coding sequence (green) (nucleotides 5151-6995), synthetic intron (IVS) (orange) (nucleotides 7040-7269), the 2nd internal ribosome entry site (IRES) (purple) (nucleotides 7327-7900), human VPS35 coding sequence (gold) (nucleotides 8023-10413), the 3rd IRES (purple) (nucleotides 10455-11028) and the poly A termination sequence (red) (nucleotides 11199-11634).

[External] RE: Request to re-use material

Carry Koolbergen <C.Koolbergen@iospress.nl>

Thu 9/7/2023 1:56 PM

To: Bracewell, Joshua (Postgraduate Researcher) <j.bracewell@lancaster.ac.uk>

This email originated outside the University. Check before clicking links or attachments.

DOI: 10.3233/JAD-215457

Journal: [Journal of Alzheimer's Disease](#), vol. 86, no. 3, pp. 1201-1220, 2022

Dear Joshua Bracewell,

We hereby grant you permission to reproduce the below mentioned material in **print and electronic format** at no charge subject to the following conditions:

1. If any part of the material to be used (for example, figures) has appeared in our publication with credit or acknowledgement to another source, permission must also be sought from that source. If such permission is not obtained then that material may not be included in your publication/copies.
2. Suitable acknowledgement to the source must be made, either as a footnote or in a reference list at the end of your publication, as follows:

"Reprinted from Publication title, Vol number, Author(s), Title of article, Pages No., Copyright (Year), with permission from IOS Press".
"The publication is available at IOS Press through [http://dx.doi.org/\[insert DOI\]](http://dx.doi.org/[insert DOI])"
3. This permission is granted for non-exclusive world **English** rights only. For other languages please reapply separately for each one required.
4. Reproduction of this material is confined to the purpose for which permission is hereby given.

Yours sincerely

Carry Koolbergen (Mrs.)

Contracts, Rights & Permissions Coordinator

Not in the office on Wednesdays

IOS Press | Nieuwe Hemweg 6B, 1013 BG Amsterdam, The Netherlands

Tel.: +31 (0)20 688 3355/ +31 (0) 687 0022 | c.koolbergen@iospress.nl | www.iospress.nl

Twitter: @IOSPress_STM | Facebook: publisheriospress

View the latest IOS Press newsletter [here](#)

Confidentiality note: This e-mail may contain confidential information from IOS Press. If that is the case any disclosure, copying, distribution or use of the contents of this e-mail is strictly prohibited. If you are not the intended recipient, please delete this e-mail and notify the sender immediately.

Figure S.6: Permission for re-use of material from (Owens *et al.*, 2022) by the Journal of Alzheimer's Disease.

9. Bibliography

Alberdi, E., Sánchez-Gómez, M. V., Cavaliere, F., Pérez-Samartín, A., Zugaza, J. L., Trullas, R., Domercq, M. and Matute, C. (2010) 'Amyloid beta oligomers induce Ca²⁺ dysregulation and neuronal death through activation of ionotropic glutamate receptors', *Cell Calcium*, 47(3), pp. 264-72.

Allinson, T. M., Parkin, E. T., Turner, A. J. and Hooper, N. M. (2003) 'ADAMs family members as amyloid precursor protein alpha-secretases', *J Neurosci Res*, 74(3), pp. 342-52.

ALZFORUM (2021) *Mutations*. Available at: <https://www.alzforum.org/mutations> (Accessed: 4th August, 2021).

Ancelin, M. L., Carriere, I., Barberger-Gateau, P., Auriacombe, S., Rouaud, O., Fourlanos, S., Berr, C., Dupuy, A. M. and Ritchie, K. (2012) 'Lipid lowering agents, cognitive decline, and dementia: the three-city study', *J Alzheimers Dis*, 30(3), pp. 629-37.

Anders, A., Gilbert, S., Garten, W., Postina, R. and Fahrenholz, F. (2001) 'Regulation of the alpha-secretase ADAM10 by its prodomain and proprotein convertases', *FASEB J*, 15(10), pp. 1837-9.

Andrew, R. J., Kellett, K. A., Thinakaran, G. and Hooper, N. M. (2016) 'A Greek Tragedy: The Growing Complexity of Alzheimer Amyloid Precursor Protein Proteolysis', *J Biol Chem*, 291(37), pp. 19235-44.

Arispe, N., Rojas, E. and Pollard, H. B. (1993) 'Alzheimer disease amyloid beta protein forms calcium channels in bilayer membranes: blockade by tromethamine and aluminum', *Proc Natl Acad Sci U S A*, 90(2), pp. 567-71.

Arriagada, P. V., Growdon, J. H., Hedley-Whyte, E. T. and Hyman, B. T. (1992) 'Neurofibrillary tangles but not senile plaques parallel duration and severity of Alzheimer's disease', *Neurology*, 42(3 Pt 1), pp. 631-9.

Augustinack, J. C., Schneider, A., Mandelkow, E. M. and Hyman, B. T. (2002) 'Specific tau phosphorylation sites correlate with severity of neuronal cytopathology in Alzheimer's disease', *Acta Neuropathol*, 103(1), pp. 26-35.

Baldi, L., Hacker, D. L., Adam, M. and Wurm, F. M. (2007) 'Recombinant protein production by large-scale transient gene expression in mammalian cells: state of the art and future perspectives', *Biotechnol Lett*, 29(5), pp. 677-84.

Bandyopadhyay, B., Li, G., Yin, H. and Kuret, J. (2007) 'Tau aggregation and toxicity in a cell culture model of tauopathy', *J Biol Chem*, 282(22), pp. 16454-64.

Belyaev, N. D., Kellett, K. A., Beckett, C., Makova, N. Z., Revett, T. J., Nalivaeva, N. N., Hooper, N. M. and Turner, A. J. (2010) 'The transcriptionally active amyloid precursor protein (APP) intracellular domain is preferentially produced from the 695 isoform of APP in a {beta}-secretase-dependent pathway', *J Biol Chem*, 285(53), pp. 41443-54.

Belyaev, N. D., Nalivaeva, N. N., Makova, N. Z. and Turner, A. J. (2009) 'Neprilysin gene expression requires binding of the amyloid precursor protein intracellular domain to its promoter: implications for Alzheimer disease', *EMBO Rep*, 10(1), pp. 94-100.

Bennett, B. D., Denis, P., Haniu, M., Teplow, D. B., Kahn, S., Louis, J. C., Citron, M. and Vassar, R. (2000) 'A furin-like convertase mediates propeptide cleavage of BACE, the Alzheimer's beta -secretase', *J Biol Chem*, 275(48), pp. 37712-7.

Bolduc, D. M., Montagna, D. R., Gu, Y., Selkoe, D. J. and Wolfe, M. S. (2016) 'Nicastrin functions to sterically hinder γ -secretase-substrate interactions driven by substrate transmembrane domain', *Proc Natl Acad Sci U S A*, 113(5), pp. E509-18.

Braak, H., Alafuzoff, I., Arzberger, T., Kretschmar, H. and Del Tredici, K. (2006) 'Staging of Alzheimer disease-associated neurofibrillary pathology using paraffin sections and immunocytochemistry', *Acta Neuropathol*, 112(4), pp. 389-404.

Buxbaum, J. D., Liu, K. N., Luo, Y., Slack, J. L., Stocking, K. L., Peschon, J. J., Johnson, R. S., Castner, B. J., Cerretti, D. P. and Black, R. A. (1998) 'Evidence that tumor necrosis factor alpha converting enzyme is involved in regulated alpha-secretase cleavage of the Alzheimer amyloid protein precursor', *J Biol Chem*, 273(43), pp. 27765-7.

Cacace, R., Slegers, K. and Van Broeckhoven, C. (2016) 'Molecular genetics of early-onset Alzheimer's disease revisited', *Alzheimers Dement*, 12(6), pp. 733-48.

Caillé, I., Allinquant, B., Dupont, E., Bouillot, C., Langer, A., Müller, U. and Prochiantz, A. (2004) 'Soluble form of amyloid precursor protein regulates proliferation of progenitors in the adult subventricular zone', *Development*, 131(9), pp. 2173-81.

Canevari, L., Abramov, A. Y. and Duchon, M. R. (2004) 'Toxicity of amyloid beta peptide: tales of calcium, mitochondria, and oxidative stress', *Neurochem Res*, 29(3), pp. 637-50.

CDC (2003) 'From the Centers for Disease Control and Prevention. Public health and aging: trends in aging--United States and worldwide', *JAMA*, 289(11), pp. 1371-3.

Cerdà-Costa, N. and Gomis-Rüth, F. X. (2014) 'Architecture and function of metallopeptidase catalytic domains', *Protein Sci*, 23(2), pp. 123-44.

Chasseigneaux, S. and Allinquant, B. (2012) 'Functions of A β , sAPP α and sAPP β : similarities and differences', *J Neurochem*, 120 Suppl 1, pp. 99-108.

Chasseigneaux, S., Dinc, L., Rose, C., Chabret, C., Couplier, F., Topilko, P., Mauger, G. and Allinquant, B. (2011) 'Secreted amyloid precursor protein β and secreted amyloid precursor protein α induce axon outgrowth in vitro through Egr1 signaling pathway', *PLoS One*, 6(1), pp. e16301.

Chen, J., Kanai, Y., Cowan, N. J. and Hirokawa, N. (1992) 'Projection domains of MAP2 and tau determine spacings between microtubules in dendrites and axons', *Nature*, 360(6405), pp. 674-7.

Cheung, Y. T., Lau, W. K., Yu, M. S., Lai, C. S., Yeung, S. C., So, K. F. and Chang, R. C. (2009) 'Effects of all-trans-retinoic acid on human SH-SY5Y neuroblastoma as in vitro model in neurotoxicity research', *Neurotoxicology*, 30(1), pp. 127-35.

Chiu, Y. J., Hsieh, Y. H., Lin, T. H., Lee, G. C., Hsieh-Li, H. M., Sun, Y. C., Chen, C. M., Chang, K. H. and Lee-Chen, G. J. (2019) 'Novel compound VB-037 inhibits A β aggregation and promotes neurite outgrowth through enhancement of HSP27 and reduction of P38 and JNK-mediated inflammation in cell models for Alzheimer's disease', *Neurochem Int*, 125, pp. 175-186.

Chow, V. W., Mattson, M. P., Wong, P. C. and Gleichmann, M. (2010) 'An overview of APP processing enzymes and products', *Neuromolecular Med*, 12(1), pp. 1-12.

Cissé, M. A., Sunyach, C., Lefranc-Jullien, S., Postina, R., Vincent, B. and Checler, F. (2005) 'The disintegrin ADAM9 indirectly contributes to the physiological processing of cellular prion by modulating ADAM10 activity', *J Biol Chem*, 280(49), pp. 40624-31.

Corbett, G. T., Gonzalez, F. J. and Pahan, K. (2015a) 'Activation of peroxisome proliferator-activated receptor alpha stimulates ADAM10-mediated proteolysis of APP', *Proc Natl Acad Sci U S A*, 112(27), pp. 8445-50.

Corbett, G. T., Gonzalez, F. J. and Pahan, K. (2015b) 'Activation of peroxisome proliferator-activated receptor α stimulates ADAM10-mediated proteolysis of APP', *Proc Natl Acad Sci U S A*, 112(27), pp. 8445-50.

Cui, J., Wang, X., Li, X., Wang, X., Zhang, C., Li, W., Zhang, Y., Gu, H., Xie, X., Nan, F., Zhao, J. and Pei, G. (2015) 'Targeting the gamma-/beta-secretase interaction reduces beta-amyloid generation and ameliorates Alzheimer's disease-related pathogenesis', *Cell Discov*, 1, pp. 15021.

D'Andrea, M. R. and Nagele, R. G. (2010) 'Morphologically distinct types of amyloid plaques point the way to a better understanding of Alzheimer's disease pathogenesis', *Biotech Histochem*, 85(2), pp. 133-47.

Dahms, S. O., Hoefgen, S., Roeser, D., Schlott, B., Gührs, K. H. and Than, M. E. (2010) 'Structure and biochemical analysis of the heparin-induced E1 dimer of the amyloid precursor protein', *Proc Natl Acad Sci U S A*, 107(12), pp. 5381-6.

Dai, J., Liu, Z. Q., Wang, X. Q., Lin, J., Yao, P. F., Huang, S. L., Ou, T. M., Tan, J. H., Li, D., Gu, L. Q. and Huang, Z. S. (2015) 'Discovery of Small Molecules for Up-Regulating the Translation of Anti-amyloidogenic Secretase, a Disintegrin and Metalloproteinase 10 (ADAM10), by Binding to the G-Quadruplex-Forming Sequence in the 5' Untranslated Region (UTR) of Its mRNA', *J Med Chem*, 58(9), pp. 3875-91.

Dar, N. J. and Glazner, G. W. (2020) 'Deciphering the neuroprotective and neurogenic potential of soluble amyloid precursor protein alpha (sAPP α)', *Cell Mol Life Sci*, 77(12), pp. 2315-2330.

Das, A. T., Tenenbaum, L. and Berkhout, B. (2016) 'Tet-On Systems For Doxycycline-inducible Gene Expression', *Curr Gene Ther*, 16(3), pp. 156-67.

Dawson, G. R., Seabrook, G. R., Zheng, H., Smith, D. W., Graham, S., O'Dowd, G., Bowery, B. J., Boyce, S., Trumbauer, M. E., Chen, H. Y., Van der Ploeg, L. H. and Sirinathsinghji, D. J. (1999) 'Age-related cognitive deficits, impaired long-term potentiation and reduction in synaptic marker density in mice lacking the beta-amyloid precursor protein', *Neuroscience*, 90(1), pp. 1-13.

de Medeiros, L. M., De Bastiani, M. A., Rico, E. P., Schonhofen, P., Pfaffenseller, B., Wollenhaupt-Aguiar, B., Grun, L., Barbé-Tuana, F., Zimmer, E. R., Castro, M. A. A., Parsons, R. B. and Klamt, F. (2019) 'Cholinergic Differentiation of Human Neuroblastoma SH-SY5Y Cell Line and Its Potential Use as an In vitro Model for Alzheimer's Disease Studies', *Mol Neurobiol*, 56(11), pp. 7355-7367.

Demars, M. P., Bartholomew, A., Strakova, Z. and Lazarov, O. (2011) 'Soluble amyloid precursor protein: a novel proliferation factor of adult progenitor cells of ectodermal and mesodermal origin', *Stem Cell Res Ther*, 2(4), pp. 36.

Deng, Y., Wang, Z., Wang, R., Zhang, X., Zhang, S., Wu, Y., Staufenbiel, M., Cai, F. and Song, W. (2013) 'Amyloid-beta protein (A β) Glu11 is the major beta-secretase site of beta-site amyloid-beta precursor protein-cleaving enzyme

1(BACE1), and shifting the cleavage site to Abeta Asp1 contributes to Alzheimer pathogenesis', *Eur J Neurosci*, 37(12), pp. 1962-9.

DeTure, M. A. and Dickson, D. W. (2019) 'The neuropathological diagnosis of Alzheimer's disease', *Mol Neurodegener*, 14(1), pp. 32.

Dhillon, S. (2021) 'Aducanumab: First Approval', *Drugs*, 81(12), pp. 1437-1443.

Dickerson, B. C., Stoub, T. R., Shah, R. C., Sperling, R. A., Killiany, R. J., Albert, M. S., Hyman, B. T., Blacker, D. and Detolledo-Morrell, L. (2011) 'Alzheimer-signature MRI biomarker predicts AD dementia in cognitively normal adults', *Neurology*, 76(16), pp. 1395-402.

Dickson, T. C. and Vickers, J. C. (2001) 'The morphological phenotype of beta-amyloid plaques and associated neuritic changes in Alzheimer's disease', *Neuroscience*, 105(1), pp. 99-107.

Ding, S., Wu, X., Li, G., Han, M., Zhuang, Y. and Xu, T. (2005) 'Efficient transposition of the piggyBac (PB) transposon in mammalian cells and mice', *Cell*, 122(3), pp. 473-83.

Doody, R. S., Raman, R., Farlow, M., Iwatsubo, T., Vellas, B., Joffe, S., Kieburtz, K., He, F., Sun, X., Thomas, R. G., Aisen, P. S., Siemers, E., Sethuraman, G., Mohs, R., Committee, A. S. D. C. S. S. and Group, S. S. (2013) 'A phase 3 trial of semagacestat for treatment of Alzheimer's disease', *N Engl J Med*, 369(4), pp. 341-50.

Du, H., Guo, L., Fang, F., Chen, D., Sosunov, A. A., McKhann, G. M., Yan, Y., Wang, C., Zhang, H., Molkentin, J. D., Gunn-Moore, F. J., Vonsattel, J. P., Arancio, O., Chen, J. X. and Yan, S. D. (2008) 'Cyclophilin D deficiency attenuates mitochondrial and neuronal perturbation and ameliorates learning and memory in Alzheimer's disease', *Nat Med*, 14(10), pp. 1097-105.

Egan, M. F., Kost, J., Tariot, P. N., Aisen, P. S., Cummings, J. L., Vellas, B., Sur, C., Mukai, Y., Voss, T., Furtek, C., Mahoney, E., Harper Mozley, L., Vandenberghe, R., Mo, Y. and Michelson, D. (2018) 'Randomized Trial of Verubecestat for Mild-to-Moderate Alzheimer's Disease', *N Engl J Med*, 378(18), pp. 1691-1703.

Ehehalt, R., Michel, B., De Pietri Tonelli, D., Zacchetti, D., Simons, K. and Keller, P. (2002) 'Splice variants of the beta-site APP-cleaving enzyme BACE1 in human brain and pancreas', *Biochem Biophys Res Commun*, 293(1), pp. 30-7.

Ellis, C. R. and Shen, J. (2015) 'pH-Dependent Population Shift Regulates BACE1 Activity and Inhibition', *J Am Chem Soc*, 137(30), pp. 9543-6.

Elmer, B. M., Swanson, K. A., Bangari, D. S., Piepenhagen, P. A., Roberts, E., Taksir, T., Guo, L., Obinu, M. C., Barneoud, P., Ryan, S., Zhang, B., Pradier, L., Yang, Z. Y. and Nabel, G. J. (2019) 'Gene delivery of a modified antibody to Abeta reduces progression of murine Alzheimer's disease', *PLoS One*, 14(12), pp. e0226245.

Findlay, J. A., Hamilton, D. L. and Ashford, M. L. (2015) 'BACE1 activity impairs neuronal glucose oxidation: rescue by beta-hydroxybutyrate and lipoic acid', *Front Cell Neurosci*, 9, pp. 382.

Fol, R., Braudeau, J., Ludewig, S., Abel, T., Weyer, S. W., Roederer, J. P., Brod, F., Audrain, M., Bemelmans, A. P., Buchholz, C. J., Korte, M., Cartier, N. and Müller, U. C. (2016) 'Viral gene transfer of APP α rescues synaptic failure in an Alzheimer's disease mouse model', *Acta Neuropathol*, 131(2), pp. 247-266.

Furukawa, K., Barger, S. W., Blalock, E. M. and Mattson, M. P. (1996) 'Activation of K⁺ channels and suppression of neuronal activity by secreted beta-amyloid-precursor protein', *Nature*, 379(6560), pp. 74-8.

Gertsik, N., Chiu, D. and Li, Y. M. (2014) 'Complex regulation of γ -secretase: from obligatory to modulatory subunits', *Front Aging Neurosci*, 6, pp. 342.

Gimenez-Cassina, A., Lim, F. and Diaz-Nido, J. (2006) 'Differentiation of a human neuroblastoma into neuron-like cells increases their susceptibility to transduction by herpesviral vectors', *J Neurosci Res*, 84(4), pp. 755-67.

Goedert, M. and Spillantini, M. G. (2019) 'Ordered Assembly of Tau Protein and Neurodegeneration', *Adv Exp Med Biol*, 1184, pp. 3-21.

Grant, M. K. O., Handoko, M., Rozga, M., Brinkmalm, G., Portelius, E., Blennow, K., Ashe, K. H., Zahs, K. R. and Liu, P. (2019) 'Human cerebrospinal fluid 6E10-immunoreactive protein species contain amyloid precursor protein fragments', *PLoS One*, 14(2), pp. e0212815.

Gu, Y., Chen, F., Sanjo, N., Kawarai, T., Hasegawa, H., Duthie, M., Li, W., Ruan, X., Luthra, A., Mount, H. T., Tandon, A., Fraser, P. E. and St George-Hyslop, P. (2003) 'APH-1 interacts with mature and immature forms of presenilins and nicastrin and may play a role in maturation of presenilin.nicastrin complexes', *J Biol Chem*, 278(9), pp. 7374-80.

Guglielmotto, M., Monteleone, D., Giliberto, L., Fornaro, M., Borghi, R., Tamagno, E. and Tabaton, M. (2011) 'Amyloid-beta(4)(2) activates the expression of BACE1 through the JNK pathway', *J Alzheimers Dis*, 27(4), pp. 871-83.

Güner, G. and Lichtenthaler, S. F. (2020) 'The substrate repertoire of γ -secretase/presenilin', *Semin Cell Dev Biol*, 105, pp. 27-42.

Guo, J. L., Buist, A., Soares, A., Callaerts, K., Calafate, S., Stevenaert, F., Daniels, J. P., Zoll, B. E., Crowe, A., Brunden, K. R., Moechars, D. and Lee, V. M. (2016) 'The Dynamics and Turnover of Tau Aggregates in Cultured Cells: INSIGHTS INTO THERAPIES FOR TAUOPATHIES', *J Biol Chem*, 291(25), pp. 13175-93.

Gurtu, V., Yan, G. and Zhang, G. (1996) 'IRES bicistronic expression vectors for efficient creation of stable mammalian cell lines', *Biochem Biophys Res Commun*, 229(1), pp. 295-8.

Haag, M. D., Hofman, A., Koudstaal, P. J., Stricker, B. H. and Breteler, M. M. (2009) 'Statins are associated with a reduced risk of Alzheimer disease regardless of lipophilicity. The Rotterdam Study', *J Neurol Neurosurg Psychiatry*, 80(1), pp. 13-7.

Haass, C., Lemere, C. A., Capell, A., Citron, M., Seubert, P., Schenk, D., Lannfelt, L. and Selkoe, D. J. (1995) 'The Swedish mutation causes early-onset Alzheimer's disease by beta-secretase cleavage within the secretory pathway', *Nat Med*, 1(12), pp. 1291-6.

Haass, C. and Selkoe, D. J. (2007) 'Soluble protein oligomers in neurodegeneration: lessons from the Alzheimer's amyloid beta-peptide', *Nat Rev Mol Cell Biol*, 8(2), pp. 101-12.

Hardy, J. and Allsop, D. (1991) 'Amyloid deposition as the central event in the aetiology of Alzheimer's disease', *Trends Pharmacol Sci*, 12(10), pp. 383-8.

Hartl, D., Klatt, S., Roch, M., Konthur, Z., Klose, J., Willnow, T. E. and Rohe, M. (2013) 'Soluble alpha-APP (sAPP α) regulates CDK5 expression and activity in neurons', *PLoS One*, 8(6), pp. e65920.

Hashimoto, T., Serrano-Pozo, A., Hori, Y., Adams, K. W., Takeda, S., Banerji, A. O., Mitani, A., Joyner, D., Thyssen, D. H., Bacskai, B. J., Frosch, M. P., Spires-Jones, T. L., Finn, M. B., Holtzman, D. M. and Hyman, B. T. (2012) 'Apolipoprotein E, especially apolipoprotein E4, increases the oligomerization of amyloid β peptide', *J Neurosci*, 32(43), pp. 15181-92.

Herms, J., Anliker, B., Heber, S., Ring, S., Fuhrmann, M., Kretschmar, H., Sisodia, S. and Müller, U. (2004) 'Cortical dysplasia resembling human type 2 lissencephaly in mice lacking all three APP family members', *EMBO J*, 23(20), pp. 4106-15.

Hinderer, C., Katz, N., Buza, E. L., Dyer, C., Goode, T., Bell, P., Richman, L. K. and Wilson, J. M. (2018) 'Severe Toxicity in Nonhuman Primates and Piglets Following High-Dose Intravenous Administration of an Adeno-Associated Virus Vector Expressing Human SMN', *Hum Gene Ther*, 29(3), pp. 285-298.

Hioki, H., Kameda, H., Nakamura, H., Okunomiya, T., Ohira, K., Nakamura, K., Kuroda, M., Furuta, T. and Kaneko, T. (2007) 'Efficient gene transduction of neurons by lentivirus with enhanced neuron-specific promoters', *Gene Ther*, 14(11), pp. 872-82.

Hitzenberger, M., Götz, A., Menig, S., Brunschweiler, B., Zacharias, M. and Scharnagl, C. (2020) 'The dynamics of γ -secretase and its substrates', *Semin Cell Dev Biol*, 105, pp. 86-101.

Holsinger, R. M., McLean, C. A., Beyreuther, K., Masters, C. L. and Evin, G. (2002) 'Increased expression of the amyloid precursor beta-secretase in Alzheimer's disease', *Ann Neurol*, 51(6), pp. 783-6.

Honig, L. S., Vellas, B., Woodward, M., Boada, M., Bullock, R., Borrie, M., Hager, K., Andreasen, N., Scarpini, E., Liu-Seifert, H., Case, M., Dean, R. A., Hake, A., Sundell, K., Poole Hoffmann, V., Carlson, C., Khanna, R., Mintun, M., DeMattos, R., Selzler, K. J. and Siemers, E. (2018) 'Trial of Solanezumab for Mild Dementia Due to Alzheimer's Disease', *N Engl J Med*, 378(4), pp. 321-330.

Hook, V. Y., Toneff, T., Aaron, W., Yasothornsrikul, S., Bunday, R. and Reisine, T. (2002) 'Beta-amyloid peptide in regulated secretory vesicles of chromaffin cells: evidence for multiple cysteine proteolytic activities in distinct pathways for beta-secretase activity in chromaffin vesicles', *J Neurochem*, 81(2), pp. 237-56.

Hsiao, K., Chapman, P., Nilson, S., Eckman, C., Harigaya, Y., Younkin, S., Yang, F. and Cole, G. (1996) 'Correlative memory deficits, A β elevation, and amyloid plaques in transgenic mice', *Science*, 274(5284), pp. 99-102.

Hsu, C. H., Wang, S. E., Lin, C. L., Hsiao, C. J., Sheu, S. J. and Wu, C. H. (2016) 'Neuroprotective Effects of the Herbal Formula B401 in Both Cell and Mouse Models of Alzheimer's Disease', *Evid Based Complement Alternat Med*, 2016, pp. 1939052.

Hu, X., Hicks, C. W., He, W., Wong, P., Macklin, W. B., Trapp, B. D. and Yan, R. (2006) 'Bace1 modulates myelination in the central and peripheral nervous system', *Nat Neurosci*, 9(12), pp. 1520-5.

Huang, M. T. and Gorman, C. M. (1990) 'Intervening sequences increase efficiency of RNA 3' processing and accumulation of cytoplasmic RNA', *Nucleic Acids Res*, 18(4), pp. 937-47.

Huang, Y. R. and Liu, R. T. (2020) 'The Toxicity and Polymorphism of β -Amyloid Oligomers', *Int J Mol Sci*, 21(12).

Hussain, I., Powell, D., Howlett, D. R., Tew, D. G., Meek, T. D., Chapman, C., Gloger, I. S., Murphy, K. E., Southan, C. D., Ryan, D. M., Smith, T. S., Simmons, D. L., Walsh, F. S., Dingwall, C. and Christie, G. (1999) 'Identification of a novel aspartic protease (Asp 2) as beta-secretase', *Mol Cell Neurosci*, 14(6), pp. 419-27.

Hwang, E. M., Kim, S. K., Sohn, J. H., Lee, J. Y., Kim, Y., Kim, Y. S. and Mook-Jung, I. (2006) 'Furin is an endogenous regulator of alpha-secretase associated APP processing', *Biochem Biophys Res Commun*, 349(2), pp. 654-9.

Iqbal, K., Gong, C. X. and Liu, F. (2013) 'Hyperphosphorylation-induced tau oligomers', *Front Neurol*, 4, pp. 112.

Ittner, L. M., Ke, Y. D., Delerue, F., Bi, M., Gladbach, A., van Eersel, J., Wölfing, H., Chieng, B. C., Christie, M. J., Napier, I. A., Eckert, A., Staufenbiel, M., Hardeman, E. and Götz, J. (2010) 'Dendritic function of tau mediates amyloid-beta toxicity in Alzheimer's disease mouse models', *Cell*, 142(3), pp. 387-97.

Iwatsubo, T., Odaka, A., Suzuki, N., Mizusawa, H., Nukina, N. and Ihara, Y. (1994) 'Visualization of A beta 42(43) and A beta 40 in senile plaques with end-specific A beta monoclonals: evidence that an initially deposited species is A beta 42(43)', *Neuron*, 13(1), pp. 45-53.

Jang, S. K., Kräusslich, H. G., Nicklin, M. J., Duke, G. M., Palmenberg, A. C. and Wimmer, E. (1988) 'A segment of the 5' nontranslated region of encephalomyocarditis virus RNA directs internal entry of ribosomes during in vitro translation', *J Virol*, 62(8), pp. 2636-43.

Jiang, S., Li, Y., Zhang, X., Bu, G., Xu, H. and Zhang, Y. W. (2014) 'Trafficking regulation of proteins in Alzheimer's disease', *Mol Neurodegener*, 9, pp. 6.

Jonson, M., Pokrzywa, M., Starkenberg, A., Hammarstrom, P. and Thor, S. (2015) 'Systematic A β Analysis in Drosophila Reveals High Toxicity for the 1-42, 3-42 and 11-42 Peptides, and Emphasizes N- and C-Terminal Residues', *PLoS One*, 10(7), pp. e0133272.

Jonsson, T., Stefansson, H., Steinberg, S., Jonsdottir, I., Jonsson, P. V., Snaedal, J., Bjornsson, S., Huttenlocher, J., Levey, A. I., Lah, J. J., Rujescu, D., Hampel, H., Giegling, I., Andreassen, O. A., Engedal, K., Ulstein, I., Djurovic, S., Ibrahim-Verbaas, C., Hofman, A., Ikram, M. A., van Duijn, C. M., Thorsteinsdottir, U., Kong, A. and Stefansson, K. (2013) 'Variant of TREM2 associated with the risk of Alzheimer's disease', *N Engl J Med*, 368(2), pp. 107-16.

Jorissen, E., Prox, J., Bernreuther, C., Weber, S., Schwanbeck, R., Serneels, L., Snellinx, A., Craessaerts, K., Thathiah, A., Tesseur, I., Bartsch, U., Weskamp, G., Blobel, C. P., Glatzel, M., De Strooper, B. and Saftig, P. (2010) 'The disintegrin/metalloproteinase ADAM10 is essential for the establishment of the brain cortex', *J Neurosci*, 30(14), pp. 4833-44.

Kamata, S., Oyama, T., Saito, K., Honda, A., Yamamoto, Y., Suda, K., Ishikawa, R., Itoh, T., Watanabe, Y., Shibata, T., Uchida, K., Suematsu, M. and Ishii, I. (2020) 'PPARalpha Ligand-Binding Domain Structures with Endogenous Fatty Acids and Fibrates', *iScience*, 23(11), pp. 101727.

Kandalepas, P. C., Sadleir, K. R., Eimer, W. A., Zhao, J., Nicholson, D. A. and Vassar, R. (2013) 'The Alzheimer's β -secretase BACE1 localizes to normal presynaptic terminals and to dystrophic presynaptic terminals surrounding amyloid plaques', *Acta Neuropathol*, 126(3), pp. 329-52.

Kanemaru, K., Takio, K., Miura, R., Titani, K. and Ihara, Y. (1992) 'Fetal-type phosphorylation of the tau in paired helical filaments', *J Neurochem*, 58(5), pp. 1667-75.

Kennedy, M. E., Stamford, A. W., Chen, X., Cox, K., Cumming, J. N., Dockendorf, M. F., Egan, M., Ereshefsky, L., Hodgson, R. A., Hyde, L. A., Jhee, S., Kleijn, H. J., Kuvelkar, R., Li, W., Mattson, B. A., Mei, H., Palcza, J., Scott, J. D., Tanen, M., Troyer, M. D., Tseng, J. L., Stone, J. A., Parker, E. M. and Forman, M. S. (2016) 'The BACE1 inhibitor verubecestat (MK-8931) reduces CNS β -amyloid in animal models and in Alzheimer's disease patients', *Sci Transl Med*, 8(363), pp. 363ra150.

Kim, H. S., Kim, E. M., Lee, J. P., Park, C. H., Kim, S., Seo, J. H., Chang, K. A., Yu, E., Jeong, S. J., Chong, Y. H. and Suh, Y. H. (2003) 'C-terminal fragments of amyloid precursor protein exert neurotoxicity by inducing glycogen synthase kinase-3 β expression', *FASEB J*, 17(13), pp. 1951-3.

Kim, Y. H., Lee, S. M., Cho, S., Kang, J. H., Minn, Y. K., Park, H. and Choi, S. H. (2019) 'Amyloid beta in nasal secretions may be a potential biomarker of Alzheimer's disease', *Sci Rep*, 9(1), pp. 4966.

Knopman, D. S., Jones, D. T. and Greicius, M. D. (2021) 'Failure to demonstrate efficacy of aducanumab: An analysis of the EMERGE and ENGAGE trials as reported by Biogen, December 2019', *Alzheimers Dement*, 17(4), pp. 696-701.

Kohutek, Z. A., diPierro, C. G., Redpath, G. T. and Hussaini, I. M. (2009) 'ADAM-10-mediated N-cadherin cleavage is protein kinase C- α dependent and promotes glioblastoma cell migration', *J Neurosci*, 29(14), pp. 4605-15.

Kong, J., Wan, L., Wang, Y., Zhang, H. and Zhang, W. (2020) 'Liraglutide Attenuates A β 42 Generation in APP^{swe}/SH-SY5Y Cells Through the Regulation of Autophagy', *Neuropsychiatr Dis Treat*, 16, pp. 1817-1825.

Konietzko, U. (2012) 'AICD nuclear signaling and its possible contribution to Alzheimer's disease', *Curr Alzheimer Res*, 9(2), pp. 200-16.

Kornhuber, J., Weller, M., Schoppmeyer, K. and Riederer, P. (1994) 'Amantadine and memantine are NMDA receptor antagonists with neuroprotective properties', *J Neural Transm Suppl*, 43, pp. 91-104.

Kovalevich, J. and Langford, D. (2013) 'Considerations for the use of SH-SY5Y neuroblastoma cells in neurobiology', *Methods Mol Biol*, 1078, pp. 9-21.

Kreis, A., Desloovere, J., Suelves, N., Pierrot, N., Yerna, X., Issa, F., Schakman, O., Gualdani, R., de Clippele, M., Tajeddine, N., Kienlen-Campard, P., Raedt, R., Octave, J. N. and Gailly, P. (2021) 'Overexpression of wild-type human amyloid precursor protein alters GABAergic transmission', *Sci Rep*, 11(1), pp. 17600.

Kuhn, P. H., Koroniak, K., Hogg, S., Colombo, A., Zeitschel, U., Willem, M., Volbracht, C., Schepers, U., Imhof, A., Hoffmeister, A., Haass, C., Roßner, S., Bräse, S. and Lichtenthaler, S. F. (2012) 'Secretome protein enrichment identifies physiological BACE1 protease substrates in neurons', *EMBO J*, 31(14), pp. 3157-68.

Kumar, D., Ganeshpurkar, A., Modi, G., Gupta, S. K. and Singh, S. K. (2018) 'Secretase inhibitors for the treatment of Alzheimer's disease: Long road ahead', *Eur J Med Chem*, 148, pp. 436-452.

Lammich, S., Kojro, E., Postina, R., Gilbert, S., Pfeiffer, R., Jasionowski, M., Haass, C. and Fahrenholz, F. (1999) 'Constitutive and regulated alpha-secretase

cleavage of Alzheimer's amyloid precursor protein by a disintegrin metalloprotease', *Proc Natl Acad Sci U S A*, 96(7), pp. 3922-7.

Lashley, T., Schott, J. M., Weston, P., Murray, C. E., Wellington, H., Keshavan, A., Foti, S. C., Foiani, M., Toombs, J., Rohrer, J. D., Heslegrave, A. and Zetterberg, H. (2018) 'Molecular biomarkers of Alzheimer's disease: progress and prospects', *Dis Model Mech*, 11(5).

Le Gall, S. M., Bobé, P., Reiss, K., Horiuchi, K., Niu, X. D., Lundell, D., Gibb, D. R., Conrad, D., Saftig, P. and Blobel, C. P. (2009) 'ADAMs 10 and 17 represent differentially regulated components of a general shedding machinery for membrane proteins such as transforming growth factor alpha, L-selectin, and tumor necrosis factor alpha', *Mol Biol Cell*, 20(6), pp. 1785-94.

Lee, T. H., Park, S., You, M. H., Lim, J. H., Min, S. H. and Kim, B. M. (2016) 'A potential therapeutic effect of saikosaponin C as a novel dual-target anti-Alzheimer agent', *J Neurochem*, 136(6), pp. 1232-1245.

Levy-Lahad, E., Wasco, W., Poorkaj, P., Romano, D. M., Oshima, J., Pettingell, W. H., Yu, C. E., Jondro, P. D., Schmidt, S. D. and Wang, K. (1995) 'Candidate gene for the chromosome 1 familial Alzheimer's disease locus', *Science*, 269(5226), pp. 973-7.

Li, H., Wolfe, M. S. and Selkoe, D. J. (2009) 'Toward structural elucidation of the gamma-secretase complex', *Structure*, 17(3), pp. 326-34.

Lin, L. F., Jhao, Y. T., Chiu, C. H., Sun, L. H., Chou, T. K., Shiue, C. Y., Cheng, C. Y. and Ma, K. H. (2022) 'Bezafibrate Exerts Neuroprotective Effects in a Rat Model of Sporadic Alzheimer's Disease', *Pharmaceuticals (Basel)*, 15(2).

Liu, K., Doms, R. W. and Lee, V. M. (2002) 'Glu11 site cleavage and N-terminally truncated A beta production upon BACE overexpression', *Biochemistry*, 41(9), pp. 3128-36.

Liu, L., Lauro, B. M., Ding, L., Rovere, M., Wolfe, M. S. and Selkoe, D. J. (2019a) 'Multiple BACE1 inhibitors abnormally increase the BACE1 protein level in neurons by prolonging its half-life', *Alzheimers Dement*, 15(9), pp. 1183-1194.

Liu, P. P., Xie, Y., Meng, X. Y. and Kang, J. S. (2019b) 'History and progress of hypotheses and clinical trials for Alzheimer's disease', *Signal Transduct Target Ther*, 4, pp. 29.

Lopez-Perez, E., Zhang, Y., Frank, S. J., Creemers, J., Seidah, N. and Checler, F. (2001) 'Constitutive alpha-secretase cleavage of the beta-amyloid precursor protein in the furin-deficient LoVo cell line: involvement of the pro-hormone convertase 7 and the disintegrin metalloprotease ADAM10', *J Neurochem*, 76(5), pp. 1532-9.

Luo, R., Su, L. Y., Li, G., Yang, J., Liu, Q., Yang, L. X., Zhang, D. F., Zhou, H., Xu, M., Fan, Y., Li, J. and Yao, Y. G. (2020) 'Activation of PPARA-mediated autophagy reduces Alzheimer disease-like pathology and cognitive decline in a murine model', *Autophagy*, 16(1), pp. 52-69.

Manzine, P. R., Pelucchi, S., Horst, M. A., Vale, F. A. C., Pavarini, S. C. I., Audano, M., Mitro, N., Di Luca, M., Marcello, E. and Cominetti, M. R. (2018) 'microRNA 221 Targets ADAM10 mRNA and is Downregulated in Alzheimer's Disease', *J Alzheimers Dis*, 61(1), pp. 113-123.

Maslah, E., Terry, R. D., Mallory, M., Alford, M. and Hansen, L. A. (1990) 'Diffuse plaques do not accentuate synapse loss in Alzheimer's disease', *Am J Pathol*, 137(6), pp. 1293-7.

Mattson, M. P., Cheng, B., Culwell, A. R., Esch, F. S., Lieberburg, I. and Rydel, R. E. (1993) 'Evidence for excitoprotective and intraneuronal calcium-regulating roles for secreted forms of the beta-amyloid precursor protein', *Neuron*, 10(2), pp. 243-54.

Mattsson, N., Rajendran, L., Zetterberg, H., Gustavsson, M., Andreasson, U., Olsson, M., Brinkmalm, G., Lundkvist, J., Jacobson, L. H., Perrot, L., Neumann, U., Borghys, H., Mercken, M., Dhuyvetter, D., Jeppsson, F., Blennow, K. and Portelius, E. (2012) 'BACE1 inhibition induces a specific cerebrospinal fluid β -amyloid pattern that identifies drug effects in the central nervous system', *PLoS One*, 7(2), pp. e31084.

McGuinness, L. A., Higgins, J. P., Walker, V. M., Davies, N. M., Martin, R. M., Coulthard, E., Davey-Smith, G., Kehoe, P. G. and Ben-Shlomo, Y. (2021) 'Association of lipid-regulating drugs with dementia and related conditions: an observational study of data from the Clinical Practice Research Datalink', *medRxiv*, pp. 2021.10.21.21265131.

Mercuri, E., Muntoni, F., Baranello, G., Masson, R., Boespflug-Tanguy, O., Bruno, C., Corti, S., Daron, A., Deconinck, N., Servais, L., Straub, V., Ouyang, H., Chand, D., Tauscher-Wisniewski, S., Mendonca, N., Lavrov, A. and group, S. V.-E. s. (2021) 'Onasemnogene abeparvovec gene therapy for symptomatic infantile-onset spinal muscular atrophy type 1 (STR1VE-EU): an open-label, single-arm, multicentre, phase 3 trial', *Lancet Neurol*, 20(10), pp. 832-841.

Mietelska-Porowska, A., Wasik, U., Goras, M., Filipek, A. and Niewiadomska, G. (2014) 'Tau protein modifications and interactions: their role in function and dysfunction', *Int J Mol Sci*, 15(3), pp. 4671-713.

Mizuguchi, H., Xu, Z., Ishii-Watabe, A., Uchida, E. and Hayakawa, T. (2000) 'IRES-dependent second gene expression is significantly lower than cap-dependent first gene expression in a bicistronic vector', *Mol Ther*, 1(4), pp. 376-82.

Moss, M. L., Bomar, M., Liu, Q., Sage, H., Dempsey, P., Lenhart, P. M., Gillispie, P. A., Stoeck, A., Wildeboer, D., Bartsch, J. W., Palmisano, R. and Zhou, P. (2007) 'The ADAM10 prodomain is a specific inhibitor of ADAM10 proteolytic activity and inhibits cellular shedding events', *J Biol Chem*, 282(49), pp. 35712-21.

Mossine, V. V., Waters, J. K., Hannink, M. and Mawhinney, T. P. (2013) 'piggyBac transposon plus insulators overcome epigenetic silencing to provide for stable signaling pathway reporter cell lines', *PLoS One*, 8(12), pp. e85494.

Moussa-Pacha, N. M., Abdin, S. M., Omar, H. A., Alniss, H. and Al-Tel, T. H. (2020) 'BACE1 inhibitors: Current status and future directions in treating Alzheimer's disease', *Med Res Rev*, 40(1), pp. 339-384.

Mroczko, B., Groblewska, M., Litman-Zawadzka, A., Kornhuber, J. and Lewczuk, P. (2018) 'Cellular Receptors of Amyloid β Oligomers (A β O) in Alzheimer's Disease', *Int J Mol Sci*, 19(7).

Murillo, J. R., Goto-Silva, L., Sanchez, A., Nogueira, F. C. S., Domont, G. B. and Junqueira, M. (2017) 'Quantitative proteomic analysis identifies proteins and pathways related to neuronal development in differentiated SH-SY5Y neuroblastoma cells', *EuPA Open Proteom*, 16, pp. 1-11.

Nicolaou, M., Song, Y. Q., Sato, C. A., Orlicchio, A., Kawarai, T., Medeiros, H., Liang, Y., Sorbi, S., Richard, E., Rogae, E. I., Moliaka, Y., Bruni, A. C., Jorge,

R., Percy, M., Duara, R., Farrer, L. A., St Georg-Hyslop, P. and Rogaeva, E. A. (2001) 'Mutations in the open reading frame of the beta-site APP cleaving enzyme (BACE) locus are not a common cause of Alzheimer's disease', *Neurogenetics*, 3(4), pp. 203-6.

Niu, M., Zhao, F., Bondelid, K., Siedlak, S. L., Torres, S., Fujioka, H., Wang, W., Liu, J. and Zhu, X. (2021) 'VPS35 D620N knockin mice recapitulate cardinal features of Parkinson's disease', *Aging Cell*, 20(5), pp. e13347.

Noble, W., Hanger, D. P., Miller, C. C. and Lovestone, S. (2013) 'The importance of tau phosphorylation for neurodegenerative diseases', *Front Neurol*, 4, pp. 83.

Nonaka, T., Watanabe, S. T., Iwatsubo, T. and Hasegawa, M. (2010) 'Seeded aggregation and toxicity of alpha-synuclein and tau: cellular models of neurodegenerative diseases', *J Biol Chem*, 285(45), pp. 34885-98.

Nübling, G., Bader, B., Levin, J., Hildebrandt, J., Kretzschmar, H. and Giese, A. (2012) 'Synergistic influence of phosphorylation and metal ions on tau oligomer formation and coaggregation with α -synuclein at the single molecule level', *Mol Neurodegener*, 7, pp. 35.

Ohsawa, I., Takamura, C., Morimoto, T., Ishiguro, M. and Kohsaka, S. (1999) 'Amino-terminal region of secreted form of amyloid precursor protein stimulates proliferation of neural stem cells', *Eur J Neurosci*, 11(6), pp. 1907-13.

Owens, L., Bracewell, J., Benedetto, A., Dawson, N., Gaffney, C. and Parkin, E. (2022) 'BACE1 Overexpression Reduces SH-SY5Y Cell Viability Through a Mechanism Distinct from Amyloid-beta Peptide Accumulation: Beta Prime-Mediated Competitive Depletion of sAbetaPPalpha', *J Alzheimers Dis*, 86(3), pp. 1201-1220.

Pahlman, S., Ruusala, A. I., Abrahamsson, L., Mattsson, M. E. and Esscher, T. (1984) 'Retinoic acid-induced differentiation of cultured human neuroblastoma cells: a comparison with phorbol ester-induced differentiation', *Cell Differ*, 14(2), pp. 135-44.

Pan, H., Wang, D., Zhang, X., Zhou, D., Zhang, H., Qian, Q., He, X., Liu, Z., Liu, Y., Zheng, T., Zhang, L., Wang, M. and Sun, B. (2016) 'Amyloid beta Is Not the Major Factor Accounting for Impaired Adult Hippocampal Neurogenesis in Mice Overexpressing Amyloid Precursor Protein', *Stem Cell Reports*, 7(4), pp. 707-718.

Pan, X. and Green, B. D. (2019) 'Temporal Effects of Neuron-specific beta-secretase 1 (BACE1) Knock-in on the Mouse Brain Metabolome: Implications for Alzheimer's Disease', *Neuroscience*, 397, pp. 138-146.

Park, S. A., Ahn, S. I. and Gallo, J. M. (2016) 'Tau mis-splicing in the pathogenesis of neurodegenerative disorders', *BMB Rep*, 49(8), pp. 405-13.

Parkin, E. and Harris, B. (2009) 'A disintegrin and metalloproteinase (ADAM)-mediated ectodomain shedding of ADAM10', *J Neurochem*, 108(6), pp. 1464-79.

Parkin, E. T., Watt, N. T., Hussain, I., Eckman, E. A., Eckman, C. B., Manson, J. C., Baybutt, H. N., Turner, A. J. and Hooper, N. M. (2007) 'Cellular prion protein regulates beta-secretase cleavage of the Alzheimer's amyloid precursor protein', *Proc Natl Acad Sci U S A*, 104(26), pp. 11062-7.

Pérez, M., Valpuesta, J. M., Medina, M., Montejo de Garcini, E. and Avila, J. (1996) 'Polymerization of tau into filaments in the presence of heparin: the minimal sequence required for tau-tau interaction', *J Neurochem*, 67(3), pp. 1183-90.

Perez, R. G., Squazzo, S. L. and Koo, E. H. (1996) 'Enhanced release of amyloid beta-protein from codon 670/671 "Swedish" mutant beta-amyloid precursor protein occurs in both secretory and endocytic pathways', *J Biol Chem*, 271(15), pp. 9100-7.

Peron, R., Vatanabe, I. P., Manzine, P. R., Camins, A. and Cominetti, M. R. (2018) 'Alpha-Secretase ADAM10 Regulation: Insights into Alzheimer's Disease Treatment', *Pharmaceuticals (Basel)*, 11(1).

Pesonen, S., Helin, H., Nokisalmi, P., Escutenaire, S., Ribacka, C., Sarkioja, M., Cerullo, V., Guse, K., Bauerschmitz, G., Laasonen, L., Kantola, T., Ristimäki, A., Rajecski, M., Oksanen, M., Haavisto, E., Kanerva, A., Joensuu, T. and Hemminki, A. (2010) 'Oncolytic adenovirus treatment of a patient with refractory neuroblastoma', *Acta Oncol*, 49(1), pp. 117-9.

Pîrșcoveanu, D. F. V., Pirici, I., Tudorică, V., Bălșeanu, T. A., Albu, V. C., Bondari, S., Bumbea, A. M. and Pîrșcoveanu, M. (2017) 'Tau protein in neurodegenerative diseases - a review', *Rom J Morphol Embryol*, 58(4), pp. 1141-1150.

Postina, R. (2012) 'Activation of α -secretase cleavage', *J Neurochem*, 120 Suppl 1, pp. 46-54.

Postina, R., Schroeder, A., Dewachter, I., Bohl, J., Schmitt, U., Kojro, E., Prinzen, C., Endres, K., Hiemke, C., Blessing, M., Flamez, P., Dequenue, A., Godaux, E., van Leuven, F. and Fahrenholz, F. (2004) 'A disintegrin-metalloproteinase prevents amyloid plaque formation and hippocampal defects in an Alzheimer disease mouse model', *J Clin Invest*, 113(10), pp. 1456-64.

Repetto, E., Russo, C., Venezia, V., Nizzari, M., Nitsch, R. M. and Schettini, G. (2004) 'BACE1 overexpression regulates amyloid precursor protein cleavage and interaction with the ShcA adapter', *Ann N Y Acad Sci*, 1030, pp. 330-8.

Riegerova, P., Brejcha, J., Bezdekova, D., Chum, T., Masinova, E., Cermakova, N., Ovsepian, S. V., Cebecauer, M. and Stefl, M. (2021) 'Expression and Localization of AbetaPP in SH-SY5Y Cells Depends on Differentiation State', *J Alzheimers Dis*, 82(2), pp. 485-491.

Rogaev, E. I., Sherrington, R., Rogaeva, E. A., Levesque, G., Ikeda, M., Liang, Y., Chi, H., Lin, C., Holman, K. and Tsuda, T. (1995) 'Familial Alzheimer's disease in kindreds with missense mutations in a gene on chromosome 1 related to the Alzheimer's disease type 3 gene', *Nature*, 376(6543), pp. 775-8.

Rossjohn, J., Cappai, R., Feil, S. C., Henry, A., McKinstry, W. J., Galatis, D., Hesse, L., Multhaup, G., Beyreuther, K., Masters, C. L. and Parker, M. W. (1999) 'Crystal structure of the N-terminal, growth factor-like domain of Alzheimer amyloid precursor protein', *Nat Struct Biol*, 6(4), pp. 327-31.

Rubinsztein, D. C. (2006) 'The roles of intracellular protein-degradation pathways in neurodegeneration', *Nature*, 443(7113), pp. 780-6.

Sabo, S. L., Ikin, A. F., Buxbaum, J. D. and Greengard, P. (2003) 'The amyloid precursor protein and its regulatory protein, FE65, in growth cones and synapses in vitro and in vivo', *J Neurosci*, 23(13), pp. 5407-15.

Saftig, P. and Lichtenthaler, S. F. (2015) 'The alpha secretase ADAM10: A metalloprotease with multiple functions in the brain', *Prog Neurobiol*, 135, pp. 1-20.

Sannerud, R., Esselens, C., Ejsmont, P., Mattera, R., Rochin, L., Tharkeshwar, A. K., De Baets, G., De Wever, V., Habets, R., Baert, V., Vermeire, W., Michiels, C., Groot, A. J., Wouters, R., Dillen, K., Vints, K., Baatsen, P., Munck, S., Derua,

R., Waelkens, E., Basi, G. S., Mercken, M., Vooijs, M., Bollen, M., Schymkowitz, J., Rousseau, F., Bonifacino, J. S., Van Niel, G., De Strooper, B. and Annaert, W. (2016) 'Restricted Location of PSEN2/ γ -Secretase Determines Substrate Specificity and Generates an Intracellular A β Pool', *Cell*, 166(1), pp. 193-208.

Sato, C., Morohashi, Y., Tomita, T. and Iwatsubo, T. (2006) 'Structure of the catalytic pore of gamma-secretase probed by the accessibility of substituted cysteines', *J Neurosci*, 26(46), pp. 12081-8.

Savonenko, A. V., Melnikova, T., Laird, F. M., Stewart, K. A., Price, D. L. and Wong, P. C. (2008) 'Alteration of BACE1-dependent NRG1/ErbB4 signaling and schizophrenia-like phenotypes in BACE1-null mice', *Proc Natl Acad Sci U S A*, 105(14), pp. 5585-90.

Schneider, A., Biernat, J., von Bergen, M., Mandelkow, E. and Mandelkow, E. M. (1999) 'Phosphorylation that detaches tau protein from microtubules (Ser262, Ser214) also protects it against aggregation into Alzheimer paired helical filaments', *Biochemistry*, 38(12), pp. 3549-58.

Schupf, N., Tang, M. X., Fukuyama, H., Manly, J., Andrews, H., Mehta, P., Ravetch, J. and Mayeux, R. (2008) 'Peripheral Abeta subspecies as risk biomarkers of Alzheimer's disease', *Proc Natl Acad Sci U S A*, 105(37), pp. 14052-7.

Seaman, M. N., Marcusson, E. G., Cereghino, J. L. and Emr, S. D. (1997) 'Endosome to Golgi retrieval of the vacuolar protein sorting receptor, Vps10p, requires the function of the VPS29, VPS30, and VPS35 gene products', *J Cell Biol*, 137(1), pp. 79-92.

Seegar, T. C. and Blacklow, S. C. (2019) 'Domain integration of ADAM family proteins: Emerging themes from structural studies', *Exp Biol Med (Maywood)*, 244(17), pp. 1510-1519.

Seegar, T. C. M., Killingsworth, L. B., Saha, N., Meyer, P. A., Patra, D., Zimmerman, B., Janes, P. W., Rubinstein, E., Nikolov, D. B., Skiniotis, G., Kruse, A. C. and Blacklow, S. C. (2017) 'Structural Basis for Regulated Proteolysis by the α -Secretase ADAM10', *Cell*, 171(7), pp. 1638-1648.e7.

Serrano-Pozo, A., Das, S. and Hyman, B. T. (2021) 'APOE and Alzheimer's disease: advances in genetics, pathophysiology, and therapeutic approaches', *Lancet Neurol*, 20(1), pp. 68-80.

Sevigny, J., Chiao, P., Bussi re, T., Weinreb, P. H., Williams, L., Maier, M., Dunstan, R., Salloway, S., Chen, T., Ling, Y., O'Gorman, J., Qian, F., Arastu, M., Li, M., Chollate, S., Brennan, M. S., Quintero-Monzon, O., Scannevin, R. H., Arnold, H. M., Engber, T., Rhodes, K., Ferrero, J., Hang, Y., Mikulskis, A., Grimm, J., Hock, C., Nitsch, R. M. and Sandrock, A. (2016) 'The antibody aducanumab reduces A β plaques in Alzheimer's disease', *Nature*, 537(7618), pp. 50-6.

Shen, L. L., Li, W. W., Xu, Y. L., Gao, S. H., Xu, M. Y., Bu, X. L., Liu, Y. H., Wang, J., Zhu, J., Zeng, F., Yao, X. Q., Gao, C. Y., Xu, Z. Q., Zhou, X. F. and Wang, Y. J. (2019) 'Neurotrophin receptor p75 mediates amyloid β -induced tau pathology', *Neurobiol Dis*, 132, pp. 104567.

Shimizu, H., Tosaki, A., Kaneko, K., Hisano, T., Sakurai, T. and Nukina, N. (2008) 'Crystal structure of an active form of BACE1, an enzyme responsible for amyloid beta protein production', *Mol Cell Biol*, 28(11), pp. 3663-71.

Shintani, E. Y. and Uchida, K. M. (1997) 'Donepezil: an anticholinesterase inhibitor for Alzheimer's disease', *Am J Health Syst Pharm*, 54(24), pp. 2805-10.

Shiple, M. M., Mangold, C. A. and Szpara, M. L. (2016) 'Differentiation of the SH-SY5Y Human Neuroblastoma Cell Line', *J Vis Exp*, (108), pp. 53193.

Siemers, E., Skinner, M., Dean, R. A., Gonzales, C., Satterwhite, J., Farlow, M., Ness, D. and May, P. C. (2005) 'Safety, tolerability, and changes in amyloid beta concentrations after administration of a gamma-secretase inhibitor in volunteers', *Clin Neuropharmacol*, 28(3), pp. 126-32.

Siemes, C., Quast, T., Kummer, C., Wehner, S., Kirfel, G., Müller, U. and Herzog, V. (2006) 'Keratinocytes from APP/APLP2-deficient mice are impaired in proliferation, adhesion and migration in vitro', *Exp Cell Res*, 312(11), pp. 1939-49.

Simon, A. M., Schiapparelli, L., Salazar-Colocho, P., Cuadrado-Tejedor, M., Escribano, L., Lopez de Maturana, R., Del Rio, J., Perez-Mediavilla, A. and Frechilla, D. (2009) 'Overexpression of wild-type human APP in mice causes cognitive deficits and pathological features unrelated to Abeta levels', *Neurobiol Dis*, 33(3), pp. 369-78.

Sims, J. R., Zimmer, J. A., Evans, C. D., Lu, M., Ardayfio, P., Sparks, J., Wessels, A. M., Shcherbinin, S., Wang, H., Monkul Nery, E. S., Collins, E. C., Solomon, P., Salloway, S., Apostolova, L. G., Hansson, O., Ritchie, C., Brooks, D. A., Mintun, M., Skovronsky, D. M. and Investigators, T.-A. (2023) 'Donanemab in Early Symptomatic Alzheimer Disease: The TRAILBLAZER-ALZ 2 Randomized Clinical Trial', *JAMA*, 330(6), pp. 512-527.

Singh, G. and Correa, R. (2023) 'Fibrate Medications', *StatPearls*. Treasure Island (FL).

Skommer, J. and Brittain, T. (2012) 'Extended survival of SH-SY5Y cells following overexpression of Lys67Glu neuroglobin is associated with stabilization of DeltapsiM', *Cytometry A*, 81(7), pp. 602-10.

Small, S. A., Kent, K., Pierce, A., Leung, C., Kang, M. S., Okada, H., Honig, L., Vonsattel, J. P. and Kim, T. W. (2005) 'Model-guided microarray implicates the retromer complex in Alzheimer's disease', *Ann Neurol*, 58(6), pp. 909-19.

Smith, T. M., Tharakan, A. and Martin, R. K. (2020) 'Targeting ADAM10 in Cancer and Autoimmunity', *Front Immunol*, 11, pp. 499.

Stachel, S. J., Coburn, C. A., Steele, T. G., Jones, K. G., Loutzenhiser, E. F., Gregro, A. R., Rajapakse, H. A., Lai, M. T., Crouthamel, M. C., Xu, M., Tugusheva, K., Lineberger, J. E., Pietrak, B. L., Espeseth, A. S., Shi, X. P., Chen-Dodson, E., Holloway, M. K., Munshi, S., Simon, A. J., Kuo, L. and Vacca, J. P. (2004) 'Structure-based design of potent and selective cell-permeable inhibitors of human beta-secretase (BACE-1)', *J Med Chem*, 47(26), pp. 6447-50.

Strittmatter, W. J., Saunders, A. M., Schmechel, D., Pericak-Vance, M., Enghild, J., Salvesen, G. S. and Roses, A. D. (1993) 'Apolipoprotein E: high-avidity binding to beta-amyloid and increased frequency of type 4 allele in late-onset familial Alzheimer disease', *Proc Natl Acad Sci U S A*, 90(5), pp. 1977-81.

Swerdlow, R. H. (2018) 'Mitochondria and Mitochondrial Cascades in Alzheimer's Disease', *J Alzheimers Dis*, 62(3), pp. 1403-1416.

Tackenberg, C. and Nitsch, R. M. (2019) 'The secreted APP ectodomain sAPP α , but not sAPP β , protects neurons against A β oligomer-induced dendritic spine loss and increased tau phosphorylation', *Mol Brain*, 12(1), pp. 27.

Takuma, H., Arawaka, S. and Mori, H. (2003) 'Isoforms changes of tau protein during development in various species', *Brain Res Dev Brain Res*, 142(2), pp. 121-7.

Tan, V. T. Y., Mockett, B. G., Ohline, S. M., Parfitt, K. D., Wicky, H. E., Peppercorn, K., Schoderboeck, L., Yahaya, M. F. B., Tate, W. P., Hughes, S. M. and Abraham, W. C. (2018) 'Lentivirus-mediated expression of human secreted amyloid precursor protein-alpha prevents development of memory and plasticity deficits in a mouse model of Alzheimer's disease', *Mol Brain*, 11(1), pp. 7.

Tanaka, S., Shiojiri, S., Takahashi, Y., Kitaguchi, N., Ito, H., Kameyama, M., Kimura, J., Nakamura, S. and Ueda, K. (1989) 'Tissue-specific expression of three types of beta-protein precursor mRNA: enhancement of protease inhibitor-harboring types in Alzheimer's disease brain', *Biochem Biophys Res Commun*, 165(3), pp. 1406-14.

Tang, X. H., Luo, R. C., Ye, M. S., Tang, H. Y., Ma, Y. L., Chen, Y. N., Wang, X. M., Lu, Q. Y., Liu, S., Li, X. N., Yan, Y., Yang, J., Ran, X. Q., Fang, X., Zhou, Y., Yao, Y. G., Di, Y. T. and Hao, X. J. (2021) 'Harpertrioate A, an A,B,D-seco-Limonoid with Promising Biological Activity against Alzheimer's Disease from Twigs of *Harrisonia perforata* (Blanco) Merr', *Org Lett*, 23(2), pp. 262-267.

Taylor, C. J., Ireland, D. R., Ballagh, I., Bourne, K., Marechal, N. M., Turner, P. R., Bilkey, D. K., Tate, W. P. and Abraham, W. C. (2008) 'Endogenous secreted amyloid precursor protein-alpha regulates hippocampal NMDA receptor function, long-term potentiation and spatial memory', *Neurobiol Dis*, 31(2), pp. 250-60.

Touloukhonova, L., Metzler, W. J., Witmer, M. R., Copeland, R. A. and Marcinkeviciene, J. (2003) 'Kinetic studies on beta-site amyloid precursor protein-cleaving enzyme (BACE). Confirmation of an iso mechanism', *J Biol Chem*, 278(7), pp. 4582-9.

Tousseyn, T., Thathiah, A., Jorissen, E., Raemaekers, T., Konietzko, U., Reiss, K., Maes, E., Snellinx, A., Serneels, L., Nyabi, O., Annaert, W., Saftig, P., Hartmann, D. and De Strooper, B. (2009) 'ADAM10, the rate-limiting protease of regulated intramembrane proteolysis of Notch and other proteins, is processed by ADAMS-9, ADAMS-15, and the gamma-secretase', *J Biol Chem*, 284(17), pp. 11738-47.

Tyan, S. H., Shih, A. Y., Walsh, J. J., Maruyama, H., Sarsoza, F., Ku, L., Eggert, S., Hof, P. R., Koo, E. H. and Dickstein, D. L. (2012) 'Amyloid precursor protein (APP) regulates synaptic structure and function', *Mol Cell Neurosci*, 51(1-2), pp. 43-52.

Vagnozzi, A. N., Li, J. G., Chiu, J., Razmpour, R., Warfield, R., Ramirez, S. H. and Praticò, D. (2019) 'VPS35 regulates tau phosphorylation and neuropathology in tauopathy', *Mol Psychiatry*.

van Dyck, C. H., Swanson, C. J., Aisen, P., Bateman, R. J., Chen, C., Gee, M., Kanekiyo, M., Li, D., Reyderman, L., Cohen, S., Froelich, L., Katayama, S., Sabbagh, M., Vellas, B., Watson, D., Dhadda, S., Irizarry, M., Kramer, L. D. and Iwatsubo, T. (2023) 'Lecanemab in Early Alzheimer's Disease', *N Engl J Med*, 388(1), pp. 9-21.

Volloch, V. and Rits-Volloch, S. (2022) 'The Amyloid Cascade Hypothesis 2.0: On the Possibility of Once-in-a-Lifetime-Only Treatment for Prevention of Alzheimer's Disease and for Its Potential Cure at Symptomatic Stages', *J Alzheimers Dis Rep*, 6(1), pp. 369-399.

- von Rotz, R. C., Kohli, B. M., Bosset, J., Meier, M., Suzuki, T., Nitsch, R. M. and Konietzko, U. (2004) 'The APP intracellular domain forms nuclear multiprotein complexes and regulates the transcription of its own precursor', *J Cell Sci*, 117(Pt 19), pp. 4435-48.
- Wang, P., Yang, G., Mosier, D. R., Chang, P., Zaidi, T., Gong, Y. D., Zhao, N. M., Dominguez, B., Lee, K. F., Gan, W. B. and Zheng, H. (2005) 'Defective neuromuscular synapses in mice lacking amyloid precursor protein (APP) and APP-Like protein 2', *J Neurosci*, 25(5), pp. 1219-25.
- Wang, Y. and Ha, Y. (2004) 'The X-ray structure of an antiparallel dimer of the human amyloid precursor protein E2 domain', *Mol Cell*, 15(3), pp. 343-53.
- Wang, Z., Wang, B., Yang, L., Guo, Q., Aithmitti, N., Songyang, Z. and Zheng, H. (2009) 'Presynaptic and postsynaptic interaction of the amyloid precursor protein promotes peripheral and central synaptogenesis', *J Neurosci*, 29(35), pp. 10788-801.
- Wen, L., Tang, F. L., Hong, Y., Luo, S. W., Wang, C. L., He, W., Shen, C., Jung, J. U., Xiong, F., Lee, D. H., Zhang, Q. G., Brann, D., Kim, T. W., Yan, R., Mei, L. and Xiong, W. C. (2011) 'VPS35 haploinsufficiency increases Alzheimer's disease neuropathology', *J Cell Biol*, 195(5), pp. 765-79.
- Wilcock, G. K., Gauthier, S., Frisoni, G. B., Jia, J., Harlund, J. H., Moebius, H. J., Bentham, P., Kook, K. A., Schelter, B. O., Wischik, D. J., Davis, C. S., Staff, R. T., Vuksanovic, V., Ahearn, T., Bracoud, L., Shamsi, K., Marek, K., Seibyl, J., Riedel, G., Storey, J. M. D., Harrington, C. R. and Wischik, C. M. (2018) 'Potential of Low Dose Leuco-Methylthioninium Bis(Hydromethanesulphonate) (LMTM) Monotherapy for Treatment of Mild Alzheimer's Disease: Cohort Analysis as Modified Primary Outcome in a Phase III Clinical Trial', *J Alzheimers Dis*, 61(1), pp. 435-457.
- Wilkinson, G. W. and Akrigg, A. (1992) 'Constitutive and enhanced expression from the CMV major IE promoter in a defective adenovirus vector', *Nucleic Acids Res*, 20(9), pp. 2233-9.
- Wojtowicz, S., Strosznajder, A. K., Jezyna, M. and Strosznajder, J. B. (2020) 'The Novel Role of PPAR Alpha in the Brain: Promising Target in Therapy of Alzheimer's Disease and Other Neurodegenerative Disorders', *Neurochem Res*, 45(5), pp. 972-988.
- Wójtowicz, S., Strosznajder, A. K., Jezyna, M. and Strosznajder, J. B. (2020) 'The Novel Role of PPAR Alpha in the Brain: Promising Target in Therapy of Alzheimer's Disease and Other Neurodegenerative Disorders', *Neurochem Res*, 45(5), pp. 972-988.
- Woods, N. K. and Padmanabhan, J. (2013) 'Inhibition of amyloid precursor protein processing enhances gemcitabine-mediated cytotoxicity in pancreatic cancer cells', *J Biol Chem*, 288(42), pp. 30114-24.
- World Health Organisation (WHO) (2020) *Dementia*. Available at: <https://www.who.int/news-room/fact-sheets/detail/dementia> (Accessed: September 21, 2020).
- Wu, L., Xie, J., Li, T., Mai, Z., Wang, L., Wang, X. and Chen, T. (2017) 'Gene delivery ability of polyethylenimine and polyethylene glycol dual-functionalized nanographene oxide in 11 different cell lines', *R Soc Open Sci*, 4(10), pp. 170822.

- Xicoy, H., Wieringa, B. and Martens, G. J. (2017) 'The SH-SY5Y cell line in Parkinson's disease research: a systematic review', *Mol Neurodegener*, 12(1), pp. 10.
- Xie, H. R., Hu, L. S. and Li, G. Y. (2010) 'SH-SY5Y human neuroblastoma cell line: in vitro cell model of dopaminergic neurons in Parkinson's disease', *Chin Med J (Engl)*, 123(8), pp. 1086-92.
- Xie, T., Yan, C., Zhou, R., Zhao, Y., Sun, L., Yang, G., Lu, P., Ma, D. and Shi, Y. (2014) 'Crystal structure of the γ -secretase component nicastrin', *Proc Natl Acad Sci U S A*, 111(37), pp. 13349-54.
- Xue, Y., Lee, S. and Ha, Y. (2011) 'Crystal structure of amyloid precursor-like protein 1 and heparin complex suggests a dual role of heparin in E2 dimerization', *Proc Natl Acad Sci U S A*, 108(39), pp. 16229-34.
- Yaar, M., Zhai, S., Pilch, P. F., Doyle, S. M., Eisenhauer, P. B., Fine, R. E. and Gilcrest, B. A. (1997) 'Binding of beta-amyloid to the p75 neurotrophin receptor induces apoptosis. A possible mechanism for Alzheimer's disease', *J Clin Invest*, 100(9), pp. 2333-40.
- Yamazaki, K., Mizui, Y. and Tanaka, I. (1997) 'Radiation hybrid mapping of human ADAM10 gene to chromosome 15', *Genomics*, 45(2), pp. 457-9.
- Yang, H. C., Chai, X., Mosior, M., Kohn, W., Boggs, L. N., Erickson, J. A., McClure, D. B., Yeh, W. K., Zhang, L., Gonzalez-DeWhitt, P., Mayer, J. P., Martin, J. A., Hu, J., Chen, S. H., Bueno, A. B., Little, S. P., McCarthy, J. R. and May, P. C. (2004) 'Biochemical and kinetic characterization of BACE1: investigation into the putative species-specificity for beta- and beta'-cleavage sites by human and murine BACE1', *J Neurochem*, 91(6), pp. 1249-59.
- Yu, X., Geng, W., Zhao, H., Wang, G., Zhao, Y., Zhu, Z. and Geng, X. (2017) 'Using a Commonly Down-Regulated Cytomegalovirus (CMV) Promoter for High-Level Expression of Ectopic Gene in a Human B Lymphoma Cell Line', *Med Sci Monit*, 23, pp. 5943-5950.
- Zempel, H., Thies, E., Mandelkow, E. and Mandelkow, E. M. (2010) 'Abeta oligomers cause localized Ca(2+) elevation, missorting of endogenous Tau into dendrites, Tau phosphorylation, and destruction of microtubules and spines', *J Neurosci*, 30(36), pp. 11938-50.
- Zhang, F., Gannon, M., Chen, Y., Yan, S., Zhang, S., Feng, W., Tao, J., Sha, B., Liu, Z., Saito, T., Saido, T., Keene, C. D., Jiao, K., Roberson, E. D., Xu, H. and Wang, Q. (2020) ' β -amyloid redirects norepinephrine signaling to activate the pathogenic GSK3 β /tau cascade', *Sci Transl Med*, 12(526).
- Zhang, H., Gao, Y., Qiao, P. F., Zhao, F. L. and Yan, Y. (2015) 'PPAR- α agonist regulates amyloid- β generation via inhibiting BACE-1 activity in human neuroblastoma SH-SY5Y cells transfected with APP^{swe} gene', *Mol Cell Biochem*, 408(1-2), pp. 37-46.
- Zhang, J. and Herrup, K. (2011) 'Nucleocytoplasmic Cdk5 is involved in neuronal cell cycle and death in post-mitotic neurons', *Cell Cycle*, 10(8), pp. 1208-14.
- Zhang, M., Deng, Y., Luo, Y., Zhang, S., Zou, H., Cai, F., Wada, K. and Song, W. (2012) 'Control of BACE1 degradation and APP processing by ubiquitin carboxyl-terminal hydrolase L1', *J Neurochem*, 120(6), pp. 1129-38.
- Zhou, W., Cai, F., Li, Y., Yang, G. S., O'Connor, K. D., Holt, R. A. and Song, W. (2010) 'BACE1 gene promoter single-nucleotide polymorphisms in Alzheimer's disease', *J Mol Neurosci*, 42(1), pp. 127-33.

